Technical Report SERDP-99-3
September 1999

US Army Corps of Engineers
Engineer Research and Development Center

Tri-Service Site Characterization and Analysis Penetrometer System (SCAPS) Accelerated Sensor Development Project - Final Report

by Ernesto R. Cespedes, ERDC
Stephen H. Lieberman, Space and Naval Warfare Systems Command
Bruce J. Nielsen, U.S. Air Force Research Laboratory
George E. Robitaille, U.S. Army Environmental Center

Prepared for Headquarters, U.S. Army Corps of Engineers

The contents of this report are not to be used for advertising, publication, or promotional purposes. Citation of trade names does not constitute an official endorsement or approval of the use of such commercial products.

The findings of this report are not to be construed as an official Department of the Army position, unless so designated by other authorized documents.

Technical Report SERDP-99-3
September 1999

Tri-Service Characterization and Analysis Penetrometer System (SCAPS) Accelerated Sensor Development Project - Final Report

by Ernesto R. Cespedes

U.S. Army Engineer Research and Development Center
Waterways Experiment Station
3909 Halls Ferry Road
Vicksburg, MS 39180-6199

Stephen H. Lieberman

Space and Naval Warfare Systems Command
53605 Hull Street
San Diego, CA 92152-5410

Bruce J. Nielson

U.S. Air Force Research Laboratory
139 Barnes Drive
Tyndall Air Force Base, Florida 32403-5323

George E. Robitaille

U.S. Army Environmental Center
Aberdeen Proving Ground, Maryland 21010-5401

Final report

Prepared for U.S. Army Corps of Engineers
Washington, DC 20314-1000

Waterways Experiment Station Cataloging-in-Publication Data

Tri-Service Characterization and Analysis Penetrometer System (SCAPS) Accelerated Sensor Development Project : final report / by Ernesto R. Cespedes ... [et al.] ; prepared for U.S. Army Corps of Engineers.
184 p. : ill. ; 28 cm.—(Technical report ; SERDP-99-3)
Includes bibliographic references.
1. Tri-Service Site Characterization and Analysis Penetrometer System (SCAPS) 2. Penetrometer. 3. Hazardous wastes — Environmental aspects. I. Cespedes, Ernesto R. II. United States. Army. Corps of Engineers. III. U.S. Army Engineer Research and Development Center. IV. Strategic Environmental Research and Development Program (U.S.) V. Series: Technical report SERDP ; 99-3.
TA7 W34 no.SERDP-99-3

Contents

List of Figures

List of Tables

Preface

The Tri-Service Site Characterization and Analysis Penetrometer System (SCAPS) Accelerated Sensor Development Project was sponsored by the Strategic Environmental Research and Development Program (SERDP), Washington, DC, under Project Number 94-729. Mr. Bradley P. Smith is the Executive Director, SERDP.

As a Tri-Service effort, the management and execution of this project were performed by representatives from each of the Services. Dr. Ernesto R. Cespedes, Environmental Laboratory (EL), U.S. Army Engineer Research and Development Center (ERDC), was responsible for overall technical and financial management of the project and was the Principal Investigator responsible for the Army portion of the project. Dr. Stephen H. Lieberman, Space and Naval Warfare Systems Command, was the Principal Investigator responsible for the Navy portion of the effort. Mr. Bruce Nielsen, U.S. Air Force Research Laboratory, was the Principal Investigator responsible for the Air Force efforts. Mr. George E. Robitaille, U.S. Army Environmental Center, was the Principal Investigator responsible for managing the 6.3 technical demonstration portion of the project. This report, which summarizes the results of the 4-year SERDP effort, was compiled and prepared by Dr. Cespedes and Ms. Diane Cargile, EL, ERDC, based on input provided by each of the Tri-Service Principal Investigators. Researchers from the three services contributed technical material included in this report, and appropriate authorship credit is given at the beginning of each chapter that describes a specific SCAPS technology development effort.

This report was prepared under the general supervision of Mr. Norman R. Francingues, Chief, Environmental Engineering Division, EL, and Dr. John W. Keeley, Director, EL.

At the time of publication of this report, Dr. Lewis E. Link was Acting Director of ERDC, and COL Robin R. Cababa, EN, was Commander.

This report should be cited as follows:

Cespedes, E.R., Lieberman, S.H., Nielsen, B.J., and Robitaille, G.E. 1999. "Tri-Service Site Characterization and Analysis Penetrometer System (SCAPS) Accelerated Sensor Development Project - Final Report." Technical Report SERDP-99-3, U.S. Army Engineer Research and Development Center, Vicksburg, MS.

Conversion Factors, Non-SI to SI Units of Measurement

Non-SI units of measurement used in this report can be converted to SI units as follows:

Multiply	By	To Obtain
acres	4046.8564224	squar meters
cubic feet	0.02831685	cubic meters
Fahrenheit degrees	5/9 x F-32	Celsius or Kelvin[1]
feet	0.3048	meters
inches	0.0254	meters
pound (force) inches	0.1129848	newton meters or joules
miles (U.S. statute)	1.609347	kilometers
pounds (force) per square foot	47.88026	pascals
pounds (mass)	0.4535924	kilograms
tons	0.9072	kilograms

[1] To obtain Celsius (C) temperature readings from Fahrenheit (F) readings, use this following formula: C=(5/9) (F - 32). To obtain Kelvin (K) readings, use: K= (5/9) (F - 32) + 273.15.

1 Introduction

Background

The Site Characterization and Analysis Penetrometer System (SCAPS) has proven to be a cost-effective, versatile tool for rapid subsurface screening of contaminated sites. Since the fielding of the first SCAPS vehicle at the U.S. Army Engineer Waterways Experiment Station (WES) during 1990, the Tri-Service SCAPS fleet has grown to seven vehicles (four Army and three Navy). In addition, the Department of Energy (DOE) operates two SCAPS vehicles, the Environmental Protection Agency (EPA) operates one SCAPS vehicle, and private contractors, under licensing agreements, operate a number of SCAPS technologies that support Department of Defense (DoD), DOE, and EPA site characterization efforts.

The basic SCAPS platform consists of a 20-ton[1] truck equipped with vertical hydraulic rams capable of pushing a cone penetrometer (CPT) into the ground at a speed of 2 cm/sec to depths of over 50 m in nominally consolidated soils. During a push, SCAPS is capable of collecting subsurface stratigraphy data with spatial resolutions of 2 cm, as well as chemical contaminant data by means of sensors and samplers incorporated into the penetrometer head. The initial application of SCAPS technology was to characterize sites contaminated with heavy petroleum, oils, and lubricants (POLs) by means of a laser induced fluorescence (LIF) sensor (Lieberman et al. 1991). Successful fielding of the LIF technology led to increased interest in expanding SCAPS capabilities to address other contaminants (Cespedes, Miles, and Lieberman 1994).

In 1994 the Strategic Environmental Research and Development Program (SERDP) funded a Tri-Service effort to accelerate the development and testing of advanced sensors and sampling technologies for SCAPS to allow characterization of sites containing explosives, metals, volatile organic compounds (VOCs), light POLs, and radioactive wastes (SERDP 1995). The project was funded for 4 years, but work continued until the end of Fiscal Year (FY) 1998. The objective of this report is to document the progress and

[1] A table for converting Non-SI to SI units is presented on page xiii.

accomplishments that resulted from the SERDP-funded Tri-Service SCAPS Accelerated Sensor Development project.

Project Management Overview

Dr. Ernesto Cespedes, WES, was responsible for the overall management and execution of the SERDP-funded Tri-Service SCAPS Project. In addition to coordinating and overseeing the wide variety of research tasks, Dr. Cespedes was also responsible for providing monthly financial and detailed quarterly progress reports to the SERDP Executive Office and for presenting technical and program briefings at numerous SERDP-sponsored events. The SERDP Executive Office and the Scientific Advisory Board (SAB) evaluated the progress of the SCAPS projects during yearly In-Process Reviews. In addition, the SAB recommended that an independent Peer Review Panel be established to evaluate the SCAPS project on a yearly basis and recommend changes and redirection of specific technology development efforts. The Peer Review Panel met three times during the life of this project. During the course of the project, a number of efforts were modified, accelerated, deleted, and/or added at the direction of the SAB and the Peer Review Panel and with the concurrence of the SERDP Program Office. These changes are described in detail in the appropriate chapters of this report. The yearly Peer Review Panel meetings included government, industry, and academic researchers and SCAPS users, and provided a forum for information exchange with others outside of the SERDP program.

The Peer Review Panel was composed of the following members:

Dr. Jeff Marqusee
Office of Deputy Under Secretary of Defense
for Environmental Security (ODUSD (ES))
3000 Defense Plaza
Washington, DC 20301-3000

Dr. Caroline Purdy and Mr. Eric Lightner
U.S. Department of Energy
Office of Science and Technology, EM-50
19901 Germantown Road
Germantown, MD 20874-1290

Dr. Greg Rosasco
Chief, Process Measurement Division
National Institute of Standards and Technology
Chemical Science and Technology Laboratory
Gaithersburg, MD 20899

Dr. Carl Enfield
Robert S. Kerr Environmental Research Laboratory
U.S. Environmental Protection Agency
919 Kerr Research Drive
Ada, OK 74820

Project Technical Overview

The Tri-Service Accelerated SCAPS Sensor Development Project was initially composed of seven 6.2 Applied Research areas as follows:

a. Laser Induced Breakdown Spectroscopy (LIBS) sensor development for detecting metals in soils.

b. LIF sensor development for detecting
(1) Lighter POL contaminants
(2) Explosive contaminants

c. Fiber Optic Raman Sensor (FORS) development for detecting volatile organic compounds (VOC) (Light nonaqueous phase liquids (LNAPLS) and dense nonaqueous phase liquids (DNAPLS)).

d. Electrochemical sensors for detecting
(1) Explosive contaminants
(2) VOCs

e. Spectral Gamma probe for detecting radioactive waste.

f. SCAPS sampler development
(1) Thermal desorption VOC sampler
(2) Multiport sampler

g. Data processing methodologies to provide onsite three-dimensional (3-D) visualization and to interface emerging sensors into the SCAPS data acquisition, processing, and visualization systems.

In addition to these seven 6.2 Research Areas, there was a 6.3 Technology Demonstration task component which was managed by Mr. George Robitaille, U.S. Army Environmental Center (AEC), who also served as the Tri-Service SCAPS coordinator responsible for facilitating the validation, certification, and transfer of new technologies to SCAPS users.

The technical portions of this report are organized into seven chapters which describe the progress achieved in each of the first six research areas listed above as well as the X-Ray Fluorescence (XRF) sensor development effort which was added after the second Peer Review Panel meeting. The contributions of research area VII - Data processing methodologies, and of the 6.3 Technology Demonstrations have been incorporated into the appropriate technology chapters.

2 Research Area I: Laser Induced Breakdown Spectroscopy (LIBS)

By: Brian H. Miles, WES
Gregory A. Theriault, SPAWAR
Javier Cortes, WES

Introduction

The focus of this research area was to develop and evaluate LIBS sensors for the delineation of metal contamination in soils. Under SERDP support, two parallel approaches for the implementation of LIBS technology for SCAPS applications were investigated. WES developed a downhole laser LIBS (DL-LIBS) probe while the Space and Naval Warfare Systems Command (SPAWAR (formerly NRaD)) developed a fiber-optic LIBS (FO-LIBS) probe to reduce technical risks. As a result, two types of SCAPS LIBS probes were designed, fabricated, evaluated, and both were transitioned to the Environmental Security Technology Certification Program (ESTCP) for Demonstration/Validation.

There are several physical differences between the two probes. First, the DL-LIBS probe utilizes a laser within the probe, while the FO-LIBS probe's laser is in the SCAPS truck. The DL-LIBS probe incorporates a recessed window, while the FO-LIBS window is in contact with the soil. While both probes rely on optical fibers to bring plasma light from downhole to the surface, the FO-LIBS probe utilizes a single fiber to transmit laser light and to receive plasma light from the sample. The DL-LIBS acquires data during probe retraction, while FO-LIBS typically acquires data during the push phase. The DL-LIBS probe incorporates an integrated microwave soil moisture sensor, and both probes utilize geophysical sensors to provide subsurface soil classification (i.e., stratigraphy).

The LIBS technology is well suited for in situ SCAPS measurements because it requires no sample preparation and can be performed with only optical

interrogation of the sample. In a typical LIBS measurement, the high-powered infrared emission from a pulsed Nd:YAG laser is focused to a small spot, generating power densities in excess of several GW/cm^2. Under these conditions, ablation and ionization of a small amount of the sample material occurs. The subsequent atomic emission of the plasma constituents can then be spectroscopically analyzed. The time-resolved spectral emission of the LIBS plasma is initially characterized by a broadband continuum due to Bremsstrahlung and recombination radiation. As the plasma cools, this broadband background decays leaving atomic emission lines at discrete wavelengths that characterize the thermally excited elemental species that were present in the plasma. By using a time-gated detector, the atomic emission can be separated from the broadband background and concentrations of the emitting elements can be quantified.

Laboratory Development

DL-LIBS laboratory development

The initial phase of the effort conducted by WES researchers consisted of laboratory experiments to collect LIBS signatures of heavy metals in solid form, in dissolved aqueous solutions, and in soil samples. Laboratory investigations were conducted on metal spiked sand, silt, and clay soils at three different moisture contents. Results of this research indicated that fine grain soils produce a weaker LIBS signal than large-grain soils with the same contaminant concentration. Similarly, moist soils displayed weaker signals than dry soils, and moist soils required higher irradiances to achieve breakdown than dry soils.

Each acquisition of a single LIBS spark requires integration of the spark light using a gated detection system. Early research sought to understand how to choose the best parameters for acquisition. The detection parameters including integration time and delay needed to be determined. Figure 1 displays a plot of the temporal history of LIBS spectra of solid lead. At the earliest times (rear most trace in figure) after the plasma creation, the plasma's spectrum is intense and similar to that of a blackbody. As the plasma cools, the blackbody component of the radiation decays and atoms return to their ground states. As the atoms transition to lower quantum states, light is emitted proportional in wavelength to the energy difference between the quantum states. Within Figure 1 are 50 spectra of LIBS plasmas formed on solid lead. The rearmost spectrum is at an early time after plasma creation (130 ns). Note the high baseline intensity of the early spectra. Each subsequent spectrum is separated by 50 ns (i.e., the second spectrum from the rear was collected at 180 ns after plasma creation). Note the emergence of the 405.783-nm lead peak as time increases. From a quantitative standpoint, signal-to-noise is improved if the onset of peak integration is delayed until the blackbody component has died down but while the emission peak is still strong. The duration of the integration is typically several μs to ensure that all of the metal emission line is recorded. The integration delay utilized in the DL-LIBS probe is typically set at approximately 220 ns, while the integration time is approximately 80 μs.

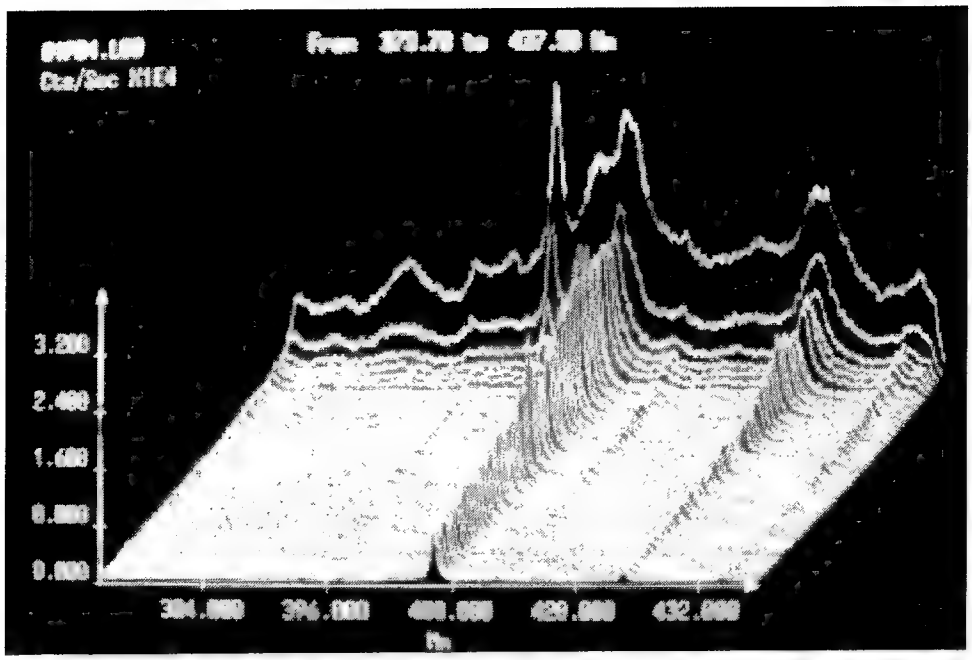

Figure 1. Temporal evolution of LIBS plasma of lead

Laboratory studies were conducted in soil matrices of Yuma sand and sea sand provided by the Fisher Scientific Company. The chemicals used were water-soluble compounds with the exception of mercury where an acetone-soluble compound was used. A solution of $HgCl_2$ and acetone was used to prepare the Hg samples. All the samples were certified by WES analytical laboratory.

WES laboratory instrumentation consisted of an excitation laser, focusing optics, spectrometer, control electronics, and data acquisition hardware. The excitation laser is an Nd:YAG Continuum Surelite 20 laser operating at a wavelength of 1,064 nm. The spectrometer is an Instruments S.A. model HR 640, which has a focal length of 640 mm with a 2,400-groove/mm grating. A Princeton Instruments intensified 1,024-element photodiode array controlled by Princeton Instruments PG-200 programmable pulse generator was used to acquire the diffracted spectra. A bundle of 19 optic fibers, 1 m long, transmits the light from the laser spark to the spectrometer.

The optimum parameters for WES laboratory instrumentation were determined to be: laser power of 100 mJ, integration delay of 350 ns, integration width of 100 μs, and entrance slit width of 10 μm. The detection limits analyses were performed by integrating the area below the peak of a metal of interest and rationing against the area of a large background peak in the same spectral region (usually an Fe peak). The standard deviation and the average value were calculated for each sample. The average ratio value of each metal was plotted against its certified concentration. A least squares fit was conducted and the slope was obtained from the data for each metal. The lower detection limit was calculated using the relation.

$$D_L = \frac{2^*Std}{M}$$

where

D_L = lower detection limit (concentration)

Std = standard deviation of the lowest concentration used

M = slope of calibration curve

The University of Nebraska-Lincoln (UNL), under SERDP support through WES, performed LIBS research to validate and extend WES results. The UNL conducted similar experiments in sand, silt, clay, and kaolin. In this study, the intensity of the contaminant lines were ratioed to the intensity of a silica line or titanium line present within the same spectrum. The metals of interest and their respective emission lines analyzed were: As at 278.02 nm, Cd at 479.99 nm, Cr at 425.44 nm, Hg at 435.83 nm, Pb at 405.78 nm, and Zn at 481.05 nm. The combined detection limits results for both WES and UNL studies are presented in Table 1.

Table 1
Lower Detection Limits For As, Cd, Cr, Hg, Pb, and Zn in Soils, ppm

	WES Research		UNL Research			
Element	Yuma sand	Fisher sea sand	Sand	Silt	Clay	Kaolin
As	*	*	530	?	?	?
Cd	*	1.1	3.3	160	360	830
Cr	*	1.6	0.4	74	73	83
Hg	*	3.8	11	1,800	1,100	?
Pb	9.1	3.3	1.4	150	210	340
Zn	*	1.0	1.6	190	510	300

Note: * = not used; ? = could not be determined from data.

From these laboratory measurements, it was determined that LIBS was capable of meeting and exceeding regulatory action levels for most toxic metals in soils. Thus, efforts were directed to implement LIBS technology in a SCAPS probe. It should be noted that the high mercury detection limits observed by the UNL researchers in silt and clay were later determined to have been caused by contaminant evaporation during drying which significantly decreased the contaminant concentrations of the spiked samples. From these experiments, it was also determined that breakdown can be generated over dry soil with as little as 10 mJ, but that higher laser power provided better signal-to-noise ratio while sampling a larger amount of soil per laser shot (thereby reducing shot-to-shot variability). It was also determined that high spectral resolution was required in

order to separate emission lines of metal contaminants from background interferences attributed to the soil matrix.

FO-LIBS laboratory development

Shortly after receipt of initial SERDP funding in FY94, and prior to prototype probe fabrication, the SPAWAR team simulated and tested the essential elements of an FO-LIBS based cone penetrometer probe using the laboratory configuration shown in Figure 2. The laser used was a Continuum NY61 Nd:YAG laser operating at 1,064 nm at 10 Hz at a pulse width of 20 ns. The intensity of the linearly polarized laser output was varied while maintaining a constant pulse width by the use of a half waveplate and beamsplitter combination mounted on the laser bench. The laser energy was monitored by the use of a beamsplitter to divert part of the beam to an energy meter. The majority (95 percent) of the laser light passed through the beamsplitter and was focused onto the face of a single 600 μm fused silica core fused silica clad optical fiber. The laser light passed through the excitation fiber and was reflected by a mirror that was highly reflecting at 1,064 nm and highly transparent from 400 to 600 nm. The excitation beam was focused by an f-number 0.63 aspheric lens onto a soil sample that was spiked with known quantities of a selected metal. The spot size at the sample was calculated to be 200 μm.

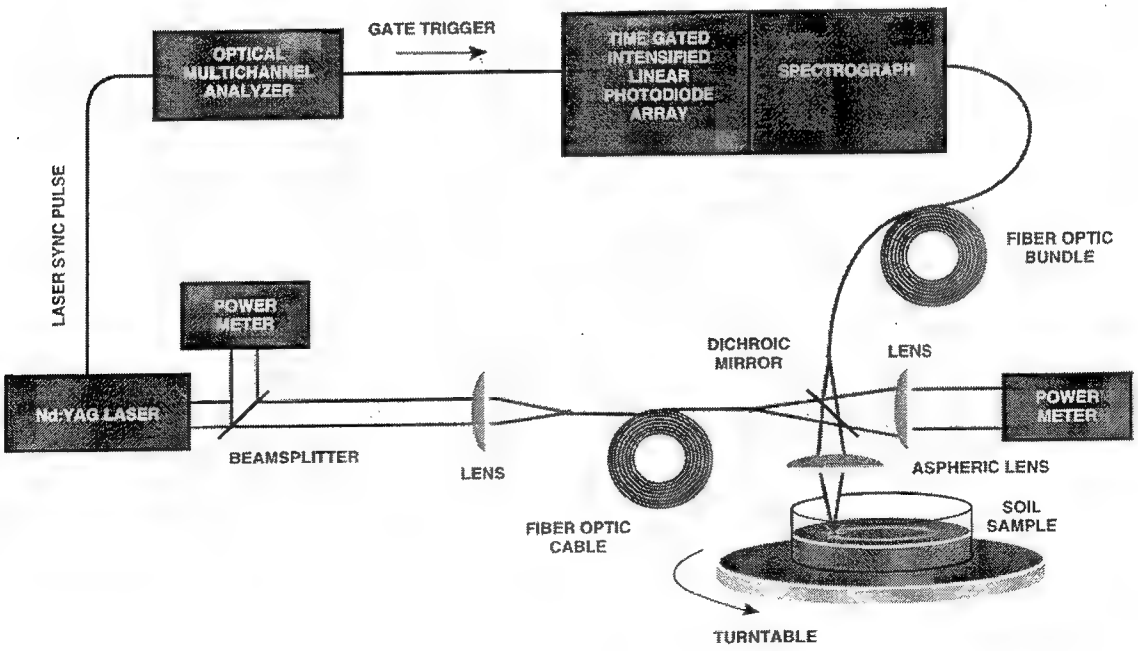

Figure 2. FO-LIBS laboratory verification configuration

Because the elemental emission from the metal contaminant on the vaporized soil sample was at a shorter wavelength (i.e., Pb 405.78 nm) than the excitation wavelength, it could be collected by the aspheric lens and focused through the dichroic mirror onto a 10-m-long bundle of five fibers. The output of the five-fiber bundle was arranged in a line and focused and f/# matched onto the input slit of a Spex 750M spectrometer. The spectrometer dispersed the spark emission over an EG&G 1420 gated intensified linear photodiode array (PDA). The PDA detector was controlled by an EG&G 1460 optical multichannel analyzer system. The timing of the detector gate was slaved to the sync pulse from the laser. The duration of the detector time gate pulse was 1 μsec, and it was applied after the broadband background light had decayed.

It was observed that the spark incident on the soil sample during the measurement created a significant shock that effectively displaced sand from the focal region of the aspheric lens. This variation of the soil surface position with respect to the focal point of the lens had the effect of varying the power density at the sample significantly. To ensure that a new sample was presented to the detector for each laser shot and to minimize the variation of the sample position with respect to the focal point of the aspheric lens, the soil sample was rotated on a turntable and simultaneously agitated. Typically, the emission spectra from 1,000 sparks were accumulated. This experimental procedure had the desired effects of reducing shot-to-shot variations in system response due to soil displacement and presenting a larger volume of sample to the detector for averaging of spatial inhomogeneities.

Using the laboratory configuration represented in Figure 3, the concept of using fiber-optic beam delivery and collection in a LIBS probe was proven. The detection capability possible with a fiber-optic probe was demonstrated to be generally at or below EPA site screening requirements. Additionally, several key variables related to probe design and use were identified including lens-to-sample distance, soil grain size, soil moisture content, fiber damage characteristics, and soil spark initiation threshold.

Probe Design

DL-LIBS probe

Based on the technical risks associated with the optical fiber power handling limits, and in view of the signal-to-noise advantages associated with high laser irradiances on the soil sample, the development group at WES chose to use a laser in the probe rather than fiber illumination. WES developed a SCAPS probe that incorporated a compact 80 mJ pulsed laser in collaboration with Los Alamos National Laboratory and Kigre Corp.

There are several advantages to using a laser in the probe. If the laser is in the probe and no fiber is used for transmission of the laser pulse to the soil, then diffraction limited spot sizes can be achieved. The diffraction limited spot size results in plasma irradiances of over 1,000 GW/cm^2 compared to 10 GW/cm^2 for

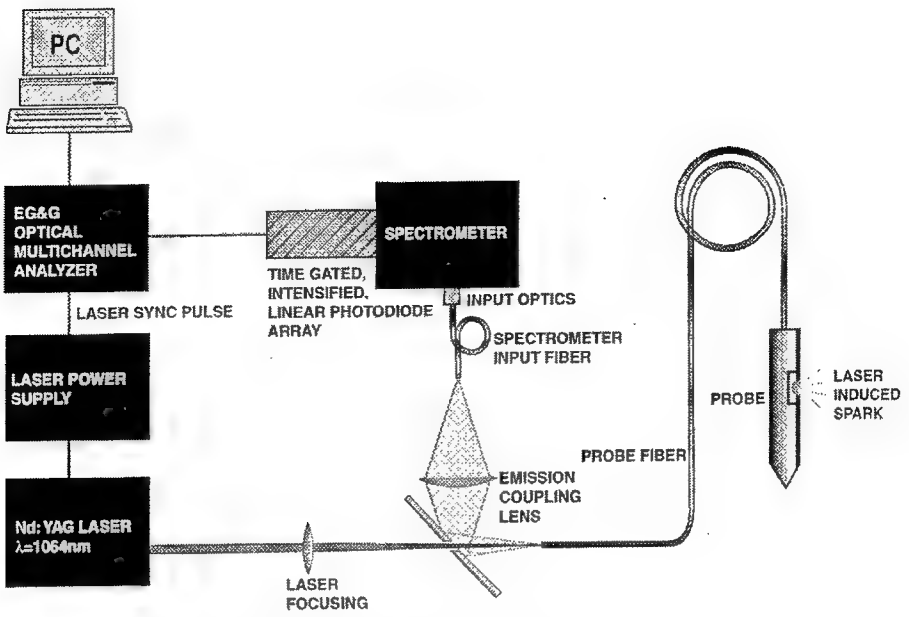

Figure 3. FO-LIBS laboratory verification configuration using fiber-optic beam delivery and light collection

a multimode fiber illuminated system. The higher irradiance leads to a hotter plasma, yielding a stronger signal and more complete ionization of the soil sample.

A second concern in the design process was the output window. Early work indicated that if the probe laser output window and soil are in contact, the formation of the plasma at the interface can damage the window. Damage to the window varies from minor surface pitting (similar in appearance to pitting on an auto's windshield from small stones) to complete fracture of the window into several pieces. A fractured or pitted window will provide signal attenuation that exhibits a complex dependence on the degree of pitting of the window. If the same portion of the window is used for transmitting and receiving, then clearly the laser and the plasma will both be attenuated. Furthermore, the quartic spectral dependence on scattering with respect to light frequency indicates how the relative line strengths will be affected. Specifically, as window condition worsens, the shorter wavelengths will scatter much more (4th power) than the longer wavelengths.

In light of these experiences, the WES development team decided to design a probe with a recessed window. A steel sacrificial sleeve was added to the design to protect the window during the push. After reaching the desired depth, the sleeve drops away and exposes the recessed window.

The fracturing problem was avoided by providing a separation between the soil and output window, allowing for very low irradiance values at window surfaces (~0.01 GW/cm^2) and eliminating the chance of damage. Comparison of various operational scenarios led to selection of a recessed window which would

allow operation during probe retraction. A slot with a gradual slope was chosen to minimize clogging. After the successful testing of a 1:2-scale model of this geometry, a full-scale probe was designed using the recessed window and slot geometry configuration. The probe diameter served to prepare the soil and define the separation between the soil wall and window. Note that different soil types (e.g., expansive clays) may expand to reduce the window-soil offset. This expansion is usually small and inconsequential for a delivery system having a large depth of focus. A large depth of focus and high-pulse peak irradiance ensure that minimum breakdown thresholds are maintained for slight offsets in the window-soil standoff distance.

A detailed closeup view of the slot geometry housing the recessed window is shown in Figure 4. The laser output window is below the snap ring. The optical receive fiber (small bright spot just above right of window) is illuminated from uphole for demonstration purposes. The larger bright item above and to the right of the window and flush with the probe surface is a locking screw. The sacrificial sleeve is slid down a bit and shown at bottom left. The probe tip is out of the picture at bottom left, and for scale, the window is 1 cm in diameter and the illuminated fiber image is approximately 1 mm in diameter.

Figure 4. Closeup view of recessed window area and slot geometry of DL-LIBS probe

Based on WES experience and published results, soil moisture and soil grain size significantly affected the LIBS signal. WES developed sensors for these parameters in a LIBS system in the attempt to create a multisensor LIBS metals detection system. In the absence of such information, a LIBS sensor alone could record equivalent signals from a highly contaminated wet clay and a slightly contaminated dry sand due to the dependencies previously mentioned.

The DL-LIBS probe uses a cone and sleeve soil classification sensor that yields estimates of average grain size for soils encountered during probe pushing. A handheld microwave soil moisture instrument was modified and incorporated into the DH-LIBS probe. The entire DH-LIBS probe, including the soil moisture sensor, is shown in operation in the SCAPS truck in Figure 5. Note the sacrificial sleeve has been removed for the photo and is located near the probe tip. The recessed window geometry can be seen above the soil moisture electrode rings.

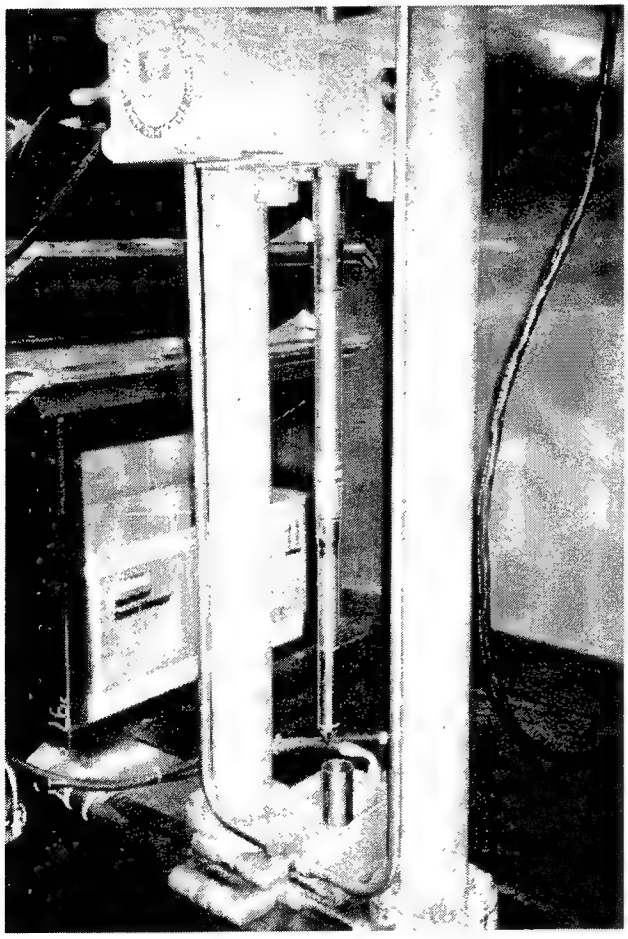

Figure 5. DL-LIBS probe including soil moisture and stratigraphy sensors, shown installed in SCAPS truck

During the push phase a dedicated Windows-based program acquires volumetric soil moisture information as well as soil stratigraphy information. The cone and sleeve sensors used for stratigraphy are visible at the far right of the conceptual block diagram in Figure 6. The moisture sensor electrodes and microwave electronics board are just to the left of the soil class sensors in the same figure.

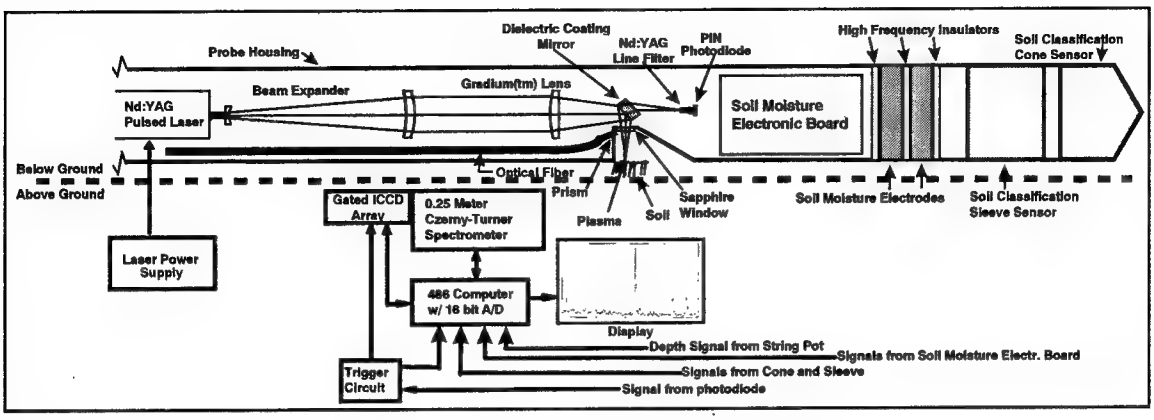

Figure 6. Block diagram of DL-LIBS probe and associated components

The retract operation sequence and timing as well as the other components involved (Figure 6) are detailed as follows: The laser (e.g., a 1.25-in.- diam, 15-in.-long, 80 mJ Nd:YAG laser) provides the master timing control for the system. When the laser is fired, a portion of the energy bleeds through the dielectric coated turning mirror and the Nd:YAG laser line filter and illuminates a PIN photodiode. The majority of the energy is focused on the soil wall creating a plasma. A portion of the plasma light is conveyed uphole to a Czerny-Turner spectrometer equipped with a microchannel plate intensified charge coupled device (CCD) array. The electrical pulse from the PIN photodiode travels uphole to a trigger circuit that defines the CCD integration time and integration delay. The trigger circuit then instructs the PC to read out the CCD. The data are acquired via a Windows-based program developed at WES. This program provides peak detection capabilities, indicating which atomic element is present, as well as an indication of confidence in peak labeling.

FO-LIBS probe

The first prototype FO-LIBS probe, shown schematically in Figure 3, was built in FY 96 and based on lessons learned during FY94 and FY95 using a laboratory prototype system. In this scheme, the Q-switched output of an Nd:YAG laser operating at 30 Hz at 1,064 nm is delivered via a single fused-silica fiber to the probe. Sample power densities of greater than 10 GW/cm^2 are available using fiber-optic delivery of the laser light, while the spark initiation threshold on dry soil is typically less than 0.5 GW/cm^2.

To ensure reliable and repeatable long-term operation of the system, an initial concern was the power handling capability of the fused-silica fiber. To achieve a comfortable margin in power density over the spark initiation threshold at the sample, without exceeding the power handling capabilities of the optical fiber (1-5 GW/cm^2), a low f/# optical system (typically f/# ~1) is required. This minimizes the size of the focused image of the optical fiber face on the sample but introduces a high dependence of the sample power density on the lens-to-sample distance, as shown in Figure 7.

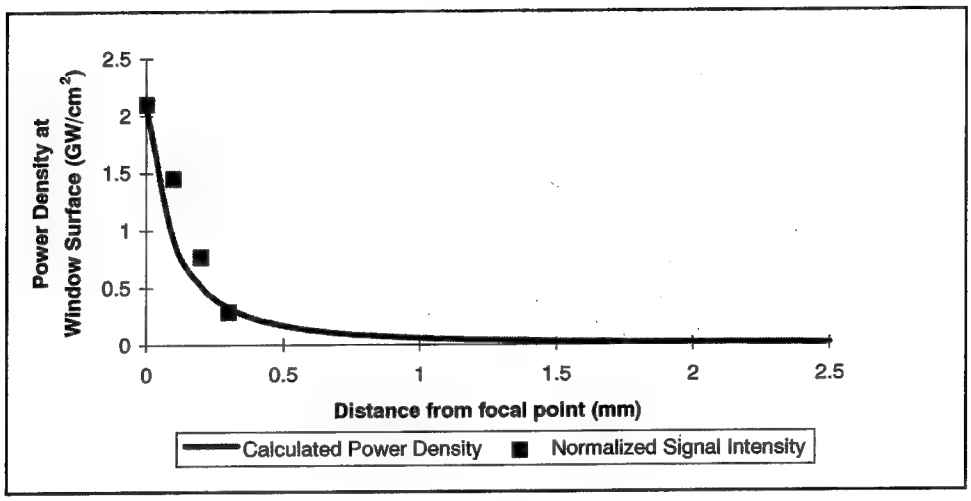

Figure 7. Dependence of sample power density as a function of lens-to-sample distance

The initial design used to keep the sample-to-lens distance fixed to within a small tolerance incorporated a disposable optical window at the sample/probe interface as shown in Figure 8. In this design, the light emitted from the fiber is collimated, turned by a quartz prism, and focused by a short-focal-length quartz lens through a sapphire window in the probe. Since the soil is pressed against the window, the lens-to-sample distance is held fixed. Contamination is not an issue because the probe is entirely sealed, allowing for operation below the water table. The symmetry of the single-fiber design for both excitation delivery and emission collection is advantageous because the fiber is self-aligned. This configuration avoids any alignment difficulties that could be present in a probe with a multiple-fiber design. The choice of a 90-deg prism rather than a mirror to turn both of the collimated beams (IR excitation and the UV/visible emission) is robust in terms of damage threshold. A prism can also be used in widely separated spectral regions without component substitution. This is an attractive feature, because LIBS can be used for simultaneous analysis of multiple components.

After several thousand laser pulses, it was observed that the sapphire window is pitted by the LIBS spark causing reduced window transmission. To minimize the effect of this pitting on the integrity of the in situ data, the spark is repositioned on the window surface by scanning the fiber and focusing optics using the modified probe design shown in Figure 9. The design, built in FY 96,

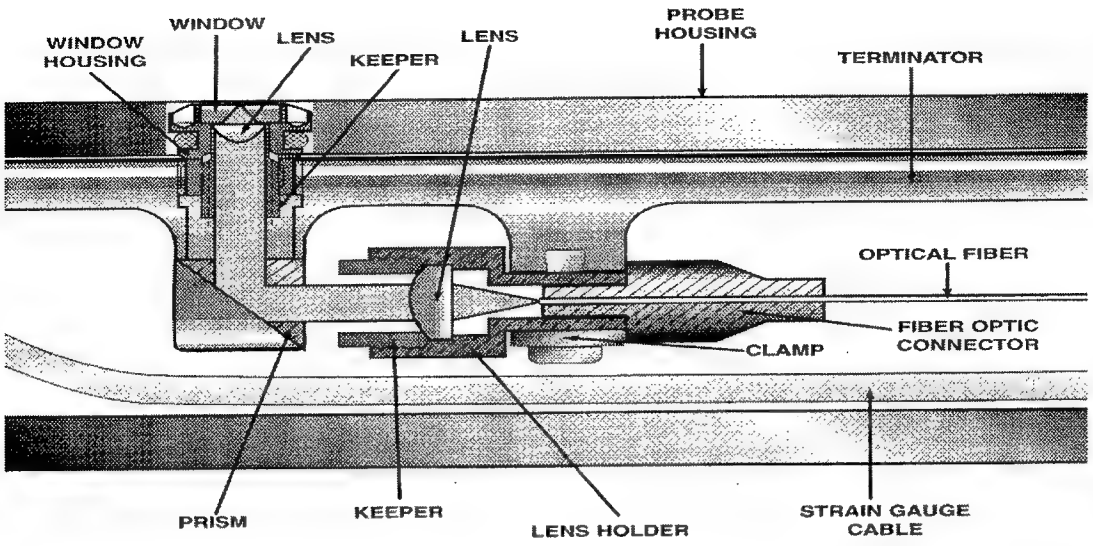

Figure 8. Initial FO-LIBS beam delivery/collection design

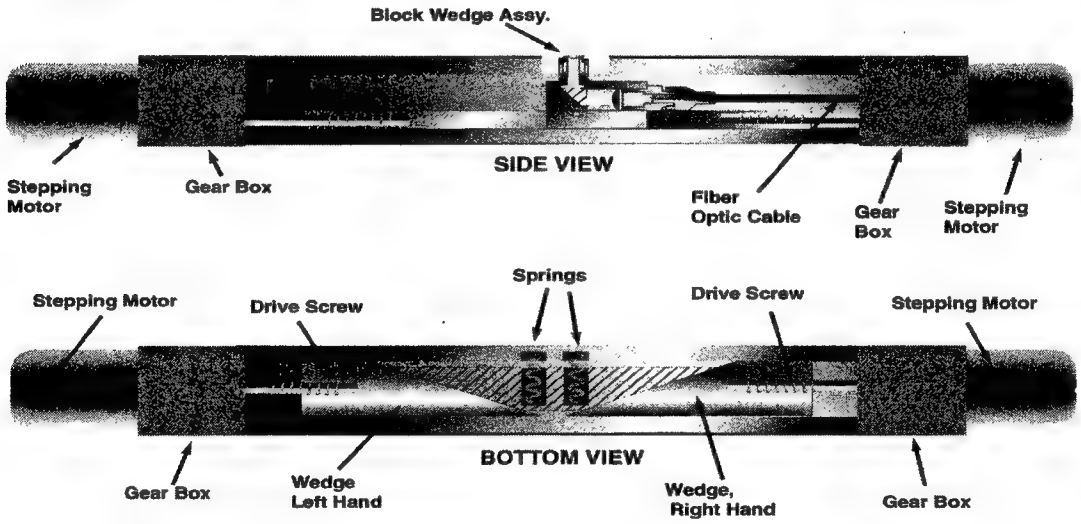

Figure 9. Modified FO-LIBS scanning beam delivery/collection design

incorporates two stepping motors to drive a block that houses the optics. The design provides for two-axis control of the position of the spark on the window surface. Because of the relatively small size of the focused spot compared to the size of the sapphire window, the number of discrete positions available is in excess of 1,000.

The excitation and emission light are decoupled using the configuration shown in Figure 3. The excitation beam is focused by a 25-cm focal length lens through a 2-in. aluminum mirror containing a small hole at 45 deg. Since the returning LIBS signal fills the entire numerical aperture of the fiber, most of the return signal is turned 90 deg by the mirror with only a small loss (~5 percent) through the hole. Like the probe design, this configuration is robust and can be operated over a large spectral range to allow the analysis of different spectral regions with no system adjustment or component substitution.

The spark emission is fiber-optically coupled to a spectrograph that disperses the light onto a time-gated, intensified, linear photodiode array detector (EG&G model 1420). The time gating of the detector during data collection is crucial due to the initial broadband background continuum created during the evolution of the plasma. Resolution of the signal from the metal emission is enhanced by delaying the application of the gate pulse to the detector until after the short-lived broadband background has decayed. The duration of the gate pulse is chosen to correspond with the duration of the metal emission to optimize the signal-to-noise ratio. Each measurement is the result of a few hundred single-shot spectra accumulated in the memory of the optical multichannel analyzer detector controller (EG&G OMA model 1460). Because signal averaging tends to reduce the detection limit of the system, the actual number of shots used for a given situation can be chosen to yield the required detection limit in the minimum amount of time.

FO-LIBS Probe Laboratory Investigations

To estimate the detection limits of the FO-LIBS probe with respect to the USEPA site screening levels (SSLs) and to measure the effects of variable grain size and moisture content on the probe's efficiency, laboratory measurements were performed on several contaminated soils.

Measurement standard deviation. In this study, detection limits are specified with a 99-percent confidence level by the 3S/m convention, where S is the measurement standard deviation and m is the slope of the concentration vs. detector response curve. The relative standard deviations obtained were typically in the 10-percent range when 100 shots were averaged. A plot of the standard deviation of the LIBS measurements as a function of the number of laser shots averaged per measurement is shown in Figure 10.

In this study, 10 samples were averaged of measurements involving 1, 5, 10, 50, and 100 shots per measurement. Predictably, the standard deviation decreases as the square root of the number of laser shots. Because of the high standard deviation for a single laser shot per measurement, averaging of hundreds of shots is typically required. Because the repetition rate of the Nd:YAG laser is 30 Hz, a measurement with a standard deviation in the range of 10 percent or less is obtainable in a few seconds.

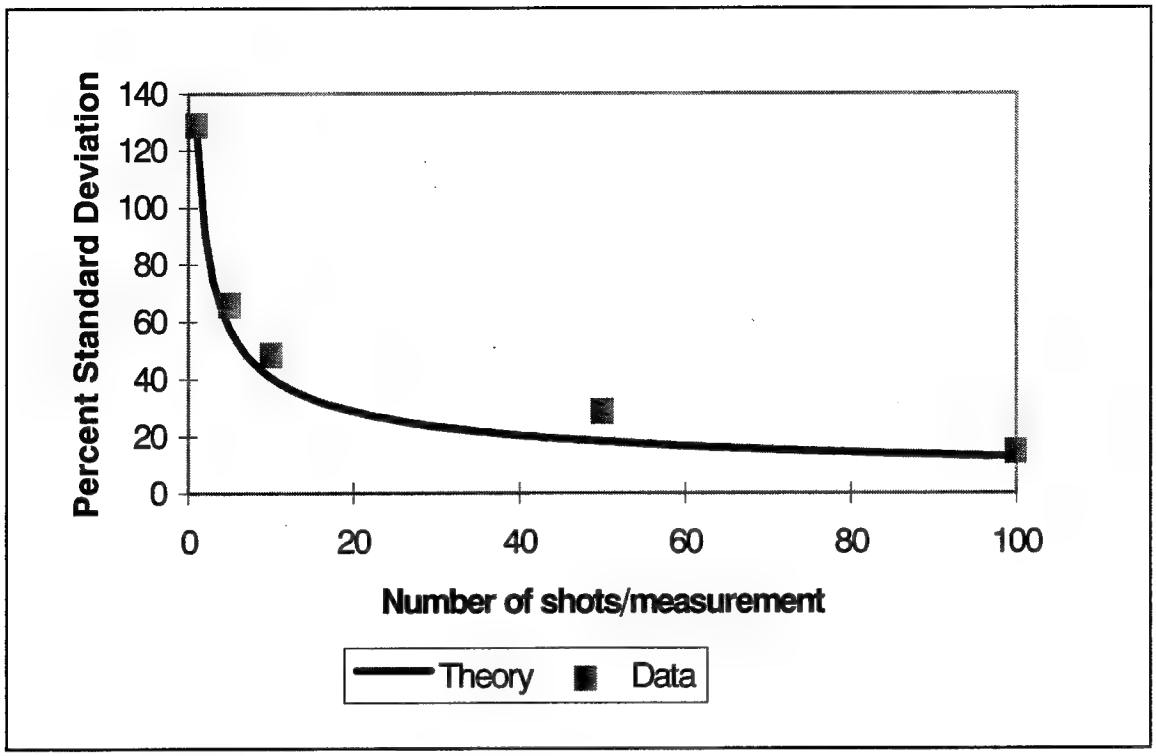

Figure 10. Standard deviation of LIBS measurement as a function of the number of laser pulses averaged

Measurement slope. The FO-LIBS probe is subject to matrix effects that scale with grain size. Figures 11 and 12 show representative examples of the results of probe calibration studies on Pb and Cr in which the grain size was varied from 800 μm down to less than 106 μm. It is observed that the slope decreases with grain size. One explanation of the variation of detection limit with grain size involves a consideration of the soil surface area over which the contaminant is spread. Because a fine-grain material has a larger total surface area per unit mass than a coarse-grain material, the total surface over which equal contaminant concentrations by mass are dispersed is larger for the fine-grain material and smaller for the coarse-grain material. This results in a thicker surface layer of contamination on coarse-grain materials. Since the LIBS measurement uses a fixed spot size to essentially ablate the contamination on the surface of the grains while exciting the plasma, there is an overall larger volume of contaminant in the plasma for coarse-grain materials. Because of this effect, the detection limits on fine materials, such as clays, are higher than the detection limits on coarse materials, such as sands. The detection limit dependence on the grain size is summarized in Table 2.

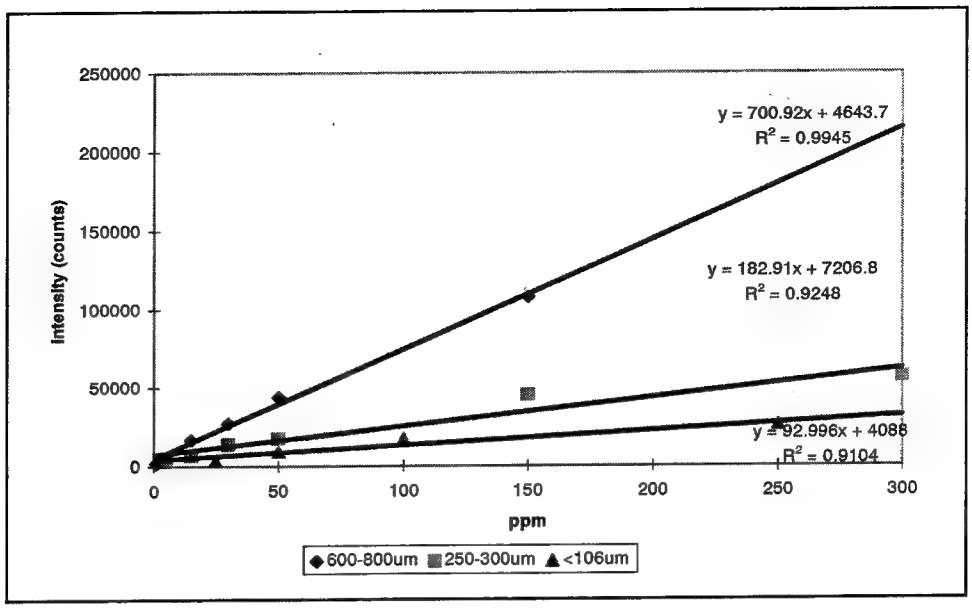

Figure 11. FO-LIBS probe calibration curves as a function of grain size for lead

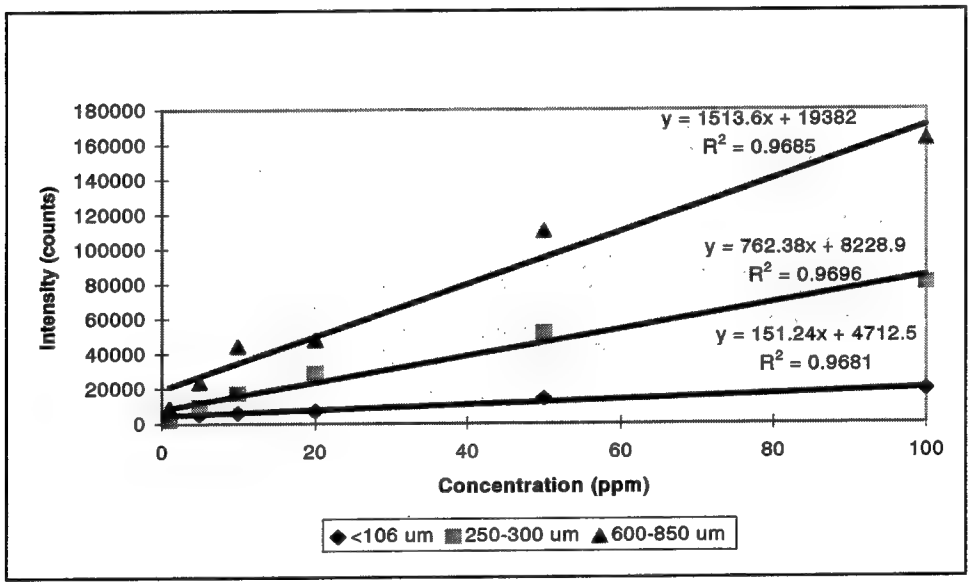

Figure 12. FO-LIBS probe calibration curves as a function of grain size for chromium

Table 2
Grain Size Effects on FO-LIBS Detection Limits

Metal	EPAs SSL	<106 mm	250-300 mm	600-800 mm	No. shots
Lead	400	53.1	13.5	0.7	200
Cadmium	6	306	24.8	19	500
Chromium	19	31.3	10.7	5.2	300

Water Effect

The sensitivity of the probe is reduced by the presence of water on the sample. A plot of the response vs. Pb concentration for the 600- to 800-μm sieved sand for a 200-shot average is shown in Figure 13. The detection limit is increased from 0.72 ppm on dry sand to 444 ppm on wet sand (2g H_2O per 15g sand). Since SSL of the EPA is 400 ppm for Pb in soil, the LIBS probe will likely be capable of achieving the SSL in this matrix by use of further signal averaging as previously discussed.

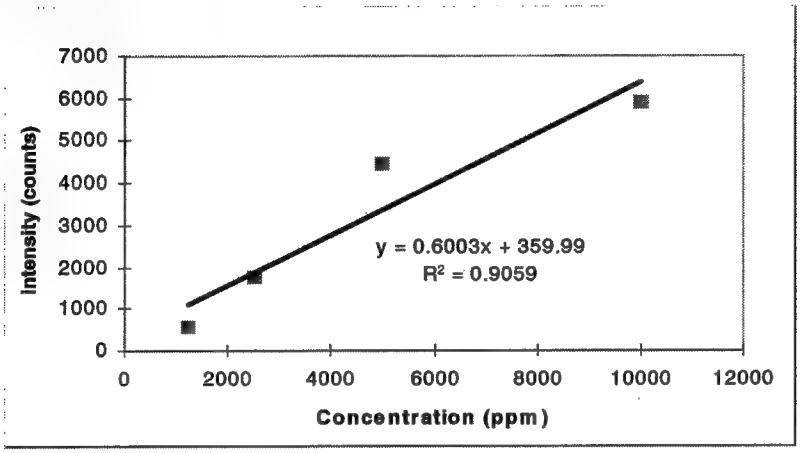

Figure 13. FO-LIBS probe calibration curve for wet sand

Discussion

Matrix effects affect all in situ measurement techniques. The prime benefits of cone penetrometer-based techniques are that the measurements are done in situ and the results are available onsite in near real-time. As a result, onsite decisions can be made as to the best course of action in the site delineation process. The use of LIBS technology for the purpose of field screening places emphasis on the timeliness of the measurements. This is in contrast with the approach of most analytical techniques, which avoid the problem of matrix effects by removing the matrix, by acid digestion or solvent extraction, at the expense of time.

Since LIBS cone penetrometer testing (CPT) technology will be used primarily as a site-screening tool, a number of factors affect calibration and interpretation of LIBS sensor results. First, as demonstrated by FO-LIBS data gathered on sieved laboratory samples (rather than naturally occurring mixtures of fine- and coarse-grain materials), Table 2 presented an extreme range of variation of the detection limit with grain size that is not likely to be encountered in the field. Second, calibration considerations must be tempered by the fact that LIBS is most sensitive in sands, the regions of the soil with the highest hydraulic conductivity. As such, sands pose the highest threat to ecology, groundwater,

and human health by contaminant transport and bioavailability. With this in mind, even with no calibration for grain size variation, a larger signal can be interpreted as a larger threat due to either a relatively small concentration in a coarse matrix or a relatively high concentration in a fine matrix.

It is clear that to obtain the most quantitative results from the LIBS probe, information on soil grain size and soil moisture must be used to calibrate the results. We anticipate two approaches to in situ grain size calibration. The first involves the use of information gathered by strain gauge sensors that are mounted on the probe (i.e., the cone tip and sleeve sensors). A method is immediately available for determining soil type by use of an algorithm relating probe tip pressure to sleeve friction and has been used with other sensors in the SCAPS sensor development program. The strain gauge technique can be visualized as a volumetric average of the grain sizes present in the vicinity of the probe. These measurements are currently made by the cone and sleeve sensors incorporated into the LIBS probes to help account for grain size effects on the LIBS signal. Because of the small spot sizes that are used in the LIBS probes, a calibration technique that provides finer-scale grain size information is expected to improve the quantitative capabilities of the probe. An effort is currently underway at SPAWAR to incorporate a downhole CCD camera into a CPT probe which, when used in conjunction with particle size analysis software, is expected to provide a second, improved calibration technique. The results of comparisons between these two calibration techniques will be the focus of future field work.

Likewise, there are two possibilities for calibration of probe response with changing water content during operations that penetrate the water table. First, the depth of the water table can be measured with a well and calibration of the data can be performed assuming a dry soil above the water table, a saturated soil below the water table, and a modeled capillary fringe. Second, moisture can be measured directly by auxiliary sensors installed in the probe. The DL-LIBS probe embodies the second approach by incorporating a microwave volumetric soil moisture sensor developed at WES. In parallel with the in situ camera effort for grain size, an effort is underway at SPAWAR to incorporate a moisture sensor into the CPT probe to make in situ determinations of water content. The eventual incorporation of this water sensor will provide a second alternative to data calibration in the presence of water and is expected to further improve the quantitative capability of the probe, particularly in the capillary fringe region.

Field Investigations

DL-LIBS probe

The first DL-LIBS probe was fabricated at WES during FY96. The first system check out was performed at WES in early August 1996. Prior to installation in the SCAPS truck, basic laboratory system operation tests were performed to ensure system operability. During FY96-97 the DL-LIBS probe

underwent field investigations at WES, Louisiana Army Ammunition Plant (LAAP), Joliet Army Ammunition Plant (JAAP), Illinois, Red River Army Depot (RRAD), Texas, and Keesler Air Force Base (AFB), Mississippi. Naturally occurring chromium was verified at WES, while chromium contamination was verified in a sludge landfill at LAAP. Lead azide was the target metal at JAAP while particulate lead was the target at RRAD and Keesler AFB.

Perhaps the most interesting of all of these tests was the Keesler AFB firing range. Sixteen penetrometer pushes were made at a small-arms firing range at Keesler AFB. The area tested was at the base of an earthen bullet impact berm (Figure 14) which stopped bullets from two parallel firing ranges. The area investigated overlapped both firing ranges including an intermediate "dead" zone where no bullets impacted. In reference to the figure, when facing the impact berms the left berm is barren and is in the upper right of the figure. The tall grassy area seen at top right of Figure 14 is the dead zone, while the right impact berm is just outside the center and bottom right of the figure. Three parallel rows of flags can be seen indicating the location of the pushes. If little leaching of lead occurred, one would expect the contamination to be primarily near the surface. Furthermore, intuition would indicate (and results should show) a "dead" zone with little or no lead contamination between the two firing ranges. Figure 15 displays a calibrated and interpolated color-coded subsurface volume plot of lead concentration. It is clear, as was theorized, that the bulk of the concentration is in two regions, separated by the dead zone mentioned. The data acquired indicate that lead contamination is shallow, within the upper 3 ft of soil. The depth dimension is exaggerated for clarity and covers just 5 ft; the longest dimension is parallel to the three rows of flags and covers 82 ft (top to bottom in Figure 14) and the across-row distance is 12 ft (left to right in Figure 14). WES-developed visualization software was used to produce Figure 15.

FO-LIBS probe

The scanning fiber-optic LIBS probe was evaluated during FY97 at three sites contaminated with lead as well as several uncontaminated sites near San Diego. Probe operation is controlled by a windows-based software package that was developed during FY94 and FY95. The three contaminated sites were a former shooting range at San Diego Naval Training Center, a former submarine battery dump at Mare Island Naval Shipyard, and a former explosives manufacturing site at JAAP. In each case, a site-specific calibration curve was prepared to calibrate the FO-LIBS sensor response for typical soil conditions (i.e., soil type and moisture content) encountered at the site.

Two pushes were completed at the San Diego Naval Training Center shooting range with lead hits occurring in the top 2 ft of soil at concentrations in the range of 0 to 1,500 ppm. At this site, the Pb is distributed inhomogeneously, consistent with lead bullet debris, with the highest concentrations occurring at or near the surface. A typical Pb spectrum from the site is shown in Figure 16.

Figure 14. Small-arms firing range used as a DL-LIBS investigation site, Keesler AFB

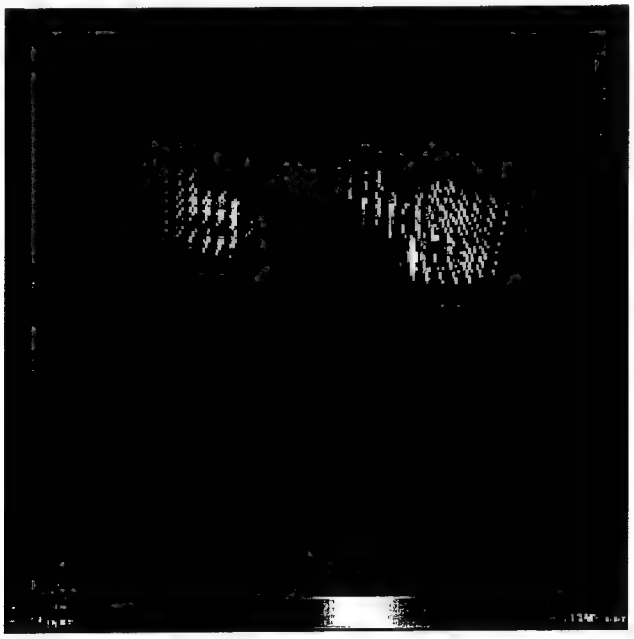

Figure 15. Lead contamination plot of the subsurface, Keesler AFB

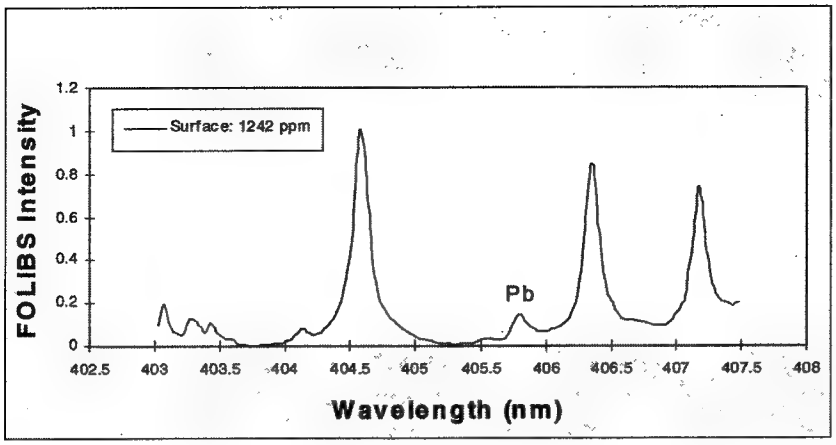

Figure 16. Typical spectra of lead taken at the San Diego Naval Training Center investigation site

An FO-LIBS field investigation was conducted at a lead battery dumpsite at Mare Island Naval Shipyard in July 1997. The distribution of the battery waste at the site was inhomogeneous and several hot spots consisting of plastic battery casings and metal were evident at the surface. A typical transect characterizing one of these areas is shown in Figure 17. In this figure, six CPT pushes were conducted on 1-ft centers with 1-in.-depth resolution, and the concentration of lead vs. depth was plotted. The distribution is consistent with acidic runoff from discretely located leaking batteries. The concentration was extrapolated using the intensity of the 405.78-nm lead emission line.

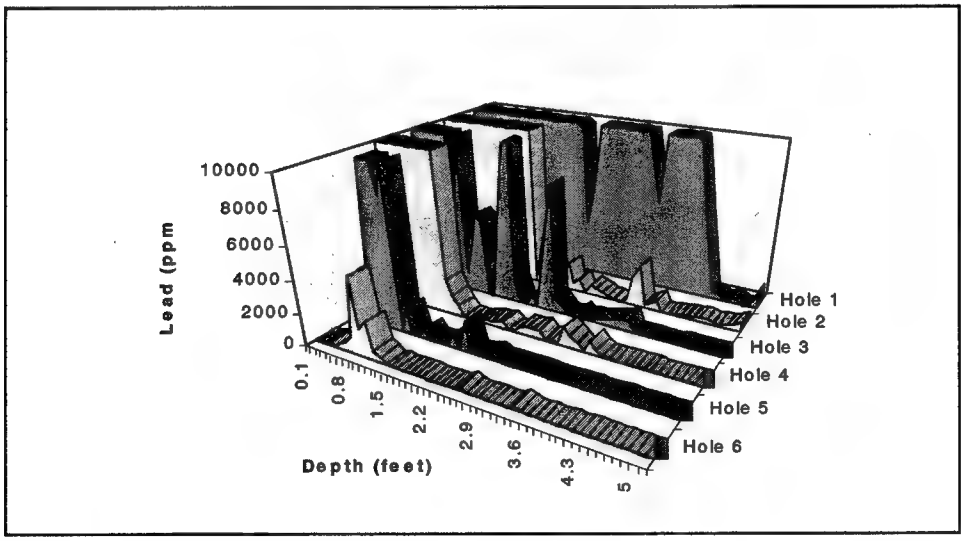

Figure 17. Lead concentration as a function of depth for six pushes at the Mare Island Naval Shipyard, San Diego, CA

A field investigation was conducted during October 1997 at JAAP. At this site the Pb contamination was homogeneously distributed in a former lead azide waste pond. A total of nine pushes were conducted and data regarding lead contamination were obtained from all nine holes. Figure 18 is a 3-D representation of the distribution of Pb at the site.

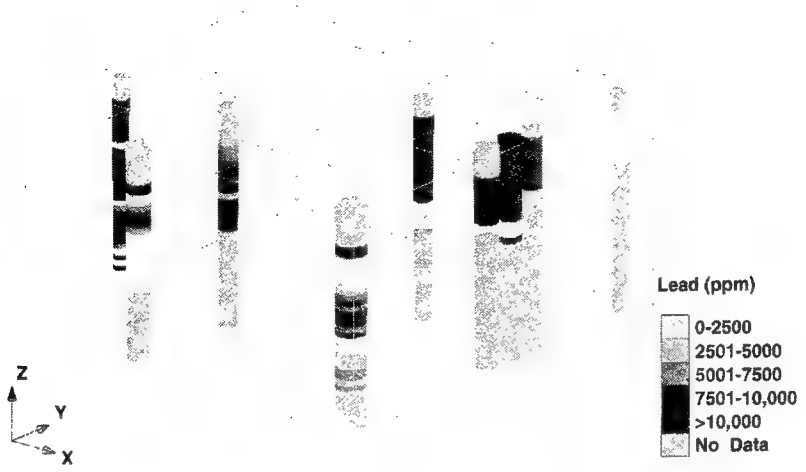

Figure 18. Lead concentration for pushes acquired at JAAP

Conclusion

Two unique LIBS technologies (i.e., probes) have been successfully developed and field demonstrated for in situ field screening of heavy metal contaminated soils. The DL-LIBS probe incorporates a laser in the probe, a recessed window geometry, microwave soil moisture measurement, and soil classification sensors. The FO-LIBS probe utilizes a unique fiber-optic laser induced breakdown spectroscopy configuration and also incorporates soil classification sensors. Although moisture is not measured by the FO-LIBS probe, the detection limits can meet the EPA's SSL's for several key metal contaminants in soil in near real-time. Investigations of calibration techniques are underway which are expected to improve the quantitative capabilities of both probes by accounting for soil matrix effects.

Transition

The DL-LIBS and FO-LIBS sensor systems have been transitioned to the ESTCP Demonstration/Validation program under the SCAPS Heavy Metal Sensor Project. An X-Ray fluorescence sensor developed by Naval Research Laboratory is part of the same ESTCP program. This project will conduct side-by-side demonstration/validations of the three direct push metal sensor systems.

Upon completion of the ESTCP program, DL-LIBS and FO-LIBS technologies are expected to be transitioned to Tri-Service, other government, and private sector users.

3 Research Area II: Laser Induced Fluorescence (LIF)

By: Bruce J. Nielsen, (U.S. Air Force Research Laboratory)
Gregory D. Gillispie, Dakota Technologies Inc. (DTI)
Stephen H. Lieberman (SPAWAR)
Ernesto R. Cespedes (WES)
William M. Davis (WES)

Introduction

When the SERDP-funded SCAPS program was initiated in 1994, the objective of this research area consisted of two distinct sensor development efforts; the first was to improve and demonstrate the first- and second-generation SCAPS LIF systems for improved detection of POL contaminants, and the second was to evaluate photofragmentation/laser induced fluorescence (PF/LIF) as a method for in situ detection of explosive contaminants in soils and groundwater. During the course of the SERDP project, it was determined that the PF/LIF approach would not be feasible for SCAPS implementation because (a) the technique would only work with explosives in the gas phase, (b) it could not achieve the required sensitivities, (c) it would be inferior to the electrochemical sensor probe developed in parallel as part of the SERDP SCAPS project for vadose zone applications, and (d) it would not operate in the saturated zone. As a result, the PF/LIF effort was discontinued in FY96 and a different technology that incorporates a fiber-optic flow-through biosensor with an improved groundwater sampler was approved to address the groundwater problem. In addition, based on the poor sensitivities observed in laboratory and field tests conducted under Research Area III - Fiber Optic Raman Sensors (FORS) for detecting DNAPLS, an additional effort was added to Research Area II to investigate the feasibility of using LIF to infer the presence of nonfluorescing DNAPLS such as trichloroethylene (TCE) that are used to dissolve POLs. This chapter describes the technologies developed under SERDP sponsorship for detecting POLs, explosives, and DNAPLS via LIF, as well as the flow-through biosensor for explosives in groundwater.

POL Techniques

The first fielded SCAPS technology for in situ detection of chemical contaminants was based on measuring the fluorescence of POL contaminants when excited by pulsed laser light via fiber optics to raise molecules to excited states. Several classes of organic, bio-organic, and inorganic molecules subsequently return to lower energy states by emitting longer wavelength fluorescence photons. For example, most fuels contain aromatic hydrocarbons, almost all of which fluoresce over a broad range of wavelengths when excited by an ultraviolet source. The original SCAPS LIF probe was developed during the late 1980s by WES (U.S. Patent 5,128,882) and was adapted from a sensor designed by SPAWAR researchers for seaborne applications. The first generation SCAPS LIF probe was first field demonstrated in 1990 and has since been extensively used to characterize U.S. Army, Air Force, Navy, and DOE sites. In addition, this technology has been licensed to private industry, and a number of commercial firms are currently using similar cone penetrometer systems (U.S. Environmental Protection Agency (USEPA) 1995).

The first generation SCAPS LIF sensor, shown in Figure 19, consists of a probe with dual fibers for excitation and emission and a flush-mounted 6.35-mm-diam sapphire window for transmitting the laser illumination to the outside of the penetrometer probe. The ultraviolet (UV) energy source for this system consists of a pulsed nitrogen laser source with an output of 1.4 millijoules (mJ), 0.8-ns pulsewidth, 10-Hz repetition rate, at 337 nanometers (nm) (Lieberman et al. 1991). This excitation source represented a mature, commercially available technology that could be readily incorporated into a field LIF system at the time that this effort was initiated in 1989. Another advantage of the 337-nm excitation source, identified at that time, was that the attenuation of energy at this wavelength is relatively modest, permitting transmission of the excitation energy over fiber lengths of 100 m or more. This permits the LIF sensor system to be used to the full push capability of the standard 20-ton penetrometer system (i.e., approximately 50 m).

The system uses a spectrograph coupled to an intensified photodiode array and OMA detection system. Because this system uses a diffraction grating to disperse the fluorescence emission signal over a 1,024-diode array detector, it is possible to read an entire spectral signature from the fluorescing fingerprint signal with a resolution of 0.5 nm or better in approximately 16 ms. In practice, the system usually integrates the emission from 10 to 20 laser shots which require a total analysis time of from 1 to 2 secs to collect a fluorescence emission spectral signature. In addition to the optical sensors, the probe also incorporates geophysical sensors that provide continuous soil classification and stratigraphy during the penetrometer push. The LIF probe is also equipped with a grouting system that is used to seal the hole as the probe is being retracted to prevent migration of contaminants between soil layers.

When advanced at the 2-cm per second standard push rate, the LIF probe collects contaminant information and soil classification data with a spatial resolution of 2 cm. Figure 20 presents an example of the data that are collected

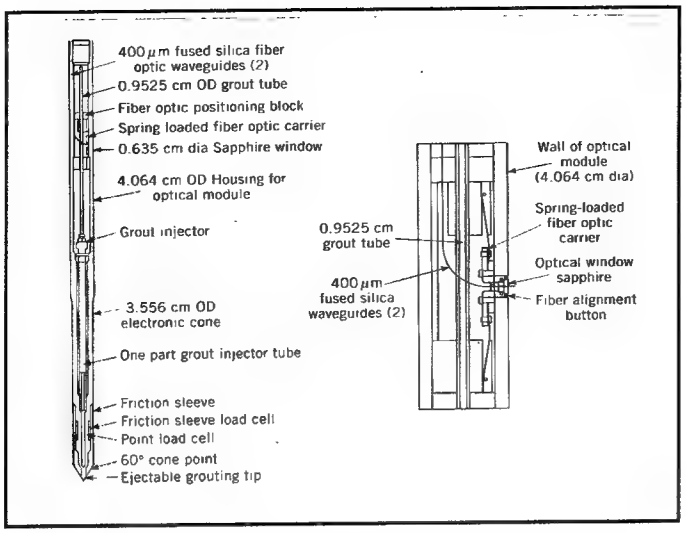

Figure 19. Cross-sectional view of the SCAPS LIF probe, with a close-up of the optical window (U.S. Patent 5,128,882)

by the SCAPS LIF probe. These plots, which are displayed in real-time during the penetrometer push, show the geophysical sensor information which is used to compute the soil classification vs. depth, as well as a summary of the LIF data (fluorescence intensity and wavelength at peak vs. depth). This particular penetrometer push indicates an area of significant POL contamination in a layer 4.2 to 4.4 m below ground surface. In addition to the data displayed in Figure 20, the SCAPS data acquisition system collects and stores the complete fluorescence spectrum (1,024 points from 270 to 800 nm) for each laser pulse (or average of pulses). After a representative number of penetrometer pushes, the geophysical and fluorescence data are used to develop a model of the subsurface contaminant plume as shown on Figure 21.

A limitation of the 337-nm excitation source identified early in the SCAPS development is that it does not induce fluorescence in single ring aromatic compounds such as the BTEX (benzene, toluene, ethylbenzene and xylene) components of fuels. In fact, the lightest weight polycyclic aromatic hydrocarbon (PAH) compound that is excited appears to be the disubstituted naphthalene. In general, the 337-nm source is most effective for inducing fluorescence in PAH's with three rings or more (Lieberman 1993). This lack of capability of the nitrogen-based LIF sensor to detect BTEX and light fuels (e.g., JP-4, JP-5, and unleaded gasoline) has led to a number of efforts to test shorter wavelength sources for incorporation into SCAPS. One of the second-generation SCAPS LIF probes resulting from these efforts is a tunable LIF SCAPS probe currently designated the Rapid Optical Screening Tool (ROST™). ROST™ was originally developed for the U.S. Air Force Armstrong Laboratory (USAFAL), Tyndall AFB, by North Dakota State University (NDSU), and Dakota Technologies Incorporated (DTI), and produced commercially by Fugro Geosciences, Inc., Houston, TX. The system was initially designed as a field

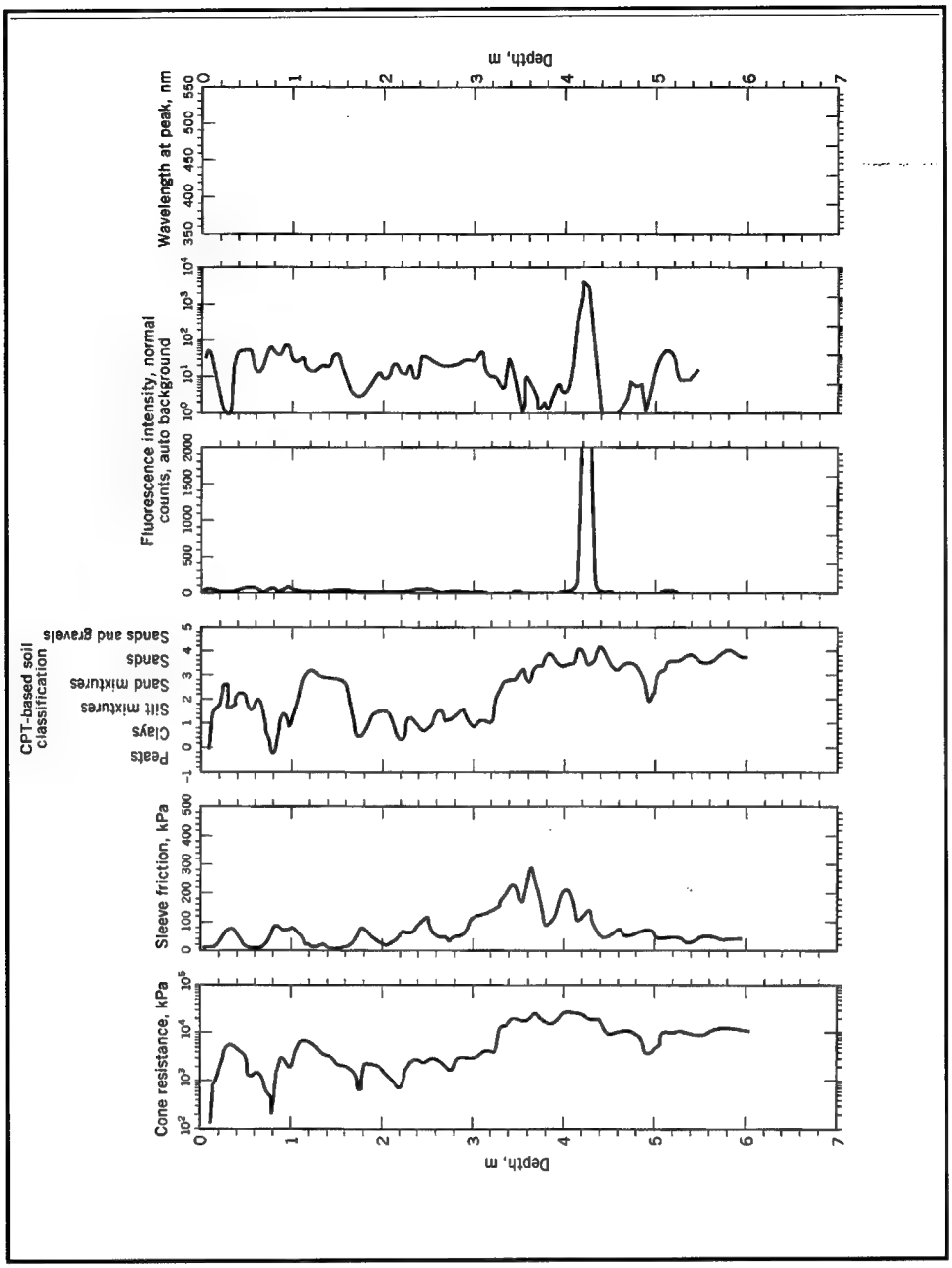

Figure 20. Typical data output of the SCAPS LIF probe at a petroleum-contaminated site

portable LIF sensor to analyze liquid samples containing aromatic hydrocarbons and fuels in monitoring well applications. Subsequently, the sensor was installed in a cone penetrometer probe, and field tested in a number of sites (Bratton, Shinn, and Bratton 1993). The system makes use of a frequency-doubled Nd:YAG laser to pump a dye laser whose output is then frequency doubled to generate UV light in the range of 230 to 300 nm. In this system, the Nd:YAG laser can also be used directly with harmonic frequency conversion to produce 266, 355, and 532 nm outputs. The advantages of these alternative excitation

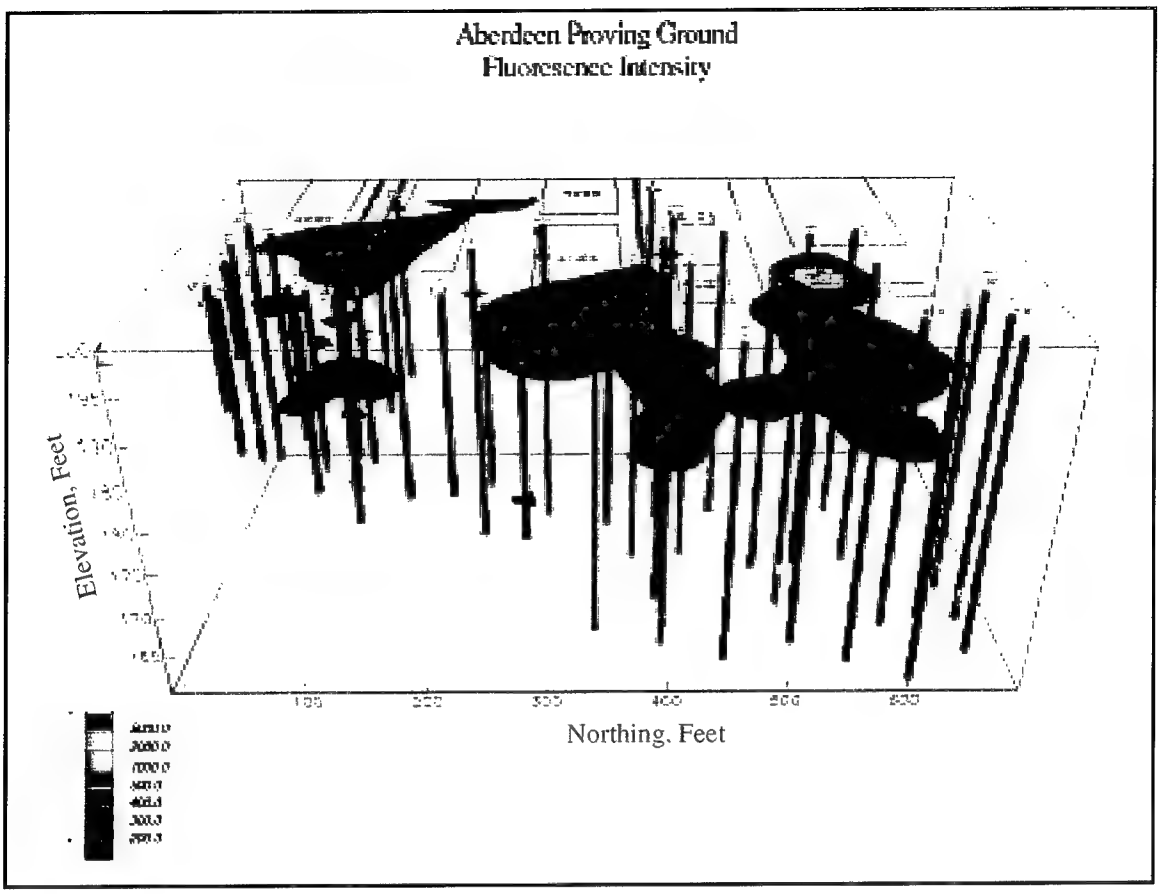

Figure 21. Three-dimensional visualization of LIF probe data, showing underground plume of POLs

wavelengths include the capability to excite lighter-weight aromatic compounds (one- and two-ring aromatic compounds) and to select in the field the most appropriate excitation wavelength for the particular contaminant of interest and the site-specific conditions. One penalty suffered by using shorter wavelength excitation light in the cone penetrometer is that energy losses in the transmission fiber increase dramatically at wavelengths shorter than 290 nm.

Unlike the fixed wavelength LIF system, the NDSU system uses a monochromator, photomultiplier tube, and digital storage oscilloscope to detect fluorescence. A major difference with this approach compared to the OMA detector used by the original SCAPS LIF system is that in the dynamic or push mode the detector measures the time decay or lifetime of the fluorescence signal at a single wavelength selected by the monochromator. Full spectral-time decay data matrices can be generated by moving the monochromator in 10-nm increments and recording the time-dependent fluorescence signal at each wavelength. With the present (50-Hz) laser system, this procedure requires approximately 2 min. to collect a wavelength-time matrix (WTM) consisting of 21 different wavelengths with a spectral resolution of 10 nm (Gillispie and St. Germain 1995).

As part of this effort, researchers at SPAWAR developed and field-tested an improved POL sensor using a 308-nm XeCl laser system. The XeCl system provides enhanced capability over the nitrogen laser for lightweight fuel products such as JP4 and JP5, etc. The 308-nm XeCl laser represents an attractive alternative to the 290 nm commonly employed by the ROST system because it is effective for exciting lighter-weight aromatic compounds, but it does not suffer the energy losses in the transmission fiber that are experienced at wavelengths shorter than about 290 nm. A practical advantage of the 308-nm excitation source is that the laser is less expensive than the tunable Nd:YAG pumped dye laser used by the ROST system and does not require flowing gas used by the nitrogen laser system.

Based on successful field tests of the XeCl laser system conducted at NAS North Island, the XeCl laser system was transitioned to Naval Facilities Engineering Command (NAVFAC) and installed on two SCAPS systems operated by Navy Public Works Centers in San Diego, CA, and Jacksonville, FL. These systems are now in an operational status. An enhanced windows-based software data/acquisition and processing system was also developed and field-tested and transitioned to the Navy-operated SCAPS systems as part of this effort.

In collaboration with developers at MIT Lincoln Labs, SPAWAR System Center also developed and evaluated a microchip laser-based LIF probe. The advantage of the microchip laser system is that its small size permits generation of 266-nm light in the probe. The "downhole" Nd:YAG generates 266-nm excitation energy in the probe using 808-nm light generated at the surface and delivered over a fiber. Because the 266-nm light is generated in the probe near the sapphire window, there is little attenuation of the low wavelength excitation energy. This permits efficient excitation of single ring aromatic compounds (BTEX) not possible with longer wavelength excitation sources (e.g., 290 and 337 nm). The downhole Nd:YAG laser system was successfully field-tested for first time at NAS North Island. A total of six pushes were done with the downhole Nd:YAG laser probe at the fuel farm site. Emission spectra at some push locations showed significant spectral shifts as the probe passed through a layer of JP-5 contamination located near the top of the saturated zone, suggesting compositional changes in the JP-5.

The microchip laser-based LIF probe was successfully transitioned to the ESTCP Dem/Val program. Two demonstration validations were completed at NAS North Island and Naval Construction Battalion, Pt. Hueneme, CA.

Phenomenology studies

A major thrust of this research area was aimed at improving the capabilities of the SCAPS LIF sensors and involved developing a better understanding of the phenomenology affecting the in situ fluorescence of POL contaminants in various soil matrices. At the start of the SERDP project, the ROST and the SCAPS nitrogen laser fluorescence systems were already being successfully used

for field screening sites for subsurface POL contamination. However, the question about the quantitative nature of the results is invariably raised. A better understanding of the relationship between composition and total observed fluorescence, the influence of the soil matrix, and other environmental effects is needed. Researchers at USAFAL, DTI, and NDSU studied several important phenomena that undoubtedly play a role. Their work began with a study of quenching by ions dissolved in solution (relevant to groundwater studies), then examined energy transfer in bulk fuels, and concluded with an investigation of what the fluorescence would be in the absence of energy transfer and quenching.

Fluorescence quenching by ions

Brief literature review. Pioneering work in anion-induced fluorescence quenching was performed by Jett and West. Förster also performed quenching studies in the 1950's. He proposed that electron transfer was responsible for energy transfer from anions to excited molecules.

In 1973 and 1974, A. R. Watkins published three articles that described the quenching of aromatic hydrocarbons by butylated anions. He found the nitrate ion's quenching efficiency was between the iodide and bromide ions. Watkins was also the first to propose a charge transfer mechanism involving anion-induced radiationless transitions from the excited state mainly to the triplet state. This was attributed to higher lying charge transfer states, implying that neither the electron transfer mechanism nor the heavy atom effect were valid considerations.

In 1978 and 1980, Japanese chemists Shizuka, Nakamura, and Morita investigated Watkins' results. They found no evidence of exciplex or excimer formation. Linear Stern-Volmer plots were found and the group proposed that the following electron transfer was the most plausible mechanism:

$$ {}^1A^* + {}^1X^- \xleftrightarrow{diffusion} {}^1A^* \bullet\bullet\bullet {}^1X^- \xleftrightarrow{electron\ transfer} {}^2A^{-2}\,X $$

In this mechanism $^2A^{-2}X$ represents the charge transfer complex, where $^1A^*\cdots{}^1X^-$ represents the collision complex formed from the interaction of the polycyclic aromatic hydrocarbons (PAH) compound (A) and halide (X^-). Shizuka, Nakamura, and Morita concluded that electron transfer is an important step in the anion-induced quenching of aromatic systems.

The debate was resumed by Mac and Najbar, Jagiellonian University, Poland, with their studies of quenching of aromatic molecules by anions. They propose the mechanisms are dependent on the DG between the inorganic ions and the singlet excited PAH. For positive DG, the quenching efficiency is higher with negligible temperature dependence. For DGs between 0 and -0.2 eV, the fluorescence quenching is a temperature dependent electron transfer process. For a DG < -0.25 eV, the electron transfer process dominates. Later papers by

these authors further concluded that the fluorescence quenching is also dependent on solvent polarity and the influence of solvent dielectric properties.

Stern-Volmer relationship. A simple system to study fluorescence quenching and Stern-Volmer behavior was desired to test methods that would eventually be applied to more complex systems involving other PAHs. We began with naphthalene as the fluorophore and simple ions as the quenchers. Preliminary literature searches have not located any articles that describe the quenching of polynuclear aromatic hydrocarbons with simple cations and anions in aqueous solutions.

The Stern-Volmer equation, which is the usual way to describe quenching behavior, is briefly derived in the following text. Equation 1 expresses the fluorescence lifetime in terms of the rate constants: k_r (radiative processes), k_{nr} (nonradiative processes), k_p (photochemical processes) and finally $k_q[Q]$ (quenching rate x quencher concentration):

$$\tau = \frac{1}{(k_r + K_{nr} + k_p + k_q\,[Q])} \tag{1}$$

In the absence of a quencher, this equation simplifies to:

$$\tau_o = \frac{1}{(k_r + K_{nr} + K_P)} \tag{2}$$

Equations 1 and 2 may now be combined to form the Stern-Volmer equation:

$$\frac{\tau_o}{\tau} = 1 + (k_{sv}\,[Q]) \tag{3}$$

where

$$K_{sv} = \frac{k_q}{(k_r + K_{nr} + K_p)}$$

K_{sv} is the Stern-Volmer rate constant and is graphically determined from the slope of a plot of $(t_o/t - 1)$ vs. quencher concentration. An alternative form of the S-V equation is obtained by dividing both sides of the K_{sv} expression by k_q.

$$\frac{\tau_o}{\tau} = 1 + \tau_o\,(k_q\,[Q]) \tag{4}$$

The constant k_q, which is simply the ratio of the S-V constant to the lifetime, is of special interest because it can be related to the diffusion controlled rate

constant (k_d), which is a function of the specific solvent viscosity and temperature, according to Equation 5.

$$k_d = \frac{8\,R\,T}{3\,\eta} \tag{5}$$

The efficiency of quenching is the ratio of the second order quenching rate constant to the diffusion controlled rate constant.

$$\text{Quenching Efficiency} = \frac{k_q}{k_d} \tag{6}$$

The k_d for water at 25 °C is $6.6 \times 10^9\ M^{-1}s^{-1}$

Experimental procedure. A stock solution of 25 ppm naphthalene in water was prepared. Concentrated aqueous stock solutions of NaBr, NaCl, and NaI were also prepared. The salt solutions were diluted (Table 3 gives specific concentrations) and then spiked with naphthalene. The final naphthalene concentration was 2 ppm (1.54×10^{-5} M) in each case. Lifetimes were analyzed for the 335-nm monitoring wavelength by the phase plane method. The quality of the lifetime fits was noticeably degraded for lifetimes shorter than a few nanoseconds.

Results. Lifetimes were measured over a range of concentrations to construct Stern-Volmer plots. Five acquisitions were averaged to obtain the following data. The data are shown in Table 3. Stern-Volmer plots (Figures 22 through 24) for each ion follow.

Table 3
Lifetimes, ns, of Naphthalene in Sodium Salt Solutions

Conc. [M]	NaCl	NaBr	NaI
0	35.83	35.40	34.95
0.0005			32.00
0.005			16.08
0.01			10.37
0.05		22.78	2.89
0.07			2.51
0.1	35.25	16.93	1.89
0.4		6.68	
0.5	33.49		
0.7		4.39	
1.0	31.63	3.28	

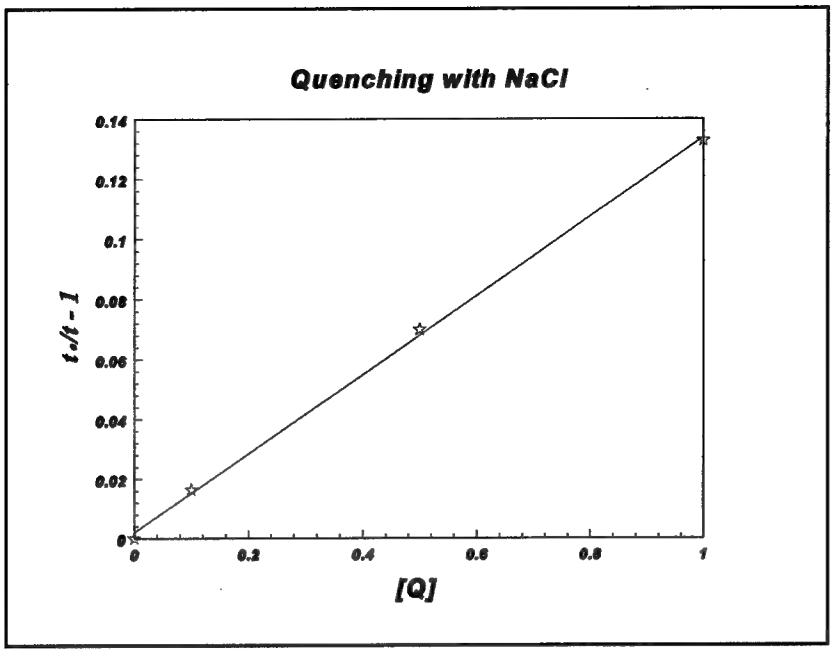

Figure 22. Stern-Volmer plot of fluorescence lifetime of naphthalene vs. concentration of quenching ion, Cl^-. These data are presented in tabular form in Table 3

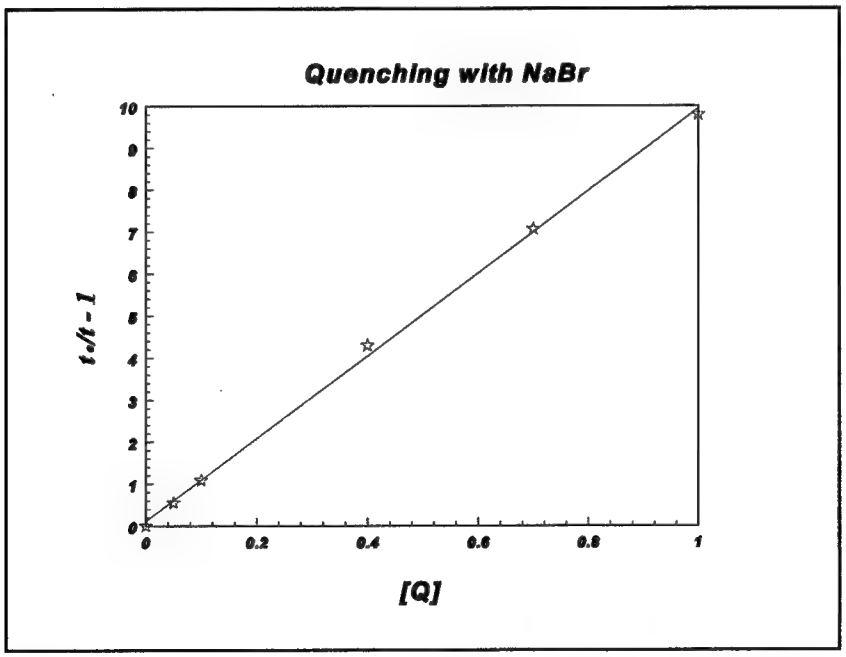

Figure 23. Stern-Volmer plot of fluorescence lifetime of naphthalene vs. concentration of quenching ion, BR^-. These data are preseneted in tabular form in Table 3

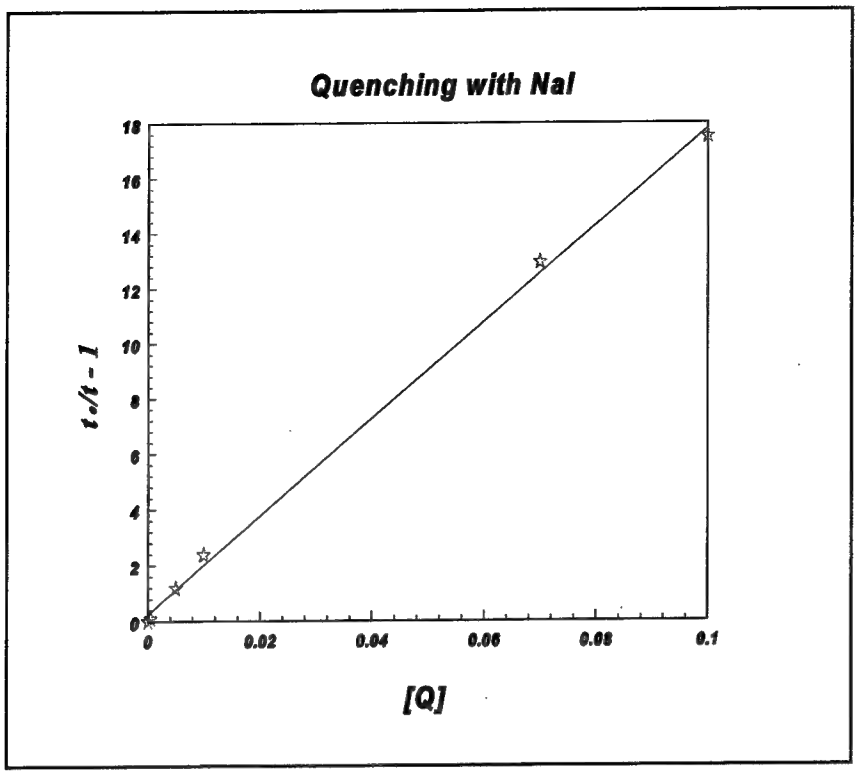

Figure 24. Stern-Volmer plot of fluorescence lifetime of naphthalene vs. concentration of quenching ion, I^-. These data are preseneted in tabular form in Table 3, note that the 0.05M data point is not included on the graph

The quenching rate constants and efficiencies for each of the ions were tabulated. See Table 4 for results. The units for k_q and k_d are $M^{-1}s^{-1}$ or L/mol s.

Table 4
Quenching Rate Constants and Efficiencies of Anions

Quenching Ion (Compound Used)	Quenching Rate Constant (Correlation Coeff.)	Efficiency = k_q/k_d (in percent)
Cl^- (NaCl)	3.64×10^6 (0.9996)	0.0549
Br^- (NaBr)	2.78×10^8 (0.9993)	4.21
I^- (NaI)	5.20×10^9 (0.9946)	78.8

Discussion. Two proposed mechanisms for quenching by ions in polar solution are electron transfer and the external heavy atom effect. We believe that the quenching is caused by the heavy atom effect. The dependence of the quenching rate on the atomic number, z, of the quencher is of interest. The intra-atomic spin-orbit coupling matrix element is predicted to follow a z^4-dependence. At most, the quenching should be proportional to the square of the

matrix element, making for a z^8 dependence. The z-dependence can be found from a log-log plot as shown in Figure 25. The slope from this graph equals the z-dependence, which in this case is approximately 6.4. There are many reasons why the idealized z^8-dependence is not expected, including the fact that we are not dealing with point particles and that solvent interactions are ignored.

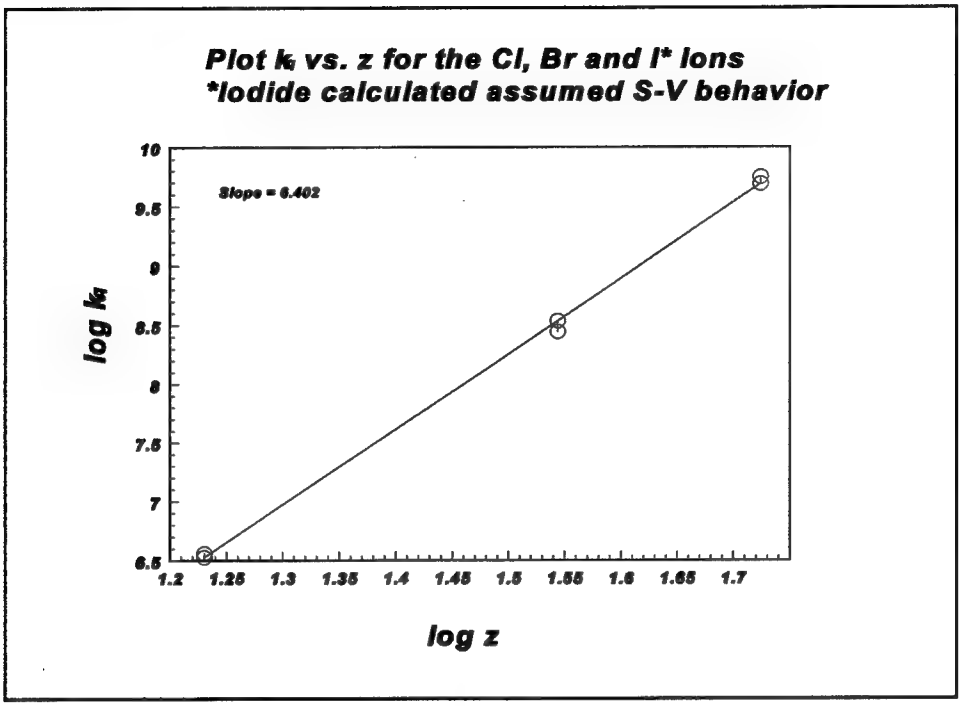

Figure 25. Plot of log (quenching rate constant) vs. log (nuclear charge) results indicate a $z^{6.4}$ dependence; ideal heavy atom quenching would show z^8 dependence

Quenching studies may also be run using steady-state fluorescence and the data interpreted using the following equation.

$$\frac{I_0}{I} - I = K_{SV}\,[Q] \quad \textit{Intensity Data} \tag{7}$$

where

$$K_{sv} = k_q\,\tau_0$$

A comparison of the results of time resolved fluorescence lifetime data (TRF) vs. steady state (SS) is shown in Table 5. Note that when measurements can be carried out, as in the case of Mn^{++}, the agreement between the two methods is good. In certain cases, steady state measurements are not feasible because the absorption spectrum of the quencher overlaps the absorption of the fluorophore. The result of the 'inner filter effect' of overlapping absorption is that I_0 (see equation above) in effect becomes a function of the quencher

concentration. In extreme cases, as with Cu^{++}, the quencher absorbs enough of the excitation light to completely eliminate any fluorescence from the naphthalene.

Table 5
Quenching Rate Constants and Efficiencies of Transition Metals

Quenching Ion (Compound Used)	Quenching Rate Constant (Correlation Coeff.)	Efficiency = k_q/k_d %
Cu^{2+} ($CuSO_4$) TRF	7.56×10^9 (G)	115
Cu^{2+} ($CuSO_4$) SS	N/A	N/A
Mn^{2+} ($MnSO_4$) TRF	1.50×10^8 (G)	2.27
Mn^{2+} ($MnSO_4$) SS	1.53×10^8	2.3
G = Global Analysis Required		

Energy transfer in solutions

We now turn our attention to the fluorescence of bulk fuels, such as gasoline, diesel, and jet fuel. Most of the work has been done for diesel. Chemical analysis of diesel fuel suggests that the main contributors to the fluorescence excited around 290 nm are naphthalene, anthracene, phenanthrene, and fluorene. However, within each class there are many different compounds that differ in the position of alkyl substituents. We have always been struck by the relatively low contribution of naphthalenes to the diesel fuel fluorescence even though they are a major component. It has been proposed that the reason diesel fluorescence observed contains little naphthalene is attributed to energy transfer mechanisms.

Experimental procedure. Methanol solutions containing 10^{-5} M naphthalene with concentrations of 10^{-3}, 10^{-4}, and 10^{-5}M phenanthrene were prepared. The naphthalene concentration was kept low to avoid energy transfer to itself. Time resolved fluorescence emission scans were taken over a range from 300 to 500 nm in steps of 5 nm. The fluorescence lifetime (t) was determined at a sufficiently short wavelength (330 nm) so that only naphthalene would contribute. Five acquisitions were averaged to obtain the following data. The results for each of the different concentrations of naphthalene are presented in tabular form in Tables 6 through 8. The results of each study were also graphed (see Figures 26 through 28).

Table 6
Lifetimes of Naphthalene (Concentration = 0.001M) in Phenanthrene Solution

Phenanthrene Conc. [M]	Lifetime in ns (c^2)	$(t_0/t) - 1$
0	14.83 (0.0000792)	0
0.00001	14.70 (0.000262)	0.0088435
0.0001	14.29 (0.0001409)	0.037789
0.001	10.24 (0.003376)	0.44824

Table 7
Lifetimes of Naphthalene (Concentration = 0.0001M) in Phenanthrene Solution

Phenanthrene Conc. [M]	Lifetime in ns (c^2)	$(t_0/t) - 1$
0	14.74 (0.000395)	0
0.00001	14.03 (0.000239)	0.050605
0.0001	12.24 (0.0012)	0.20425
0.001	5.81 (0.0020)	1.5370

Table 8
Lifetimes of Naphthalene (Concentration = 0.00001M) in Phenanthrene Solution

Phenanthrene Conc. [M]	Lifetime in ns (c^2)	$(t_0/t) - 1$
0	13.42 (0.000409)	0
0.00001	11.63 (0.0025)	0.15391
0.0001	7.54 (0.0052)	0.76812
0.001	6.65 (0.0048)	1.1404

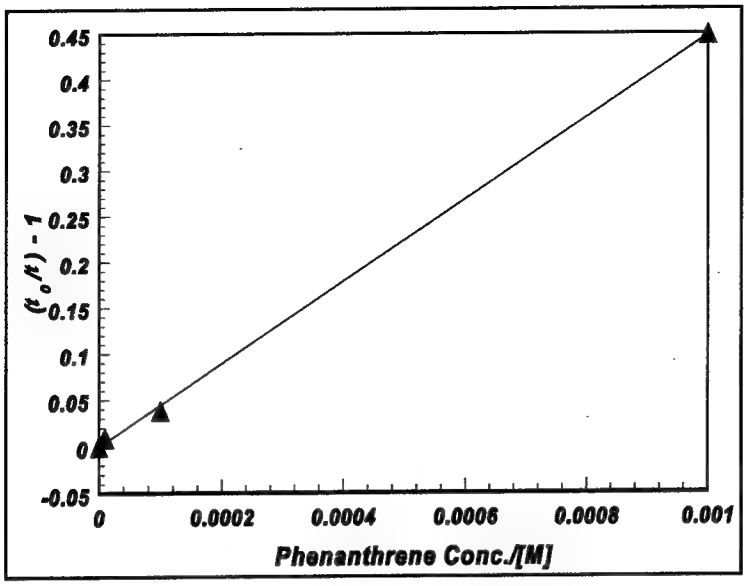

Figure 26. Stern-Volmer plot of fluorescence lifetime of naphthalene (0.001M) vs. concentration of phenanthrene solution

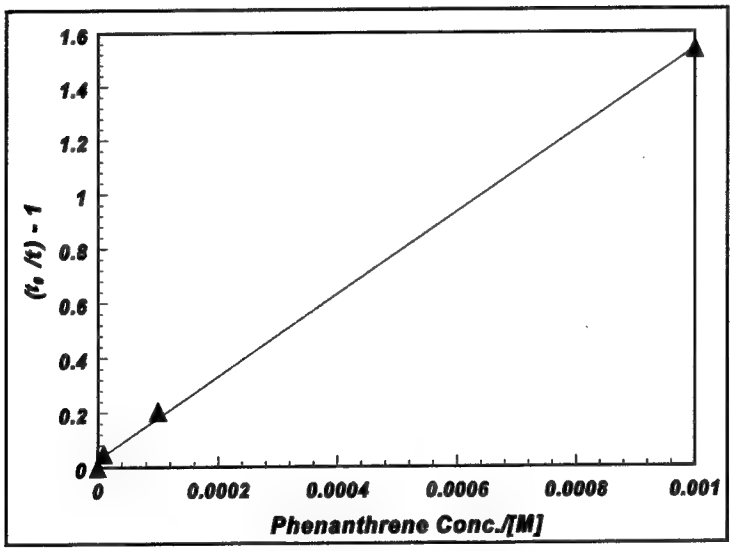

Figure 27. Stern-Volmer plot of fluorescence lifetime of naphthalene (0.0001M) vs. concentration of phenanthrene solution

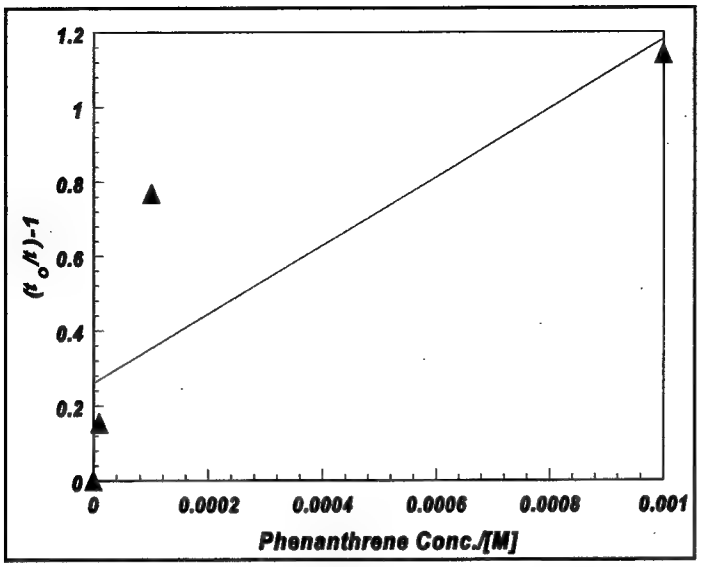

Figure 28. Stern-Volmer plot of fluorescence lifetime of naphthalene (0.00001M) vs. concentration of phenanthrene solution

The slope of the graphs, quenching rates, and correlation coefficients of the three sets of data are tabulated in Table 9.

Table 9
Slope of the Graphs, Quenching Rates, and Correlation Coefficients of the Data

Data Set	Slope	Quenching Rate, k_q	Correlation Coefficient
0.001M Naphthalene	486	3.24×10^{10}	0.9998
0.0001M Naphthalene	1511	9.98×10^{10}	0.9995
0.00001M Naphthalene	902	6.01×10^{10}	0.838
k_d (Methanol) = 1.10×10^{10}			

Conclusion. If strict Stern-Volmer quenching kinetics were active in this system, the three quenching rate constants, k_q, should be equivalent to within experimental error. As is evident, the agreement is poor. In addition, few of the decay profiles could be fit with a single exponential. The diffusion controlled rate constant for methanol at 25 °C was calculated to be 1.18×10^{10} $M^{-1}s^{-1}$. This means that the apparent efficiency of quenching is 256 percent. Nevertheless, energy transfer from naphthalene to phenanthrene is exceedingly efficient. Even low concentrations of phenanthrene, far below what are found in diesel fuel, affect the lifetime of naphthalene. At 0.001 M phenanthrene, already about one-third of the naphthalene fluorescence is quenched. If quantitative analysis of the diesel fuel composition were obtained, further validation of quenching of diesel fuel fluorescence could be performed. There are other PAH components that

exist in diesel fuel, fluorene, and anthracene. Separate energy transfer systems with these molecules could also be investigated.

The possibility of exciplex formation in a toluene solution of naphthalene and phenanthrene was investigated. Emission spectra of each analyte were studied separately and compared to the emission spectrum of the mixture. If energy transfer is not active, the emission spectrum of the mixture would be a linear combination of the two separate emission spectra. If exciplex formation is involved, fluorescence from the complex should be observed as follows:

$$N + h\nu \rightarrow N^* \tag{8}$$

$$N^* + P \rightarrow (N \bullet\bullet\bullet P)^* \rightarrow N + P + h\nu \text{ (“Exciplex”)}$$

No fluorescence was detected which could be attributed to exciplex formation. A normalized linear combination of the naphthalene emission spectrum and the phenanthrene emission spectrum matched the emission spectrum of the mixture with no additional long wavelength fluorescence noted.

Fuel fluorescence in solids

Naphthalene and phenanthrene isolated in Zeonex™ polymer film. To understand the fluorescence spectrum of a fuel on soil, it is necessary to understand the intrinsic fluorescence properties of the fuel components and the effect of the interaction with the adjacent soil matrix on those fluorescence properties. Typically, the fluorescence properties are studied for individual components in a dilute liquid solution. In a solid matrix there are many more opportunities for energy transfer and quenching. It would be advantageous to incorporate the fuel components in a solid matrix that still allowed the individual species to fluoresce independently. Such a sample would also be useful as a reference material. We have found that Zeonex™, an amorphous polyolefin, has favorable properties for such an application. Zeonex™ appears to be an attractive alternative to other plastic hosts such as polymethyl methacralates (PMMA).

Important features of this material include:

a. Good UV transparency properties.

b. Large solvent and chemical resistance.

c. Low water absorption and permeability.

d. Heat resistance high relative to other imbedding agents.

e. Low levels of impurities.

Thin films can be cast on glass plates from a stock solution of Zeonex™ beads dissolved in spectrophotometric grade toluene. Film thicknesses of 20 to 30 μm are convenient. The fluorescent species can be dissolved into the Zeonex™ stock solution before the films are cast.

Naphthalene results. Fluorescence wavelength time matrices (WTMs) were acquired for naphthalene imbedded in Zeonex™, naphthalene in Zeonex™/toluene solution, and a blank Zeonex™ sample. The data closely resembles fluorescence observed for naphthalene in solution. The contour plots in Figure 29 represent the fluorescence from 300 to 400 nm. A large difference in the time decay is qualitatively observed between the two matrix representations seen below.

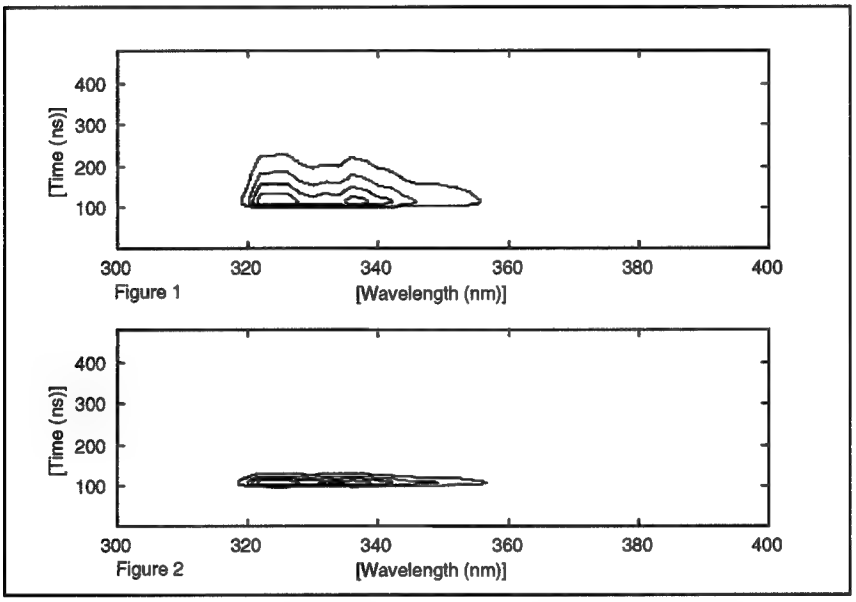

Figure 29. Contour fluorescence WTM of naphthalene imbedded into Zeonex™ (#1) and Zeonex™/toluene solution (#2)

Figure 30 shows the fluorescence lifetime data with the emission excited at 290 nm and monitored at 330 m. The fluorescence waveform obtained from the film impregnated with naphthalene is shown along with an excitation laser profile. Analysis of the waveform yields a fluorescence lifetime of 99.16 ns. No signal was generated by the clean film.

The fluorescence lifetime of the naphthalene in the solid Zeonex™ matrix is similar to the lifetime observed in a degassed alkane solution. For example, the naphthalene fluorescence lifetime in air saturated heptane is 8.6 ns. Degassing the heptane solution with nitrogen increases the lifetime to 113 ns. The increase in decay lifetime is attributed to a decrease in oxygen quenching in the degassed solution. Consequently, we infer that the naphthalene is in an oxygen poor environment when impregnated in the Zeonex™. This is reasonable if oxygen diffusion through the material is slow.

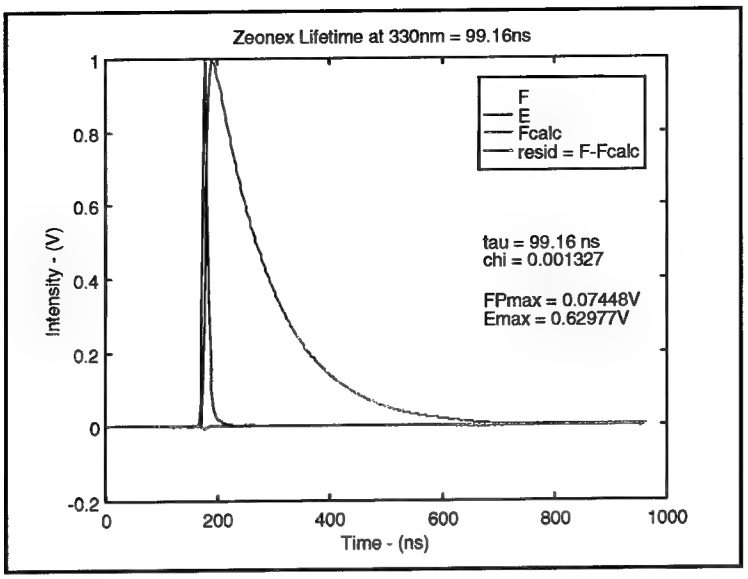

Figure 30. Fluorescence lifetime of naphthalene in Zeonex™ film

Laboratory investigations were conducted to determine whether oxygen could be "pumped" out of the film to observe a longer lifetime. Films were placed in a vacuum desiccation chamber connected to a roughing pump capable of evacuating to a few millitorr. The films were pumped for as long as 1 hr, then removed and spectra immediately acquired. No difference from the lifetime before pumping was observed.

There appears to be no appreciable lifetime difference in the naphthalene Zeonex™ samples prepared under nitrogen conditions and those prepared under atmospheric conditions. The fact that the samples have approximately the same lifetime indicates similar fluorescence emission environments for each sample. Even though oxygen may be present in different quantities, it does not quench the fluorescence because the molecules are locked into a physical space. Therefore, under vastly different preparation conditions the lifetimes remain the same, yielding a similar t_o for naphthalene in Zeonex™. This fact will be beneficial if samples are archived. There would be little effort necessary to obtain similar preparation conditions. Our conclusion is that the Zeonex™ films strongly exclude oxygen as they cure.

The WTMs were subjected to lifetime analysis across the range of wavelengths. Lifetimes of naphthalene in solution and naphthalene imbedded in the matrix were calculated by phase plane analysis across the maxima (Table 10).

Plots of ln(I) versus time were linear, indicating single exponential decay. The good precision in the lifetimes is also indicative of this fact. As originally predicted, the lifetimes are longer. This can be attributed primarily to protection from oxygen quenching.

Table 10 Lifetimes of Naphthalene in Both Environments		
Wavelength, nm	Lifetime, ns, in solution	Lifetime, ns, in matrix
330	15.97	97.75
340	16.06	96.80
350	16.22	96.85
360	15.93	97.36

Phenanthrene results. A WTM of the phenanthrene impregnated film is shown in Figure 31 (top left). The fluorescence spectrum shown in Figure 31 (bottom left) is a slice of the WTM at the time of maximum intensity. Figure 31 (right) shows the fluorescence decay profile obtained at 350 nm. Lifetime analysis yields a fluorescence lifetime of 52.9 ns for the phenanthrene in the Zeonex™ film.

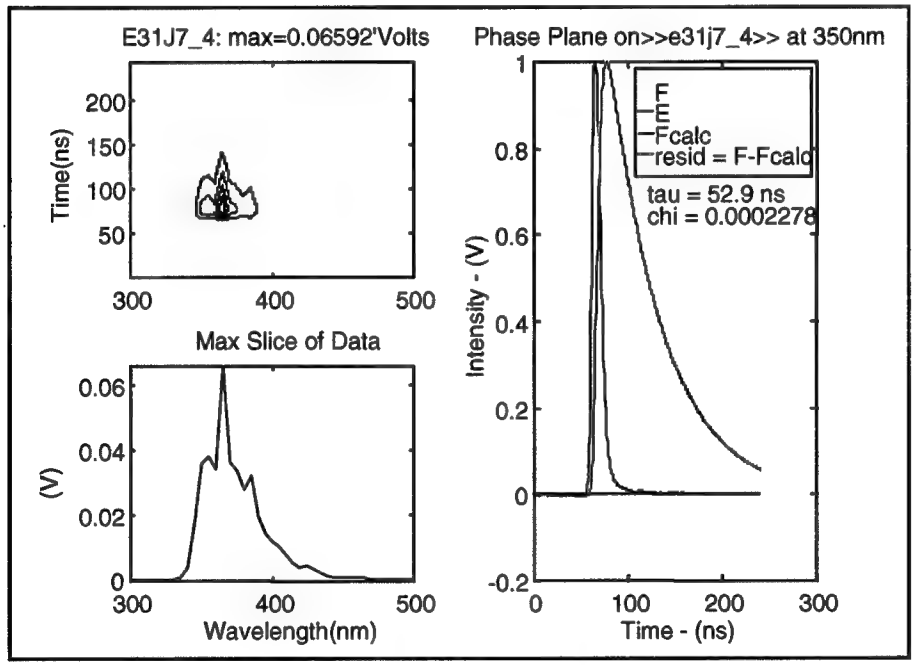

Figure 31. WTM of phenanthrene impregnated film (top left); slice of WTM at the time of maximum intensity (bottom left); fluorescence decay profile at 350 nm (right)

The linearity observed for the ln(I) versus time plot indicates that a single exponential fit of the fluorescence decay is appropriate, Figure 32.

Fluorescence data were also obtained from the solution, before the film was cast (Figure 33). The fluorescence spectrum is very similar to that obtained from the film. The fluorescence lifetime of phenanthrene in the solution is

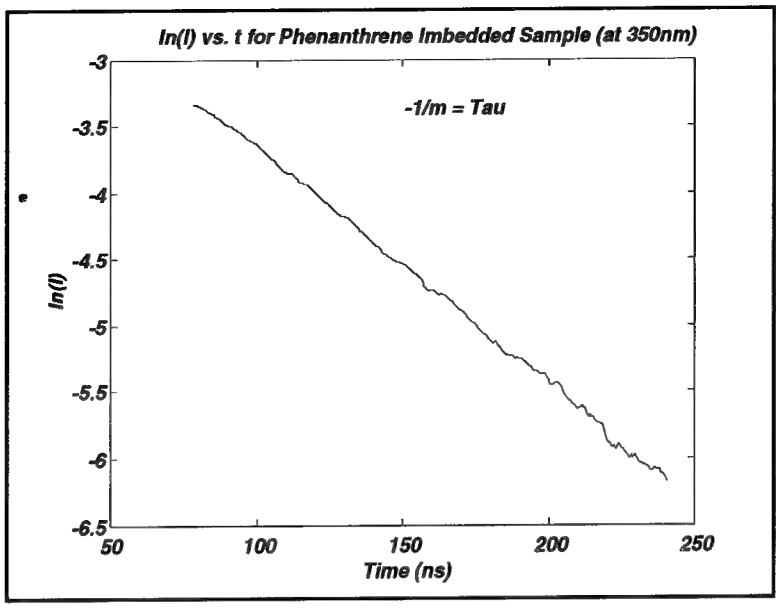

Figure 32. Ln(I) vs. time for phenanthrene imbedded sample (at 350 nm)

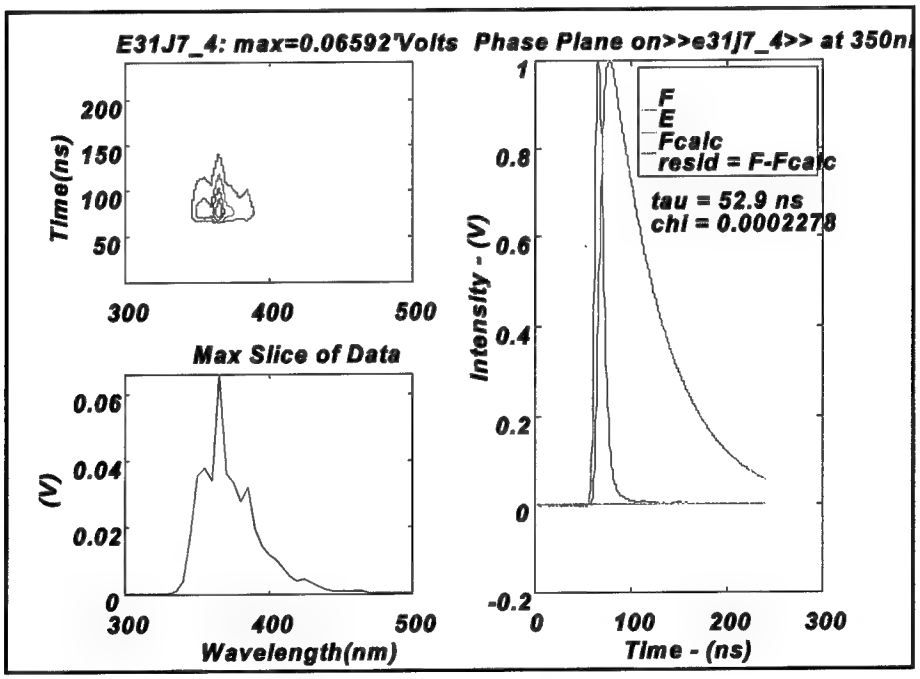

Figure 33. WTM of phenanthrene/Zeonex™ solution (top left); slice of WTM at the time of maximum intensity (bottom left); fluorescence decay profile at 350 nm (right)

considerably shorter than that in the dried film. The lifetime obtained in the solution was 15.05 ns.

These studies are an important first step toward understanding the fluorescence observed in solid matrices (i.e., soils). Other than oxygen solubility, the Zeonex™ has little effect on the interaction between the fluorescent species found in the fuels.

Fuels in Zeonex™. The next step was to compare fluorescence from diesel and jet fuel embedded in Zeonex™. Significant wavelength differences from the fluorescence spectra of the bulk fuels are expected if the Zeonex™ prevents the energy transfer that occurs in solution.

Figure 34 represents the fluorescence from neat diesel fuel and from diesel fuel isolated in a Zeonex™ film. Diesel fuel is a multicomponent mixture with many different aromatic fluorophores contributing to the fluorescence. The most likely contributors are molecules in the classes of fluorene, naphthalene, phenanthrene, and anthracene. Evidence is clearly seen for energy transfer from naphthalene to phenanthrene being turned off in Zeonex™ films. The isolated naphthalene molecules are no longer able to transfer their energy and a larger signal in the naphthalene region (320 to 330 nm emission$_{max}$) is therefore observed.

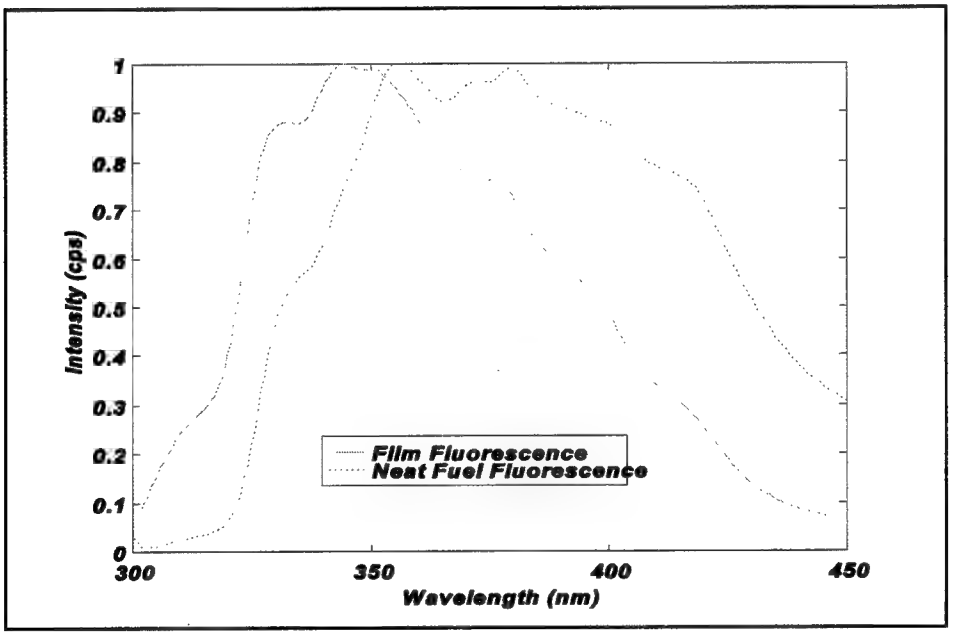

Figure 34. Normalized fluorescence of diesel of Zeonex™ (left) and neat diesel (right)

The difference between the fluorescence spectra of the imbedded diesel and neat diesel is quite dramatic. It does not appear that the shift can be attributed to the difference in molecular environments. A comparison in the shoulders of both spectra at 380, 400, and 420 nm indicates little shift in the spectra.

The differences are especially noticeable in the phenanthrene emission region from 350 to 400 nm. This is credited to a much lower mass ratio of the

diesel. Mass ratio (MR) refers to the weight ratio of diesel to Zeonex™. As the mass ratio increases, the spectra begin to acquire a more "phenanthrene like" emission (Figure 35).

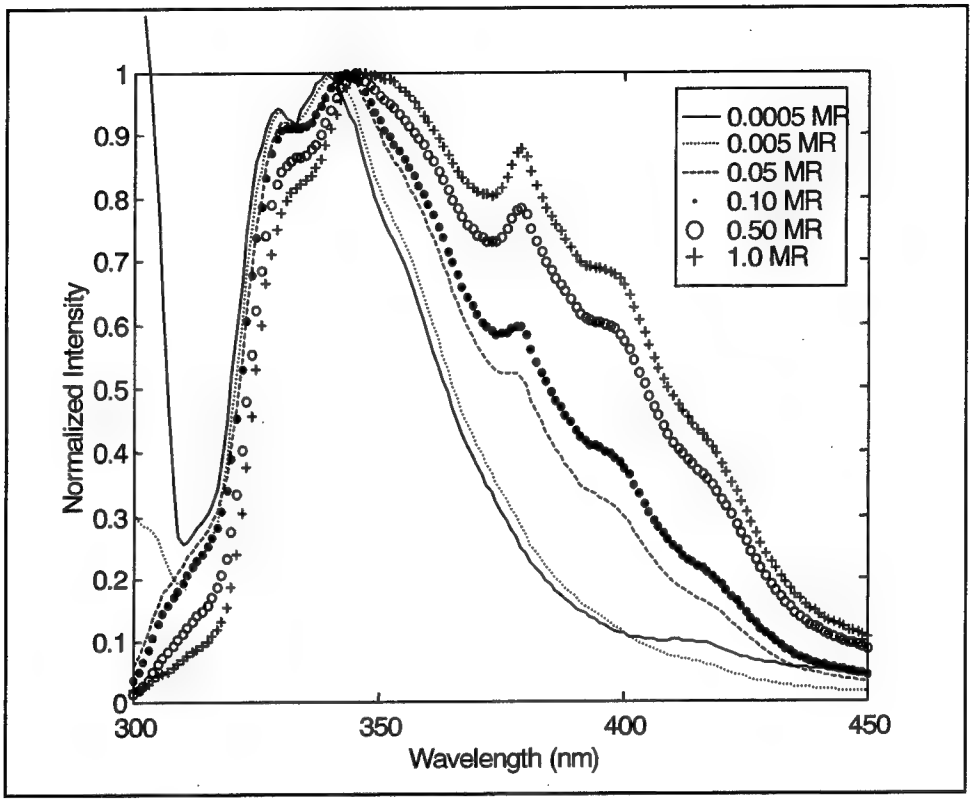

Figure 35. Increasing mass ratios of diesel in Zeonex™

The nature of these spectral changes remains unknown. Two possibilities are: (a) energy transfer is still occurring and/or (b) there is competition for photons among the fluorophores. The higher mass ratio samples (i.e., 0.5 MR and 1.0 MR) did not have their solvent completely evaporated. For this reason, it is plausible that energy transfer may still be occurring.

Because of the complex chemical nature of diesel fuel, tests were also performed on a simpler two component system of naphthalene and phenanthrene imbedded into Zeonex™. These molecules were chosen because they represent two of the four largest contributing aromatic fluorophores. By measuring the fluorescence and calculating their individual lifetimes, we should be able to distinguish if energy transfer is occurring within the film.

The WTMs of both samples (Figures 36 and 37) resembled the "sailfish" WTM pattern observed for diesel fuel.

Jet fuel (JP-5) which is composed largely of naphthalene was also investigated. New films were cast with JP-5 in Zeonex™ and Zeonex™/toluene mixture. The JP-5 fluorescence is represented in Figure 38. The data indicate

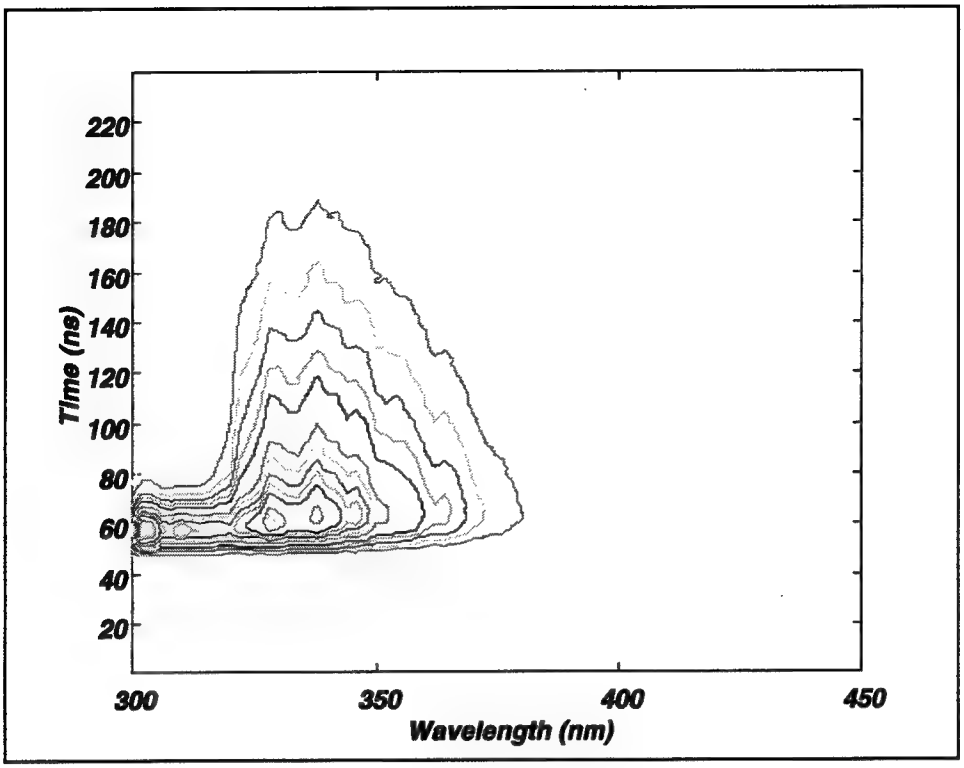

Figure 36. WTM of synthetic mixture of Zeonex™

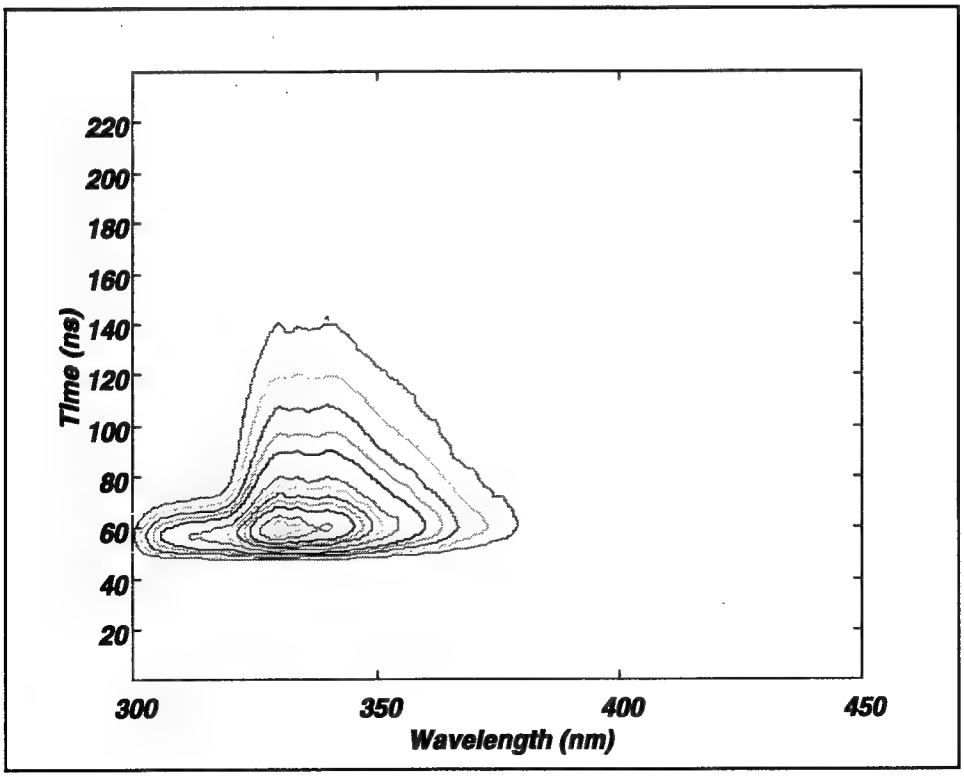

Figure 37. WTM of the 0.1 mass ratio sample of diesel in Zeonex™

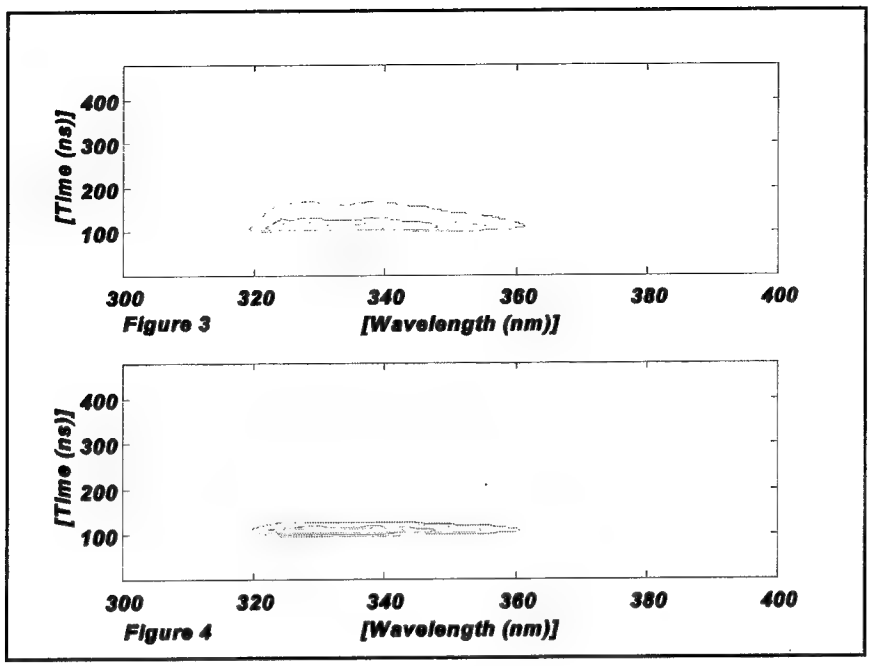

Figure 38. Contour fluorescence WTM of JP-5 imbedded into Zeonex™ (#3) and contour fluorescence WTM of JP-5 dissolved in Zeonex™/toluene solution (#4)

no wavelength shifts, only lifetime differences. This once again is likely to be protection from oxygen quenching. Attempts made to determine lifetimes with phase plane analysis met with little success. A global analysis was performed on the sample with approximate lifetimes of 6 ns and 54 ns extracted. It is presumed that the longer component is some naphthalene contribution. The shorter-lived component cannot be ascribed to one chemical species.

Resonance Enhanced Multi-Photon Ionization (REMPI)

Background. When a molecule reaches its ionization continuum by photon absorption, it liberates an electron and leaves behind a positive molecular ion. These charged species, and/or other charged species generated by subsequent electron capture and/or ion-molecule reactions, can be efficiently collected and detected at biased electrodes. In the conventional photoionization detectors (PIDs) that are commonly used for gas chromatography, the ionization source is a vacuum ultraviolet lamp which provides sufficiently energetic photons (on the order of 10 eV) to promote molecules directly to the ionization continuum.

In a multi-photon ionization process, the energy from more than one photon is required. An N-photon MPI event can occur if the sum of the energy from the N photons exceeds the molecular ionization energy. However, the ion generation efficiency is dramatically enhanced whenever the molecule proceeds

through an excited state (a "resonance") generated by conventional one-photon absorption during the MPI process. The simplest REMPI processes are those of the 1+1 type, in which one photon is absorbed to create the resonance, from which absorption of only one more photon is necessary to reach the ionization continuum.

An important advantage of the REMPI technique over other ionization-based methods (e.g., PID, FID, and other GC detectors) is that the pulsed laser source forms the ions at a well-defined time. Under this circumstance, gated detection with a boxcar averager or digital oscilloscope contributes additional sensitivity and noise reduction over what is possible with a simple DC current measurement. It should be noted that the REMPI process depends on the square of the photon irradiance (number of photons passing through unit area per unit time). For this reason, pulsed lasers are essential to the REMPI process.

The application of REMPI in laboratory-based systems is generally reported in the literature. A real-time (<100 ms) time-of-flight (TOF) mass spectrometer analysis system for auto engine combustion products based on REMPI was developed (Weickhardt et al. 1994). A small amount of the engine exhaust is passed through a cannula to a gas valve that opens for 1 ms injecting the gas into the high vacuum chamber of the mass spectrometer. They analyzed 25 exhaust gas components by MPI including toluene, xylene, and benzene. Another group or researchers (Cool and Williams 1992) demonstrated the detection of chlorinated hydrocarbons using REMPI in a TOF pulsed molecular beam apparatus. They determined detection limits from 0.5 to 40 ppbv for vinyl chloride, 1,1 dichloroethylene, 1,2-dichloroethylene, TCE, and tetrachloroethylene.

A few examples of measurements at or near ambient pressure are reported in the literature. Trace amounts of nitric oxide (NO) in a partial pressure (560 mbar) of nitrogen carrier gas using REMPI were detected (Guizard et al. 1989). The use of MPI combined with laser photofragmentation to detect trace vapors of NO, NO_2, HNO_3, and CH_3NO_2 at ambient pressure was demonstrated (Simeonsson, Lemire, and Sausa 1994). They have patented the technique for laser-based detection of nitro-containing compounds, U.S. Pat. No. 5,364,795. Detection of nitroaromatic compounds, used in explosives, by REMPI detection of NO was determined (Marshall et al. 1994). However, all of these applications require large and expensive lasers as the source of the ionizing photons. The REMPI detection approach discussed below involves direct measurements in the air under ambient conditions and is therefore extremely simple in operation. The feasibility of measurements at atmospheric pressure in moist air has already been proven. In September 1996, Dr. Orven Swenson, NDSU, participated in a summer program at Tyndall AFB in the Armstrong Laboratory Environics Directorate. At the end of his stay, Dr. Swenson demonstrated detection of aniline and styrene at the 1 ppbv level with an ROST system built by DTI.

Scope/Approach. The REMPI is widely applied in research laboratories as a means to study and characterize the energy levels of molecules. The laboratory studies almost invariably involve high vacuum TOF and supersonic molecular

beam systems, in fact, to such a degree that it is often assumed that REMPI requires high vacuum conditions. However, the utility of REMPI for ambient air measurements was demonstrated almost 20 years ago and then more or less forgotten until recently.

Tremendous progress has been made over the course of the SCAPS Program in terms of understanding the nature of the REMPI phenomenon, in particular the process by which the ions are collected at electrodes. Four papers related to REMPI detection have been published or are in press (Swenson and Gillispie 1996; Swenson, Gillispie, Cooper, and Dvorak 1997; Swenson, Gillispie, and Walls 1997). This section highlights selected results from those papers.

There have also been two highly promising spinoffs from the REMPI work: ion mobility spectrometry (IMS) (particularly with a photoemissive source of electrons) and a new laser source which promises to dramatically drop the cost of making measurements, both downhole and for air quality purposes.

The IMS work will be continued by Dr. Swenson and the NDSU Physics Department. The laser source work relates to our recognition of a serendipitous match between the output of an Nd:KGW laser and two absorption features of benzene and toluene.

Figure 39 shows the absorbance spectra of benzene, toluene, ethylbenzene, and p-xylene taken at approximately 0.1 nm resolution with a conventional laboratory spectrophotometer. Note that both benzene and toluene show a narrow absorbance feature with a maximum near 266.7 nm. The spectra of ethylbenzene and p-xylene (and other alkylated benzenes) are not as well resolved, but all absorb light near this wavelength.

Secondly, note that the absorbance of benzene is at least 20 times lower at 266.0 nm compared to 266.7 nm, and the absorbance of the other species is reduced also. The significance of the 266.0-nm wavelength is that it corresponds to the fourth harmonic of an Nd:YAG laser, the most common solid state pulsed laser. To a first approximation, the relative intensity of the REMPI spectrum as a function of wavelength matches the conventional absorbance spectrum. Thus, the use of the Nd:YAG fourth harmonic in a REMPI apparatus exacts a high-sensitivity penalty. Having recognized the desirability of the 266.7-nm wavelength over 2 years ago, we embarked on an exhaustive search for a laser source which could provide that wavelength with comparable convenience, performance, and size to commercially available Nd:YAG lasers. In the meantime, we continued our laboratory investigations, first with the frequency-doubled output of a coumarin dye laser pumped with the 355-nm third harmonic of an Nd:YAG laser, and later with an optical parameter oscillator (OPO) system. In addition to cost and size restrictions, the problem with the coumarin dyes is that they degrade over a few hours and are not as efficient as the rhodamine dyes which are used in the ROST. Too much time is spent maintaining the dye laser to make this approach satisfactory for routine use. The OPO system, which is also pumped by the Nd:YAG third harmonic, is all solid

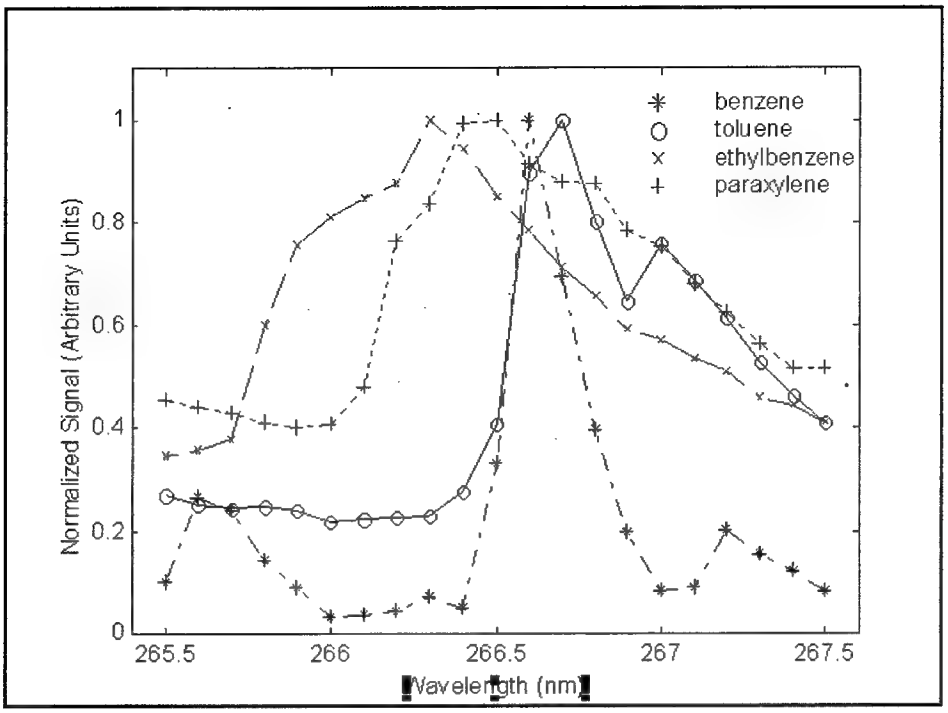

Figure 39. Normalized absorbance spectra of BTEX

state and therefore more reliable than a dye laser system, but its output is too sensitive to temperature fluctuations and the input pump power.

For these reasons, we performed a study in which the individual components of a mixture were eluted with a Gas Chromatograph (GC) and simultaneously recorded with a conventional PID and the REMPI detector. An early study (Klimcak and Wessel 1980) had used a GC to separate mixtures of aromatic hydrocarbons and detect them via REMPI. Detection limits on the order of 10 pg were found for the aromatic hydrocarbons anthracene, phenathrene, benzanthracene, acenaphthene, naphthalene, and assorted halonaphthalenes and showed spectral differentiation between co-eluting anthracene and phenathrene. This shows that the REMPI detector should be capable of reliable, defendable results even when operated in a field configuration. We further show encouraging results for freedom from interferences. The REMPI detector gives virtually no response under the usual operating conditions to aliphatic hydrocarbons, alcohols, and other possibly interfering species. It can be very specific for BTEX.

Experimental section. All of the results reported herein were acquired with a portable bread board REMPI apparatus. The third harmonic of an Nd:YAG laser (Quantel Brilliant B) pumped an OPO. The Nd:YAG pump laser and OPO were mounted on a wheeled cart along with the REMPI flow cell and digital storage oscilloscope signal processor. The signal beam emerging from the OPO was frequency doubled in a BBO crystal (266.8 nm). The ultraviolet light around 266 nm was separated from residual 355-nm pump light, the undoubled

output of the OPO, and the idler beam with a Pellin-Brocca prism and softly focused with a 50-cm lens through the center of the REMPI cell. The UV light passing through the cell was directly monitored with a pyroelectric detector, and the REMPI signal was corrected by dividing it by the square of the laser pulse energy (approximately 200 μJ). A diaphragm pump was used to draw room air through the flow cell at 900 mL/min. The air passed only through a Teflon tube probe before passing through the flow cell. The flow cell was under atmospheric pressure and the 2-cm diam/1-cm separation parallel plate electrodes were biased with a 300-volt battery. The waveforms were averaged over 64 laser shots, stored on a Tektronix 360 digital storage oscilloscope, and downloaded to a floppy disk.

The GC comparison was performed with an SRI GC with a 15-m long, 0.53-mm ID column. Mixtures of benzene, toluene, ethylbenzene, and p-xylene in methanol were directly injected. The column was held at 40 °C for 3 min after the injection and then ramped at 12 °C/min to 80 °C. The effluent was passed from the SRI PID through a 0.8-mm ID, 0.75-m stainless steel tube at room temperature and introduced in between the REMPI electrodes with a Teflon tube extension. The 2-cm diam/1-cm separation copper REMPI electrodes were in a Teflon holder mounted inside a small metal box along with the preamplifier circuitry to shield them from radio frequency (RF) noise.

Closed-loop calibration curve. Calibration curves were generated by injecting vapor with a gas tight syringe into a 5-L flask from which vapor is pumped in a closed loop through the REMPI cell. A dye laser pumped by an Nd:YAG laser was used for those studies. The vapor containing the analyte of interest was extracted from the headspace above the corresponding liquid. A portion of a similar calibration curve, but now acquired with the portable OPO REMPI system, is shown in Figure 40. Three acquisitions were made at each concentration.

Specificity/interference test. A comparison was made of the REMPI detector response to commonly used organic solvents. The probe was fixed in a lab stand to sample at the opening of the solvent bottles with the results displayed in Figure 41. This was set up next to a fume hood and the room air BTEX background was high due to solvents in the hood. No change was seen in the signal except for the m-xylene and benzene. The m-xylene was sampled at a distance of 1.5 m from the open bottle.

Comparison with GC detector. The benefits of introducing the GC into the experimental procedure, in comparison to the previously used procedure in which vapor is injected into a reservoir and gas circulated through the cell include:

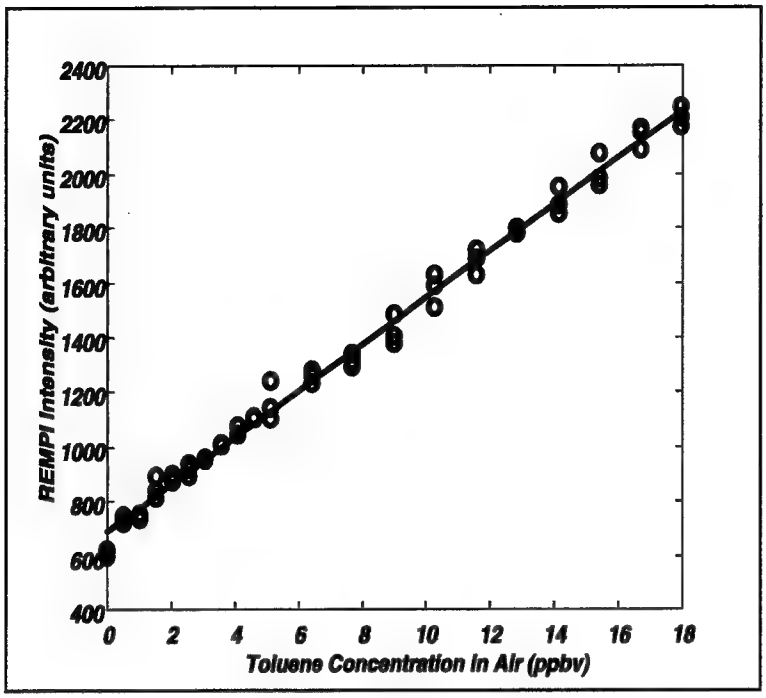

Figure 40. Toluene calibration for REMPI detection using a closed loop injection system

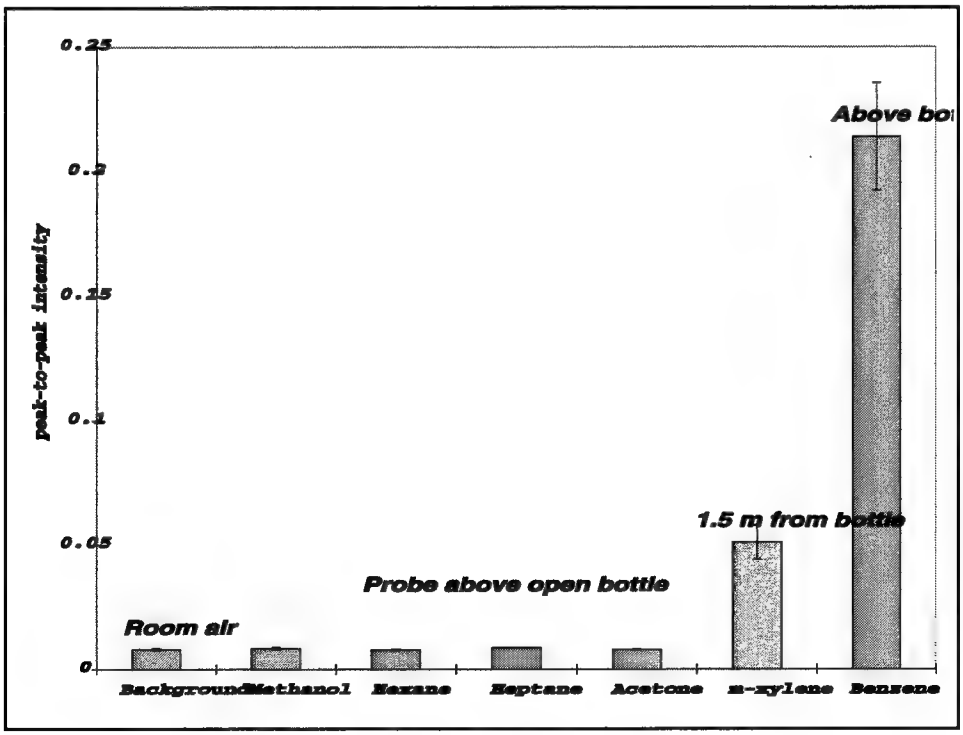

Figure 41. Comparison of REMPI detection of common solvents, the maximum peak-to-peak values have been corrected for the laser pulse energy variations

a. Samples at low concentrations/masses can be introduced more reliably into the REMPI cell. It is very difficult to reliably prepare samples at ppbv levels with other techniques because of adsorption losses.

b. We can study several different analytes at once and in doing so, test the effect of changing the laser wavelength. These experiments show that speciation of benzene and toluene from the other benzenoid species is possible with a small number of wavelengths.

c. We can show that the REMPI detector meets all the desired criteria of an analytical instrument: good precision, wide linear dynamic range, and low limits of detection.

We used the conventional PID and our REMPI detector to measure chromatograms simultaneously as a mixture of benzene, toluene, ethylbenzene, and p-xylene in methanol was eluted. We performed two sets of experiments. In one set, the OPO wavelength was fixed at 266.7 nm, which coincidentally matches sharp absorbance features of benzene and toluene and corresponds to reasonable absorbance of the other benzenoid species. We believe this may be the optimal wavelength for a fixed wavelength system for screening purposes. The second set of experiments involved variation of the laser wavelength in a narrow range around 266.7 nm, to investigate the possibilities for speciation.

The PID and REMPI chromatograms at a relatively low concentration of injected BTEX are shown in Figures 42 and 43. We wanted to have comparable REMPI signals for all four species in the mixture. We used solutions in which the benzene was 10 times more concentrated than the other species because 266.7 nm corresponds to a weak absorbance feature of benzene, with only about 5 percent of the signal of the strongest REMPI bands around 260 nm. Because the PID detector has comparable response factors for all four species, the benzene peak is much stronger in the PID chromatogram.

Background and impurity. Each injection involved 2 μL (approximately 2 mg) of methanol, approximately four to seven orders of magnitude more than the BTEX species. Even though the PID sensitivity is far higher for BTEX than for methanol and we have chromatographic separation, the tailing of the methanol peak is still evident in the PID chromatogram. Although we did observe an effect of the methanol passing through the REMPI cell also, it was much less. Moreover, the methanol levels in these experiments are far higher than we would expect to find in a real-world scenario. (Note the peak eluting at about 220 sec in the PID chromatogram. It apparently corresponds to some impurity in the mixture. We have not attempted to identify its chemical nature, but this does partially illustrate the selectivity of the REMPI detector.)

Resolution. The REMPI spectrum is not as well-resolved as the PID. Because of the low repetition rate of the OPO (10 pulses/second) and the slow data transfer time of the inexpensive digital storage oscilloscope used for these experiments, a datum was acquired only every 2.3 sec during the chromatogram

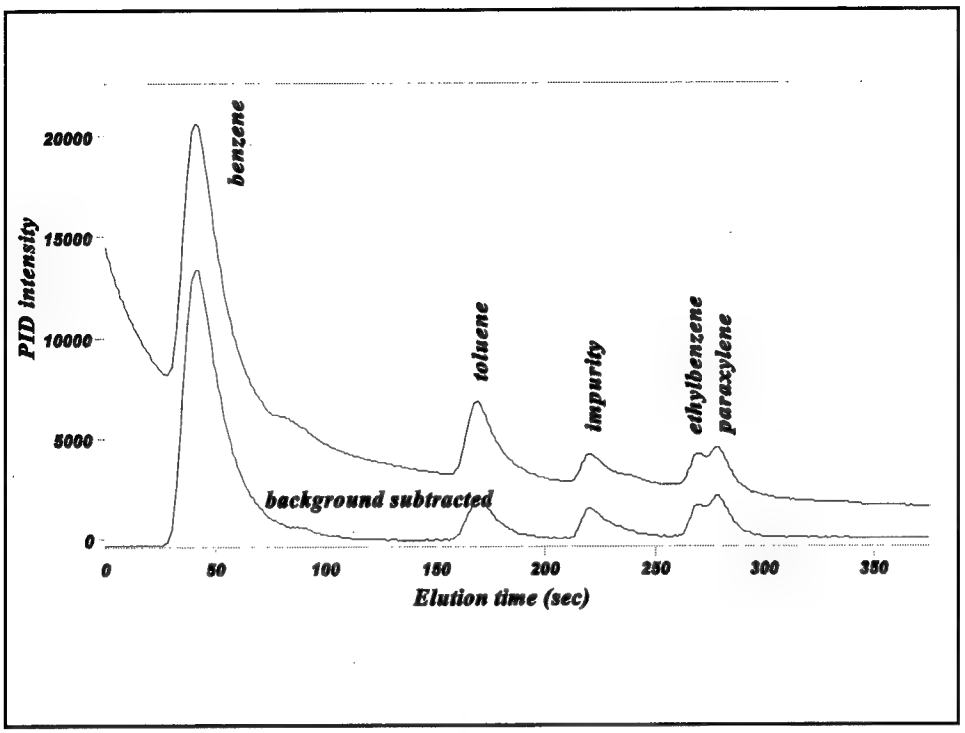

Figure 42. GC chromatogram using PID detection for injection of 10 ng benzene and 1 ng each of toluene, ethylbenzene, and p-xylene

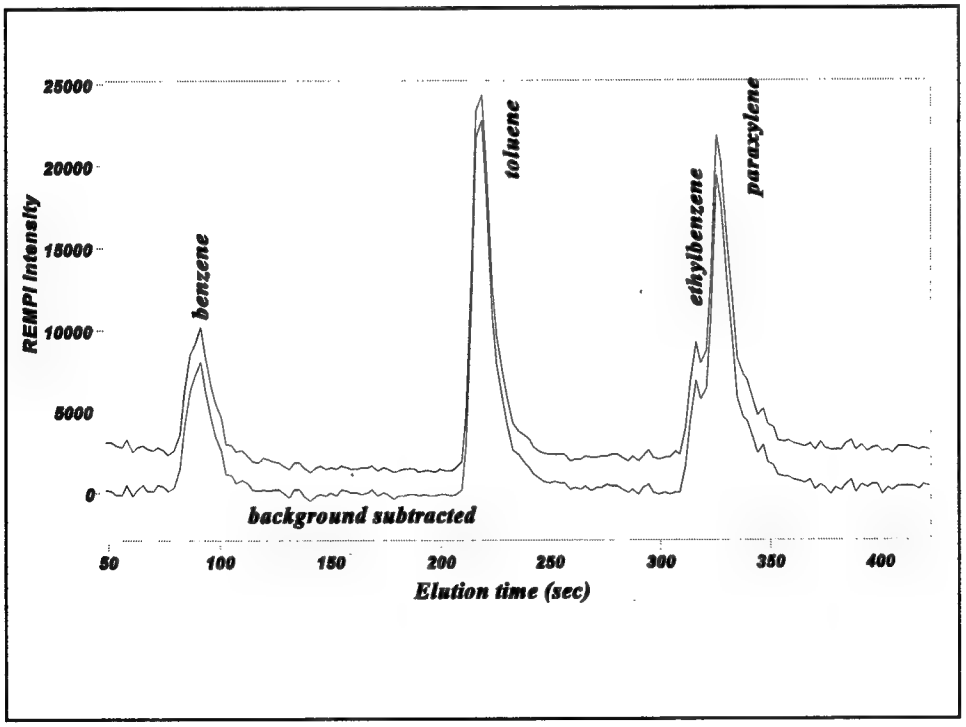

Figure 43. GC chromatogram using REMPI detection for injection of 10 ng benzene and 1 ng each of toluene, ethylbenzene, and p-xylene

versus 1 sec for the PID. It will be possible in the future to reduce the time per point to a small fraction of a second.

Calibration curves. Simultaneous PID and REMPI chromatograms were measured for injections of toluene, ethylbenzene, and p-xylene in the range of 0.25-20 ng. The corresponding benzene masses were 10 times greater. A correlation of the REMPI and PID results on a log-log format is shown in Figure 44. The ethylbenzene (E) and p-xylene (X) features were treated together as a single component in this analysis owing to their overlap. If one assumes the PID data represent a primary standard, then "perfect" REMPI performance would be a straight line with a slope of one for each component. The linear behavior is found, but the observed slopes are 0.88 for toluene, 0.91 for ethylbenzene + p-xylene, and 1.17 for benzene. The deviation from unit slope is presumably due to a nonlinearity in the response of one or both detectors. For reasons which are not completely understood at this time, the scatter in the data is significantly higher for toluene than for the other components. It appears that wavelength drift of the OPO during a 3-hr interruption in the data collection is a contributing factor, but a more in-depth analysis is hampered by the relatively broad spectral output of the OPO (see below).

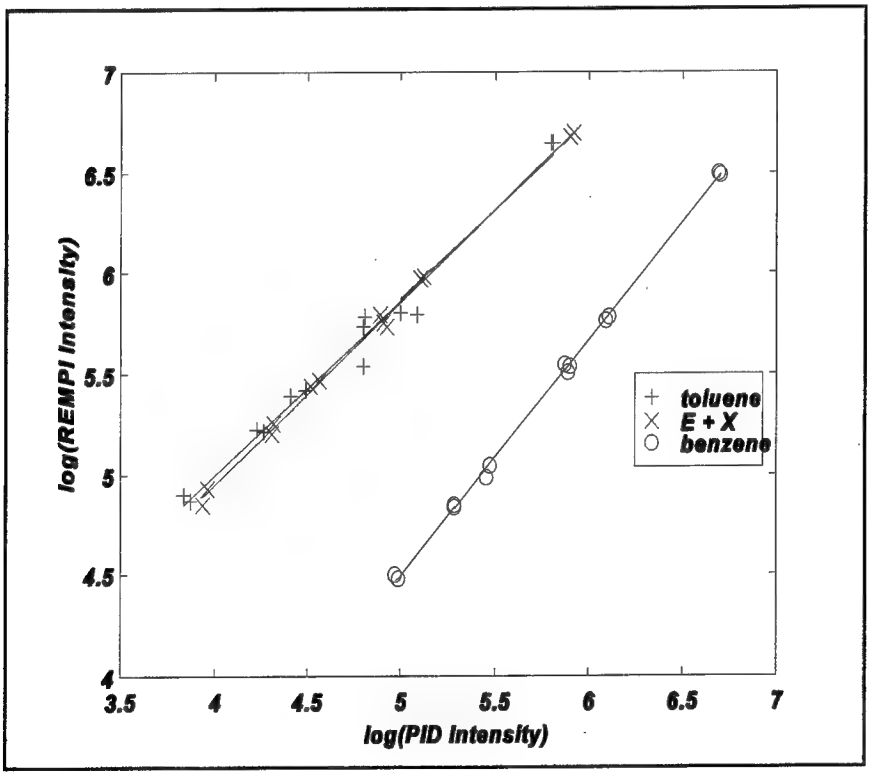

Figure 44. Correlation of PID and REMPI detectors using simultaneous GC chromatographic detection

Wavelength dependence of the REMPI chromatograms. The relative absorbance spectra, normalized to the highest value occurring in the wavelength

range between 265.5 and 267.5 nm were shown in Figure 39. The nominal resolution of the spectrophotometer used in these measurements is 0.1 nm, and the digitized data were taken in increments of 0.1 nm. We note several important features:

a. Benzene and toluene have nearly coincidental absorbance features near 266.7 nm.

b. Ethylbenzene and p-xylene also absorb well at about the same wavelength.

c. The corresponding absorbencies at 266.0 nm, corresponding to the fourth harmonic of Nd:YAG, are substantially lower, particularly for benzene.

The absorbance spectra are an excellent guide to what is possible with REMPI. We have previously shown that there is an excellent overall correspondence between the REMPI spectra and conventional absorbance spectra for benzene and toluene, which shows that the selectivity of 1+1 REMPI is predominately associated with the excitation of the initial resonance, not the second (ionization) photoprocess. However, the REMPI spectra we recorded with the frequency doubled dye laser show slightly narrower features than in the absorbance spectra, indicating that the conventional absorbance spectra are instrument limited. The OPO used in these studies is relatively broad band. We measured output profiles with a monochromator and found bandwidths of 0.1-0.2 nm (of the frequency doubled output). In addition, the band profiles tended to be asymmetric in what appears to be random fashion. For this reason, we cannot comment in detail at this time on the ultimate degree of speciation which may be possible for real-time measurements by rapidly changing the laser wavelength. Nonetheless, the REMPI spectra generated from the GC chromatograms as the wavelength was varied for repeat injections of the same mixture are encouraging. These spectra are shown in Figure 45. It appears that a very good separation of the combined benzene/toluene contribution to the total REMPI intensity can be gained with a very small switch of the wavelength from 266.7 nm to about 266.5 nm. Similarly, a move of the wavelength of the ionizing radiation to 266.9 or 267.0 nm could be used to separate the benzene contribution.

Conclusion. We have demonstrated the extremely high promise of 1 + 1 REMPI for the detection of BTEX in air using a field deployable instrument. These results show that a portable BTEX detector is feasible to measure air concentrations at or below 1 ppbv. Interferences from common solvents such as methanol, aliphatic hydrocarbons (e.g., hexanes or heptane), and acetone are very low. Component discrimination and verification of "hits" can be accomplished by changing the laser excitation wavelength as well as via ion mobility spectrometry.

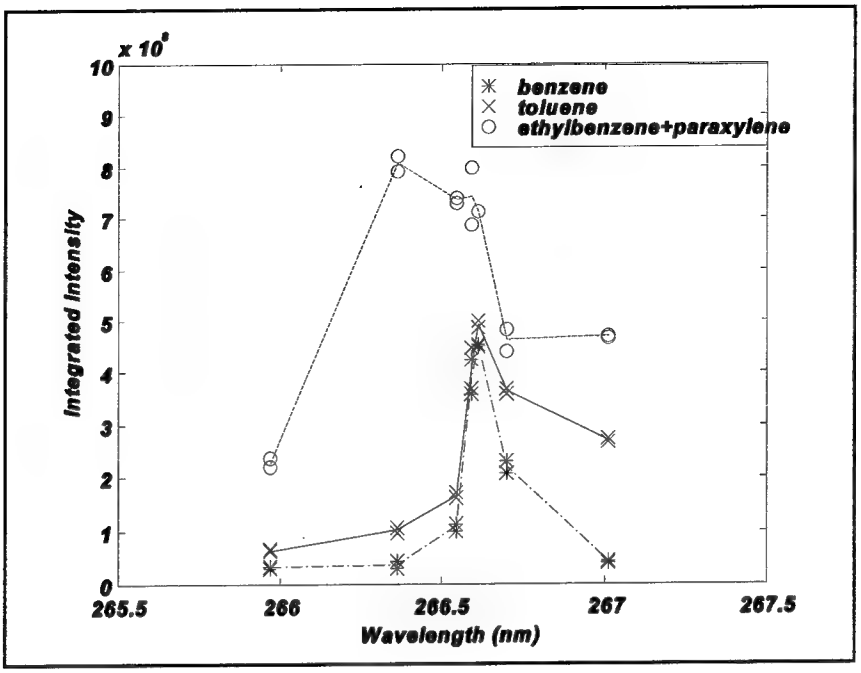

Figure 45. Comparison of benzene absorbance and GC/REMPI intensities as a function of wavelength

Explosives/Energetics Techniques

Photofragmentation/LIF sensing of explosives/energetics

Background. As stated in the introduction to this chapter, photofragmentation (PF) with LIF sensing was one of the technologies evaluated for SCAPS application as part of the original SERDP-funded project. The objective of this effort was to investigate the feasibility of adapting PF/LIF techniques to the detection of explosives in soils and groundwater using a SCAPS probe similar to the LIF probes for POL contaminants. The technique was based on successful experiments conducted by the Army Research Laboratory (ARL) and University of Iowa researchers (Lemire, Simeonsson, and Sausa 1993, and Simeonsson, Lemire, and Sausa 1994) for detecting vapor-phase nitro compounds using 266 -nm laser radiation. The method originally envisioned for SCAPS application would use a single laser to both fragment the explosive molecule and to raise the NO photofragment (characteristic of the explosive molecules of interest) to excited states that subsequently return to the ground state by emitting fluorescence photons.

Theory. The original work by Lemire, Simeonsson, and Sausa (1993) for detecting NO gases relied on laser PF followed by REMPI and detection via a time-of-flight mass spectrometer. Detection limits of 8 ppb and 24 ppb, respectively, for RDX and trinitrotoluene (TNT) vapors were established using this approach. In subsequent work, they demonstrated PF followed by LIF rather

than REMPI, which was then detected via a bandpass filter/photo multiplier tube detector. It is the latter approach that was evaluated for SCAPS implementation. In the initial SCAPS investigations, short wavelength (225 to 227 nm) laser energy was used to both photofragment and excite the energetic molecules. The reactions pertinent to the PF/LIF approach to explosives detection may be written as follows:

$$R-NO_2+hv_1 \rightarrow R+NO(X^2\Pi)+O(^1D,^3P) \quad (9)$$

$$NO(X^2\Pi)+hv_2 \rightarrow NO^*(A^2\Sigma^+,C^2\Pi) \quad (10)$$

$$NO^*(A^2\Sigma^+,C^2\Pi) \rightarrow NO(X^2\Pi)+hv_3 \quad (11)$$

where

R-NO2 represents the explosive molecule containing one or more -NO2 functional groups; Equation 9 represents the laser photofragmentation step yielding NO; Equation 10 represents the laser excitation of NO; and Equation 11 represents the resultant NO fluorescence. The processes depicted by Equations 9 and 10 are very fast and efficient since they occur in the duration of the laser pulse (~10 nsec) and require relatively small amounts of laser energy (tens of mJ). Also, hv1 = hv2 since the same laser frequency is used for both photofragmentation and subsequent fragment excitation. The process depicted by Equation 11 depends on the NO A2$\sum$+ and C2$\prod$ radiative lifetimes, approximately 200 and 20 nsec, respectively, and quenching rates for various species at a particular pressure (Sausa et al. 1996).

Laboratory evaluations of this approach identified several major technical challenges to transitioning directly to a SCAPS probe. Problems associated with optical fiber attenuation and/or downhole generation of short wavelength UV light, difficulties in rejecting the scattered laser energy from the fluorescence signal (both of which are very close to 226 nm), as well as the presence of interfering fluorescence from sapphire window used in SCAPS probes and from chemicals and minerals in the soils. As a result, the focus of this research was directed at modifying the PF/LIF to use longer-wavelength laser excitation. The thrust of this effort was to demonstrate that multiphoton processes could achieve results similar to those obtained using 226 -nm photons. The theory of multiphoton processes was described previously in the REMPI discussion, but briefly, the objective of the PF/LIF effort was focused on evaluating the efficacy of two-photon excitation at longer wavelenghts (300 to 500 nm) to fragment explosives molecules and excite NO fluorescence.

Experimental. The experimental setup used to demonstrate proof-of-principle for SCAPS application consisted of a tunable, pulsed dye laser with frequency-doubling capabilities, a variable pressure cell equipped with a photomultiplier tube coupled to a band pass filter or spectrometer, and a data acquisition and analysis system consisting of a 125-MHz digital oscilloscope,

boxcar integrator, and PC (Sausa et al. 1996). Initial TNT measurements were conducted in the gas phase where the TNT sample was heated in a vial immersed in an oil bath, and the vapors interrogated in room air at 1 atmosphere pressure (atm). The temperature was used to calculate the partial vapor pressure and concentration of TNT.

Results. Laboratory experiments verified that measurable fluorescence signals were obtained from NO, NO2 , and TNT gasses when excited at 226 nm, 382 nm, and 452 nm. Unfortunately, these tests demonstrated that the lowest detection limit obtained for TNT (in the gas phase, at 1 atm) was 60 ppm. In addition, no detectable NO levels were produced when solid or liquid phase TNT samples were excited by laser energy in these ranges.

Conclusion. Laboratory experiments conducted at ARL and WES determined that lasers operating in the 382 to 452 nm region were not effective in photofragmenting solid or liquid phase TNT molecules and that a heat source (similar to that used in the SCAPS electrochemical TNT sensors) would be required to volatilize and fragment the TNT molecules to produce sufficient NO gas for sensing via LIF. This approach would provide no advantage to the existing electrochemical probes, since both would be restricted to operation in the vadose zone. The PF/LIF probe would be more complex/costly, and the limits of detection would be more than an order of magnitude higher than electrochemical methods. As a result, the PF/LIF effort was discontinued from the SERDP SCAPS project, and a more promising technology based on a fiber optic biosensor for groundwater applications was proposed and accepted by the SERDP Peer Review Panel and the Executive Office.

SCAPS fiber-optic explosives biosensor groundwater probe

The objective of this task, which was added at the recommendation of the third Peer Review Panel in 1997, was to interface the Naval Research Laboratory (NRL) Fiber-optic Explosives Biosensor (FEB) to the Hydrosparge II VOC Sensor (HSII). The objective of this effort was to develop a combined sensor that would be capable of detecting explosives contaminants in groundwater at multiple depths during a single SCAPS penetration. The NRL originally developed the FEB for ex situ detection of TNT in groundwater sampled from conventional or direct push wells (Shriver-Lake, Donner, and Ligler 1997). As part of this SERDP-funded effort, the NRL developed a fiber-optic explosives biosensor for RDX and combined it with the TNT sensor to make a combined sensor.

The original FEB used <1-m fiber to interface the biosensing fiber module to the fluorometer detector module. Operation of the FEB with the HSII would require transmission of the biosensor fluorescent signal from downhole to the fluorometer operated in the SCAPS truck. Therefore, during this project the FEB was operated over long lengths of fiber (50 m). Laboratory experiments indicated there was no significant loss of signal or sensitivity when the FEB was operated with 50 m of fiber-optic cable.

The HSII was designed to allow multiple groundwater samplings and analyses in a single SCAPS penetration. The probe has a pneumatic piston sampling port opening into a 40-mL chamber designed to collect a 30-mL groundwater sample. Once the groundwater is sampled and analyzed at a particular depth, the port is opened and the groundwater sample is expelled. The probe is then advanced to the next sampling depth and the process repeated. Laboratory test of the HSII probe indicated the design worked well in relatively clean, nonsilty groundwater.

During the period of execution of this project, the HSII was field tested for the detection of VOC contaminants in groundwater. Two field tests were conducted at sites with clay and flowing sands. The piston port allowed soil to flow into the sample chamber, causing the piston to malfunction. The probe was modified with the addition of a fritted filter to protect the piston. The third field test of the modified probe was performed at a site with silty groundwater. The probe functioned correctly about 50 percent of the time (i.e., multiple groundwater sampling and analysis events in a single penetration). The remainder of the time the HSII obtained no water due to clogging of the fritted filter.

The ultimate implementation of the combined FEB with the HSII will depend on the function of the HSII in situ under actual field conditions. Although the FEB was demonstrated to be capable of interfacing to the HSII, additional modifications are required before any benefit can be achieved from interfacing the FEB to the HSII. The SERDP funding for this task was withdrawn. No additional work on this prototype SCAPS sensor was conducted.

Transition

The Nitrogen and Tunable LIF systems were successfully transitioned to the ESTCP Dem/Val program and were certified for environmental screening applications by the USEPA, the California EPA, and the Interstate Technology Regulatory Cooperation (ITRC) Workgroup. The XeCl LIF system has been incorporated in the Navy-operated SCAPS trucks operated by Naval Facilities Engineering Command. The microchip laser-based LIF probe has successfully transitioned to the ESTCP Demonstration/Validation Program. In addition to the LIF probes described in this Applied Research Associates (ARA) have deployed LIF probes based on adaptations of the initial SCAPS LIF sensor design.

4 Research Area III: Fiber Optic Raman Sensor (FORS)

By: Bruce J. Nielsen, USAFRL
Gregory D. Gillispie, DTI
Stephen H. Lieberman, SPAWAR
Pamela A. Mosier-Boss, SPAWAR

Introduction

TCE is the cause of many groundwater contamination problems and has been found in at least 791 of the 1,300 hazardous waste sites on the National Priorities List identified by the EPA. Over the years, a real-time method for detection of TCE in the soil has been elusive. Although LIF, via fiber optics, is an accepted technique for real-time detection of polyaromatic hydrocarbons in soil and groundwater, TCE does not fluoresce and therefore LIF cannot be utilized. TCE has been identified by Raman spectroscopy using fiber-optic probes. Previous laboratory studies have also confirmed that neat TCE can be identified using a 35-m fiber-optic probe. However, the inherent weakness of the Raman signal, the attenuation in the fiber-optic probe, and luminescent background often make remote Raman spectroscopy difficult.

Under SERDP support, two parallel approaches for the implementation of Raman sensors for SCAPS applications were investigated. The Air Force efforts concentrated on Resonance Raman enhancement. The initial objective of the Navy program at SPAWAR was to develop a fiber-optic sensor based upon conventional Raman spectroscopy. However, despite the advances in instrumentation in recent years, it was found that a sensor based upon conventional Raman spectroscopy was hampered by the insensitivity of the technique. The SPAWAR program was redirected to develop a fiber-optic sensor based upon surface enhanced Raman spectroscopy (SERS) via thiol coated substrates.

Resonance Enhancement

The objective of this effort was to determine the degree of resonance enhancement of TCE solutions at laser excitation wavelengths of 355, 299, and 266 nm.

Experimental. It has been extolled that resonance enhancement can yield an increase of several orders of magnitude in the Raman cross section. However, the enhancement varies from molecule to molecule and may be small, or not affect the Raman cross section at all. The degree of resonance enhancement in neat TCE and a mixture of TCE and hexanes was calculated.

The excitation wavelengths for this experiment were 355, 299, and 266 nm. The 355- and 266-nm lights were generated from a Quanta Ray GCR 11, 10 Hz Nd:YAG laser, third and fourth harmonic, respectively. The 299-nm light was generated from a custom-built molecular hydrogen Raman shifter. Focusing the fourth harmonic of the Nd:YAG laser into the Raman cell yields wavelengths of light shifted from the excitation source in intervals of 3760 cm^{-1}, the vibrational frequency of molecular hydrogen. The shifted wavelengths were dispersed with a Pellin Broca prism. All wavelengths except the first stokes-shifted wavelength, 299 nm, were spatially filtered.

The excitation light was focused into a fiber-optic probe and delivered to a cuvette with side excitation. The scattered photons were collected at 90 deg from the excitation source and imaged into a Chromex 500IS imaging spectrograph with f-matched optics. The spectrograph, controlled by software provided by the manufacturer, has a 1,200-grove/mm grating. The slit widths were set at 10 μm. At the exit plane of the spectrograph, a Princeton Instruments thermo-electric cooled (-42 °C) CCD camera (1,024 × 256 pixel array) was mounted. To reduce on spherical aberration only some of the pixels were used, pixels 1,024 × (110 to 40). The CCD camera was controlled by a controller box via WinSpec software from Princeton Instruments. The output of the CCD camera was downloaded to a PC for further analysis.

Discussion

Since the Raman scattering intensity is proportional to $1/\lambda^4$, a normalization process had to be implemented to distinguish between resonance enhancement and normal $1/\lambda^4$ enhancement. We assumed that the C-H stretches would show no enhancement beyond the $1/\lambda^4$ dependence and could be used as internal normalization. Since benzene and toluene should show no resonance enhancement between 355 and 299 nm, spectra of benzene and toluene were taken at these two wavelengths to test this hypothesis. The benzene spectra were normalized to the 3,100-cm^{-1} C-H stretch and the toluene spectra were normalized to the 3,100-cm^{-1} stretch. Since little enhancement of the C=C bond (» 1,000 cm^{-1}) and other bonds can be found (Figures 46 and 47) upon

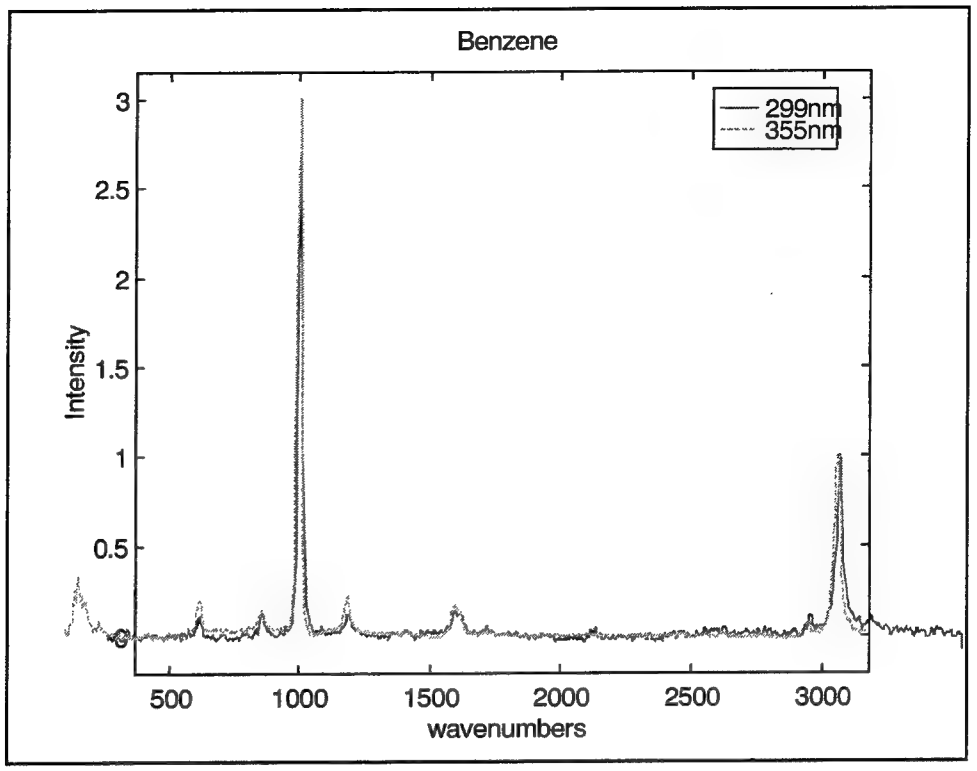

Figure 46. Neat benzene excited at 299 and 355 nm

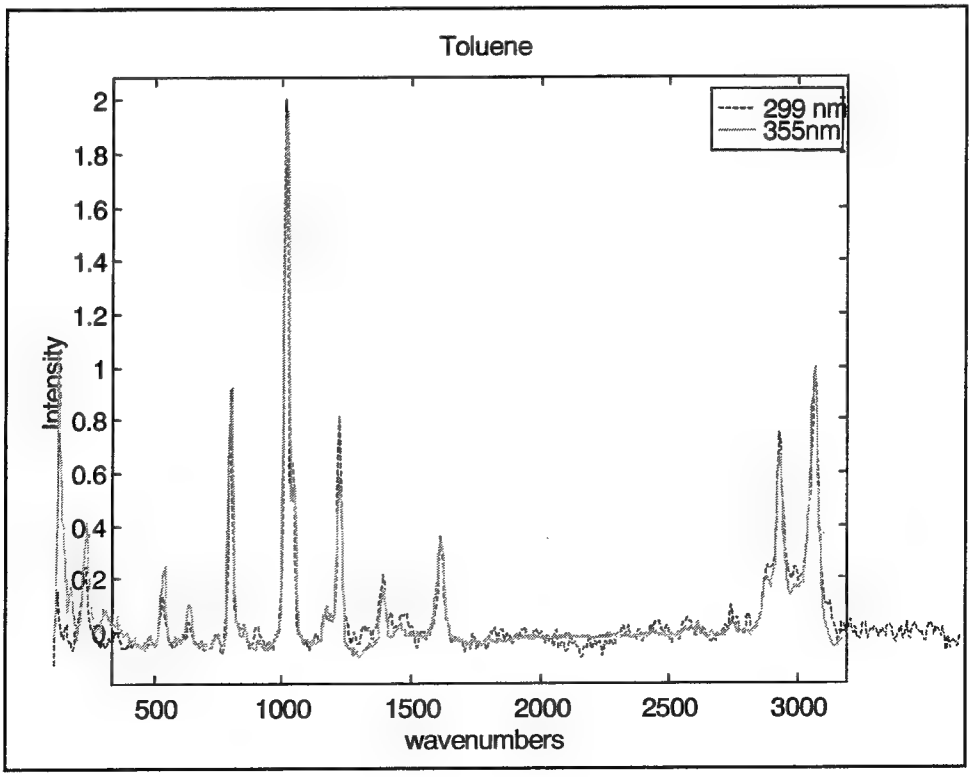

Figure 47. Neat toluene excited at 299 and 355 nm

normalizing the spectra to the C-H stretch, we decided our assumption was correct.

Spectra of neat TCE were collected at 355 and 299 nm. Upon normalization to the C-H stretch at 3,100-cm^{-1} the ratio of the C=C stretch, 1,589-cm^{-1}, showed an enhancement factor of 1.9 beyond the $1/\lambda^4$ enhancement. The Raman bands below 1,000 cm^{-1} showed a negative enhancement, (decrease in signal) when 299 nm was compared to 355 nm. This is caused by reabsorption of the Raman scattered photons by the TCE (Figure 48).

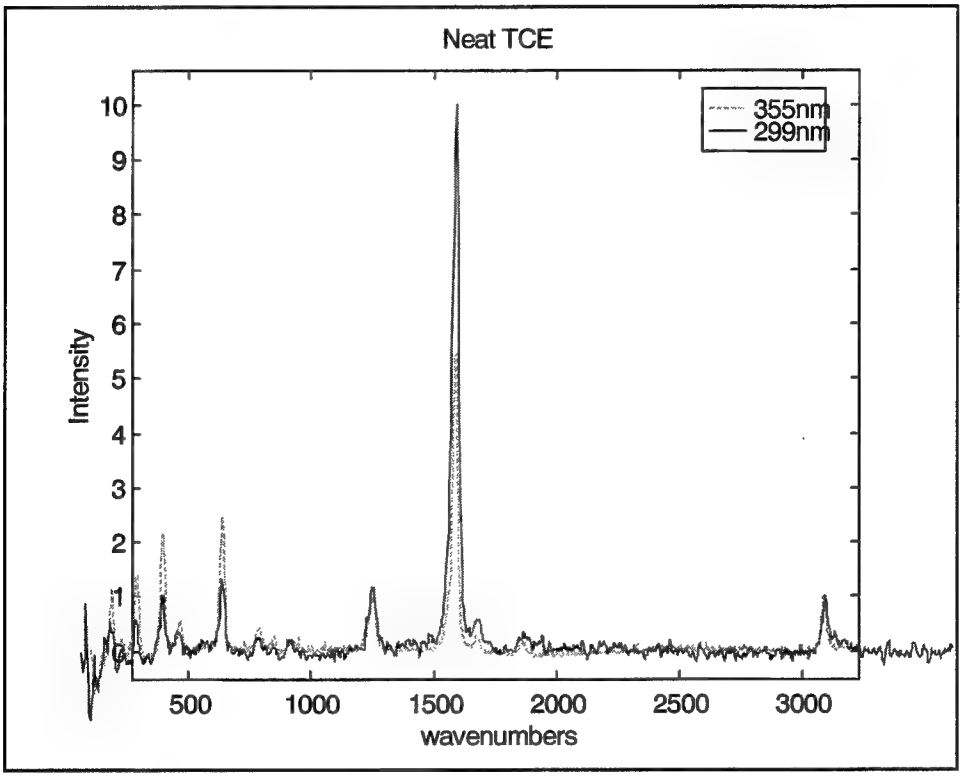

Figure 48. Neat TCE excited at 299 and 355 nm

Neat TCE absorbs 266 nm light so strongly that no Raman scatter could be detected. This is due to complete absorption of the excitation source and/or reabsorption of the Raman scattered photons.

Samples of TCE in hexanes do yield a Raman signal. Spectra of 1 percent and 10 percent solutions (by volume) of TCE in hexanes were collected. Both solutions were normalized to the 2,865 cm^{-1} C-H stretch of hexanes. The enhancement of the C=C stretch, 1,589-cm^{-1}, was compared between 266 and 355 nm. The enhancement of the 1 percent TCE solution could not be determined because the 1,589-cm^{-1} band is nearly unnoticeable with 355 nm excitation (Figure 49). Although the band was observed with 266-nm excitation, an enhancement factor would be difficult to assign. The enhancement factor for

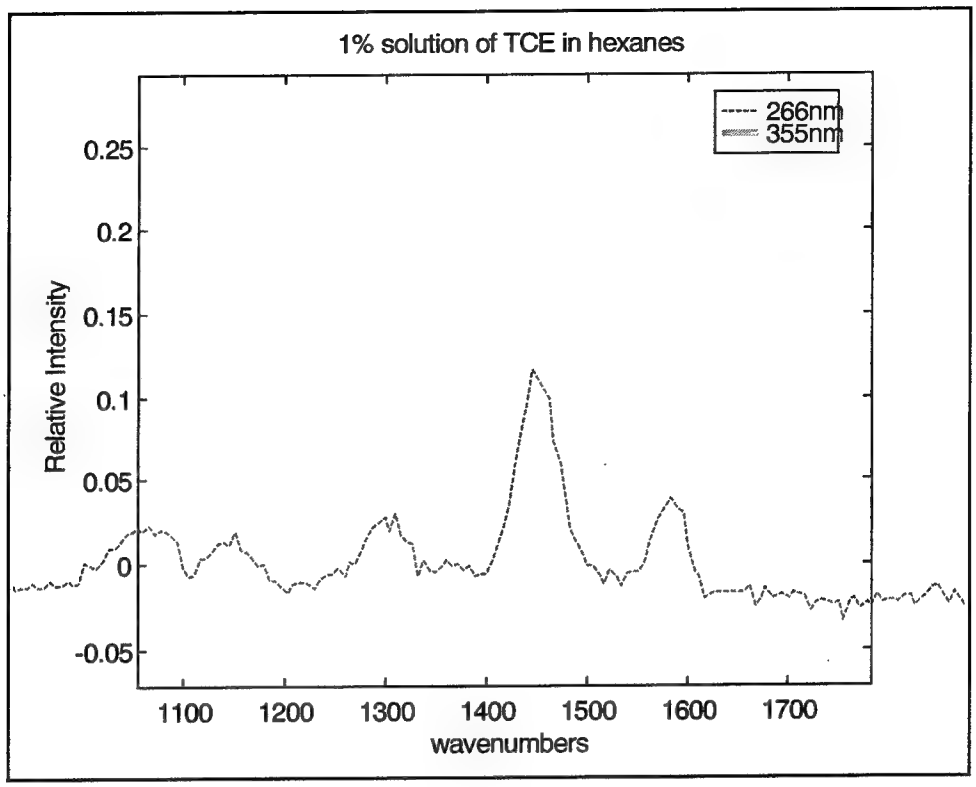

Figure 49. 1-percent TCE in hexanes excited at 266 and 355 nm

the 10-percent TCE solution determined by the ratio of the peak intensities is 3.78 (Figure 50).

Conclusions

The degree of resonance enhancement for TCE is modest, 1.9 for 299-nm and 3.78 for 266-nm excitations when compared to 355-nm excitation. The enhancement might be larger in dilute solutions than concentrated solution due to absorption and reabsorption effects. These experiments determined that the choice of excitation wavelength for field measurements depends more critically on factors such as fiber transmittance and total number of photons than resonance enhancement.

Raman intensity of TCE and TCE saturated sand samples. Signal to noise of the Raman intensity of neat TCE and TCE saturated sand were measured and compared.

Experimental. A custom-built frequency doubled Bethune cell dye laser, 292.5 nm, was pumped by the second harmonic of a Big Sky Nd:YAG laser operating at 50 Hz. The 6-ns excitation pulse was focused into a ST terminated fiber-optic probe. The probe consists of two optical fibers with a core diameter

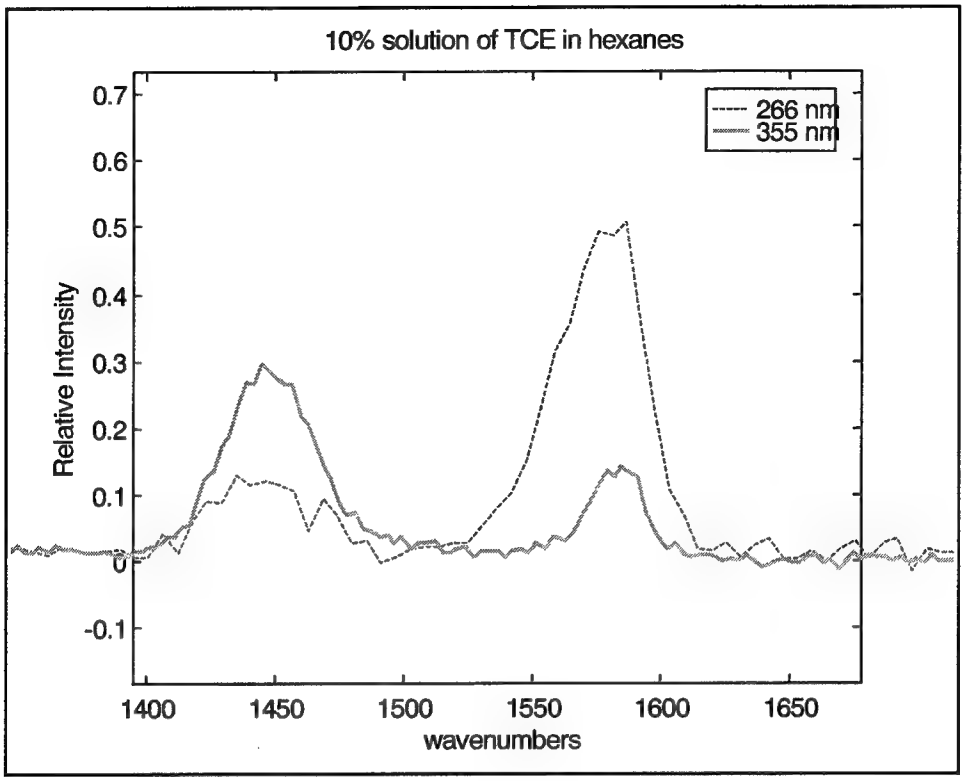

Figure 50. 10-percent TCE in hexanes excited at 266 and 355 nm

of 600 μm, 2 m long, one for excitation and the second for collection and delivery to the detector. The probe tip was placed perpendicular to the face of a quartz cuvette at a distance of 1 mm. The scattered photons collected by the second fiber were imaged into a ISA HR320 monochromator, with slits at 750 μm, and detected by a photo-multiplier tube (PMT). The output of the PMT was collected by a digital storage oscilloscope (Tektronix TDS 620A) and then downloaded to a PC for further analysis.

The TCE was placed in a quartz cuvette and a wavelength time matrix was collected between 305 to 314 nm in 0.25-nm increments. This range incorporates the 1,589 cm^{-1} stretching of the C=C double bond with 292.5-nm excitation. The cuvette was then filled half full with sand. The TCE was poured into the cuvette until it was 7 mm above the level of the sand and left to settle and saturate the sand for 10 min. After saturation, a wavelength time matrix was collected over the same wavelength region with the probe directed at the TCE saturated sand.

Conclusion. The most intense waveform of the neat TCE (85.9 mV) is five times larger than the most intense TCE saturated sand waveform (16.9 mV). Figure 51 shows the time integrated spectra of TCE (upper) and TCE saturated sand (lower). The time integrated spectrum is 14.6 times larger for the neat TCE (1.0663 nano-volt-seconds) compared to the TCE saturated sand (0.0730 nano-volt-seconds).

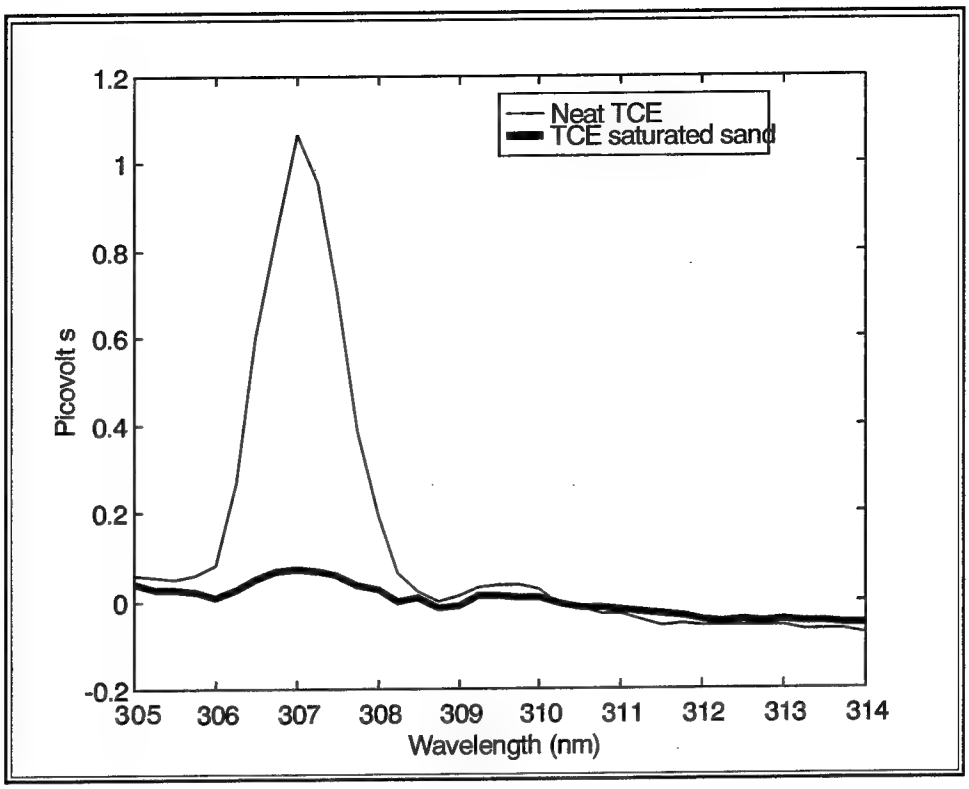

Figure 51. Time integrated spectrum of neat TCE and TCE saturated sand

FO Raman probe based on conventional Raman spectroscopy

Raman spectra can be obtained remotely over optical fibers in real-time and there have been significant advances in the development of inexpensive, portable Raman spectrometers and CCD detectors. The approach of SPAWAR was to take conventional, off-the-shelf technology to quickly build and field a FORS system. Technical issues that were addressed during development of the FORS probe included interferences due to Raman scattering emissions in the fibers, fluorescence interferences from the background, and low sensitivity.

Probe design

A cone penetrometer FORS sensor was built. A schematic of the sensor is shown in Figure 52. The system is comprised of a Chromex Raman One imaging spectrograph and a Princeton Instruments thermoelectrically cooled CCD detector with controller. The excitation source was a water-cooled, argon ion laser. The 488-nm line was focused into the excitation fiber using a 5X microscope objective lens. To reject the Rayleigh line, a holographic notch filter from Kaiser Optical Systems was used. The optical fibers used in the cone penetrometer probe were high *OH*, silica/silica clad, 70 m long, and 365 mm in diameter. To increase light collection efficiency, six collection fibers surround the single excitation fiber.

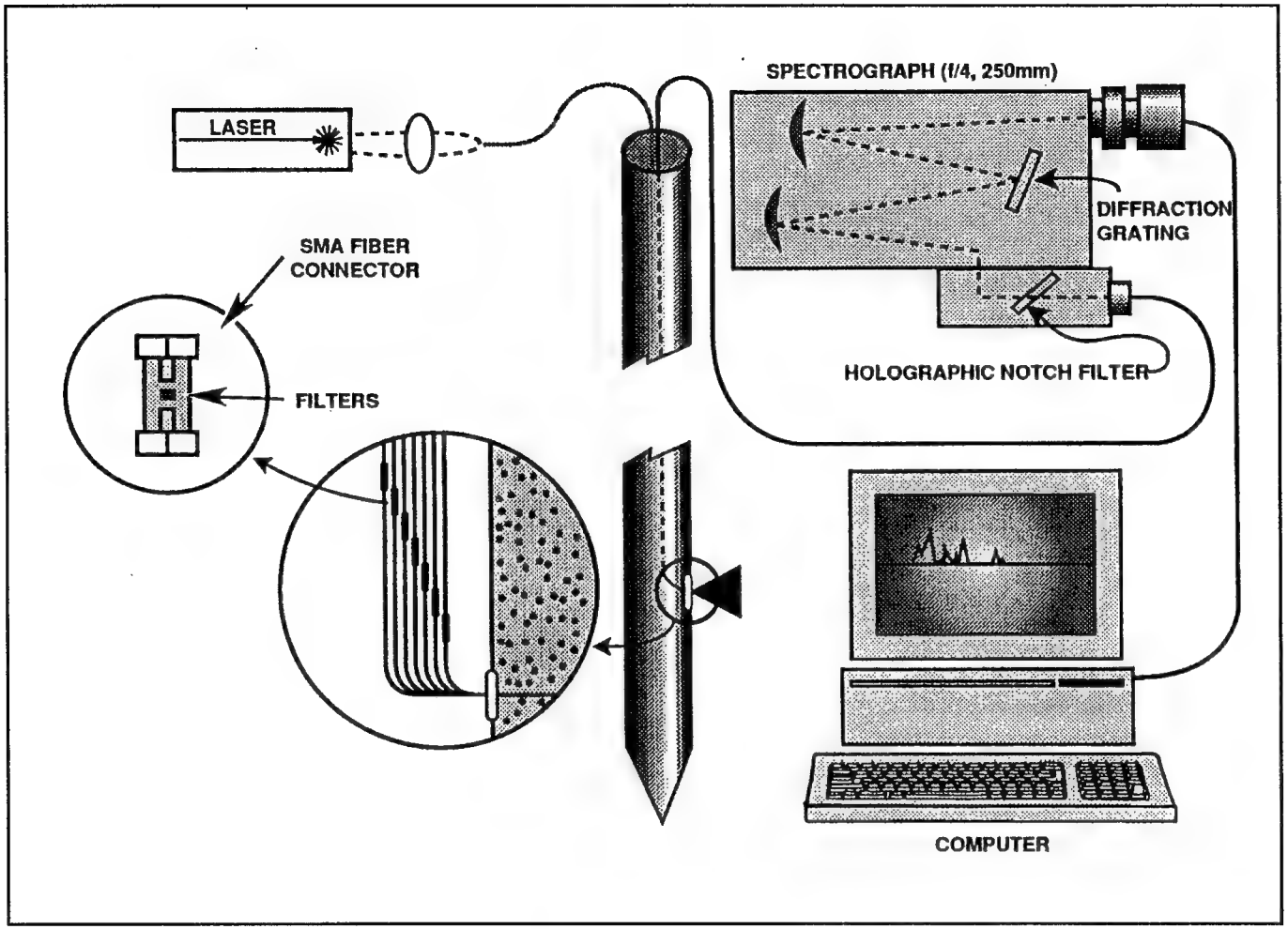

Figure 52. Schematic of FORS sensor for the cone penetrometer. Sensor consists of a single excitation fiber surrounded by six collection fibers. Inside the probe, each fiber is equipped with a filter module which houses bandpass filters for the excitation fiber and longpass filters for the collection fibers. These filters eliminate the interference due to fiber Raman emissions

The fiber bundle is oriented in a compound angle to minimize Rayleigh backscatter. To eliminate interferences due to fiber Raman emissions, filter modules housing bandpass filters for the excitation fiber and longpass filters for the collection fibers were spliced into the optical fibers. The filters were 3 mm in diameter and 1 mm thick. Because of their thickness, it was not necessary to use collimating lenses. Index matching gel was used between the terminated fibers and filters to increase light throughput. Raman spectra were obtained through an anti-reflection (AR) coated sapphire window. Instrument operation and data collection were under computer control. With few optical components, the probe exhibits very high light throughput and no alignment problems. Alignment was a consideration because the target compounds are chlorinated solvents. These materials make up a class of compounds referred to as dense nonaqueous phase liquids, DNAPLs. Because they are more dense than water, DNAPLs tend to migrate downward through the subsurface until they reach an impermeable layer. These materials will then migrate laterally following the structure of the impermeable layer. Since these materials exhibit low solubility in water, they are generally present as a separate liquid phase. Although Raman spectroscopy is an insensitive technique, it should be possible to detect the droplets of DNAPLs that separate out of the aqueous phase.

Laboratory Developments

In the laboratory, samples of naphthalene, toluene, and TCE were prepared on Fisher sea sand and on soil from Naval Air Station North Island (NASNI). Figure 53 shows Raman spectra and calibration curves obtained for naphthalene on Fisher sea sand and NASNI soil. The soil obtained from NASNI is darker and much finer than the Fisher sea sand. The Raman spectra in Figure 53 show that there is more fluorescence observed for the samples prepared from the NASNI soil. On Fisher sea sand, the main naphthalene peak at 1,375 cm^{-1} can be clearly seen for 5,000 ppm naphthalene. This peak is barely visible above the noise for 10,000 ppm naphthalene on NASNI soil. The calibration curves of naphthalene obtained for both Fisher sea sand and NASNI soil, Figure 53, are linear. However, the intensities of the naphthalene peaks are approximately four times stronger on Fisher sea sand. This is attributed to the fact that the NASNI soil is much finer than the Fisher sea sand. Finer soils have a higher surface area. Significantly different surface areas result in much different layer thicknesses on a grain for a given amount of contaminant. Since the sensor only 'sees' contaminants on the first grain layer at the grain/window interface, this results in a much lower response in high surface area materials.

On Fisher sea sand, 50,000 ppm TCE could not be detected. TCE is not as good a Raman scatterer as naphthalene. However, with the addition of water, droplets of TCE would separate out and those droplets could be detected. The same was not true for TCE samples prepared using NASNI soil. The results for toluene on the two soil types were similar to those obtained for naphthalene.

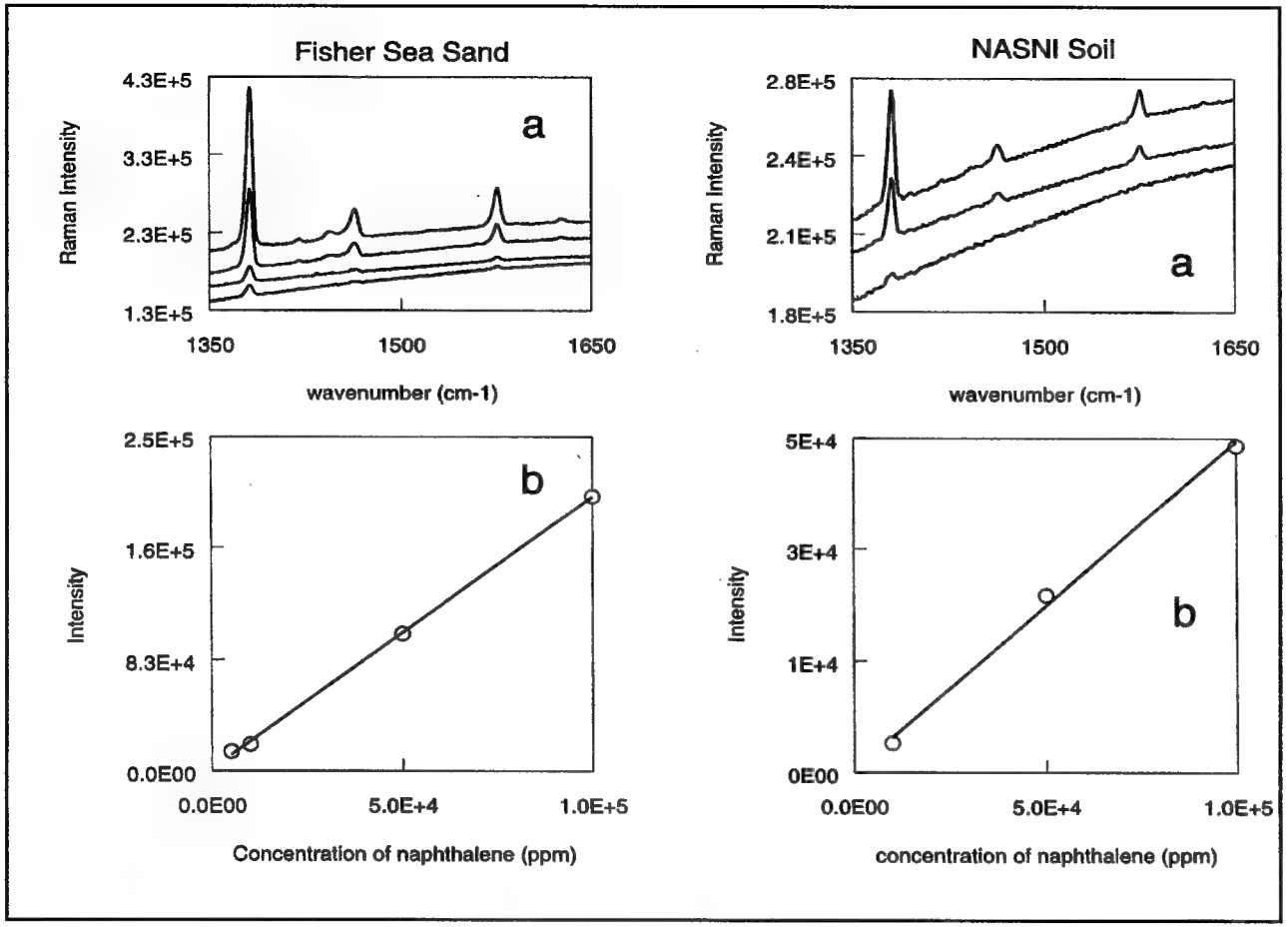

Figure 53. Summary of results obtained on Fisher sea sand and NASNI soil. Fisher sea sand: (a) Raman spectra obtained for naphthalene on Fisher sea sand. Concentration of naphthalene on Fisher sea sand (top to bottom) is 100,000, 50,000, 10,000, and 5,000 ppm; (b) Calibration curve plots intensity of the 1,375 cm^{-1} naphthalene peak, corrected for background, versus concentration of naphthalene in ppm; NASNI soil: (a) Raman spectra obtained for naphthalene on NASNI soil. Concentrations of naphthalene on NASNI soil (top to bottom) are 100,000, 50,000, and 10,000 ppm; (b) Calibration curve plots intensity of the 1,375 cm^{-1} naphthalene peak, corrected for background, versus concentration of naphthalene in ppm

Field Investigations

The performance of the probe was demonstrated at a site at NASNI in which the contaminants of primary concern are chlorinated solvents. The geological data indicated that the site is a low-lying coastal area of shallow groundwater with seawater intrusion. Groundwater occurs approximately 8 ft below ground surface (bgs). The upper 250 ft consists of a 100-ft sand layer, a 14-ft-thick 'B' clay layer, another 40-ft sand layer, followed by a 30-ft-thick 'C' clay layer. There is no evidence of hydraulic continuity between the two water-bearing zones. Monitoring wells indicated the presence of chlorinated solvents above the 'B' clay and nothing above the 'C' clay. In July 1995 the FORS probe was deployed in a cone penetrometer on a 20-ton truck. The probe was robust and survived pushes through shell beds and compacted soils. However, the probe reached refusal at a depth of 85-ft bgs -- 5 to 10 ft shy of the surface of the 'B' clay.

Conclusion

The laboratory results indicate that field investigations using a sensor based on conventional Raman spectroscopy are hampered by matrix effects. Besides fluorescence interference, the surface area of the soil affects the intensity of the signal. Despite these effects, the greatest limitation of conventional Raman spectroscopy is still sensitivity. For this technology to be useful as a practical SCAPS solvent sensor, it was determined that the Raman signal needs to be enhanced.

Surface Enhanced Raman Spectroscopy

In the 1970s, it was discovered that Raman scattering from molecules adsorbed on such noble metals as silver, copper, or gold can be enhanced by as much as 10^6 to 10^7. The SERS can be done electrochemically or on chemically modified surfaces. Of the two SERS approaches, the coated SERS substrates were considered to be the most promising for the following reasons: (a) coated substrates can be used for both vapor and aqueous phases and, consequently, can be used in both the vadose and saturated zones; (b) the coated substrates can be thought of as a `static' chromatographic system, *i.e.*, coatings can be chosen which will selectively adsorb the contaminants of interest; (c) the SERS spectrum of the coating can act as an internal standard for calibration purposes; (d) the coating increases the lifetime of the SERS substrates from minutes or hours to months and the coated substrates are reusable; and (e) unlike electrochemical SERS, the Raman peaks of the contaminants adsorbed into the coating directly correspond with those of the neat compounds thereby facilitating species identification. As a result of these considerations, the program was redirected to develop a solvent sensor based upon thiol coated SERS substrates. Technical issues which needed to be addressed included preparation and

characterization of thiol coated SERS substrates, design and construction of a sampler probe, and design and construction of a SERS sensor module to go inside the sampler probe.

Response of Thiol-Coated Substrates

Figures 54 through 56 show Raman spectra for 3-chloro-1-propanethiol, 4-chlorobenzyl mercaptan, and 4-chlorothiophenol on chemically etched silver. These spectra are typical for the thiol-coated silver substrates. As shown in Figures 54 through 56, the monolayer coating on the SERS substrate displays a characteristic Raman spectrum and the Raman bands of the coating can be used as an internal standard for calibration purposes. The spectra also indicate that when choosing a coating, not only is chemical affinity a consideration, but there is also the availability of a spectral window to allow detection of an analyte. Of the three thiol coatings shown in Figures 54 through 56, the Raman spectrum of 4-chlorobenzyl mercaptan (Figure 55) is the most complex. Besides the ring vibrational modes at 490 to 550, 800 to 860, 1,050 to 1,120, and 1,550 to 1,590 cm^{-1}, the spectrum for 4-chlorobenzyl mercaptan exhibits peaks due to *C-Cl* out of plane deformation (320 to 480 cm^{-1}), CH_2 wag, and *C-S* stretch of a CH_2S group (620 to 770 cm^{-1}), and CH_2 wag and twist (1,140 to1,250 cm^{-1}). Despite the complexity of the spectrum of the coating, we can clearly see the Raman peaks of toluene at 538, 793, 1,003, and 1,028 cm^{-1} as it partitions into the coating both in the gas and aqueous phases, Figure 55. Figure 55 shows spectra obtained for toluene saturated water both in the presence and absence of the 4-chlorobenzyl mercaptan coated silver substrate. In the absence of the substrate, we can barely see the dominant toluene peak at 1,003 cm^{-1}. However, with the substrate present, toluene partitions into the coating and there is a considerable enhancement of the vibrational modes of toluene. Furthermore, the spectral features (*i.e.*, number of peaks as well as the shape, intensity, and position of those peaks) of the toluene peaks observable in the spectrum of the coating, Figure 55, are very similar to those observed in the spectrum obtained for neat toluene. The results obtained for benzene in 3-chloro-1-propanethiol, Figure 54, and PCE in 4-chlorothiophenol, Figure 56, are similar to those obtained for toluene in 4-chlorobenzyl mercaptan. The response of the coated substrates to the analytes is instantaneous and reversible. The coating protects the surface from deterioration. Consequently, it is expected that several samplings can be done using a single substrate.

The function of the thiol coating is to concentrate the hydrophobic organics at the SERS interface. Therefore, the use of thiol-coated SERS substrates essentially combines spectroscopy with chromatography. In order for the analyte to be detected, it must adsorb onto the substrate. Coatings are chosen that have an affinity for the analyte. The extent to which an analyte concentrates is related to its adsorption coefficient. This, in turn, depends upon the energetics and kinetics of adsorption. The energetics of adsorption include the equilibrium constant and its temperature variation, free energy, heat and entropy of adsorption, their variation with coverage, the activation energy for adsorption and desorption, and the strengths of the bonds involved in the adsorption process

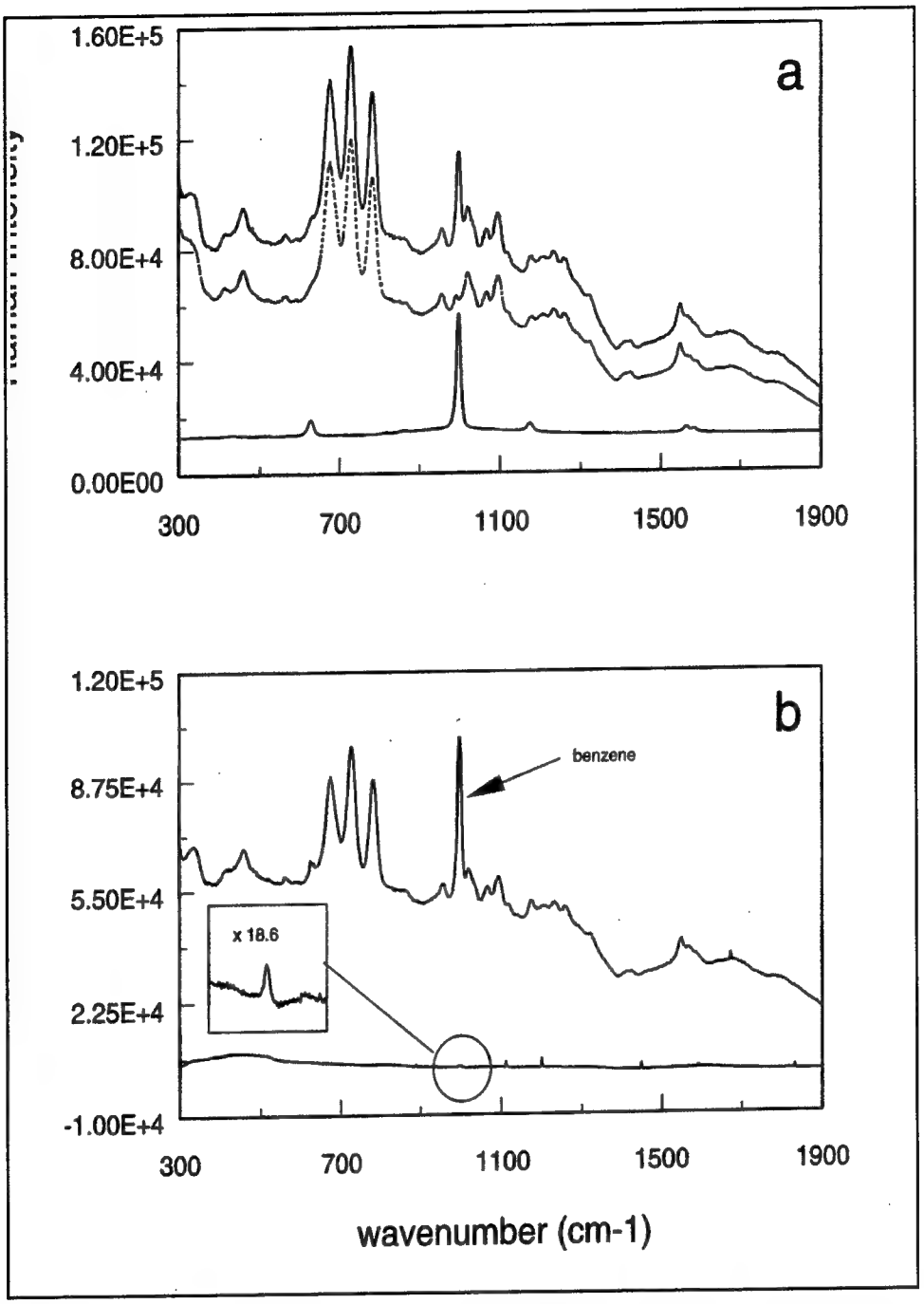

Figure 54. Raman spectra of 3-chloro-1-propanethiol adsorbed on chemically etched silver: (a) Top two spectra are of 3-chloro-1-propanethiol, the gray spectrum is of the substrate, and the black spectrum shows benzene partitioning into the coating from the gas phase, the bottom spectrum is that obtained for neat benzene and this spectrum is superimposed upon the spectra for 3-chloro-1-propanethiol; (b) Raman spectra of benzene saturated water both in the presence (top) and absence (bottom) of a 3-chloro-1-propanethiol coated silver substrate

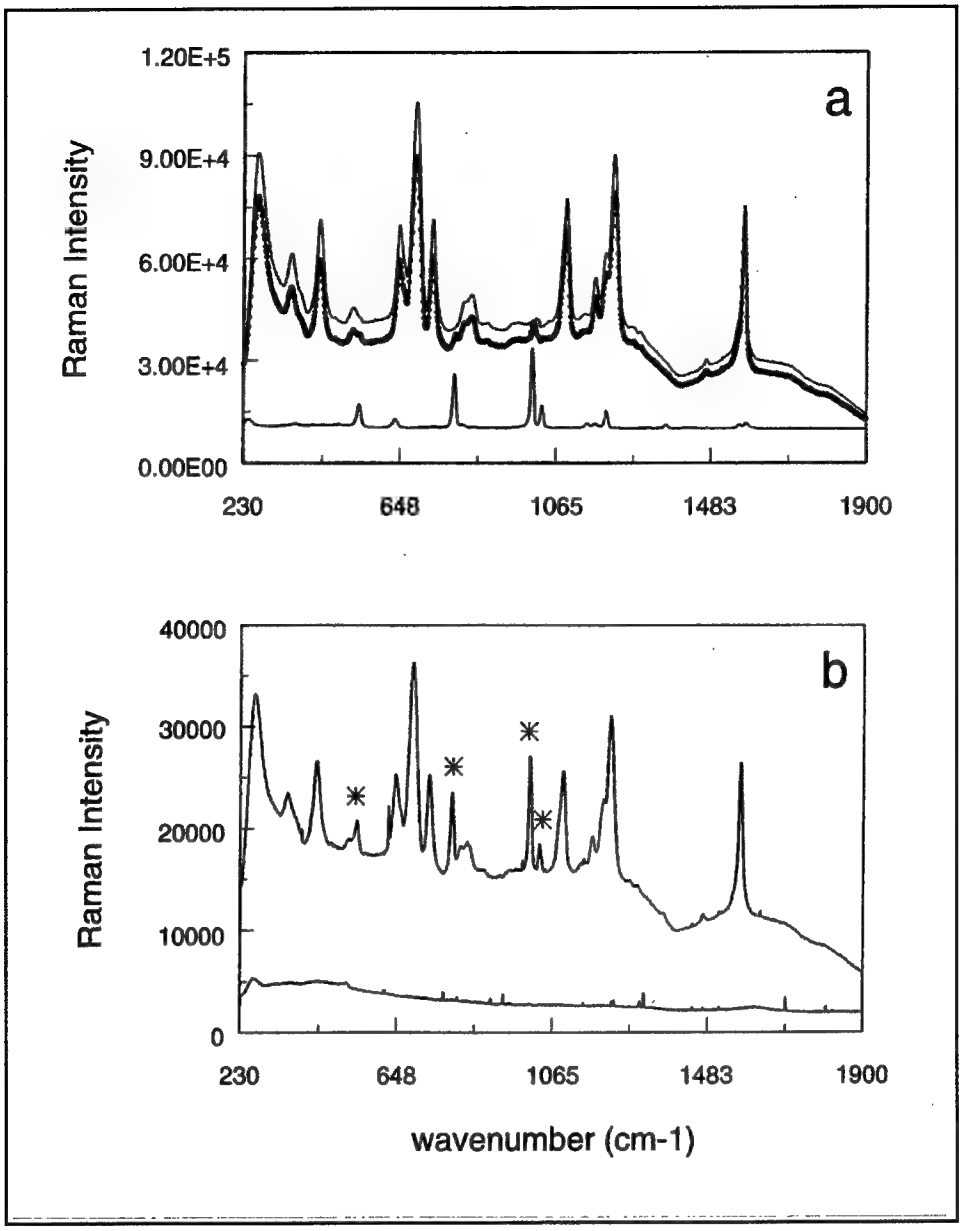

Figure 55. Raman spectra of 4-chlorobenzyl mercaptan adsorbed on chemically etched silver: (a) Top two spectra are of 4-chlorobenzyl mercaptan, the gray spectrum is of the substrate, and the black spectrum shows toluene partitioning into the coating from the gas phase, the bottom spectrum is that obtained for neat toluene and this spectrum is superimposed upon the spectra for 4-chlorobenzyl mercaptan; (b) Raman spectra of toluene saturated water both in the presence (top) and absence (bottom) of a 4-chlorobenzyl mercaptan coated silver substrate, the toluene peaks are designated by asterisks (*)

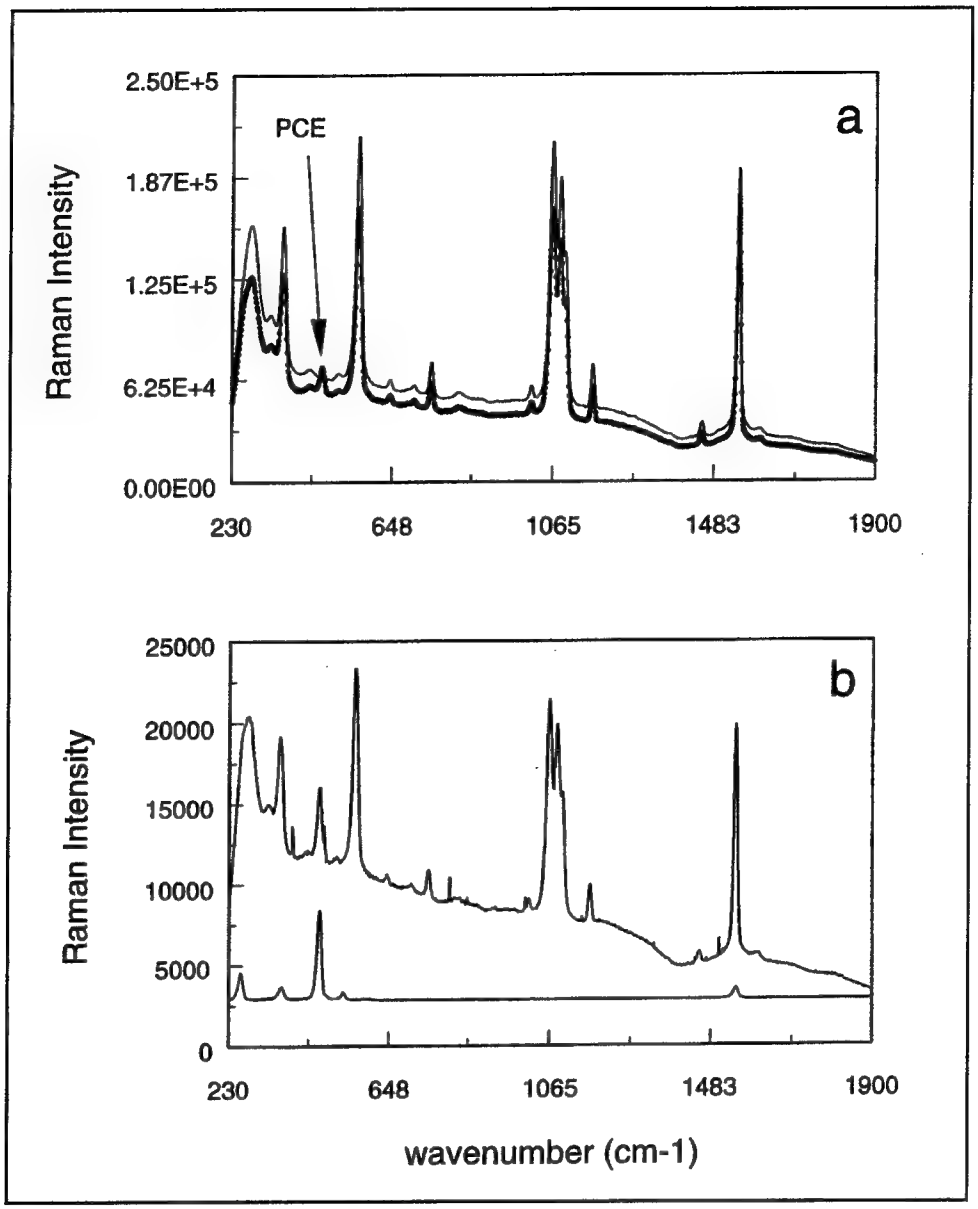

Figure 56. Raman spectra of 4-chlorothiophenol adsorbed on chemically etched silver: (a) Gray spectrum is of the substrate, and the black spectrum shows PCE partitioning into the coating from the gas phase; (b) Top spectrum shows PCE partitioning into the coating from PCE saturated water, the bottom spectrum is that obtained for neat PCE, and this spectrum is superimposed upon the spectrum for the coating

while the kinetics of adsorption is concerned with the rates of adsorption and desorption. Therefore, the adsorption coefficient depends upon the chemical nature of the coating and the analyte. In general, the old adage 'like dissolves like' can be used for guidance in the selection of coatings. Polarizable molecules such as alcohols, esters, and aromatics will exhibit dipole-dipole,

dipole-induced dipole, and p-p interactions. For nonpolar molecules, the dominant intermolecular forces are of the weaker London (dispersive) type.

Design and Construction of a Sampler Probe

The SERS technique requires intimate contact between the sample and the enhancing surface. For a penetrometer probe, this requires bringing the material inside the probe for analysis. The most logical approach is to modify an existing cone penetrometer module capable of obtaining gas or liquid samples as the CPT platform probe is advanced. One such commercially available module is the ConeSipper from Applied Research Associates shown in Figure 57. The ConeSipper module can be attached directly behind a standard CPT cone and contains a two-stage stainless steel filtration system, an integrated pneumatic valving system, and an 80-ml stainless steel sample chamber. A pneumatic line to the surface provides control for the valving of the sample chamber, while a small pneumatic controller on the surface controls the flow of inert gas or water to the module. The filtration system prevents sand and fine particulates from entering the sample chamber. Samples can be drawn into the chamber through a check valve that prevents backflow from the chamber. After sampling is complete, the internal chamber can be remotely flushed with water or gas. The sample chamber of the ConeSipper has a diameter of 1.15 in. and is 8.4 in. long. The sample chamber can be redesigned to accept a sensor package which incorporates, into a single unit, the optical fibers and associated optical components (*i.e.*, filters and lenses), and the thiol-coated SERS substrate.

The ConeSipper was modified to reduce the sampling volume and to accept a SERS sensor module. As shown in Figure 57, the sample chamber of the ConeSipper is an insert that slips inside the mandrel. The O-rings are used to provide a leak-tight seal. The insert was modified to reduce the upper sample chamber volume from 80 ml to approximately 22 ml as shown in Figure 58. An additional piece of stainless steel 304 (a corrosion resistant grade) is welded to the CPT cable pass-through tube in the lower sample collection chamber. This modification reduces the volume of the lower chamber from 20 to 10 ml. Decreasing the volume of the sample requires less sampling time and reduces the risk of clogging the filters with sediments. Two pass-through holes are found on both sides of the CPT cable pass-through tube. These holes house the two *Pt* wires which comprise the water level sensor. Platinum was chosen for its corrosion resistant properties. The *Pt* wires are insulated except at the tips. The uninsulated part of the *Pt* wires are placed at the same level as the SERS sensor module and epoxy is used to pot the *Pt* wires inside the sample insert. Each of the plenums houses four wires. Of the eight wires available, six go to the strain gauges. The other two wires are soldered to the *Pt* wires of the water level sensor in the probe. On the surface these two wires are connected to a 5-V DC power supply and simple electrical circuit. A digital multimeter is connected in parallel. A reading of 5V is indicative of the absence of water. A reading of <1 V results at saturation, indicating that the water level inside the sample chamber has reached the SERS sensor module.

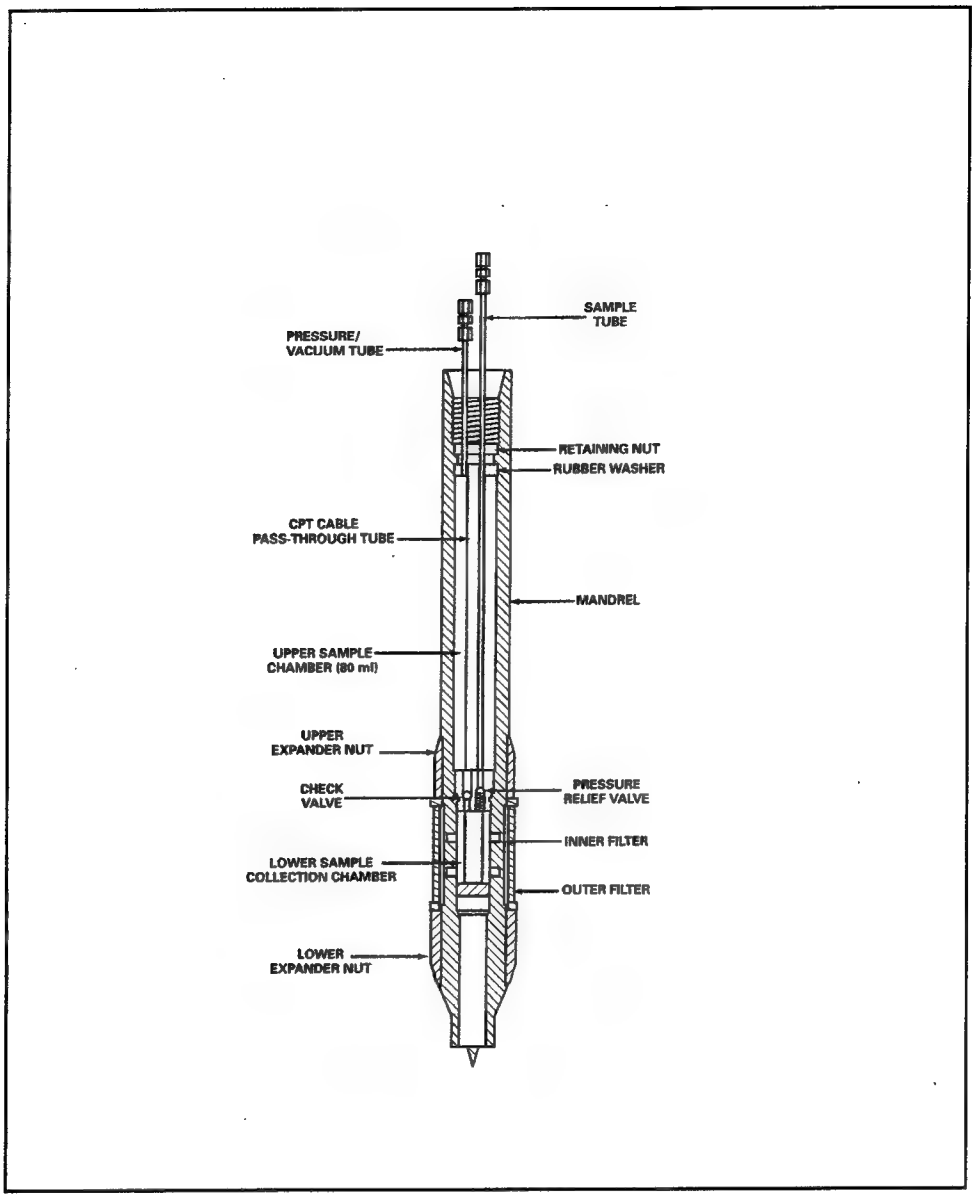

Figure 57. Schematic of the ConeSipper, a water/gas sampler manufactured by Applied Research Associates

Design and Construction of SERS Sensor Module

The design and construction of the SERS sensor module was contracted to Detection Limit, Inc. Laramie, WY. Drs. Chris Schoen and Keith Carron, Detection Limit, have experience in the design and construction of fiber-optic probes for Raman spectroscopy. The sensor module incorporates, into a compact unit, the collimating lenses, filters, dichroic mirrors, focusing lens, and mount for the SERS substrate. Figure 59 shows a schematic of the sensor

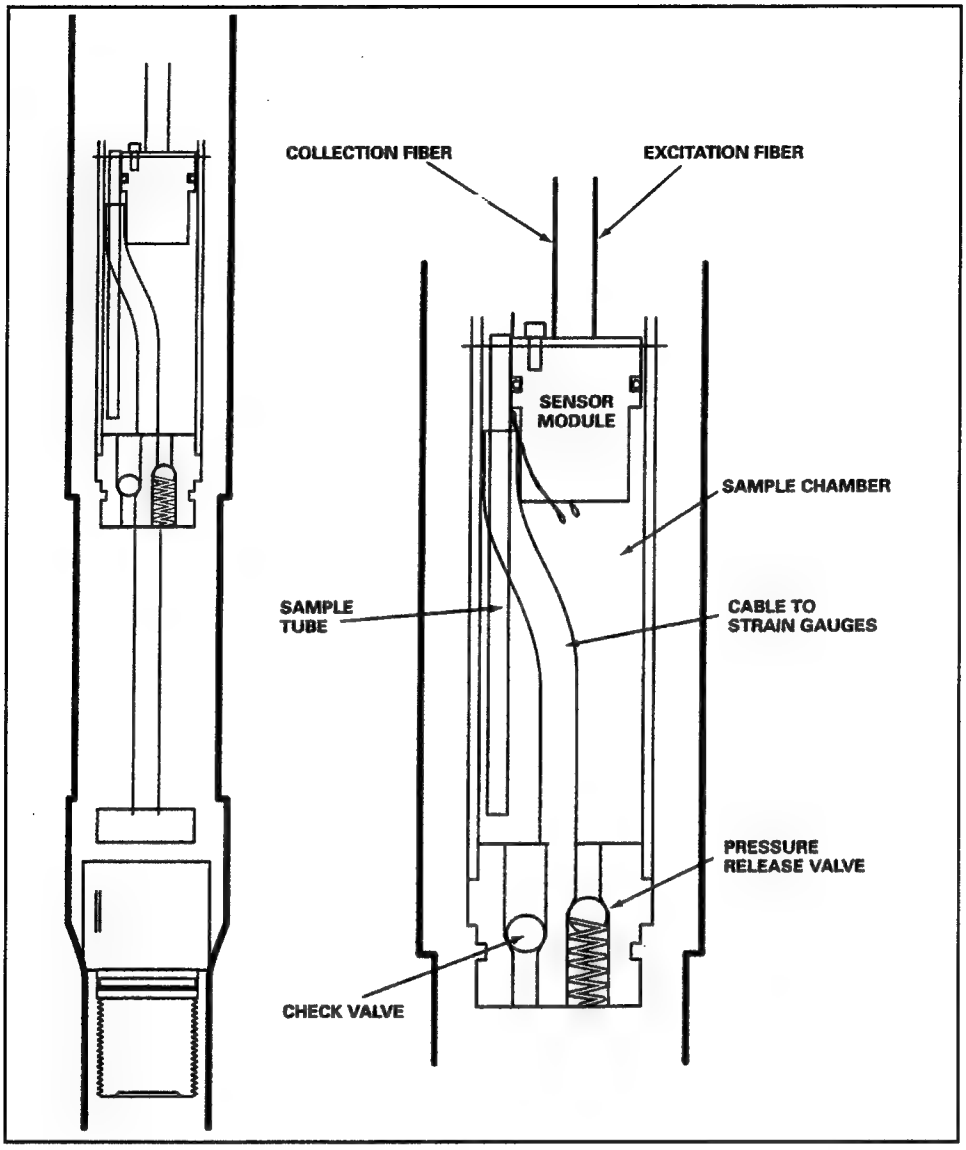

Figure 58. Schematic of the modified ConeSipper showing the orientation of the sensor module; the sample insert of the ConeSipper has been shortened to reduce the sample volume

module for SERS (the focusing lens and mount for the SERS substrate are not shown). The housing of the sensor module is machined from stainless steel 304 chosen for its chemically resistant properties. In the design shown in Figure 59, the o-ring and screws in the graded index (GRIN) collimator plate are used to align the optics of the sensor. Once aligned, the GRIN collimator plate is epoxied in place as are the mirrors, filters, and lenses. As designed, this module slips into the ConeSipper as shown in Figure 58. An o-ring provides a leak-tight seal between the sampling portion of the chamber and the upper chamber where the optical fibers, which go to the surface, are mounted. The optical fibers of the umbilical are connected to fiber pigtails of the sensor module using the

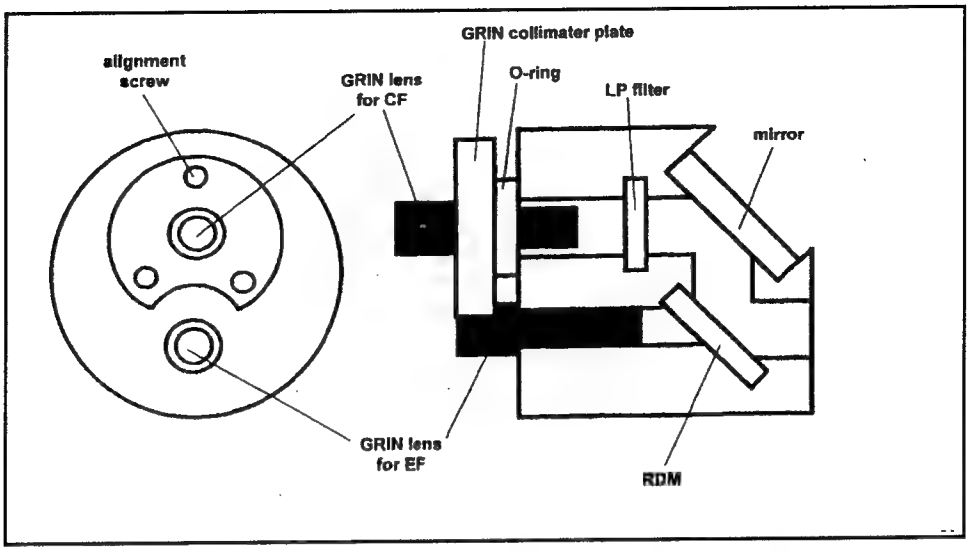

Figure 59. Schematic of the sensor module designed by Detection Limit, Inc., where LP = longpass filter, RDM = Raman dichroic mirror, EF = excitation fiber, and CF = collection fiber. The housing for the focusing lens and SERS substrate is not shown. GRIN lenses are used to collimate the light out of the optical fibers, the GRIN assemblies are epoxied to 50-mm-diam, fiber-optic pigtails that are connected to the optical fibers of the umbilical

appropriate connectors. Index matching gel between the terminated fibers can be used to improve light throughput.

Field Demonstration of the Modified Sampler Probe

After the ConeSipper sampler probe was modified for use as a SERS sensor, it was demonstrated using a dummy sensor probe. A total of five holes were pushed at the SPAWAR parking lot and at NASNI. The water level sensor inside the sample chamber worked well. There were no problems with clogging the filters of the ConeSipper with sediments. Groundwater samples were successfully brought up to the surface and were sent for laboratory analysis along with a soil sample obtained at the same depth. There has always been the question of `as long as you are bringing sample inside the probe for analysis, why not just bring it up to the surface for analysis?' The analytics on the groundwater samples were an order of magnitude less than in the soil sample. This discrepancy is probably due to a loss of analyte through the permeable teflon tubing on its way up to the surface.

Conclusion

Figure 60 shows a schematic of the fully assembled solvent sensor. However, the fully integrated system has not been field tested. A solvent sensor based upon SERS has one obvious disadvantage. Because the sample must be brought inside the probe for analysis, the CPT probe cannot be operated in a continuous mode as it is for the LIF sensor. The probe must be periodically stopped during the push, so that either vapor or groundwater can be brought inside the sample chamber for analysis. This increases the time required during sampling and, for practical purposes, reduces the number of data points obtained during a single push. Consequently, sampling should only be done in areas where the soil stratigraphy is favorable for the detection of the contaminant(s) of interest. This, in turn, requires a thorough knowledge of the geology of the site, *i.e.*, soil types and depth, faulting, monitoring well data, hydrology, *etc.* For example, chlorinated solvents tend to sink below the water table and accumulate above impermeable layers such as clays. Therefore sampling of chlorinated solvents should be done directly above the clay layer. Since sampling decisions are based upon the strain gauge data and the transport properties of the contaminant, success is for the most part left to chance.

Another indicator is required to determine when to stop the push to take a sample inside the probe for further analysis. It has been suggested that LIF could be used as that indicator. Chlorinated solvents do not fluoresce. However, chlorinated solvents have been used for decades in cleaning and degreasing operations. It has been suggested that the chlorinated solvents and dissolved fluorophores from oils and lubricants would comigrate through the soil. There have been anecdotal observations that it may be possible to detect the presence of chlorinated solvents via fluorescence from fluorophores that are dissolved in these solvents.

Video imaging is another technology that could possibly be used to indicate when a sample should be brought inside the probe for further analysis. Upon release, chlorinated solvents are trapped in the interstitial pore spaces of the soil matrix as microscale globules. These microglobules are clear and are difficult to detect visually. However, optical detection of these microglobules can be enhanced using a system of colored or fluorescent dyes that can be dispensed from the sensor probe and preferentially dissolve into the chlorinated solvent phase. Once located, a water sample would be taken inside the probe for further analysis by SERS. One candidate dye system is the tri-iodide ion, I_3^-. The tri-iodide ion exists in equilibrium with iodine, I_2, and iodide ion, I^-. Iodine is insoluble in water and partitions, preferentially, into the chlorinated solvent. In water, I_3^- is yellow-brown in color, while I_2 is red-purple in color in the chlorinated solvent. Figure 61 demonstrates the use of I_3^- to visualize microglobules of TCE in a water-saturated soil matrix. The primary criteria for a fluorescent dye to enhance visualization of the chlorinated solvent microglobules are: (a) the dye exhibits little or no fluorescence in water but a great deal of fluorescence when dissolved in the chlorinated solvent and (b) the wavelength of fluorescence is compatible with the use of optical fibers.

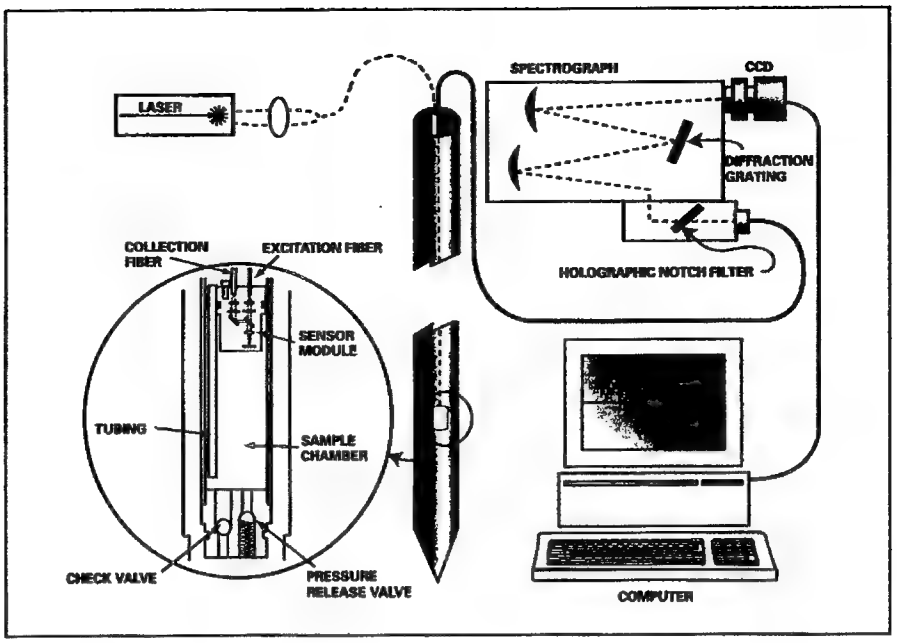

Figure 60. Schematic of fully integrated solvent sensor based upon SERS

Figure 61. Videomicroscopy image (100x) of tri-iodide strained TCE microglobules in a water-saturated soil matrix

5 Research Area IV: Electrochemical Sensors

by: Jane W. Adams, WES
William M. Davis, WES

Introduction

The DoD has responsibility for management and cleanup of sites contaminated with energetic materials such as the explosives TNT, RDX, HMX, their manufacturing intermediates, and subsequent breakdown products. Characterization of these sites is often very time and cost intensive because contaminant distribution is generally widespread over large areas. Ammunition plants typically cover many thousands of acres. The traditional methods to measure TNT and other explosives in the environment include collection, transport of samples, and extraction coupled with sophisticated laboratory analysis (Yinon and Zitrin 1981). Cone penetrometry offers cost relief and time savings. As part of this research area, a probe was designed to contain electrochemical sensors for nitroaromatic breakdown products and geophysical sensors for determining soil layering. The design uses an imbedded heating element to vaporize and decompose explosive compounds in situ into nitrogen-containing gaseous products that can be detected by this probe.

The DoD also has responsibility for management and cleanup of sites contaminated with VOC used as solvents in a range of machining, manufacturing, and degreasing operations at installations. As part of this SERDP-funded effort, a second SCAPS electrochemical sensor probe was developed which uses a cell that responds to chlorine ions to detect chlorinated hydrocarbon vapors from compounds such as TCE, carbon tetrachloride, or methylene chloride in soils. Concentrations as low as 1 ppm_{wt} may be detected, and the upper range is virtually unlimited. The sensor is especially useful because it is highly selective for chlorine, giving negligible responses to other halogens and nonchlorinated organic vapors.

Background

Many organic contaminants are compounds that can be efficiently detected by electrochemical or amperometric sensors (Stetter, Zaromb, and Findley 1985, 1991). Two innovative cone penetrometer probes, equipped with electrochemical sensors for detecting VOC and low concentrations of explosives contaminants in the soil, were developed by the DoD in cooperation with industry partners. The probes were developed jointly by WES and Transducer Research Inc. (TRI), a manufacturer of industrial environmental sensors (TRI, now TSI, Milwaukee, WI, (Muilenberg 1997)). Off-the-shelf electrochemical sensors and electronics were reconfigured for SCAPS penetrometer operation. An electrochemical sensor measures a change in current as result of contact by the electroactive analyte with the sensor electrode. The voltage response is a direct function of electroactive analyte concentration. Electrochemical sensors have the advantageous properties of small size, simple circuit requirements, low power needs, high sensitivity coupled with moderate selectivity, large dynamic range, fast recovery, and no chemical waste.

One probe detects explosive nitrogen compounds, their byproducts, and breakdown products. Another sensor probe detects chlorinated solvents from their vapors in soil. The probes are sensitive to a wide number of chemicals within a class of compounds; thus they are quantitative, not qualitative. It should be noted that these probes are limited to operation in the soil vadose zone and can be damaged if water is drawn into the probes.

This was the first electrochemical probe developed to sense explosive compounds. Explosive compounds such as TNT can be thermally decomposed into vapor. To decompose TNT in situ, the soil must be heated to release the nitrogen-containing gases that are diagnostic for explosives. Because the concept worked well, a similar probe for volatile chlorinated hydrocarbon solvents was developed according to the same basic design. VOC contaminants have high vapor pressures allowing contaminant vapor to be drawn from the soil and detected without the need for applied heat. This probe was initially called the RCl probe due to its ability to detect chlorine ions from solvent vapors. The probe was later renamed the "vadose sparge" probe to reflect the way it works to draw contaminant vapors from soil. The sensor systems will be described individually for clarity. The discussion and conclusions will be collective.

Electrochemical Probe for Explosives: Initial Probe Design

The explosives probe contains, in addition to standard geophysical soil class sensors, an electrochemical sensor that is responsive to NO, an internal pneumatic system and associated power supply and signal conditioning electronics inside the probe, and output monitors in the truck (Buttner et al. 1997). The probe is designed for air to be continuously pumped through the output ports of the probe and into the soil matrix adjacent to the probe, be collected through the vapor inlet ports and directed over the sensor, then drawn

to the surface where it is vented to the outside. A diagram of the initial design of the SCAPS explosive probe is shown in Figure 62.

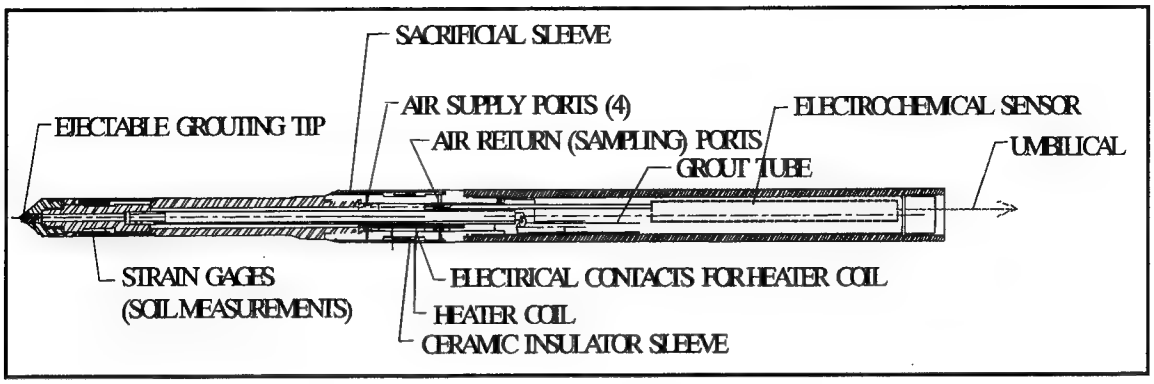

Figure 62. Illustration of the explosives detector probe showing the standard geophysical sensors and grouting system. The design included: (a) an external, open-filament heater for the *in situ* pyrolysis of explosives in soils, (b) an electrochemical sensor with associated electronics, power supply, and link to the SCAPS computer, and (c) a pneumatic system to collect vapors from the soil and transport them to the electrochemical sensor

In order for this probe to operate, the analyte vapor must be electrochemically active and must come into physical contact with the active electrode of the sensor. The NO gas sensor cannot directly measure a response from solid TNT because of its low vapor pressure. Therefore, explosive compounds must be vaporized from the soil matrix. Vaporization is accomplished by means of a heater located on the outside of the probe, in close proximetry to the sensor, to thermally degrade TNT and other explosives that are generally found in crystalline form in soil. The heater consists of a 20-cm length of 0.010-in.-diam platinum wire wound in two loops around a ceramic inset in the probe located between the output and inlet ports so that the heater wire is offset from the soil surface by 0.15 in. A commercial zirconium oxide ceramic paint is used as an electrical insulator between the platinum wire and the probe's surface.

During operation the wire is heated briefly to ~900 °C. The surrounding soil located from 0.15 to 0.25 cm from the filament is warmed to roughly 125 to 150 °C. The explosives in the soil sublime, and the heat dissociates the NO_2 groups that are weakly bound to the main portion of energetic molecules. The resulting vapor contains CO_2, H_2O, CO, and NO_2. The NO_2 molecules are further dissociated into NO + O. The NO fragment, nitric oxide, is the dominant gaseous product. A more detailed description of the theory of the device and testing procedures is included in Cespedes et al. (1994), Adams et al. (1995), and Buttner et al. (1997).

Explosives Sensor Verification/Calibration

Standard practice with all SCAPS sensors includes both traditional laboratory analyses and soil sampling to verify each new and developing technology. The explosives probe system was comprehensively evaluated in the laboratory using custom-built fixtures and soils spiked with known levels of TNT. Laboratory results indicated that the probe is very sensitive to low concentrations of TNT in dry soil. The response of the probe is linear over a broad range of concentrations, as shown in Figure 63. The calculated lower detection limit based on the signal equivalent to three times the noise is 0.5 ppm_{wt} (Adams et al. 1995).

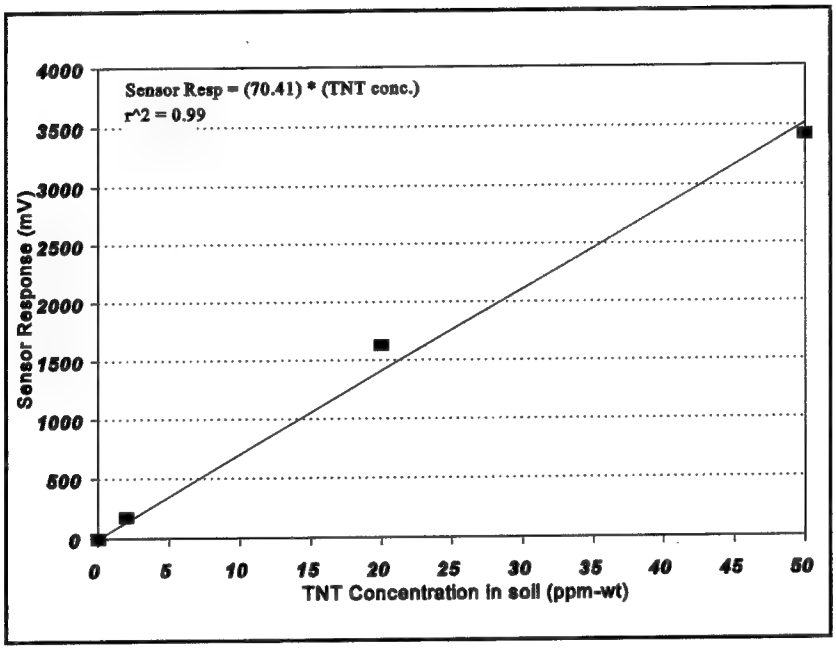

Figure 63. TNT calibration curve for the electrochemical explosives sensor probe

Explosives Sensor Field Operations

The standard method of operating the SCAPS explosives sensor in the field consists of calibrating the stratigraphy, electrochemical sensors, and air flow prior to pushing the probe. A known concentration of NO in nitrogen gas is used to calibrate the explosives electrochemical sensor. Then the probe is pushed to the full depth of interest at a constant rate of 2 cm per second to collect soil stratigraphy data according to American Society for Testing and Materials (ASTM) Method D3441. After pushing to the maximum depth, the probe is retracted approximately 30 cm to release a sacrificial sleeve that protects the pyrolyzer unit during the downward push. The sleeve is designed to fall off, exposing the Pt wire heater and the module's vapor delivery and sampling ports. Sensor readings are made at discrete depths during retraction,

increasing in number when a positive sensor response is recorded (Figure 64). Each data cycle consists of a short stabilization period of 30 sec to 1 min, activation of the heating elements to thermally degrade explosives in the surrounding soil for 30 sec, followed by another stabilization period of approximately 30 sec while the sensor recovers. The probe is then moved upward to the next sampling point. The probe may be pushed to the full depth allowed by umbilical cable length. The minimum depth the sensor is able to operate is 4 in. below the surface, otherwise the characteristics of gas flow and soil heating are not the same as at lower depths.

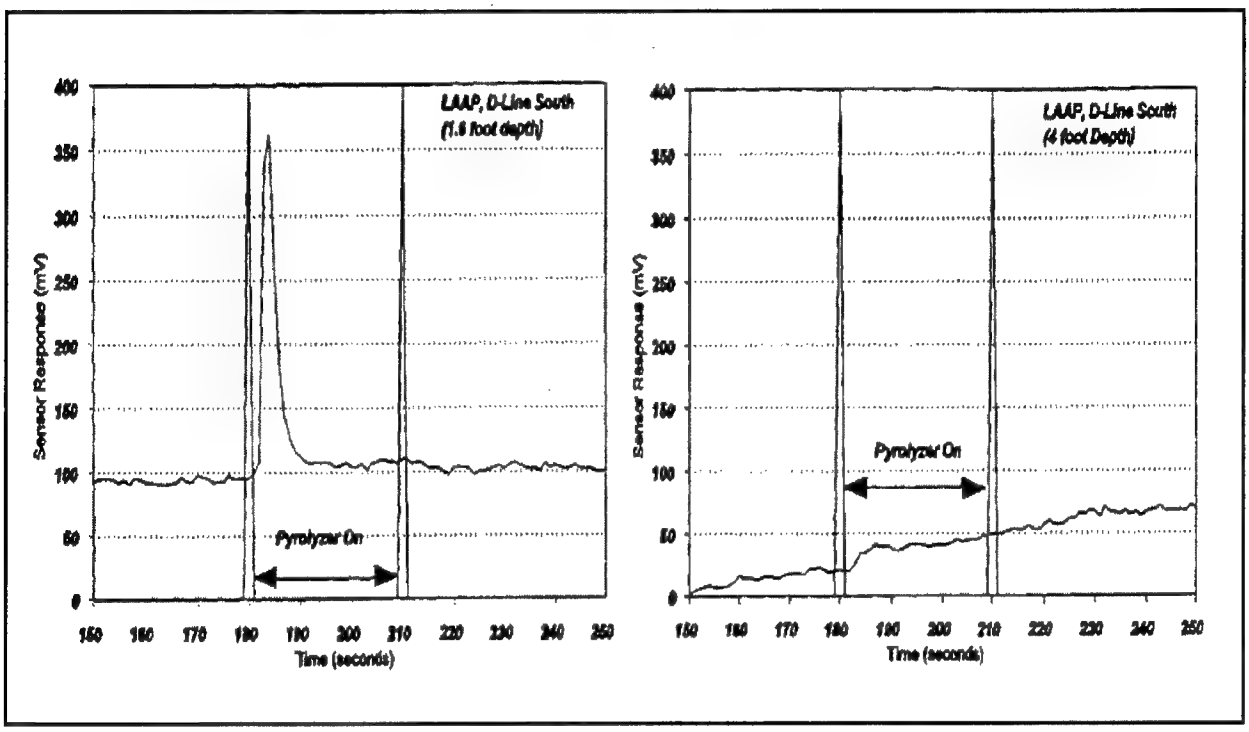

Figure 64. Typical response obtained from the explosives sensor in situ at LAAP

Subsurface soil samples for confirmation analysis were collected from each sampling location at the site. During the first four field demonstrations, cores were taken using a commercial direct push split sleeve sampler to take soil within a 30-cm radius from the sensor push location at depths that correspond to the sensor depth. Efforts to collect valid verification samples were sometimes hampered by moisture, soil texture or rubble in the soil. Cores deemed accurate representations were sectioned into samples for both laboratory analysis and for analysis on site using a colorimetric screening procedure for explosive compounds (RDX, HMX, TNT, etc.). The field screening method used was developed by Jenkins and Walsh (1992) and is commercially available as test kits (EnSys Soil Test System, Strategic Diagnostics Inc., Newark, DE). The test is highly effective but is not compound specific. Laboratory samples were kept refrigerated until they were analyzed at the WES Environmental Chemistry Branch analytical laboratory using EPA Method 8330. In addition, verification samples from Volunteer Army Ammunition Plant (AAP) in 1996 were analyzed by the SERDP National Test Site laboratory, and in 1997 a high performance

liquid chromatograph (HPLC) was taken to the field in a mobile laboratory to allow EPA Method 8330 to be performed on site.

Revised Probe Designs

The first revision to the probe design consisted of minor modifications to enhance gas flow. Next, an electrochemical CO sensor was added to the sensor module. This change was based on detailed laboratory experiments conducted to determine thermal decomposition processes of a variety of interfering nitrogen-containing compounds, such as fertilizers, that might be encountered during field investigations (Shorter et al. 1997). The multiple sensors permit discrimination of organic nitroaromatic compounds from inorganic nitrogen compounds that do not give off CO_x compounds when dissociated by heat. Figure 65 and Table 11 show the responses of nitroaromatic explosives vs. nitrate compounds.

Although the open-heater filament probe was used safely and successfully at four sites, there was concern from the user community about the possibility that the hot Pt wire could ignite a concentrated deposit of subsurface explosive. The design was modified to alleviate this danger. The heating element was isolated from direct contact with the soil by a 0.07-in-thick steel housing designed to push soil away from the ports as shown in Figure 66. The ceramic paint was replaced by a Macor™ machined ceramic sleeve to insulate the filament from the metal cover. These additions resulted in much slower heating rates and the soil surrounding the probe does not reach the same temperature as the open-filament design. The heating cycle had to be extended to several minutes to warm the soil sufficiently to vaporize and decompose explosive compounds into nitrogen-containing gaseous products. The recovery cycle was also substantially longer. However, extensive reevaluation both in the laboratory and the field showed that the probe gives the expected response.

A problem unique to explosives contaminants is that, because of the fact that they are not very soluble crystalline compounds, they tend to be dispersed very heterogeneously (Jenkins et al. 1997). Solid TNT tends not to be uniformly distributed in soils but instead exists in soil as localized particles. Under these circumstances, samples collected from nearly identical site locations and depths can have significantly different contamination levels. Although not exact, the explosives sensor probe readings correspond well with the laboratory results obtained by EPA method 8330 and the field screening method. Any discrepancy between the three methods could be attributed to inhomogeneity of explosives in environmental samples (Jenkins et al. 1997). Nonetheless, data variability hampered efforts to validate the probes operation. Furthermore, the sampling method is destructive, so it is not possible to repeat a measurement in the same location. Therefore, a revised validation sampling method was conceived.

After initial sensor measurements indicate explosives contamination in a particular area, a direct push soil sampler is used to obtain 18-in. cores at depths suspected of having explosives contaminants. The verification soil samples are analyzed in the field using the colorimeter screening procedure previously

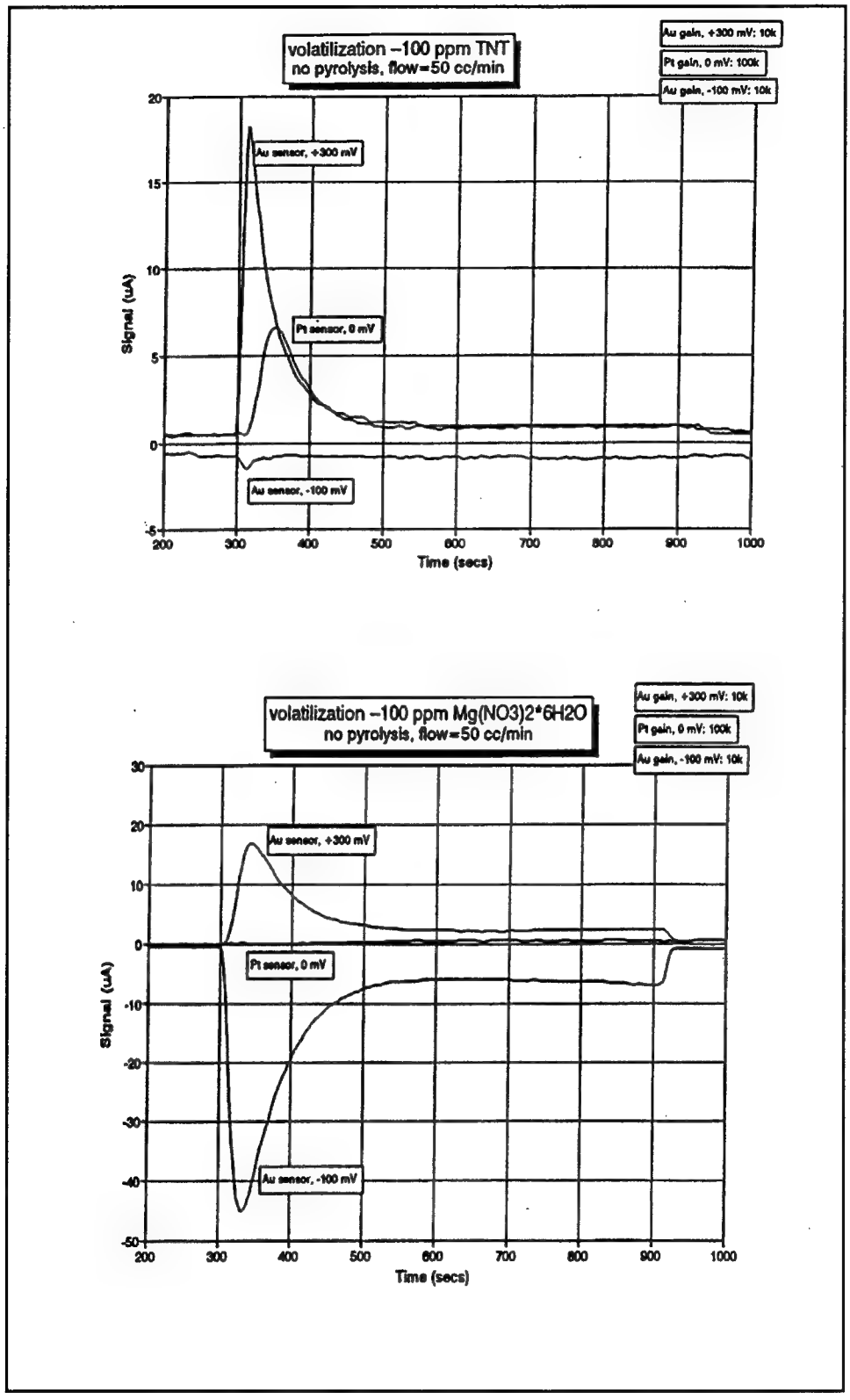

Figure 65. Explosives sensor responses to (a) explosives and (b) nitrate compounds

Table 11
SCAPS Explosives Sensor Responses to Low-Temperature Operation that Volatilizes the Explosive and Nitrate Compounds. Use of Multiple Sensors Achieves Selectivity and Discrimination between Explosives and Naturally Occurring Nitrates and Fertilizers

Compound evaluated	Sensor Response		
	NO	CO	NO_2
TNT	+	+	–
$Mg(NO_3)_2$	+	–	+

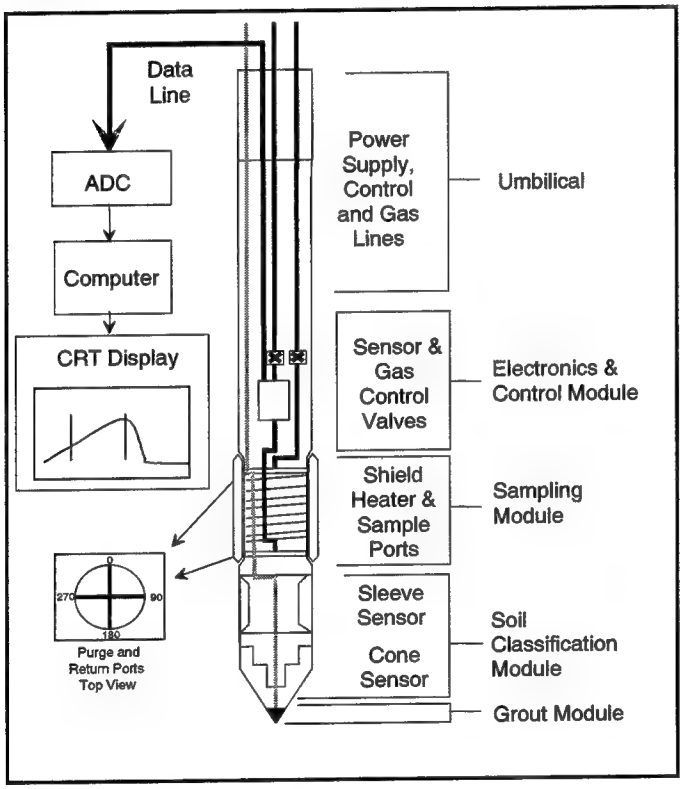

Figure 66. Schematic of the revised explosives probe, this design incorporates a fixed, enclosed heater and four sampling ports for carrier gas to flow outward over the warmed soil surface and inward to carry vapor across the sensor

described (Jenkins and Walsh 1992). The soil sampler has a 1.50-in. outer diameter (OD). In an attempt to overcome the uncertainty introduced by the heterogeneous distribution of explosives contaminants, the explosives sensor is then pushed into the pervious boring produced by the soil sampling event. The explosives probe has a 1.84-in. OD, therefore it makes contact with soil that was

no more than 0.24 in. away from any depth where a verification sample was obtained.

Field Investigations Completed -- Explosives

Seven field demonstrations were performed in the course of developing the explosives sensor probe and establishing operation procedures. TRI personnel participated in all field demonstrations except those performed at JAAP in 1997.

a. LAAP, Louisiana, 12-16 Sept 1994
First prototype tested ·
Heterogeneous TNT/RDX contamination
Wet clay conditions
Improvements identified.

b. Department of Energy Pantex Assembly Plant, Texas, 6-10 Mar 1995
Dry sand / clay conditions
Heterogeneous RDX / HMX contamination
Improved gas pneumatic system
Coordinated with and trained the Tulsa District SCAPS crew using their truck.

The primary objective of this field test was to evaluate the performance of the prototype SCAPS explosives sensor under soil conditions different from those encountered at the LAAP. A second objective was to collect data to support the Corps' project to characterize and remediate Landfill No. 3.

c. Volunteer Army Ammunition Plant (VAAP), Tennessee, 3-7 Apr 1995
SERDP National Test Site
Used an improved pneumatic system
Improved data acquisition / display system
Moist clay conditions
Homogeneous (near surface) TNT contamination.

At the time of this demonstration VAAP was a part of the SERDP National Environmental Technical Test Site (NETTS) program. The site is a former munitions facility that was in operation for nearly 50 years. It has areas with considerable TNT and RDX contamination. Area 806 TNT production line had been previously screened for TNT contamination by TRW, Inc.

d. Longhorn Army Ammunition Plant (LHAAP), Texas, 24-27 Sept 1995
Heterogeneous soil (sand and clay)
Homogeneous (near surface) TNT contamination
Coordinated with and trained the Tulsa District SCAPS crew using their truck.

Investigation of a former burn pit (Site 17) and a former burning ground (Site 63) for reject materials were known to have explosives contamination present. Wet clay hampered some sensor readings from the burn pit, but

significant responses were recorded when this did not happen. No positive responses were measured at Site 63.

e. VAAP, Tennessee, 15-22 Oct 1996
SERDP NETTS
Probe redesigned to operate at lower temperatures (enclosed heating elements)
First use of new validation sampling method.

f. JAAP, Illinois, 19-23 May 1997
EPA Method 8330 for Explosives analysis performed in the field
Revised validation sampling method not possible due to glacial till at site
Validation samples obtained by hand auger
Tetryl manufacturing area was surveyed.

g. JAAP, Illinois, 08-12 Sept 1997
During this demonstration the effects of soil moisture and heating duration were further evaluated. A former subsurface drain pipe (12 ft below ground surface) that carried red water from the TNT line to the waste treatment area during plant operation was investigated. The SCAPS explosives probe confirmed that the sectioned, vitrified clay pipe had not leaked explosive compounds into the surrounding soil at the sample location.

Explosives Results/Data

The first analysis of the explosives sensor response is a qualitative comparison with validation soil sample results analyzed using EPA Method 8330. This contingency analysis involves evaluation of the frequency of explosives sensor true positive and negative response as determined by the validation soil sample results. True positive sensor response is assigned whenever the validation soil sample indicates the presence of explosives at a location where the sensor yielded response above background. Similarly, a true negative is assigned where the validation soil sample and the explosive sensor both yield no response above background.

The results obtained from field tests of the open-filament design (Table 12) indicate that the electrochemical explosives sensor yields a high percentage of true positive and true negative responses. The false positive responses observed may have been due to explosive near probe but not in verification sample or the presence of nonexplosives nitrogen species present in the soils. Sensor response was calculated from the difference between the maximum counts and the averaged background. In Table 12, all sensor responses less than 50 millivolts (mV) above mean background were classified as nondetects (ND) for the open filament design. Field and laboratory tests with the closed-filament design probe indicate that a 1-mV response can be assumed to semiquantitatively be equivalent to 1 ppm_{wt} explosive in soil. It should be noted that the explosives

Table 12
Contingency Analysis for Explosives Sensor Response and Verification Soil Samples

Site	Positives true	Positives false	Negative true	Negative false
VAAP 95	8	2	1	2
VAAP 96	16	0	0	2
LAAP	4	0	0	0
Pantex	4	0	3	1
LHAAP	4	1	5	0
Total	36	3	9	5
Total(%)	88	25	75	13

sensor was designed as a rapid site screening tool to distinguish areas of contamination from areas without contamination. As such, it was developed as a semiquanitative tool and the validation sampling and analyses were conducted to verify the utility of the sensor for the intended application.

Electrochemical Probe for Chlorinated Solvents (EC-RCl)

Probe design and operation

The sensor has been highly selective for volatile organochlorine compounds. It was extensively evaluated against both traditional laboratory analysis by EPA Method 8260 and in the laboratory using custom-built fixtures and spiked soils. The advantage that this design has over standard soil gas sampling is that 7-in^2 soil surface area is purged as opposed to a single point tube inserted into the soil. A schematic of the probe is shown in Figure 67.

The EC-RCl VOC sensor consists of a standard geophysical cone module coupled to a soil vapor sensing module within the probe that contains a sensor for chlorine ions. The stratigraphy sensor is operated in accordance with ASTM Method D3441. Geophysical data are collected in real-time as the probe is advanced to the depth of interest. This probe also has a sacrificial sleeve that protects the vapor delivery and sampling port openings during the downward push. The sleeve falls off on retraction, and data are taken during probe retraction.

After the sleeve falls off downhole to expose the vapor ports, air controlled by two pumps flows through the system. One pushes air out of the sensor purge ports and the other pulls the sample soil vapor back through the in-line sensor. Surface air regulated to ~ 200 ml m^{-1} is pumped out of four ports located at 0, 90, 180, and 270° at the bottom of the vapor sampling module. The pumped air

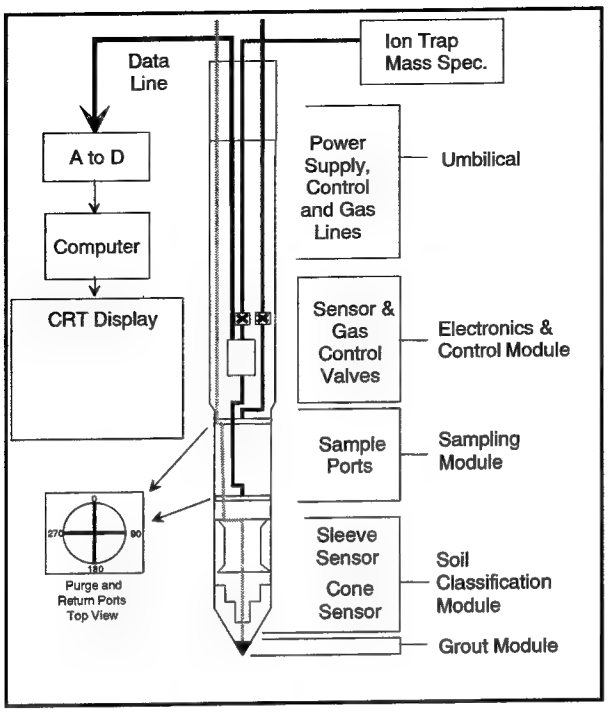

Figure 67. Schematic of the RCI electrochemical sensor

purges a cylindrical soil surface area around the probe corresponding to an area ~4 in. long by 1.75-in. diameter so that soil vapors are transferred to the purge gas and then captured by four intake ports that feed the vapor through a manifold to the electrochemical sensor in the probe. The voltage output signal is conducted through the umbilical and interfaced to an onboard computer for real-time display. Alternatively, purged VOC sample vapors may be delivered via the purge-gas tubing to an in situ sparge inlet for input to a Direct Sampling Ion Trap Mass Spectrometer (DSITMS) that gives quantitative compound-specific analysis (Wise et al. 1997; and Davis et al. 1997; Davis, Furey, and Porter 1998).

Calibration

The electrochemical RCI VOC sensor is calibrated on site, daily during each field deployment. A known concentration of a specific analyte vapor, e.g., TCE, is injected into a calibration sleeve that fits on the probe. The calibration sleeve covers the vapor ports to create an annular space equivalent to that of the probe in the soil. It has an inlet port to which a gas calibration bag may be attached. The purge-gas flow rate is checked and sensor response to the calibration gas is measured (Figure 68). This must be done for each VOC of interest.

The probe sensitivity is excellent. In situ soil vapor measurements made with this sensor correlate well with contaminant concentrations from soil measured by gas chromatography/ mass spectrometry. The SCAPS RCI VOC

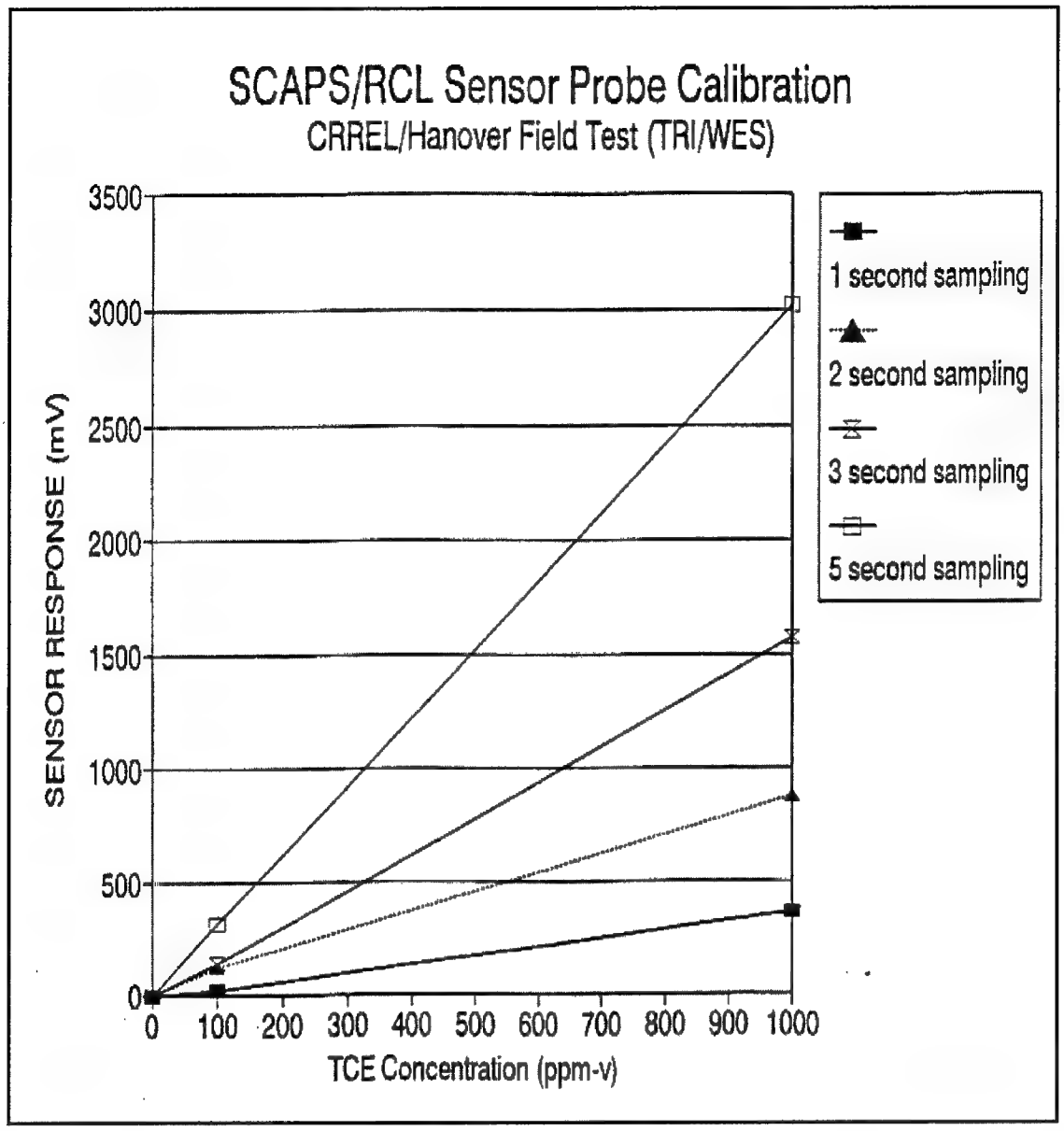

Figure 68. Typical calibration curves obtained for analysis of TCE vapor samples at different sampling intervals using the calibration sleeve

probe has been used at several sites to record TCE vapor levels between 10 and >10,000 ppm. The response has been temperature independent.

RCl sensor field operations

The standard method of operating the SCAPS RCl sensor in the field consists of calibrating the push load, stratigraphy, electrochemical sensor, and air flow prior to pushing the probe. A known concentration of a contaminant of interest, frequently TCE, is used to calibrate the probe using the calibration sleeve fixture. Then the probe is pushed to the full depth of interest at a constant

rate of 2 cm per sec to collect soil stratigraphy data according to ASTM Method D3441. After pushing to the maximum depth, the probe is retracted approximately 30 cm to release the sacrificial sleeve that protects the probe openings during pushing. The sleeve is designed to fall off to expose the outflow and inflow ports. Sensor readings are made at discrete depths of interest during retraction. Each data cycle consists of the acquisition of a baseline reading of air only before the solenoids are opened to flush air onto the soil surface. Air sparges the soil surface for approximately 60 sec followed by another stabilization period of several minutes while the sensor recovers to baseline level (Figure 69). Then the probe is moved upward to the next sampling point. The probe may be pushed to the full depth allowed by umbilical cable length, roughly 150 ft. The deepest RCl sensor penetration to date is 125 ft below ground surface (bgs).

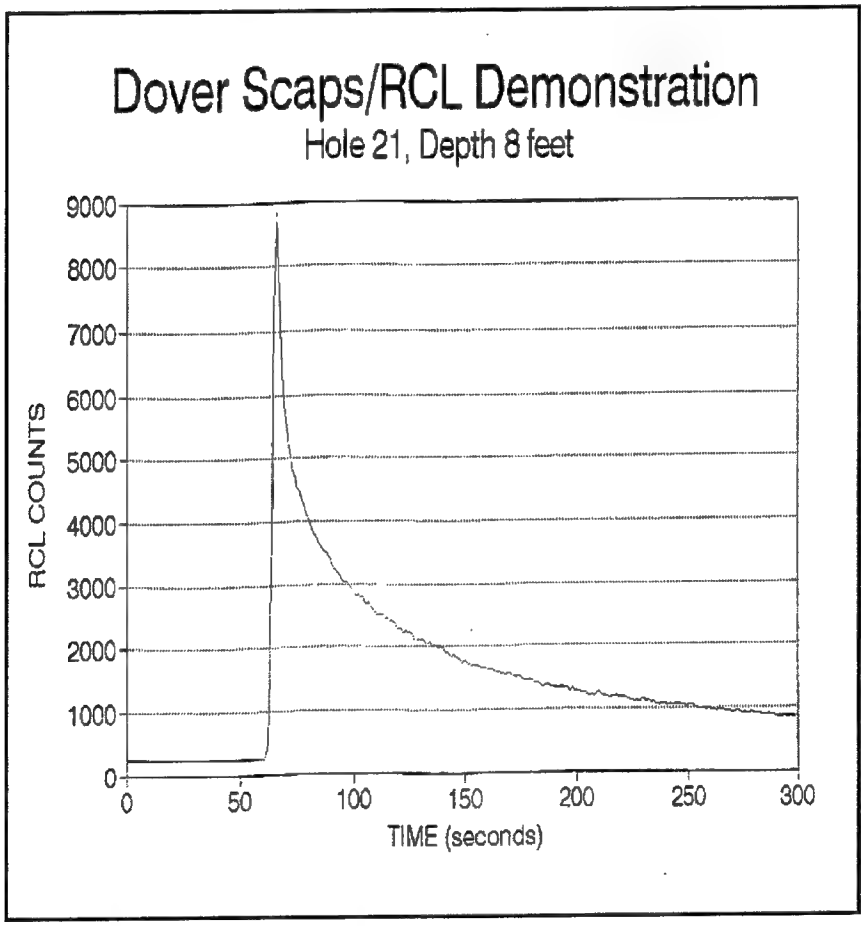

Figure 69. Typical response of RCl sensor under normal in situ operation at Dover AFB, May 1995

Subsurface soil samples for confirmation analysis are collected from each sampling location at the site. During the first four field demonstrations, cores were taken using a commercial direct push split sleeve sampler to take soil within a 30-cm radius from the sensor push location at depths that correspond to

the sensor depth. Efforts to collect valid verification samples were sometimes hampered by moisture, soil texture, or rubble in the soil.

Field Investigations Completed – Chlorinated VOCs

Dover AFB, Delawar, May 1995
- First prototype probe successfully demonstrated
- 3 sensor penetrations, 14 verification samples

USAE Cold Regions Research and Engineering Laboratory (CRREL), New Hampshire, Jan 1996
- Modified RCl/CO probe demonstrated: CO sensor added to identify nonchlorinated VOCs
- Performed lateral and vertical characterization of abandoned ice well
- Depth of interest was ~120 ft bgs
- 4 sensor penetrations, 11 verification samples

USAE CRREL, July 1996
- Improved pneumatic system
- Trained Savannah District personnel
- 6 sensor penetrations, 14 verification samples obtained

USAE CRREL, June 1997
- Interfaced sensor with an ITMS at surface
- First use of probe for continuous push
- Extended plume characterization
- Leveraged validation samples with SCAPS Thermal Desorption Sampler (TDS) probe: samples analyzed by Dr. Alan Hewitt, USACE CRREL

RCl VOC Data Results

The RCl sensor has been demonstrated to yield rapid field screening data to characterize VOC contaminant distribution in the vadose zone. Typical comparisons between validation data and in situ sensor measurements indicate the sensor provides accurate relative measurement of subsurface VOC contamination (Figure 70). The data collected at CRREL during January 1996 were used by the site manager to place additional soil borings to further characterize the site.

Contingency analysis of field data collected using the RCl sensor and data form verification sample analysis support the use of the sensor for rapid site screen (Table 13). The very low number of false positives and false negatives obtained during validation efforts indicate the utility of the RCl sensor for rapid site screening. It should be noted that the electrochemical sensor is extremely sensitive and has a very slow recovery time (i.e., to return to baseline) (Figure 69). This is especially true when an extremely high-level sample is

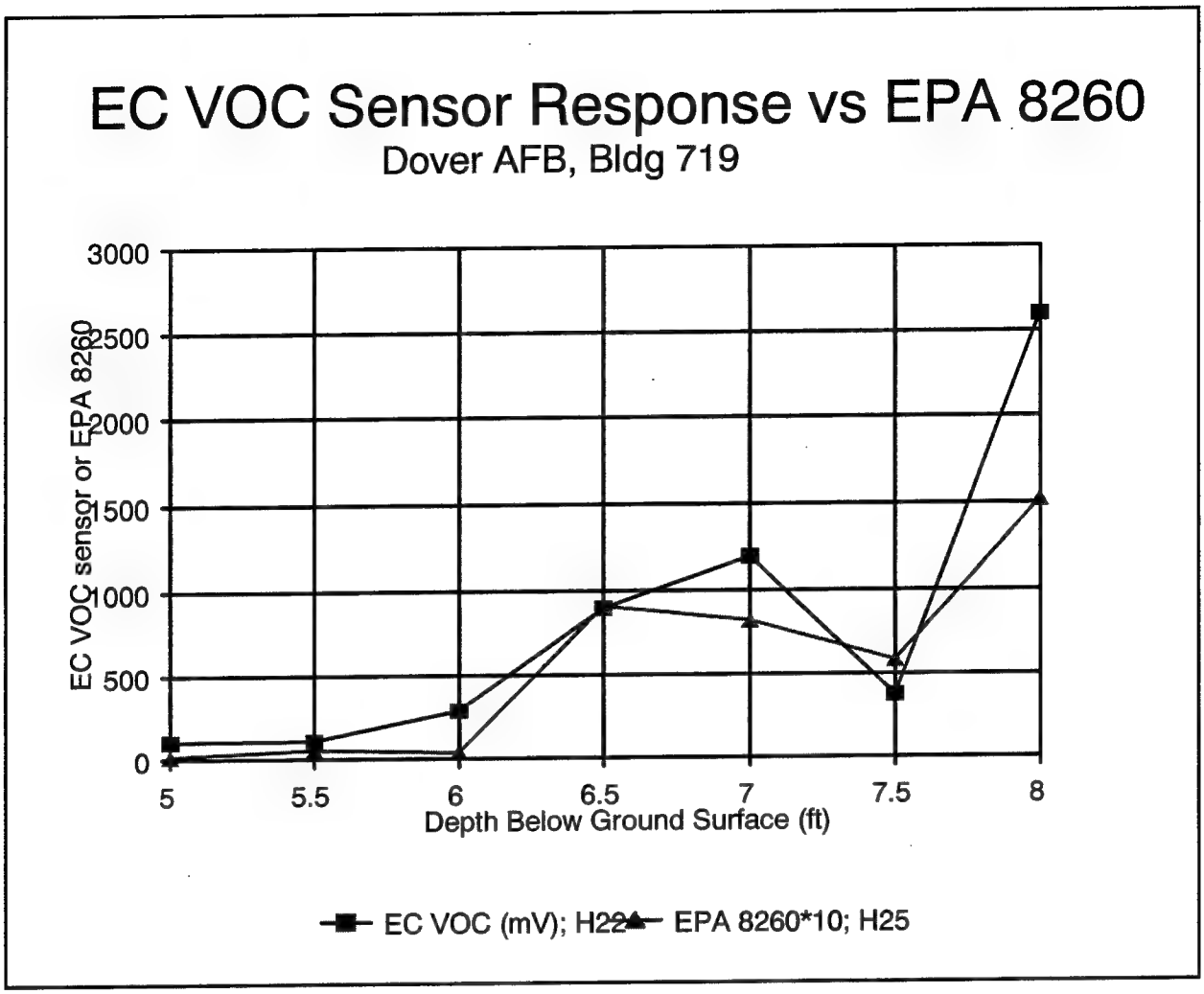

Figure 70. Comparison of RCI sensor response to results of verification sample analyses

Table 13
Contingency Analysis for Electrochemical VOC Sensor (RCI) Response and Verification Sample Analyses by EPA Method 8260

Site	True Positives	False Positives	True Negatives	False Negatives
Dover AFB	14	0	0	0
CRREL 1/96	11	0	0	0
CRREL 7/96	14	0	4	1
Total	39	0	4	1
Total (%)	97.5	0	100	2.5

encountered. The slow recover time limits the use of the sensor to discrete sampling applications. The DSITMS is very sensitive and has a very rapid recovery time (milliseconds). This makes the DSITMS an ideal detector for use with the RCl probe in applications for continuous monitoring of VOC contaminants in the subsurface. Initial investigation of the DSITMS interfaced to the RCl probe were conducted at CRREL in June 1997. The results indicated that the combined system was capable of continuous monitoring VOC contaminants during probe retraction (Figure 70).

Discussion

The initial version of the SCAPS explosives probe used an open heating element to warm the surrounding soil to release nitroaromatic vapors. It was evaluated safely at four sites. Later, to address safety concerns, the heater was redesigned to be enclosed in a steel jacket. Although the operation cycles increased in time due to slower heating, the modified probe also operated successfully. The major disadvantage of this probe is that it cannot operate in saturated soil, wet silts, or wet clays that tend to clog the gas ports. Detailed laboratory assessment, and subsequent field investigations, of thermal decomposition processes of explosive compounds has made it possible to distinguish the presence of nitroaromatic compounds from inorganic nitrates, for example, fertilizer, and from naturally occurring nitrates that may also be present in explosive-contaminated soils. During SERDP field demonstrations, the probe was pushed to more than 30 ft bgs. Although most explosive compounds at manufacturing sites found in the subsurface are shallow, this probe is extremely useful for explosive contamination detection found in landfills and burning pits because it is faster and more economical than core drilling.

The advantage of the current RCl design is that the VOC analytes are sampled by purging a cylindrical soil surface during probe retraction. The technique is different from soil gas sampling in that soil gas sampling consists of a single point (usually a tube) inserted at depth through which a soil gas sample is withdrawn by vacuum. By contrast, the EC VOC sensor contains four purge-gas delivery ports (at 0-, 90-, 180-, and 270-deg locations around the probe, Figure 67) and four purge gas recovery ports (4 in. above at the same radial locations). A significant advantage of the RCl VOC probe over conventional soil gas is that it purges a known surface area while the soil sample volume of a soil gas sampler is not known. Previous field trials of the RCl VOC probe have demonstrated good correlation between verification samples obtained at depth and probe response (Figure 70 and Table 13).

Conclusions

Field evaluations of SCAPS electrochemical sensor probes have shown that they possess the advantage of rapid, highly sensitive detection of explosives and chlorinated solvents below the ground surface in the vadose zone. Electrochemical sensors are ideally incorporated into rugged probes that are

accurate and of reasonable cost. Calibration procedures are simple, data are obtained quickly, analytical equipment is not needed, and the need for extensive personnel training is negligible.

Extensive laboratory tests were performed during the development and field use of these probes. Field demonstrations of each of these probes have been performed at a variety of sites to evaluate probe performance and to refine operational procedures. The explosives probe was funded in 1997 by the Environmental Security Technology Certification Program (ESTCP) to gain regulatory acceptance and to transition these technologies to SCAPS users. During FY97 the ESTCP program was leveraged against SERDP funding for the two field demonstrations conducted at JAAP during 1997.

The Corps of Engineers District SCAPS teams have been trained to use the RCl and Explosives sensors (Tulsa District - RCl and Explosives sensors; Savannah District - RCl). The prototype probes currently reside at WES and have been made available to the Corps of Engineers District SCAPS programs on an as-needed basis. The RCl probe is currently deployed using the DSITMS, because the manufacturer of the electrochemical RCl sensor has discontinued production of the RCl sensor.

6 Research Area V: Spectral Gamma Sensor

by: John C. Morgan, IITRI
Jane W. Adams, WES

Objective and Project Background

In situ spectroscopic measurement of radionuclide concentrations in the subsurface has previously been limited to well logging measurements. Direct measurement of subsurface radionuclide contamination is currently accomplished by taking core samples of soil for analysis by standard nuclear industry techniques. Although this approach provides a high degree of precision and accuracy for any specific sample, it is extremely costly. The expense involved includes the costs of physical sampling procedures, the safety restrictions inherent in handling radioactive materials, the equipment involved in counting the samples, and sample disposal. A lower-cost method to determine the distribution of subsurface radionuclides, the SCAPS Spectral Gamma probe, was developed at WES with funding from the DOE Office of Science and Technology (EM50), and SERDP. The success of the SCAPS Spectral Gamma Probe was achieved due to the SERDP-funded design changes that moved the diagnostic electronics to the surface.

In 1992, the DOE funded WES to design, fabricate, and test the first cone penetrometer-based spectral gamma sensor for the SCAPS to address DOE needs. The WES and Pacific Northwest Laboratory (PNL) provided data acquisition/processing/display software and radionuclide calibration/identification software for the system. Initial spectral gamma sensor field demonstrations were conducted at the DOE Fernald Facility, Ohio, September 1994. The data were not sufficiently conclusive.

Design improvements to minimize the downhole components, associated electronic noises, and to add fault tolerance to the system were identified as a result of this initial field deployment. In FY 94, SERDP provided funding for WES to design an enhanced spectral gamma system with the goal of higher resolution and less expense than the first-generation spectral gamma sensor system.

During the August 1995 SERDP Peer Review, it was recommended that SERDP support for spectral gamma sensor research be discontinued, since this work was not seen to address a DoD requirement. The SERDP support of this research area was discontinued at the end of FY 95. Work on the SCAPS spectral gamma probe continued during FY 96/97 under DOE funding.

Technical Approach to the Initial Probe Design

The spectral gamma probe consists of a sodium iodide (NaI) scintillation crystal, which is optically coupled to a PMT, power supply, microprocessor, and high-voltage supply. When a gamma ray strikes the crystal, it emits a photon that is detected by the PMT and converted into an electrical voltage. The amplitude of this voltage is proportional to the energy of the photon. This analog signal passes through a high-speed A/D converter and is converted into a digital value. From the A/D converter, the resulting value is passed on to a microprocessor that sorts the value within a histogram of counts versus energy. Characteristic peaks in the gamma spectrum indicate the presence of gamma-emitting radionuclides.

The WES approach to the development was to identify a commercial vendor capable of modifying their existing sensor to operate in a SCAPS probe. The Canadian vendor, IFG, was selected to develop and fabricate the internal probe hardware. Based on their experience building well-logging systems, their design consisted of putting the entire system down-hole. Three different 1 in. × 3 in. crystal types: NaI, cesium iodide (CsI), and BGO were investigated for gamma radiation detection and robustness. The NaI was determined to be the best gamma detector of the three with sufficient resolution to meet SCAPS goals. The probe's high-voltage module, the analog to digital converter, a serial controller, a preamplifier, and the NaI gamma ray detector were packaged into a single unit as shown in Figure 71. This probe is a fully digital spectral gamma detector that samples 512 channels of gamma radiation in the energy range from 100 keV to 3 MeV at a rate of one complete spectrum every 2 sec. The detector is controlled by an on-board microprocessor that transmits the digital values along a four-conductor logging cable to a microcomputer for storage and display. The classifying software was an adaptation of a code written for analysis of germanium (Ge) detector data. The probes were delivered to PNL Hanford Calibration Facility for Gamma-Ray and Fission-Neutron Well Logging for calibration prior to field deployment.

Spectral Gamma Detector Calibration

Two NaI spectral gamma probes were calibrated by PNL at the Hanford Calibration Facility for Gamma-Ray and Fission-Neutron Well Logging. Full details of the construction and composition of the Hanford Facility are available in PNL-9958, by D. C. Stromswold (1994). Facility zones for thorium (Th), potassium (K), and uranium (U) were used to calibrate the probes. After placing the probe in the central region of the calibration zone, the spectral gamma sensor

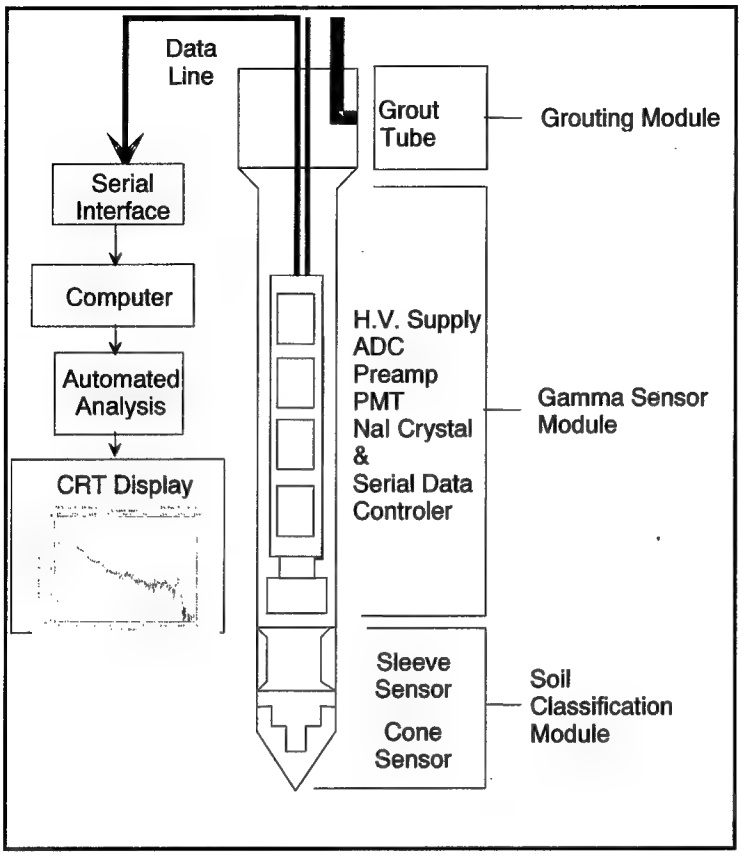

Figure 71. Schematic of the initial SCAPS spectral gamma probe

system was allowed to come to temperature equilibrium for approximately 15 min before calibration data were acquired. Spectra were analyzed and the results compared to the known compositions of the facility. The results directly determine the absolute detection efficiency of the probes as a function of gamma-ray energy.

Results of Fernald Site, Ohio, Field Demonstration

The SCAPS spectral gamma sensor was field tested at the DOE Fernald Facility, Ohio. Field tests were conducted in three stages: at a clean location adjacent to Fernald South Field, in Fernald Environmental Restoration Management Corporation (FERMCO) provided test drums, and at the Fernald South Field test location. First, the probes were lowered into test drums that had been prepared by FERMCO personnel with known amounts of contaminants. Spectral gamma data were accumulated for 1,800 sec, based on Fernald background conditions. Next, the SCAPS truck was moved onto the site where pushes were made at predetermined clean and contaminated locations.

Clean location

Background gamma radiation levels in the vicinity of South Field were established by a push at a supposed uncontaminated location. Analysis of the spectrum (using the calibration coefficients determined at the Hanford Calibration Facility) indicated background gamma activity levels for ^{40}K and ^{232}Th.

Test drums

Three 55-gal steel drums filled with soil contaminated with known levels of radionuclide contaminants were provided by FERMCO. The probe was manually lowered into a drum and data were collected for 1,800 sec. The spectral gamma sensor system successfully identified the contaminant as ^{238}U with a concentration of approximately 150 pCi/g using the automated data processing software. The analysis code also found the 766 keV and 1,001 keV peaks from ^{234m}Pa, a daughter product of ^{238}U. This closely approximated the stated value of 155 pCi/g that was provided by FERMCO. The same procedure was performed in two additional drums of contaminated soil. The automated software did not identify the contaminant in either case. FERMCO data for these drums indicated concentrations of ^{238}U at 72 pCi/g and 44 pCi/g, respectively.

Fernald South Field, Location SF11406

The SCAPS truck was driven onto the Fernald South Field for direct push demonstration in several locations. Data from location SF11406 were collected at depths of 0.5, 1.5, 3.5, 6.5, 9.5, and 12.5 ft for 1,000 sec. The probe was pushed the total depth of the intended push to collect soil stratigraphy and gross gamma data and then retracted. A representative spectrum acquired for a 3.5-ft depth is shown in Figure 72. A panel plot displayed in the truck showed soil strata and gross gamma count versus depth. The analysis of the spectral gamma data indicated that the increased gamma activity is attributable to daughter products of ^{232}Th, not ^{238}U. The elevated thorium concentrations can be seen by comparing the relative peak areas of the 1,460 keV peak from ^{40}K, which appears to be constant, and 2,614 keV peak from ^{208}Tl.

Discussion

During this initial field deployment, the automated software did not always properly identify or quantify the contaminant. Although quantitative data were obtained from this initial test, a substantial postprocessing effort was required offsite by PNL staff to reduce the data. Due to this fact, the recommendation was made for final data analysis to be performed manually. The resolution of the NaI detectors (about 14 percent) was not sufficient to observe some spectral peaks of interest. The DOE and WES objective for the first generation spectral

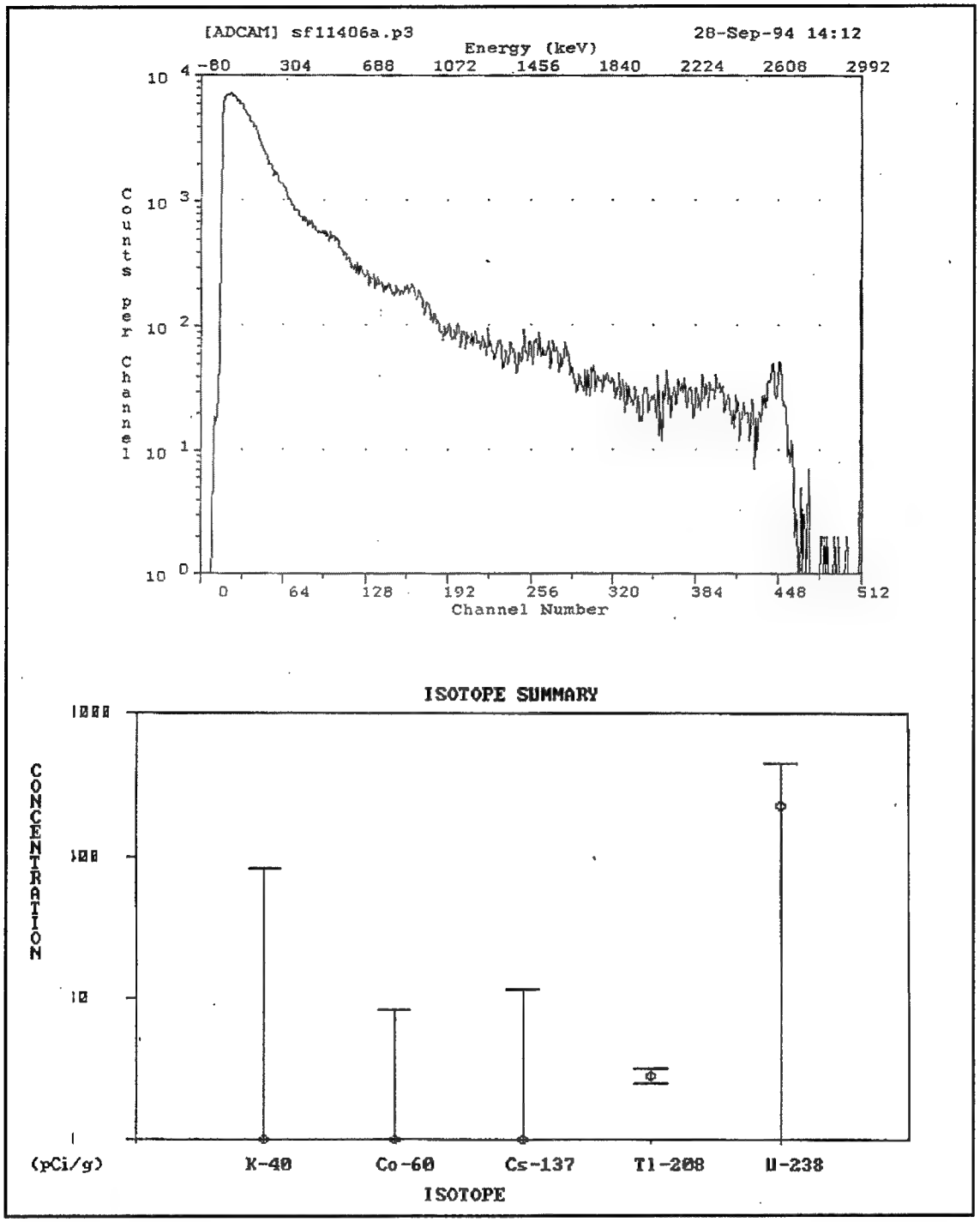

Figure 72. Results of Fernald test site spectral gamma data for location SF11406 at 3.5 ft bgs

gamma probe was to detect and identify ^{238}U concentrations as low as 50 pCi/g in soil; however, the first-generation probe demonstrated a detection limit for ^{238}U of between 60 and 80 pCi/g.

SERDP Program: Enhanced Spectral Gamma Probe Design

The SERDP funded WES to develop the design improvements for a second-generation spectral gamma probe with higher resolution and lower cost. The performance goals for the enhanced probe were that it be capable of detecting radioactive contaminants that emit gamma radiation with energies ranging from 300 KeV to 3 MeV and have sensitivities of approximately 35 pCi/g. In the first-generation probe, there was a considerable redundancy of costly electronics, since each probe contained an A/D converter, high-voltage supply, power supply, and microprocessor section. To reduce the cost and redundancy of this design, all downhole electronics were moved uphole with the exception of the detector, PMT, and preamplifier. Thus, each probe shares a common high-voltage supply, power supply, A/D converter, and microprocessor section located in the SCAPS truck. This configuration facilitates the adjustment of gain levels from an amplifier located in the SCAPS truck. Previously, any gain adjustment had to be made inside the probe. An added advantage is that with much of the costly electronics located in the truck, the cost risk is substantially reduced if a probe is broken or must be left in the ground.

The spectral gamma detection system was designed to SCAPS probe specifications using commercially available components. Field-use procedures for this probe affected the design such that it was conceived to conform to "as little as reasonably achievable" (ALARA) principles, or dose of radiation. As much flexibility as possible was designed into the system by use of industry-standard Nuclear Instrument Module (NIM) rack mounted modular components for data processing and storage. The schematic of the enhanced system is shown in Figure 73.

The probe contains a detector consisting of a high-resolution 1.0- × 3.0-in. cylindrical NaI crystal and photomultiplier tube, a temperature sensor, and a preamplifier downhole in the probe. The temperature sensor is essential to assess spectral drift due to thermal changes in the detector. During operation, analog signals are transmitted from the probe at depth through an umbilical cable to the SCAPS truck for data processing and storage. The data acquisition components consist of a spectroscopy amplifier from which the signal is split into a multichannel analyzer (MCA) buffer and to a rate meter. The MCA system yields approximately 9-percent resolution on the 662 keV line for Cs^{137}. In the current configuration, the gamma energy range for 2,048 channels is from approximately 100 to 2,000 keV, but this range can be modified by simple adjustments to the NIM mounted spectroscopy amplifier within the limits of the detector. There is some distortion in the low end of the spectrum due to scattering from the steel housing.

Data acquisition

The software program collects temperature and spectral data as it becomes available, corrects for temperature drift to prevent peak smearing, displays a raw

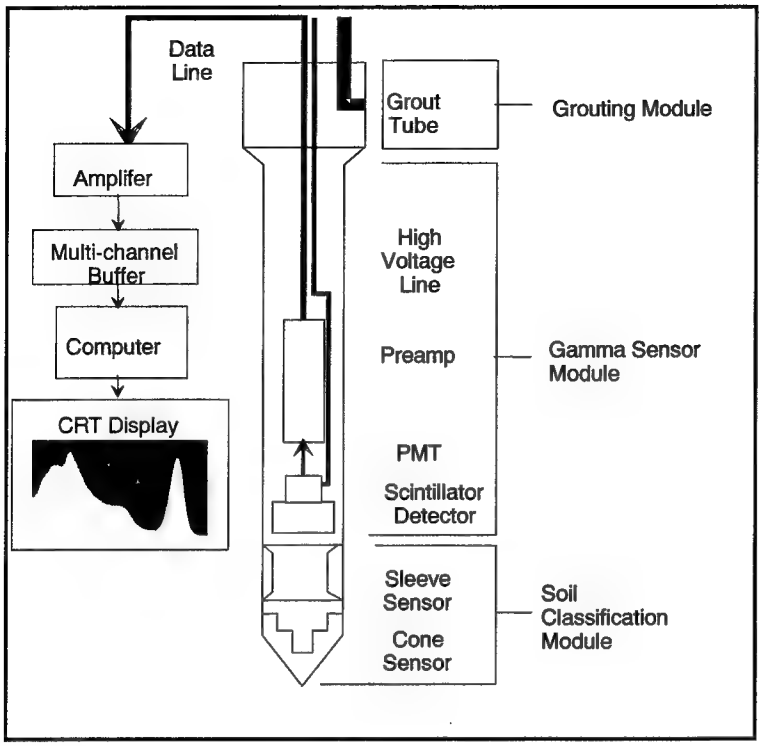

Figure 73. Enhanced spectral gamma probe

spectral data, near real-time temperature-corrected data, and a color two-dimensional (2-D) representation of the 3-D spectral information. In addition, all data are saved in an ASCII Universal histogram format for later use and flexibility in choice of analysis package.

In addition to spectral accumulation, the software collects soil stratigraphy data while the probe is being pushed. The SCAPS gamma probe may be pushed continuously to map "hot" areas within the soil subsurface, after which it can be directed to contaminated locations for a static spectral analysis of the subsurface region of interest. The SCAPS operator is able to acquire soil classification and gross gamma count versus depth in real-time and then visually analyze rate data collected during the push to select locations for additional investigation.

System calibration

Researchers from WES and the Mississippi State University Department of Physics Nuclear Group performed calibration experiments for the enhanced spectral gamma probe. Experimental measurements for the calibration of this probe were performed by pushing the probe into a barrel of radioisotope-doped soil. Spectra were acquired over a range of temperatures in a homogeneous mixture of short-lived radioisotopes and soil. (Morgan, Adams, and Ballard 1997). The loess-clay soil used in the calibration measurements was chosen for its midrange attenuation properties. Isotopes were chosen to provide a wide spectral range and short half-lives to eliminate disposal costs. The initial total

concentration was approximately 1,000 pCi/g. Care was taken to see that all of the contaminant was mixed thoroughly with the soil; after 1 week of turning the mixture, measurements using a survey meter showed equivalent count rates over the entire length of the calibration chamber (i.e., a 4-ft capped 20-in.-diam PVC pipe). A SCAPS gamma probe was inserted into the soil in the calibration chamber. The gamma response from the soil mixture was observed throughout roughly seven half-life time periods.

Spectral response and temperature data were continuously recorded with spectra saved every 15 min. Data were collected for 2 weeks. The probe was then removed and replaced with the second probe that was counted in a similar manner. This procedure was repeated changing probes every 2 weeks from October 1996 to January 1997. During the measurements, the temperature in the area where the experiment was conducted ranged from 20 to 100 °F, giving additional data for the temperature correction algorithm. The data were analyzed to give spectral response as a function of radioactive contaminant concentrations. Spectra are analyzed for peak position and areas and an algorithm to adjust gain and offset shifts as a function of temperature and energy was applied. An example spectrum of data corrected using the temperature correction algorithm is shown in Figure 74.

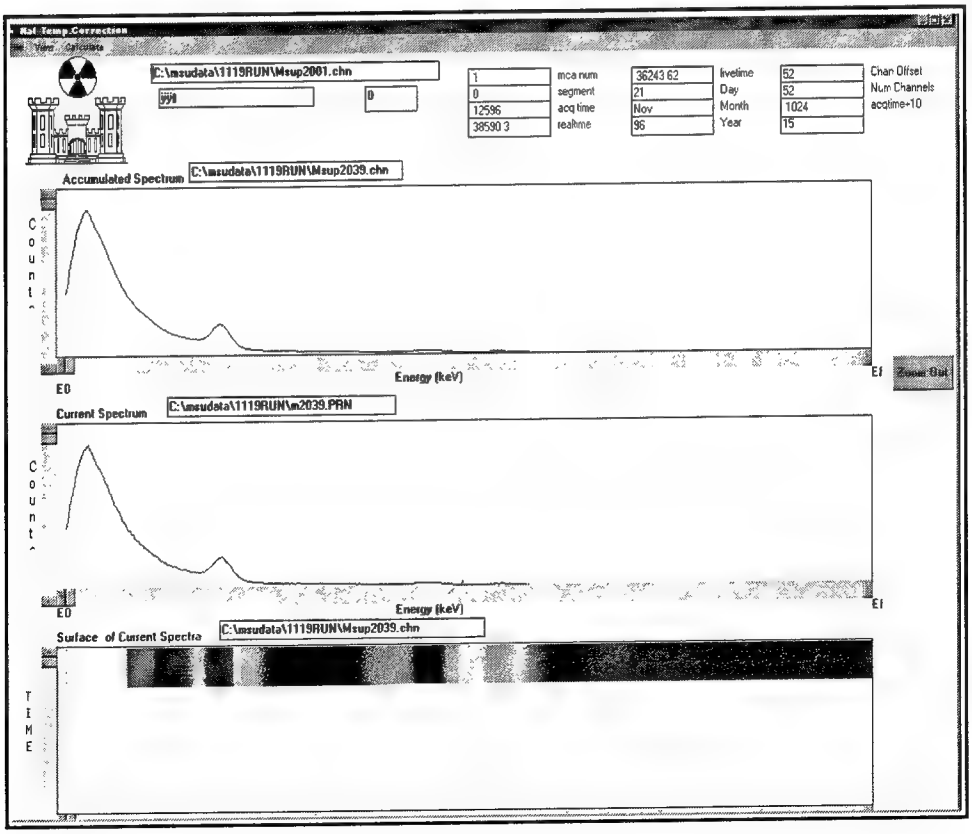

Figure 74. Spectral gamma probe temperature correction program

Results of the Savannah River Site (SRS), South Carolina, Field Demonstration

During the summer of 1997, the SCAPS Enhanced Spectral Gamma Probe was field demonstrated at the DOE's SRS. The DOE SCAPS truck was the deployment platform. The R-reactor site at the SRS has six seepage basins which were used as emergency catchments for reactor cooling water when an experimental zirconium cladding design failed during calorimetric testing in the 1950s. Approximately 2,800 Ci of waste were diverted into Basin 1, with outflow going to five other basins in series (RCRA 1995). The gamma emitter, Cs137, and the beta emitter, Sr90, dominate the contaminants expected in these basins. The water table lies approximately 20 ft below the natural clay lens that effectively form the bottom of the basins. The local geology consists of mixed clayey and silty sands. However, through past efforts to isolate the area, the basins were filled with soil from excavations, construction operations and backfill sources (mostly clayey sand soils). In 1996, an additional layer of nonradioactive soil (24 in.) and an asphaltic paving layer of 4 to 6 in. was used to cover the entire seepage basin area ~14 acres. Due to these events, there is no indigenous soil present in the basin area.

Data Analysis

One advantage of the SCAPS gamma probe over conventional well-logging methods is that it may be pushed continuously to map "hot" areas within the soil subsurface, after which the probe can be directed to contaminated locations for a static spectral analysis of the subsurface region of interest, taking longer counts as necessary. The SCAPS operator can acquire soil classification and gross gamma count versus depth and then visually analyze rate data collected during the screening push to select locations for additional investigation. This procedure was used at SRS. However, at SRS no spill classification data were collected. At the request of the on-site manager, the soil classification sensor module was removed from the probe. The push locations with the reactor basins were selected by the SRS site manager on the basis of sampling locations within the six basins for which there were laboratory data. Fifty-five pushes to depths of ~25 ft were made during mid-April to September. Spectra were collected at 1-ft intervals during each push, with additional spectra acquired to delineate contamination within the basins.

Final data analysis was performed offsite at WES. Spectral analyses consisted of a visual inspection and calibration check, as well as obtaining peak information, gross counts, and count rate for each spectrum. These data files were used as input to a temperature correction program to produce difference and gain shift-corrected spectra. Consistency between consecutive spectra was checked where peak areas were statistically significant enough to allow for comparison. From these spectra, final Cs^{137} concentration, in pCi/g, was calculated for each depth at every push location. An example spectrum is shown in Figure 75.

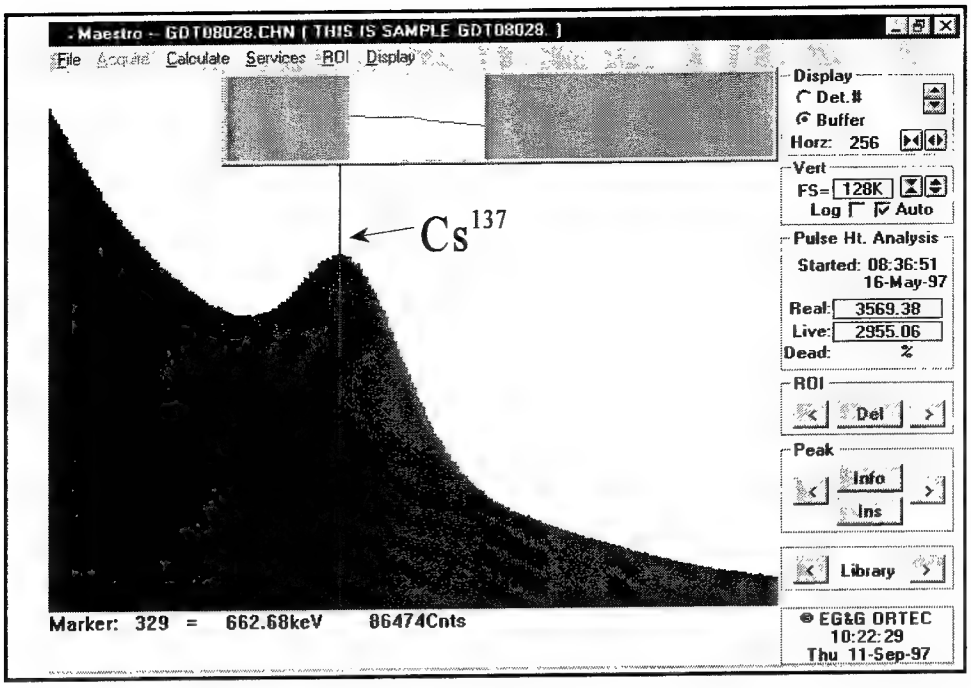

Figure 75. A representative gamma spectrum from the SRS

Assessment of gamma probe results was accomplished by a comparison of SCAPS results with previously obtained subsurface soil sample laboratory analyses. In 1996, SRS personnel took core samples from three of the basins using hand augers. Various depths to 20 ft below the surface were sampled. These cores were divided into 2-ft long sections, and these sections were then homogenized. Samples were extracted and submitted for laboratory radionuclide analyses. The background levels and contamination from three of the basins were analyzed using conventional laboratory methods (RCRA 1995).

The lack of homogeneity and soil attenuation factors makes comparison between the two data sets somewhat problematic. It should be noted that the results of the sample core analyses made in 1996 represent sample volumes that are significantly different, both in volume and material sampled, from soil volumes that are detected by the SCAPS gamma probe. Schematics of the respective sampling volumes are shown in Figure 76. Taking the example shown in Figure 76, the soil boring intercepts contaminated soil at the tip of the boring. Upon homogenization of the soil column, there will be a net concentration of radioactive material distributed throughout the soil volume. Since this layer lies outside the NaI detector sphere of influence in the situation diagramed in Figure 76, the detector will not register any contamination at this depth.

Push depth, gross gamma counts, gross counts, the calculated upper and lower Cs^{137} limits, and the normalized ratio of Cs^{137} to gross counts were the data used to plot the depth profile for each push (Morgan et al. in preparation). Two representative depths vs. concentration profiles for this push location are shown in Figure 77. For comparison with cone penetrometer data, the SRS core sample concentration from Basin 6 is indicated as a dashed line at ~2,300 pCi. It is

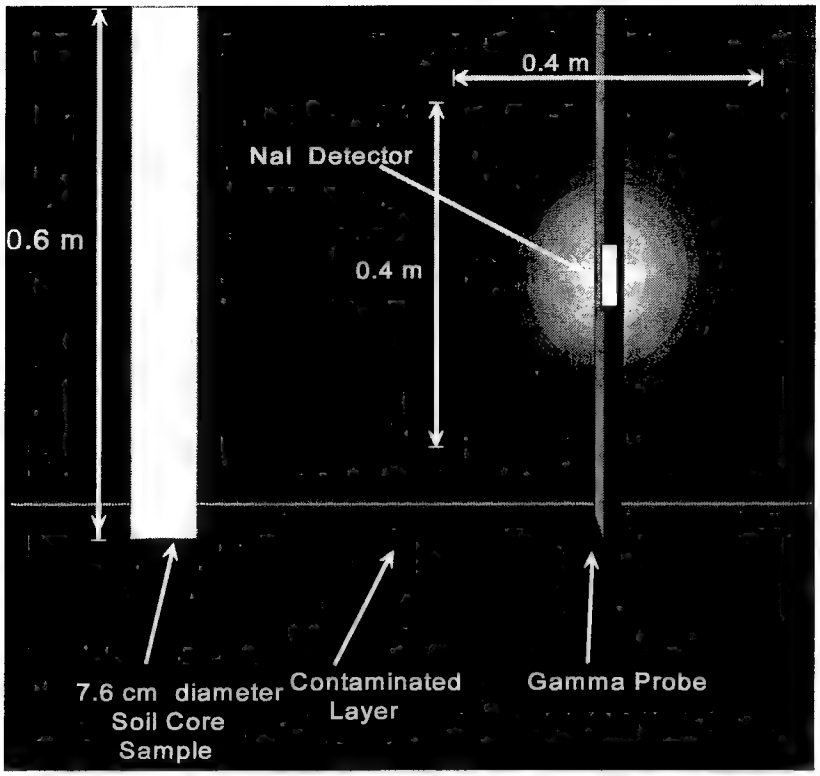

Figure 76. omparison of relative sampling volumes, core sample vs. SCAPS gamma probe

obvious from the plots of concentration vs. depth that the sources of contamination in the basins at R Reactor Area at SRS were not distributed in a homogenous manner but exist in well-defined layers. This was the case in each push location at SRS. (Argonne National Laboratory 1997).

Conclusions

The extended field investigation at the DOE, SRS, demonstrated the operational capabilities and utility of the enhanced SCAPS spectral gamma system that was designed under the sponsorship of the SERDP. Due to the sphere of influence sensed by the sodium iodide crystal, site conditions and specific push conditions must be considered to build an accurate evaluation of the subsurface contaminant distribution. The SCAPS spectral gamma probe has the advantage of in situ detection of radioactive contaminants at much reduced cost over conventional characterization costs. Future developments could lead toward higher resolution detectors, thus reducing data acquisition times.

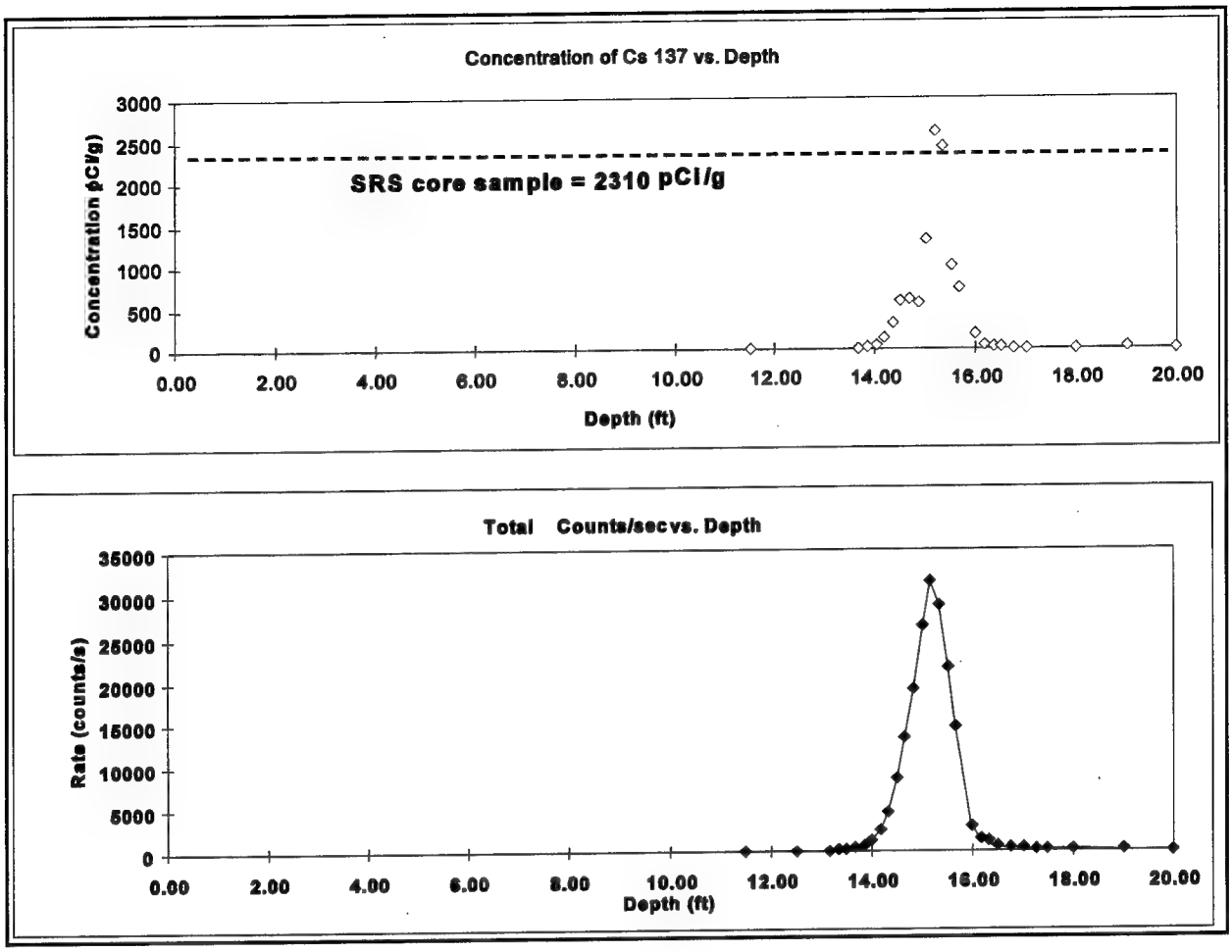

Figure 77. Cs^{137} concentration calculated from spectral gamma data as a function of depth at Basin 6 is shown by the connected points; the concentration of the core sample taken from Basin 6 measured from laboratory radioisotope measurements is indicated by the dashed line

Transition Plan

The SCAPS spectral gamma probe sensor system was used successfully during summer 1997 at DOE, SRS, with DOE contract personnel operating the DOE, SCAPS, vehicle. This project subsequently led to the development of the SCAPS Multisensor Spectral Gamma/X-ray Fluorescence probe for the DOE in 1997. WES is currently coordinating with U.S. Army Corps of Engineer District representatives to provide the SCAPS Spectral Gamma technologies developed under SERDP/DOE sponsorship including hardware, training, and data analysis to District users for Formerly Used Defense Sites (FUDS) and Formerly Utilized Sites Remedial Action Program (FUSRAP) site characterization.

7 Research Area VI: SCAPS Samplers

By: James M. Brannon, WES
Karen F. Myers, WES
Richard A. Karn, WES
Daniel R. Leavell, WES
Cynthia B. Price, WES
Dan Y. Eng, WES
Ann B. Strong, WES

Introduction

The DoD has become increasingly concerned with the environmental fate and remediation of contaminants at military installations. The DoD has responsibility for management and cleanup of sites contaminated with VOC used as solvents in a range of machining, manufacturing, and degreasing operations at installations. Management and cleanup of sites contaminated with VOCs require rapid, cost-effective, in situ sampling of contaminated soil. Current SCAPS LIF systems are capable of detecting polyaromatic organic compounds associated with petroleum, oils, and lubricants at contaminated sites but are not able to detect VOCs in soil.

Researchers at WES developed a TDS and a Multiport Sampler (MPS) for rapidly determining the concentration of VOCs in soil. Utilizing the principle of thermal desorption used in gas chromatography for soil analysis, the TDS transfers volatilized compounds to the surface where they are captured on an absorbent trap and later desorbed into an ITMS for identification and quantitation. Without being retracted, the TDS will sample discrete volumes of soil, heat and desorb the volatile compounds, eject the spent sample, and then can be pushed to successive depths where additional samples may be taken. The MPS was developed to provide a cone penetrometer with a more reliable means of obtaining multiple vapor and/or liquid samples from successive depths during a single push. It consists of a series of vertically stacked port modules, which are independently operated during sampling. As the cone penetrometer advances to a desired depth, the modules are selectively opened to capture soil pore vapor and/or liquid. The vapor and/or liquid samples may then be analyzed for

suspected contaminants or stored for other purposes. An Ion Trap Mass Spectrometer (IT/MS) or other appropriate instrumentation is normally used for direct analysis of contaminants. These samplers are especially useful because they provide quantitative, in situ, concentrations of VOCs in soil and soil gas.

Thermal Desorption Sampler

The objectives of this SERDP-funded effort were to improve the sampler mechanically to simplify operation, to evaluate additional target analytes, and field verify the mechanical and chemical functioning of the TDS.

Results and Discussion

Sampler design

The design of the TDS is illustrated in Figure 78. The TDS principle of operation is based on capturing a known volume of subsurface soil in situ and purging the VOC contaminants with nitrogen carrier gas while heating the soil. The purged VOCs are returned to the surface via a deactivated fused silica lined stainless steel analyte transfer line and interfaced to the analytical instrument for analysis. The TDS probe is pushed by the CPT to a predetermined depth, and a central actuator rod is retracted and the probe is pushed into the soil, collecting soil in an inner sample chamber. The chamber, and the soil therein, is heated to 120 to 150 °C for 5 to 15 min, depending on soil moisture and soil type, by a nichrome wire wrapped ceramic heater fitted with an inner stainless steel protective sleeve and a thermocouple to monitor temperature. The temperature of the ceramic heater can be controlled and maintained at a steady level. Immediately following initial collection of the soil in the chamber, a vacuum is applied to the outlet trap and an inert gas such as nitrogen is introduced into the sample chamber via a stainless steel tube located along the inner wall of the outer housing of the probe. The gas, which is heated as it passes over the surface of the heating coil, enters the chamber through six ports located in the top of the sample chamber and also flows upward over the soil plug. The VOCs are volatilized from the soil plug and are carried to the surface through the analyte transfer line, which is interfaced to the analytical equipment by a trap for volatilized organic contaminants.

Evaluation of additional analytes and the first field investigation

The TDS was shown to be capable of determining 1,1-dichloroethene, *cis*-1,2-dichloroethene, tetrachloroethene (PCE), naphthalene, and 2-methylnaphthalene in addition to the 12 compounds for which the TDS was designed and tested (Myers et al. 1995a). The first field investigation was conducted at Dover AFB. Field investigating showed that mechanically the probe functioned well, proving reliable and sturdy. Ejection of soil samples and closing of the probe below the surface was demonstrated. Experience gained

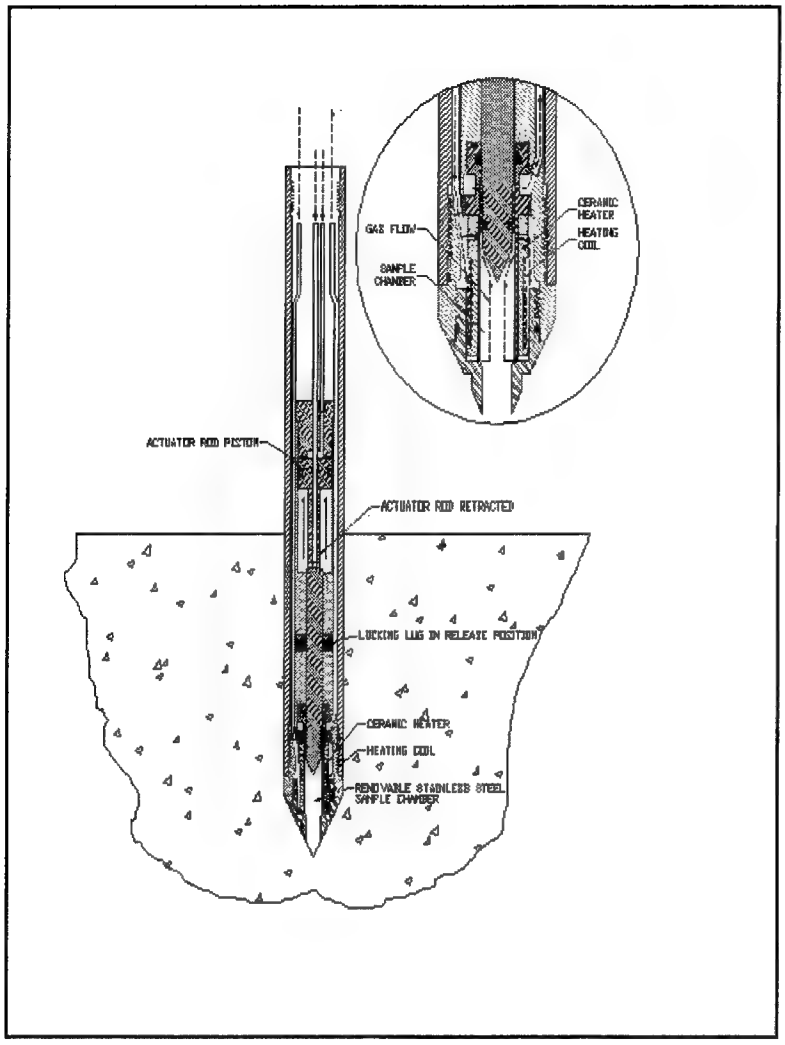

Figure 78. Schematic of TDS

from this field evaluation indicated the need for improved flow metering to measure flow during soil gas sampling. The need for an indicator to show when the probe was open or closed was also indicated. The TDS detected the contaminants present in the soil, but recoveries were generally low compared to verification samples. Results and details of the testing of additional compounds and the Dover field investigation are available (Myers et al. 1998).

Second field investigation, Aberdeen, MD

A second field investigation was conducted at Aberdeen Proving Ground, Maryland, to examine sampler operation in soils of differing characteristics and to determine if improved carrier gas flow control and mass flow meters on both the carrier gas and analyte lines could rectify the low recovery problem observed at Dover. Experimental methods were the same as those used at the Dover AFB field site (Myers et al. 1998). Data were obtained on 11 samples in four push holes before bending of the interior piston at 11 tons push pressure halted

sampling. Confirmation soil samples were taken at eight of the SCAPS sampling locations. The nature of the fill material in the vicinity of the push hole where the interior piston of the TDS buckled, caused the split spoon sampler to crack, making it impossible to take additional soil confirmation samples. The major contaminants found at the site were trichloroethane (TCA), TCE, and toluene. In all cases but one, detection of TCE by the TDS was verified by confirmation samples. The limited number of samples obtained before the TDS became inoperative showed that TCE concentrations measured with the TDS and in confirmation samples were generally comparable and exhibited a nearly 1:1 response. The number of samples, however, was too limited to draw general conclusions.

This field investigation showed that further modifications were needed to strengthen the TDS in addition to the physical improvements identified during the first field investigation. The limited number of TDS and confirmation sample analyses obtained prior to buckling of the TDS interior piston showed promise that the low recoveries observed during the first field investigation had been corrected.

Third field investigation, Eglin AFB

The objectives of this field investigation were to evaluate the changes that were made to improve the functioning and ruggedness of the TDS and to demonstrate the interface between the TDS and the IT/MS. Improvements to the TDS included; installation of a probe sensor to indicate whether the sampler tip is open or closed; hardening of the inner retractable rod; an increase in the length of the umbilical cable from 100 to 200 ft; substitution of silco steel for the stainless steel analyte line; use of a Teledyne model 3DQ IT/MS for field analysis rather than a gas chromatograph with photo-ionization detector (GC/PID); and investigation of the use of a commercial purge and trap to directly interface the TDS analyte line to the IT/MS.

Laboratory evaluation prior to field investigation. A limited laboratory evaluation of the direct purge and trap interface to the IT/MS was performed prior to the field investigation. The direct interface consisted of an OI Analytical model 4560 purge and trap sample concentrator fitted with additional manual switching valves to route sample gases from the TDS through the purge vessel and into the trap where they could be concentrated and then desorbed onto the IT/MS. The purge and trap was attached directly to the TDS analyte line via the gas manifold. The model 4560 system vent was fitted to accept a vacuum pump to assist gas transport throughout the TDS analytical system. Analytical standards were introduced through the purge vessel. The target analyte list and ions used for quantitation are given in Table 14.

TDS operation procedures. The TDS (Figure 78) was pushed to a selected depth in the subsurface. The sampler was then raised 0.1 to 0.5 in. to break contact with the soil and the interior rod was retracted. The sampler was then pushed 1.8 to 1.9 in. and the temperature monitored to gauge the amount of soil in the sample chamber. A full 1.9-in. push resulted in a soil plug approximately

Table 14
Target Analyte List

Analyte	Quant Ion	Analyte	Quant Ion
1,1-Dichloroethene	96	Tetrachloroethene	164
1,1,1-Trichloroethane	99	Chlorobenzene	112
Trichloroethene	130	Dichlorobenzene	146
Benzene	78	Ethylbenzene/T-Xylene	106
Toluene	92		

1 in. long in the sampler. Prior to the push, temperature in the probe desorption chamber was stabilized at 150 °C and gas flow was initiated at 40 ml/min. In the field, analysis for the TDS occurred one of two ways: analytes were collected and desorbed from the OI Analytical purge and trap described above or were collected on a tenax trap attached directly to the gas manifold. At the conclusion of a sampling event, contaminants on the tenax trap were desorbed with 1 ml of methanol (MeOH), and a portion of the methanol extract analyzed using the Teledyne IT/MS.

After thermal desorption was completed on the in situ soil sample, the soil was ejected and the probe flushed briefly at high pressure and then closed. The probe-tip sensor was tested by bringing the TDS probe to the surface and confirming that the tip was closed and locked. If the soil was ejected and the probe tip closed properly, the sensor displayed a green light. Display of a red light or no light meant that the probe tip was either retracted and open or that the tip was not locked in place. Once the sample had been ejected and the probe tip closed, the system was flushed with helium for 5 min and then a 5-min blank was taken to establish the status of the system prior to the next sampling event. The sampler was then pushed to a new depth where the process was repeated.

Verification samples. Verification soil samples were taken with a Mostap sampler using an 18-in. split sleeve. Samples were taken as prescribed by USEPA SW-846 Method 8260A (USEPA 1994) and by the method developed by Hewitt (1994). The Hewitt method involved quickly placing a 4-ml portion of sample into a preweighed vial containing 5 ml of methanol. The vial was mixed to extract and fix the volatile compounds and reweighed. All samples were stored and shipped at 4 °C. Laboratory analysis was performed using a Hewlett Packard 5890 Series II gas chromatograph with a mass selective detector and an OI Analytical DPM-16 discrete purging multisampler.

Field results. Three sites were visited at Eglin AFB: a) site FT-28, Eglin main base old fire training area; b) site ST-72, A.C.C. tank farm; and c) site ST-75, adjacent to a jet wash. All sites were in the vicinity of existing monitoring wells, which were used to determine approximate groundwater depths. Standing water in some wells was sampled with a Teflon bailer and the sample analyzed by IT/MS. Table 15 identifies the samples taken at the three sites and gives the status of the data and the verification samples. Five pushes with a total of 10 samples were attempted at FT-28, one push with one sample

Table 15
Status of Samples Taken at Eglin AFB

Samples taken at FT-28		Groundwater (ft bgs)	Data Status (target analytes)	Verification Sample?
P 2	S 39	38	all <0.100 mg/g	NO
P 3	S 34.5	36.3	NO sample, hit 12 tons at 34 ft	NO
P 4	S 34.5	36.3	all <0.033 mg/g	YES
	S 36.5		all <0.033 mg/g	YES
	S 37.5		all <0.033 mg/g	NO - sand fell out bottom of sleeve
P 5	S 37	36.3	data	YES
	S 39		all <0.033 mg/g	YES
Well FT-28-01 D			all <0.010 mg/ml	NO
tar sample			all <0.200 mg/g	NO
Samples taken at ST-72		**Groundwater (ft bgs)**	**Data Status (target analytes)**	**Verification Sample?**
P 1	S 35	34.7	all <0.100 mg/g	NO
Well EA-5		34.3	all <0.0025 mg/ml	NO
Well EA-7		34.7	all <0.0025 mg/ml	NO
Samples taken at ST-75		**Groundwater (ft bgs)**	**Data Status (target analytes)**	**Verification Sample?**
P 1	S 37	36.2	NO sample, hit limestone, 15 tons	NO
Well EA-14		36.2	all <0.0025 mg/ml	NO

each was attempted at ST-72 and ST-75. In addition, the water from one well was analyzed by IT/MS at FT-28 and ST-75. Water from two wells was analyzed at ST-72. A tar sample taken from FT-28 was extracted with methanol and analyzed for target analytes. Verification samples were successfully taken for 4 of the 12 field samples. Verification samples were not attempted unless the TDS data indicated the presence of target analytes.

Mechanical functioning. The first three samples attempted were lost because of a combination of gas flow problems. Gas flows from the analyte line were less than 5 ml/min even with vacuum assistance. The repositioning of the vacuum from the TDS gas manifold to the vent of the OI purge and trap combined with the additional 200 ft of gas lines offered greater resistance than expected from the laboratory evaluation. In addition, flow up the analyte line was not continuous. Once the switches on the OI purge and trap were thrown to direct the sample into the IT/MS, the flow was halted. This meant that purging of the line was stopped and that the flow meters on the TDS no longer functioned. It was also determined that the probe was leaking internally around the top of the sample chamber. The probe was disassembled and repaired and

the direct interface from the TDS gas manifold was removed. Subsequent samples were collected on tenax traps and eluted with methanol as described above. Once the leaks were eliminated from the probe sample chamber, the 200-ft umbilical offered little resistance to gas flows.

Sandy soil impeded sampling at two sites. Penetrometer pushes at FT_28P3S34.5 and ST-75P1S37 were discontinued when the truck hydraulic ram force reached 12 and 15 tons, respectively. At ST-75 the probe tip appeared to be caked with limestone (this was not confirmed). However, the hardened inner retractable rod was not deformed in any way and continued to function flawlessly. Verification soil samples for FT-28P4S37.5 were not taken because the sand fell out of the Mostap upon retrieval.

The probe sensor designed to indicate if the tip was open or closed functioned extremely well. The sensor lights accurately indicated if the tip was open or closed. In cases where grit hampered complete shutting of the probe, neither light came on to correctly indicate that the probe tip was not completely shut and locked. For the most part, the sandy plugs ejected well. O-rings had to be checked between each push location because of wear caused by the sand.

Soil sampling. In general, concentrations of target analytes were less than 0.100 mg/g for all samples except FT-28P5S37. Confirmed target analytes were toluene, chlorobenzene, and a combination of total xylenes and ethylbenzene. Concentrations taken from the TDS analysis are compared to the verification soil samples in Table 16. Sample blanks were taken at the beginning and end of each day and between every sample. There were not enough samples with high concentrations to determine if the silco steel improved the flushing of the analyte line.

IT/MS. In the electron impact mode, the IT/MS proved to be a very good screening tool. Analysis took 10 min compared to 25 min for the GC/PID system. There were conflicts with accurate identification and quantitation, however, because of the sharing of quantitation ions. For example, ion 106 is the quantitation ion for both ethylbenzene and the individual xylene isomers (Table 14). Any compound exhibiting ion 106 would positively increase the quantitation for these analytes. Near the end of the field investigation, chemical ionization (CI) IT/MS reduced the instances of false positives. This is because aromatic compounds (BTEX) have a better CI response than aliphatic (fuels).

IT/MS techniques have very good detection limits with analytical ranges from low mg/L (ppb) to mg/L (ppm). Lack of a functioning automatic gain control on the IT/MS made analytical procedures challenging. The nature of sample introduction, a quick 1-min desorption from a trap, mandated rapid selection of appropriate concentration ranges for each sample. High-concentration samples demonstrated space charging that would produce unreliable analyte concentrations. This was solved by establishing equivalencies between ranges and quickly adjusting the MS ionization time from milliseconds to microseconds as the sample appeared on the screen. Conversely, samples with low concentration needed their MS ionization times increased to add

Table 16
Comparison of Field Data to Laboratory Validation Samples

	FT28 P4 S34.5			FT28 P4 S36.5		
	TDS	Hewitt MeOH ext	EPA 8260A	TDS	Hewitt MeOH ext	EPA 8260A
	mg/g	mg/g	mg/g	mg/g	mg/g	mg/g
Toluene	<0.033	<0.25	<0.005	<0.033	<0.25	<0.005
Chlorobenzene	<0.033	<0.25	<0.005	<0.033	<0.25	<0.005
T-xylene /Ethylbenzene	<0.033	<0.25	<0.005	<0.033	<0.25	<0.005
	FT28 P5 S37			FT28 P5 S39		
	TDS	Hewitt MeOH ext	EPA 8260A	TDS	Hewitt MeOH ext	EPA 8260A
	mg/g	mg/g	mg/g	mg/g	mg/g	mg/g
Toluene	3.50	3.04	2.1	0.004	<0.25	<0.005
Chlorobenzene	<1.7	0.98	<5.0	<0.033	<0.25	<0.005
T-xylene /Ethylbenzene	21.9	6.78	50.5	0.0056	<0.25	0.0016

sensitivity. This adjustment of ionization times resulted in the differing detection limits.

Conclusions

Improvements to the TDS worked well and greatly improved its mechanical functioning. The IT/MS proved to be an excellent, rapid screening tool, although the lack of a functioning automatic gain control resulted in challenging analytical conditions. The OI Analytical purge and trap interface did not function as expected. The system was complicated and presented numerous problems during sampling and analysis and required more time in the purge mode than did the custom built sparging interface developed by Oak Ridge National Laboratory (ORNL) for the IT/MS. Collecting analytes on the trap attached to the gas manifold, followed by extraction with methanol worked well as an interface to the IT/MS but resulted in slightly higher detection limits. It was therefore decided to use the custom-built trap desorption apparatus developed at ORNL in future investigations.

Multiport Sampler (MPS)

The objectives of this SERDP-funded effort were to simplify operation of the MPS by improving it mechanically, evaluate an additional method of

collecting and analyzing analytes, and field verify the mechanical and chemical functioning of the MPS.

Results and Discussion

Sampler design

A conceptual drawing of the MPS is shown in Figure 79. The design, initial development, and the first field demonstration of the MPS at Savannah River Site, 5-10 June 1994, were funded by the Army Environmental Center (AEC) and are discussed by Leavell and Lee (1995) and Leavell, Malone, and Lee (1996). The MPS was developed to provide the cone penetrometer system with a more effective means of obtaining soil vapor and liquid samples. The MPS consists of a series of vertically stacked port modules, which are independently operated during sampling. As the cone penetrometer advances to a desired depth, the modules are selectively opened to allow entrance of soil pore vapor and/or liquid. The vapor and/or liquid samples may then be analyzed for suspected contaminants or stored for other purposes. The collection/transfer lines between the MPS and the equipment used to analyze VOCs are made of stainless steel tubing. An IT/MS containing a custom-built sparging interface unit developed by ORNL is normally used for direct analysis of contaminants. The MPS unit is the only fluid sampler that is designed to allow soil strength measurement to be made during the same push that samples are taken and to permit grout to be injected into the penetrometer hole as the probe is retracted. A patent (U.S. Patent Office 1994 (No. 5,358,057)) has been granted for the MPS system.

Field Investigation at Dover AFB

The field investigation at Dover was conducted to evaluate the MPS capability to measure the contamination levels of VOCs using the IT/MS and Drager tubes for direct measurements and contaminant traps (CT) for obtaining VOC and water samples for postanalyses. In addition, the Dover AFB field demonstration showed that improvements to the probe had corrected mechanical problems experienced during the first field demonstration at SRS.

The Dover AFB site, shown in Figure 80, was located on an aircraft parking apron, adjacent to a jet engine wash facility. The site was paved with approximately 6 to 8 in. of concrete. Before the probe could be pushed, the concrete was cored using a hand-operated coring drill that was flushed with water. The use of water during the coring operation caused the cored holes to fill with water. This situation was further complicated by rain, which filled previously cored holes. In some of the holes, water backed up under the pavement causing the holes to continually fill with water as they were being emptied. No probe was pushed in a hole before it was emptied of surface water.

Eight holes were pushed, MPS1 through MPS8. Data were obtained using both the CT and IT/MS systems for holes MPS1 through MPS7 and are shown

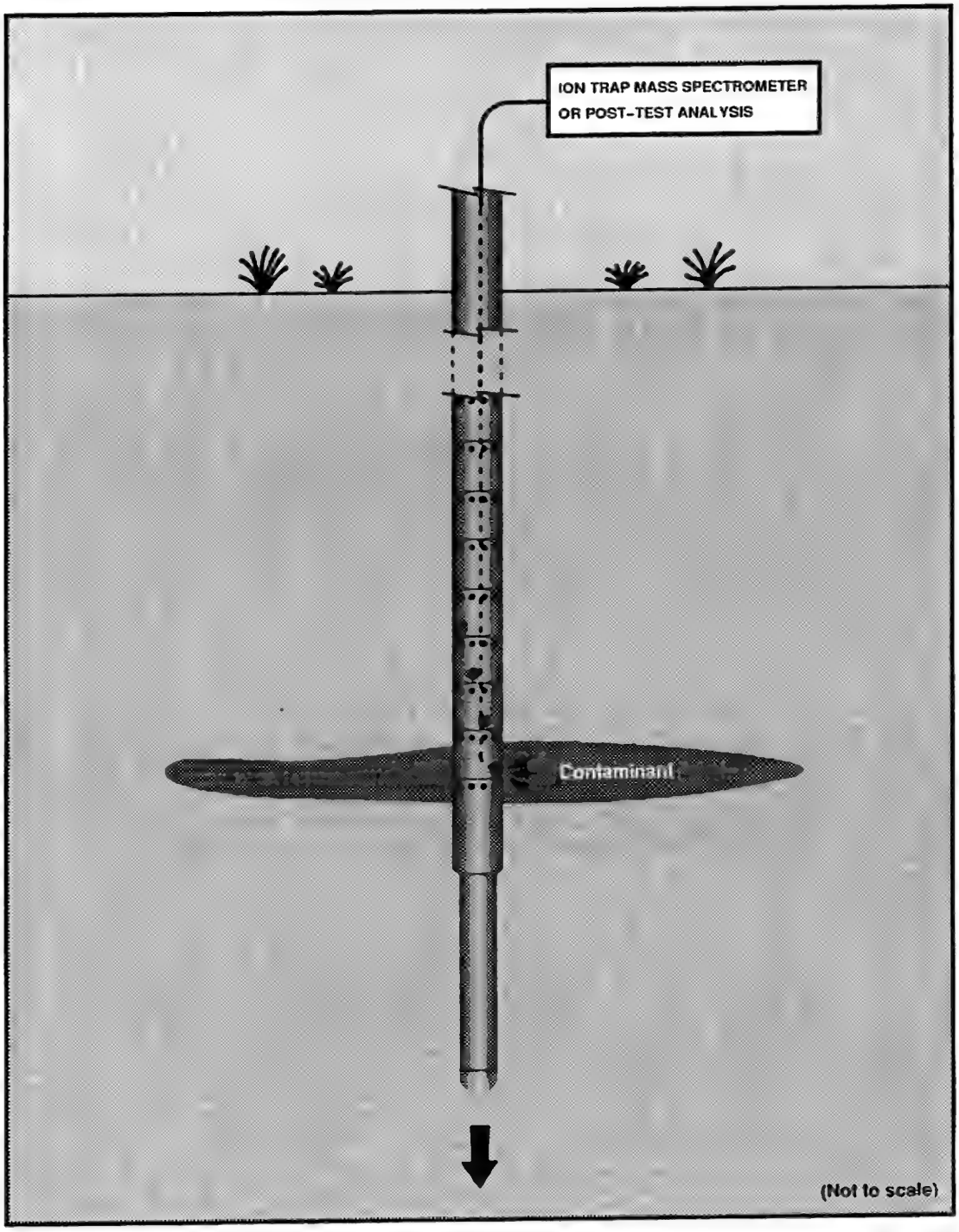

Figure 79. Conceptual drawing of the MPS

for comparison in Table 17. Hole MPS8 was used to demonstrate the Drager pump/tubes and to obtain a water sample from below the water table. Use of the Drager monitoring pump was unsuccessful, because its sampling rate was too slow (collected 1 l/hr) for field applications. However, because the Drager tubes

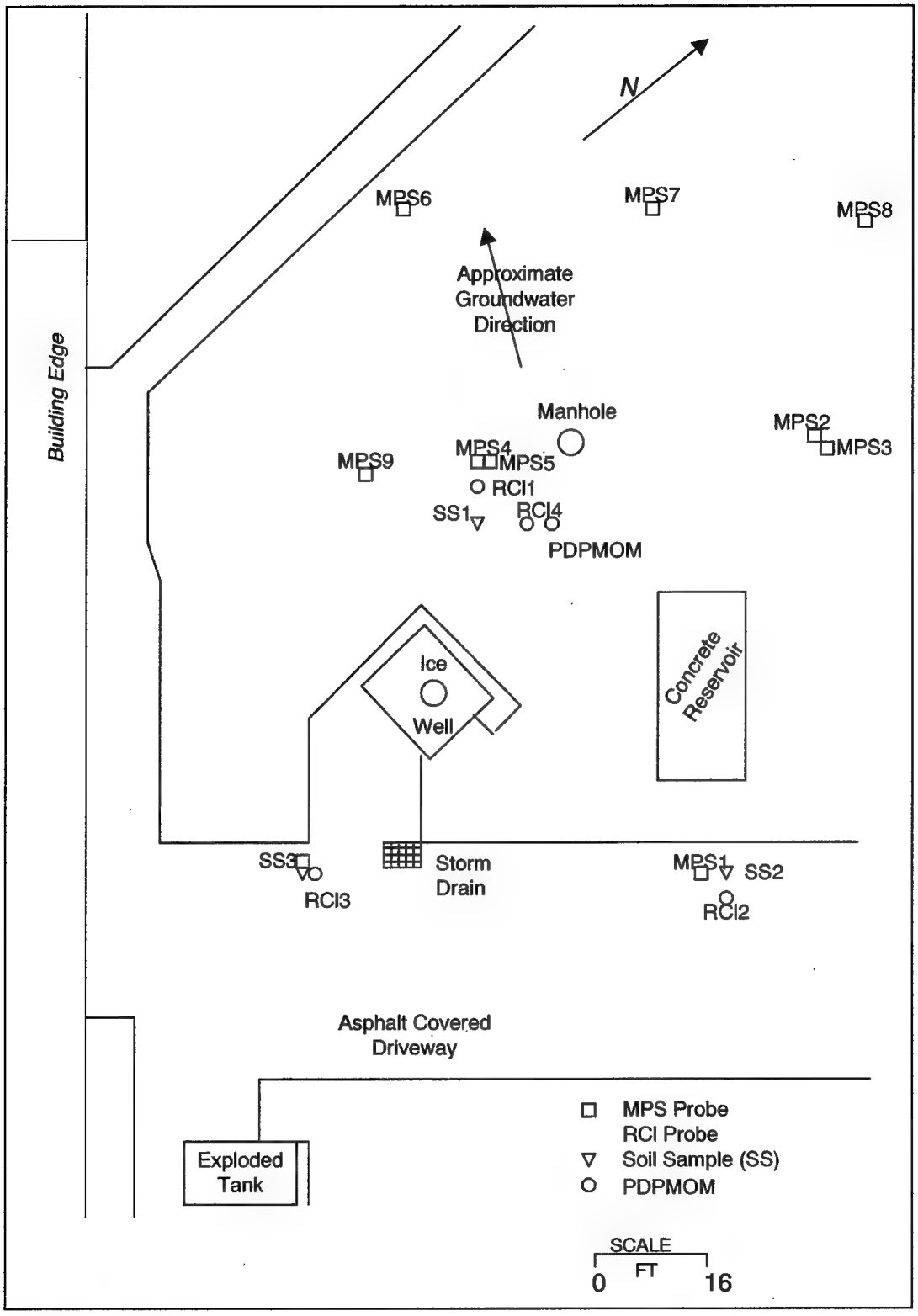

Figure 80. Site map of the Dover AFB field demonstration

Table 17
Comparison of MPS Direct Measurement and CT Data from Dover AFB Field Demonstration

Contaminant Trap Data								
Data file	Hole No.	Depth	Port No.	Sample Vol ml	1,1,1-TCA ppmv	TCE ppmv	Benzene ppmv	Toluene ppmv
MPS11	1	6.18	6	400	4	2	0	2
MPS12	1	6.83	2	45.2	46	18	0	16
MPS13	1	7.83	4	45	5,990	1,351	0	0
MPS31	3	3.83	2		ERROR	ERROR	ERROR	ERROR
MPS32	3	4.83	4	42.2	423	0	0	35
MPS33	3	5.83	6	92.6	44	0	154	28
MPS41	4	3.83	2	1.6	806	0	0	453
MPS42	4	4.83	4	5.1	149	0	117	139
MPS43	4	5.83	6	99.8	1,537	0	274	6
MPS51	5	4.33	6	143	5	0	0	0
MPS52	5	5.33	4	56.8	13	0	0	0
MPS53	5	5.83	2	0.1	8,043	0	0	0
MPS61	8	21.55	6	10	1	0	0	0
Direct Measurement Data								
				Flow Rate ml/min				
0502AR02	1	8.00	3	600 to 700	12,907	206	NA	NA
0502AR03	1	9.00	5	130 to 190	11,637	109	NA	NA
0503AR01	3	5.00	3	50	546	NA	14	23
0503AR02	4	6.00	5	50	3,083	NA	6	28
MPS7	7	7.00	4	200	166,344	4,560	NA	NA
MPS7A	7	8.00	6	200	86,766	2,382	NA	NA

could be used independent of the Drager pump, they were connected to a vacuum pump, which allowed sampling rates up to 1 l/min. This procedure was successful and gave quantitative results to within 20 percent of other collected results. Data from the Drager tube indicated hydrocarbon contamination levels of between 1,000 and 1,250 ppm with no detectable trace of TCE. This demonstration showed the Drager sampling tubes to be an inexpensive, qualitative, alternative to the IT/MS for sampling known contaminants.

A CT was used in MPS8 for collection of contaminants below the water table. Only one experiment was performed with this specially configured contaminate trap. The probe was pushed to approximately 25 ft and the natural

water head (about 10 ft) was used to push approximately 10 ml water through the CT. The analyzed data from the trap are presented in Table 17.

The major contaminant at the site was TCA. From the field data it is apparent that the contaminant concentration levels change significantly with depth and location. Therefore, minor changes in depth can result in major differences in contaminant concentration. The most valid comparisons between CT and the IT/MS data are:

a. MPS13 (CT) and 0502AR02 and 0502AR03 (IT/MS)

b. MPS32 (CT) and 0503AR01 (IT/MS)

c. MPS43 (CT) and 0503AR02 (IT/MS)

The Dover AFB field demonstration verified that problems experienced at SRS were subsequently corrected. Problems experienced at SRS, solution, and performance of the MPS at Dover AFB are listed below.

a. Maintaining port integrity during a penetration event was a problem at SRS, even though all investigations conducted at WES were successful. The WES investigations involved the use of one friction breaker in the field and no friction breaker in the laboratory. However, at SRS two friction breakers were used: one before the sampling ports and one after. It was proposed that various friction breaker configurations be investigated at WES. It was thought that configuring the MPS with one and two friction breakers and then with no friction breakers would show if the number of friction breakers caused the port sealing problem. The MPS was pushed at WES as proposed. It was found that using two friction breakers caused the ports to open as the MPS was pushed to depth. It is assumed that two friction breakers, one placed above and one placed below the MPS modules, increase the horizontal in situ stress. Therefore, only one friction breaker was used at Dover AFB, and the MPS had no port leakage or sealing problem.

b. Because of the SRS experience, a pressure monitoring system for each port is required to determine if/when a port seal is broken. The MPS control panel was modified so that a flow meter could be used to monitor and/or measure port leakage. The modified control panel worked as designed and a mass flowmeter was used to monitor port seals, pressure connections in the probe, and sampling flow rates. The mass flowmeter worked extremely well. A leakage check of each port before the penetration event ensured that the overall pressure leakage in a probe was less than 20 ml/min at a pressure of 125 psi.

c. The screws used to connect each module tend to become compacted with soil during a penetration event. The compacted soil in the screw head is difficult to remove and complicates the disassembly of the MPS. A new module connection design that eliminated the screws was developed which used three dowel pins indexed by 120 deg around the module.

The new design was successfully investigated at Dover AFB and minimized the time required for disassembly. The dowel pins also increased the connection strength 2.5 times.

d. It is difficult to determine the location of each port, with relation to the soil strata, during a sampling event. Computer software was modified to indicate "real time" port depths with the soil classification screen display. The software worked well and allowed accurate sampling of thin soil layers.

e. The connection between the sampling tube/CT and the MPS module occasionally comes loose during the pressure check. Shallow threads were used to affix the sampling tube/CT to each module. None of the sampling tubes/CTs came loose during any sampling event at Dover AFB.

Additional modifications that were made to the MPS and how they performed at Dover AFB are:

a. Some lengthened pistons were substituted for the normal pistons in an attempt to allow sealing of the ports after a sampling event. Resealing of the ports was successful about 80 percent of the time when the lengthened pistons were used. The unsuccessful attempts were caused by saturated soil flowing into the port (the zone around the probe was saturated, possibly from surface water).

b. All CTs were grooved such that a positive attachment to the o-ring-sealed quick-disconnect coupling could be made. The modified CTs worked well with no blown connections during the field investigations.

c. A special program that compensates for the dead volume in the sampling tube was developed and used to obtain the volume (to within 10 percent) of vapor sampled through the contaminant trap. The program worked well.

Field Investigation at Cold Regions Research Engineering Laboratory (CRREL), Hanover, NH

A field demonstration of the MPS and IT/MS was conducted at CRREL during 2-6 February 1996. The objectives of the investigation were to demonstrate the capability to measure the contamination levels of VOCs using the IT/MS for direct measurements, to verify that MPS modifications enhanced its in situ measurement capabilities, and to demonstrate that the MPS would operate in subfreezing weather.

Modifications made to the MPS after the demonstration at Dover AFB were:

a. The 0.125-in. nylon tubing in the umbilical cable was replaced with 0.0625-in. stainless steel tubing. The advantage of the new tubing

(stainless steel) is that it does not absorb the sampled contaminant and can be cleaned more easily. The tubing is cleaned by blowing nitrogen through it. The volume required for cleaning can be as little as the tubing volume (approximately 20 ml).

b. The maximum number of modules used in the probe at one time was reduced from 10 to 6 because of the installation of a new hydraulic chuck system in the SCAPS truck. The number of sampling tubes in the umbilical cable were also reduced from 12 to 7 (one spare). The reduction in tubes allowed spacing of the connections in the tweener rod section so that all interconnecting tubes between the modules and the umbilical cable can be made the same length. The uniform length reduced fabrication time and eliminated errors in probe assembly.

c. The 0.125-in. nylon interconnecting tubing between the modules and umbilical cable was replaced with thin-wall 0.125-in. stainless steel tubing. Replacing the nylon tubing with stainless steel allowed the probe to remain assembled for cleaning. The probe can now be assembled in the laboratory before the field trip, checked for leaks, and used repetitively in the field. The MPS will only require disassembly if problems occur in the field or for a thorough cleaning after it returns from the field.

d. The length of the new umbilical cable was increased from 120 to 150 ft during the modification to accommodate the 0.0625-in. stainless steel transfer tubes. The increased length allows the probe to be pushed to a maximum depth of approximately 90 ft. The maximum depth attained during the CRREL demonstration was 79 ft bgs at the probe tip. This exceeded the previous maximum depth of 58 ft bgs.

e. The port pistons were lengthened by 0.03 in. The additional length allowed the pistons to close after a sampling event. Percentage of ports that could be closed after a sampling event was approximately 80 percent. Ports that were closed after a sampling event were used at different depths. For hole MPS5, port #1 was used at four depths during hole penetration and at two depths during retraction of the probe.

The geology at the CRREL site indicates the top 60 ft bgs of material to be ML (cohesionless inorganic silt and very fine sands). The material from 60 ft bgs to bedrock can be classified as SM (silty sands, sand silt mixture). Both the ML and SM tend to have a low permeability to liquids with the ML being less permeable.

The weather at the CRREL site during the field demonstration was cold and dry. The temperature ranged between 10 and 40 °F on the first day, but dropped to between -9 and 15 °F for the remainder of the field demonstration. Because of the subzero temperature, the nitrogen bottle used to pressurize the MPS was moved from outside to inside the truck. Having the nitrogen warmer than the ground temperature (the ground temperature typically remains at about 60 °F year around) ensured that vapor extracted from the vadose zone would not

condense on the interior walls of the sampling tubes as it was drawn to the surface for analysis by the IT/MS.

Ten holes were attempted during the 4-day field demonstration. See Figure 81 for their locations. Three of the holes were not successful. These holes and their associated problem are:

a. MPS2 - A ductile steel pipe was hit at 7.2 ft bgs. The probe was retracted and the incident was reported. Since no fluid seeped from the hole when the probe was retracted, it was marked and abandoned.

b. MPS4 - Because of frozen ground, the probe started into the ground at an angle. The hole was abandoned. After hole MPS4 a dummy probe was used to prepush holes in the frozen ground.

c. MPS10 - Hole 10 was attempted twice without success. Data from this hole were to be used for comparison of MPS and RCL results. It is thought that the subzero temperatures froze the two layers of asphalt and underlying ground to the point that the dummy probe could not penetrate. No data were obtained for these holes and are only presented for completeness.

Difficulties were encountered with holes MPS1 and MPS6. The probe was configured without a friction breaker for hole MPS1. It was pushed to 30 ft and retracted because of port sealing problems. It is thought that the air volume contained in the 0.0625-in.-OD stainless steel tubing was not sufficient to keep the ports closed. The probe was then reconfigured with a friction breaker, and pushed to approximately 75 ft bgs. Samples were obtained every 10 ft to a depth of 72.25 ft bgs. After configuring the probe with a friction breaker no port sealing problems were observed through the remainder of the field demonstration. During reconfiguration of the probe, the cone wires were broken. Therefore, the cone and sleeve data taken for hole RCL2 is used for the soil stratification of hole MPS1.

Hole MPS6 was pushed to 22 ft bgs with sampling attempted at 10 and 20 ft bgs. No gas flow was obtained for IT/MS sampling; therefore the ports were assumed clogged with soil. The probe was retracted to determine possible causes for no flow through the ports. After probe retraction, it was found that all ports were clean and sealed. It was finally discovered that the connection for the sampling tube to the IT/MS was loose and not allowing enough suction to develop at any probe port to open the pistons. The connection was tightened and the probe was pushed in the same hole with good results.

Data for the MPS and soil samples are shown in Table 18. The data show that the top 60 ft of soil around the ice well have a relatively high concentration of TCE. The data also indicate that, as you move away from the ice well, the concentration of TCE decreases. In the lower sand layer, below 60 ft, the data indicate the TCE concentration to be approximately 5,000 ppm. Information from CRREL showed that the groundwater contains 120 ppm of dissolved TCE.

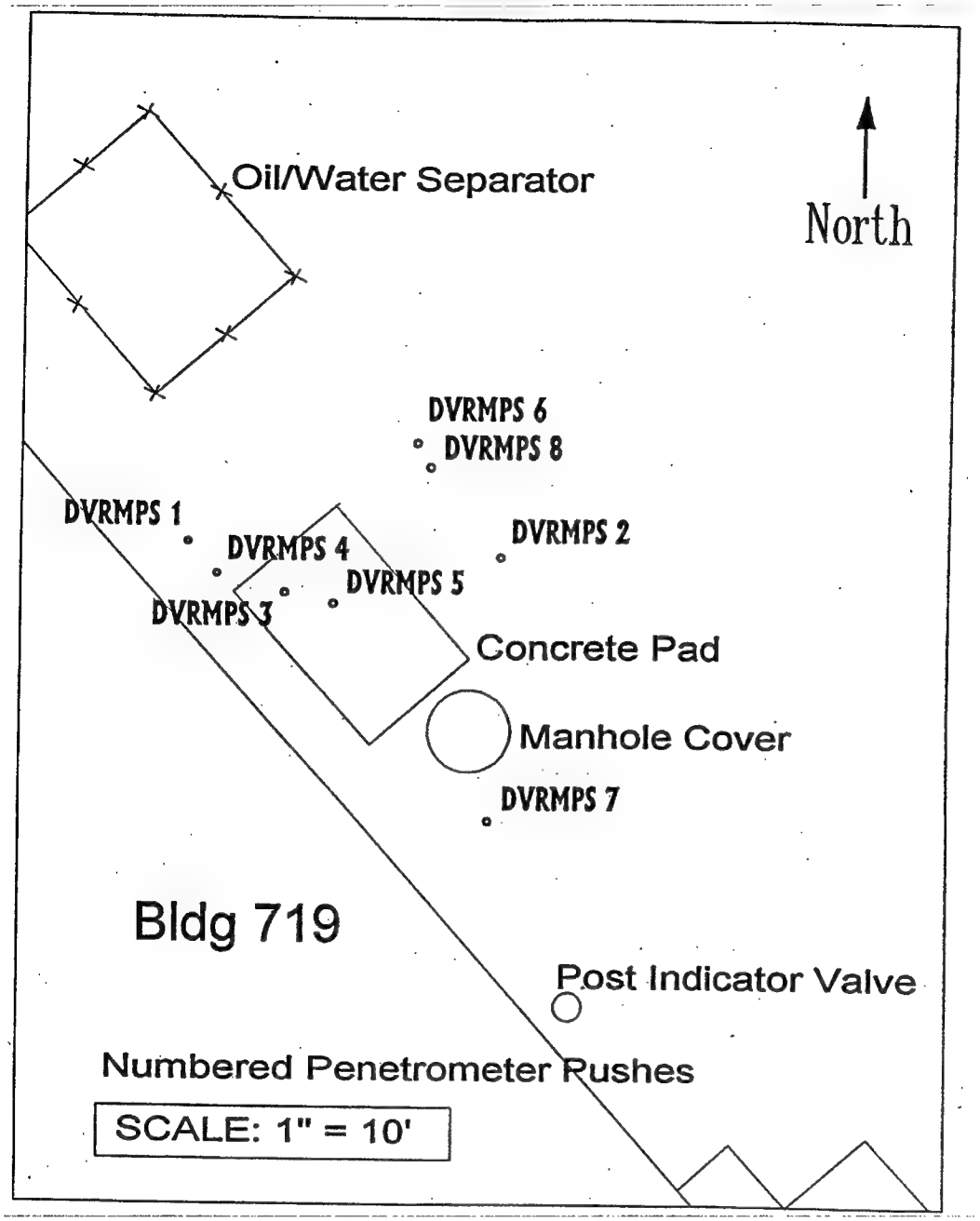

Figure 81. Site map for CRREL field demonstration

It is speculated that the source for the TCE in the sand above the water table may originate from the dissolved TCE in the groundwater.

The head space analysis technique, developed by Dr. Alan Hewitt at CRREL, was used for soil sample analysis. Contaminant data collected with the MPS are compared with the soil verification data in Figure 82. Soil sample SS2 shows a strong correlation with MPS1, while soil sample SS1 shows a more qualitative than quantitative correlation with MPS5. It is thought that the

Table 18
MPS and Soil Verification Data for CRREL Field Demonstration

	TCE Concentration, ppm								
Hole Depth, ft	MPS1	SS2	MPS3	MPS5	SS1	MPS6	MPS7	MPS8	MPS9
10	297	1,100	39	2,681	43,000	22	30	7	4,809
20	214		709	27,817		90	194	14	>55,000
30	501	340	1,294	8,404	120,000	68	107	4	2,745
40	1,416		1,402			11	1,786	7	12,877
50	290	200	1,278	5,766		105	38	1,014	11,251
55								1,310	
60	839		943	4,941	2,300	12			6,749
65						8,320			
69				3,036					
70	768		1.044						
72.3	819								
75					440				
77			818						
80		120							
98		51							

Note: SS and MPS designate Soil Sample and Multiport Sampler hole, respectively.

qualitative comparison is caused by the relative distance of MPS5 versus that of the soil sample SS1 from the ice well (Figure 81).

The field demonstration of the MPS was highly successful with all difficulties stemming from subzero weather and associated equipment. Some of the high points of the demonstration were:

a. The MPS was pushed to 77 ft bgs (previously, the maximum depth was 58 ft bgs).

b. Ports were reused several times (ports were opened and resealed during a push).

c. A new 150-ft umbilical cable was used which made use of 0.0625-in.-OD by 0.04-in.-ID stainless steel tubing as sampling tubes. The steel tubing did not retain a memory of the contaminant sampled and allowed repeated sampling through the same tube. A secondary advantage is that, in the future, the MPS probe can be configured with one or two direct sampling ports and the other four as contaminant traps.

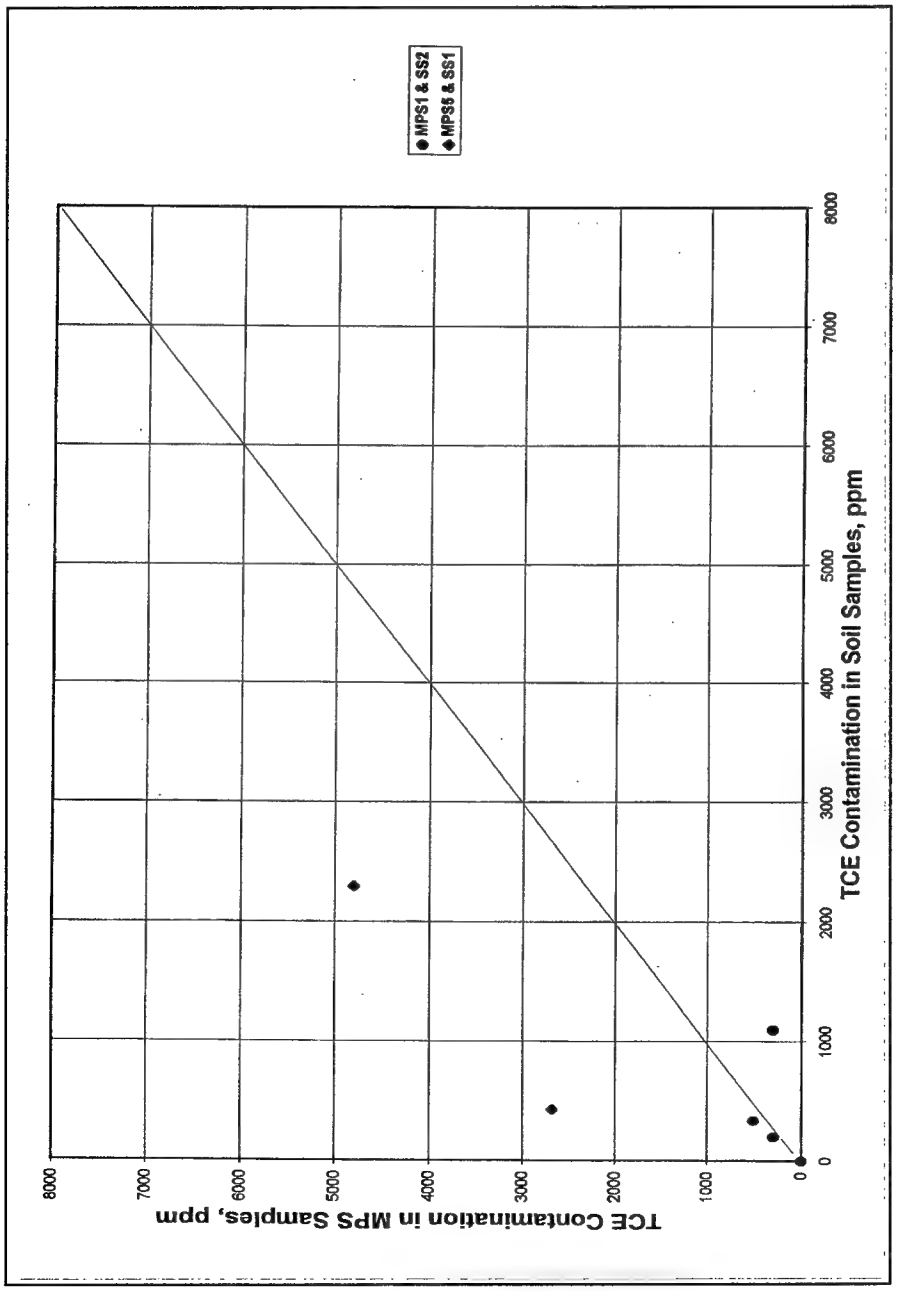

Figure 82. Comparison of TCE contamination in MPS1 and MPS5 samples vs. SS2 and SS1 samples

d. All interconnecting tubes between the umbilical cable and modules were made of stainless steel and could be used repeatedly.

e. While the truck was being repositioned for the next push, the probe was cleaned and readied without disconnecting it from the umbilical cable. This technique was successfully demonstrated several times.

f. The time required to prepare the MPS probes between pushes was reduced to less than 15 min.

g. The reduction in the number of MPS modules from 10 to 6 allowed all interconnecting tubes (tubes between the modules and umbilical cable) to be the same length. This allowed all contaminant traps to be the same length, thereby reducing fabrication time and expense.

h. The reduction in sampling tube size, from 0.125-in. to 0.0625-in-OD, decreased the available tube volume and therefore air volume required to maintain the port piston seal while the probe was being pushed. The lack of air volume required that a friction breaker be used to remove the lateral earth pressure from the ports and was successful for all holes.

i. The probe was used in temperatures as low as -9 °F with no effect on its operation. The nitrogen bottle was moved into the truck to maintain the nitrogen gas at a temperature above freezing as a precaution.

j. The demonstration showed that a probe can be assembled in the laboratory, transported to the field, and hooked up to the umbilical cable on site. The probe should not require disassembly in the field unless a problem arises.

k. Two pushes were attempted each day. Each push took approximately 2 to 2 1/2 hr (sampling every 10 ft to an average push depth of 60 ft, six samples).

l. Two bottles of nitrogen were used during the field demonstration. One bottle was used to clean and test the probe not in use, while the other bottle was used in the truck to support MPS push/sampling operations.

Although funding for development and field testing of the MPS has been terminated, it continues to require additional field work. One observation made during the CRREL demonstration was that the RCl probe was pushed to depth in excess of 100 ft. The only difference between the RCl and MPS probes is the size of the friction breaker. Therefore, it is hypothesized that if the RCl friction breaker dimensions were used on the MPS (increased in size and length), the MPS would be able to achieve greater depths before probe refusal is reached. Because of the modular construction of the MPS, this change can be easily achieved.

Conclusions

The laboratory and field investigations conducted with the TDS resulted in evaluation of additional VOCs, mechanical improvements to the TDS to simplify and improve operation, additional strength for difficult soil conditions, improvement of the analytical interface, and promising chemical investigation results. These improvements were field investigated and showed that the TDS was ready for transition into ESTCP, where field verification of the probe coupled to the IT/MS has continued.

Laboratory and field demonstrations have shown the MPS to be a viable method for sampling vapor and/or gas for contaminant analyses. The MPS is capable of collecting samples for field analyses onsite or at an offsite analytical chemistry laboratory. The ORNL equipment, the CT and the IT/MS, interface well with the MPS and add depth to its usefulness as a site characterization and vapor and/or gas sampling tool. Although there is room for further improvement, the MPS has been transitioned to the field.

8 SCAPS X-Ray Fluorescence (XRF) Metals Sensor

by: Jane W. Adams, WES
W.T. Elam, NRL

Introduction

The DoD has responsibility for management and cleanup of sites that were contaminated with various toxic metals during a wide range of military and industrial manufacturing, management, and waste processes. These sites include machine shops, painting facilities, firing ranges, load/assemble and packing operations at ammunition plants, storage depots, and landfills. Site characterization is very time- and cost- intensive due to the fact that heavy metals are widely distributed over large operational areas. As a result of technical briefings and discussions during the FY95 meeting of the Peer Review Panel, and with subsequent approval from the SERDP Scientific Advisory Board and the SERDP Executive Office, a new research area focused on the development of an XRF probe was initiated. Reasons for incorporating this technology development effort in the SCAPS program included the fact that XRF represented a fairly mature, relatively low-risk approach for detecting toxic metals in soils and groundwater and could be pursued in parallel with the ongoing LIBS efforts. As a result, in FY96, SERDP funded an effort by Naval Research Laboratory and WES researchers to design, fabricate, and evaluate a state-of-the-art XRF SCAPS probe. This chapter describes the laboratory and field investigations conducted under SERDP funding which resulted in the successful transition of XRF SCAPS technology to the ESTCP for demonstration/validation.

Background

Technical rationale

Recent advances to miniaturize x-ray fluorescence detectors have permitted XRF sensors to be placed within the SCAPS to provide information about elemental contaminants in soils. This probe is proving to be a breakthrough in environmental heavy metals analysis. This system minimizes soil excavation, provides real-time information, and dramatically reduces environmental analytical costs. The EPA established methods for metals analyses include inductively coupled plasma (ICP) and atomic absorption spectroscopy (AAS). Detection limits for ICP range from ppb to ppm, with AAS only slightly higher. Despite low detection limits, neither is an ideal technique because they are complicated laboratory methods that require well-qualified personnel. Sample preparation is complex, destructive, and not always successful in the case of unknown samples. The XRF has none of these drawbacks, and since x-ray intensity is not affected by moisture, the SCAPS XRF probe can operate in both the vadose and saturated soil zones.

X-ray fluorescence spectroscopy

The XRF spectroscopy is a well-established, nondestructive method for qualitative and quantitative chemical fingerprinting of gaseous, liquid, and solid elements and compounds. This spectroscopy is capable of determining elemental concentrations at ppm levels in complex samples and provides accuracy of 1 percent or better under optimum vacuum conditions. It can be done in ambient conditions with no sample preparation, although this causes detection levels to increase. It is a technique used widely today in all areas of characterization of materials. Auger, x-ray, and UV photoelectron spectroscopies are related techniques that can give more chemical information, but are limited to use in vacuum conditions.

The XRF determines elemental composition due to the fact that fluorescent x-rays have constant and well-known energies and are different for each elemental atom since the electron energy states that produce fluorescence x-rays originate from the core valence of the atom. The atomic process by which this works is shown in Figure 83. The diagram shows a typical set of energy levels for the electrons in an atom in the sample. As x-rays from an excitation source bombard the sample with known energy greater than the binding energy of the core electron, the core electron can be excited to a higher-energy empty state above the atomic states. The empty-core state is refilled by an electron from a higher valence. This electron has to lose energy to drop to a lower energy level (valence), thus this atom emits a secondary, fluorescent x-ray. Since the electron energy states producing the fluorescence x-ray are entirely within the atom, the x-ray is produced with a constant and well-known energy that is different for each type of atom and also independent of the chemical state of the atoms. The intensity of the secondary x-rays is directly related to the concentration of the corresponding element in the sample.

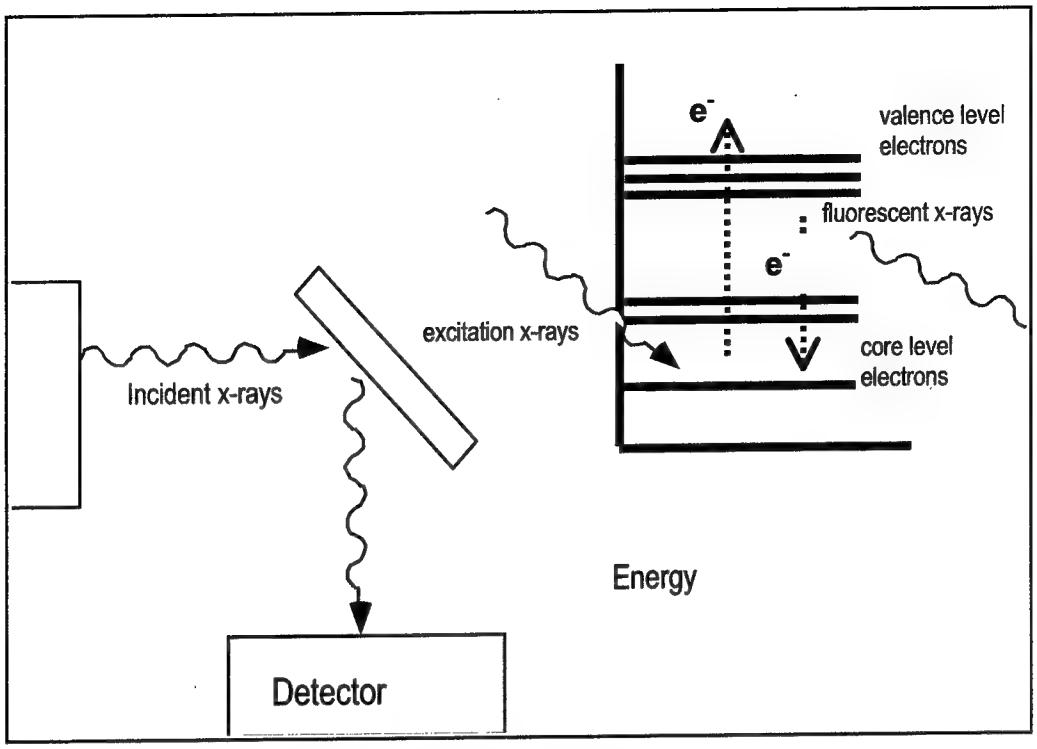

Figure 83. Schematic diagram showing the physical processes involved in x-ray energy transitions for electrons in a sample

XRF spectra normally are presented as a plot of energy of the fluoresced rays in keV as a function of electron emission in arbitrary intensity units. It is possible to detect elements with atomic weights as low as 6, carbon, in vacuum, but under ambient conditions only elements above 19, potassium, can be detected accurately. As with other spectroscopic techniques, partitioning a spectrum consisting of overlapping peaks is not always unique. However, the valence electrons of a given element will fluoresce at different energies so that there may be several diagnostic energies for a given element, as given in Table 19. Heavy metals pollutants that are targeted by the SERDP program include lead, chromium, copper, arsenic, cadmium, and mercury.

Probe Design

The successful deployment of XRF in a cone penetrometer (CPT) was dependent on having a simple and reliable detector that could be engineered to fit and perform in the CPT configuration. The commercial x-ray detector manufactured by Amptek, Inc., has the size, performance, and electronics necessary for use in a SCAPS sensor. This unique detector is the same type used on the 1997 Pathfinder Mars mission. An XR-100 x-ray detector placed on the Sojourner arm successfully performed soil and rock analyses using XRF while on Mars.

Table 19
X-Ray Emission Lines, keV (Ballard and Cullinane 1998)

No.	Element	Ka1	Ka2	Kb1	La1	La2	Lb1	Lb2	Lg1
19	K	3.3138	3.3111	3.5896					
20	Ca	3.69168	3.68809	4.0127	0.3413	0.3413	0.3449		
21	Sc	4.0906	4.0861	4.4605	0.3954	0.3954	0.3996		
22	Ti	4.51084	4.50486	4.93181	0.4522	0.4522	0.4584		
23	V	4.95220	4.94464	5.42729	0.5113	0.5113	0.5192		
24	Cr	5.41472	5.405509	5.94671	0.5728	0.5728	0.5828		
25	Mn	5.89875	5.88765	6.49045	0.6374	0.6374	0.6488		
26	Fe	6.40384	6.39084	7.05798	0.7050	0.7050	0.7185		
27	Co	6.93032	6.91530	7.64943	0.7762	0.7762	0.7914		
28	Ni	7.47815	7.46089	8.26466	0.8515	0.8515	0.8688		
29	Cu	8.04778	8.02783	8.90529	0.9297	0.9297	0.9498		
30	Zn	8.63886	8.61578	9.5720	1.0117	1.0117	1.0347		
31	Ga	9.25174	9.22482	10.2642	1.09792	1.09792	1.1248		
32	Ge	9.88642	9.85532	10.9821	1.18800	1.18800	1.2185		
33	As	10.54372	10.50799	11.7262	1.2820	1.2820	1.3170		
48	Cd	23.1736	22.9841	26.0955	3.13373	3.12691	3.31657	3.52812	3.71686
80	Hg	70.819	68.895	80.253	9.9888	9.8976	11.8226	11.9241	13.8301
81	Tl	72.8715	70.8319	82.576	10.2685	10.1728	12.2133	12.2715	14.2915
82	Pb	74.9694	72.8042	84.936	10.5515	10.4495	12.6137	12.6226	14.7644

The SCAPS probe housing is 1.75 in. in diameter by 20 in. long. A schematic diagram is shown in Figure 84. Geophysical cone and sleeve sensors for determining soil classification and postpush grouting tubes were included in the design but were not included in the prototype probes. The x-ray source, detector, and preamplifier are mounted on a rail inside the probe that also holds an x-ray collimator to direct the excitation radiation onto the soil and the fluorescence back onto the x-ray detector. The radiation exits and enters the probe housing through a robust, wear resistant x-ray transparent window. A sealed x-ray tube is used as the excitation source to provide adequate incident radiation and to avoid the use of a radioactive excitation source. The probe uses a miniaturized conventional x-ray tube which was custom made for this project but which is now commercially available. The optical design considerations for this probe have been covered in previous publications which are listed in the reference section of this report.

The Amptek XR-100 detector unit was modified to fit in the probe. It contains a silicon PIN diode with Peltier electrical cooling and is connected to a low-noise preamplifier. The x-ray window is machined from hot-pressed boron carbide (B_4C) to allow high x-ray transmission for the excitation and fluorescent x-rays and to have sufficient strength to avoid breakage during penetrometer use.

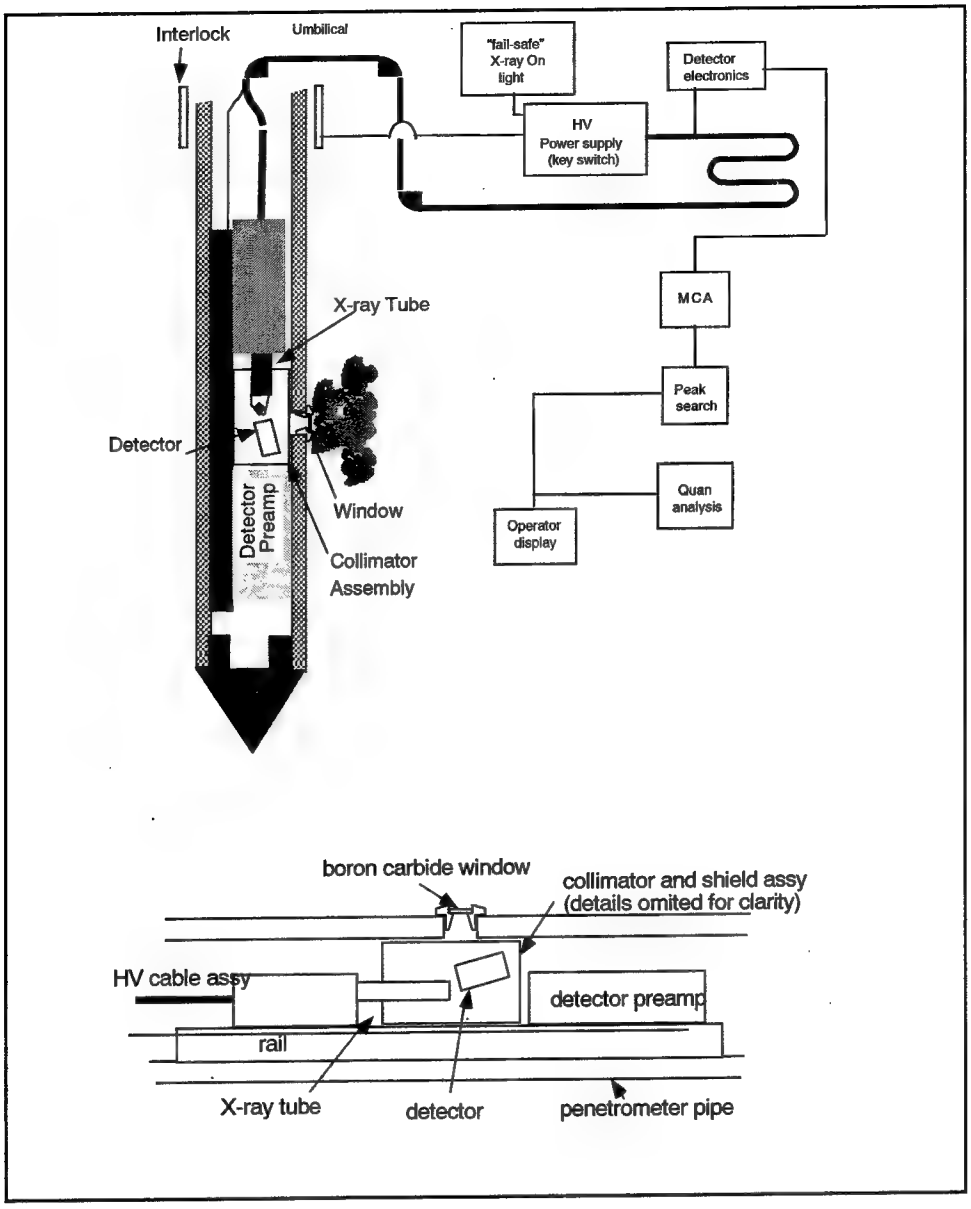

Figure 84. Engineering layout of the SCAPS XRF metals sensor

Norbide B_4C was obtained as machined disks from Norton/Saint Gobain, Worchester, MA. The windows are 1/2 in. diam with the optics designed to collect signal from the entire window diameter.

The umbilical cable supplies the high voltage as well as other power and signals required by the probe. It is shielded both for noise immunity and high voltage safety and for this particular probe is 75 ft long. There is no intrinsic limit to the umbilical cable length.

This probe design provides a sensor which has proven to be rugged and reliable. This optical arrangement permits detection limits of about 100 ppm to be achieved in 100 sec for lead in the field. The principal factor determining the

detection limits is the scattering of the continuum radiation from the x-ray tube. The flux from the incident x-ray tube is sufficient to saturate the detector, so overall counting statistics are adequate. A filter in the incident beam is used to reduce the continuum radiation in the energy region where the emission lines from the metals of interest lie. Better detection limits may be achieved with longer counting times.

A diagram of the SCAPS XRF system is shown in Figure 85. The aboveground electronics located in the truck contain a power supply for the x-ray tube, power, and a shaping amplifier for the detector, and a standard multichannel analyzer for data collection. An important feature of the system is that the x-ray power supply is also connected to a safety interlock system that ensures safe operation. The interlock system is part of the overall electronics that operate the probe. It consists of a shielded tube with sensor switches to ensure that the probe is fully inserted into the ground before the x-ray tube can be energized. Radiological safety systems appropriate to x-ray producing systems and their high-voltage power supplies are incorporated into the entire probe system to prevent accidental exposure to personnel during operation. The interlock system meets all safety requirements and regulations.

The shielding device is also configured to analyze test samples above ground via a sample introduction port. This port enables calibration samples, blanks, and test samples to be run during field operations. The remainder of the aboveground system consists of a portable computer to collect, interpret, and display the data.

Sensor Verification/Calibration

The sensor was calibrated for lead using two different calibration samples. The first were Standard Reference Materials (SRM) from the National Institute of Standards and Technology. The SRM 2709, 2711, and 2710 are soil matrices with 19, 1,162, and 5,532 ppm of lead, respectively. Additional, intermediate value samples were prepared by adding lead sulfide to silicon dioxide (sand) in known quantities and verifying the results by laboratory analysis. One calibration spectrum was taken of pure lead oxide (greater than 98 percent lead by weight). All calibration samples were measured with three to five replicates for a 100-sec acquisition time. The resulting calibration curve is shown in Figure 86. The calibration curve was a linear least-squares fit to the SRM and five prepared samples. The R value for this linear fit was 0.9906. The intensity was calibrated as the ratio of the counts in the lead L-alpha peak divided by the counts in the excitation peak, which is insensitive to variations in the x-ray tube output and other measurement conditions. A linear background was removed from each peak prior to calculating the counts. Fixed regions in the spectrum corresponding to individual peaks were used for all samples and the same regions were used for the field spectra.

This calibration provides good quantitation at low levels, where the combined errors are ~ 20 percent in the worst case. It was found that the matrix effects for silicon dioxide (sand) and the San Joaquin and Montana soils SRMs

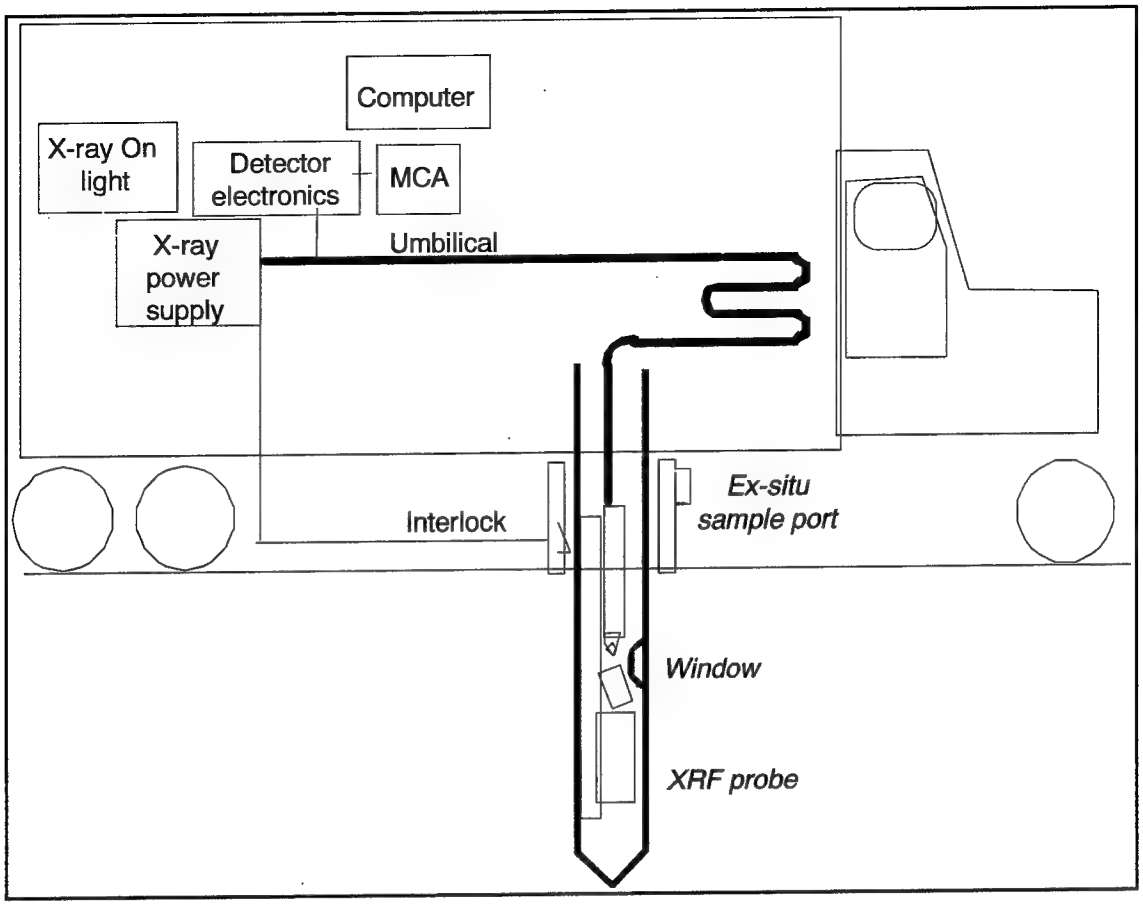

Figure 85. Diagram of the SCAPS XRF metals sensor as deployed via the SCAPS penetrometer truck, the uphole components (shown as blocks in the diagram) are in the computer room of the SCAPS truck, the sensor head is shown in schematic detail on the lower right, the interlock sleeve for electrical safety and radiation shielding surrounds the probe just above the ground surface and contains the port for measuring calibration and check samples

are small enough to be ignored in the calibration. The lead oxide value did not fit on the curve due to saturation of the detector at the high count rates and to the strong lead self-absorption in lead oxide. Some of the measured lead values from field sites have been at levels much higher than the calibration range, as high as a few percent. Extrapolation of the linear calibration curve above 10,000 ppm will produce larger errors and should be considered only semiquantitative. This is not a limitation since the XRF sensor is designed to assist in the delineation of contaminant boundaries (i.e., to screen sites for contaminant plume boundaries for the optimum placement of monitoring wells).

Sensor Field Operations

To collect in situ XRF spectra, the XRF electronics are set up in the SCAPS truck and the umbilical threaded through the penetrometer pipe. After a field

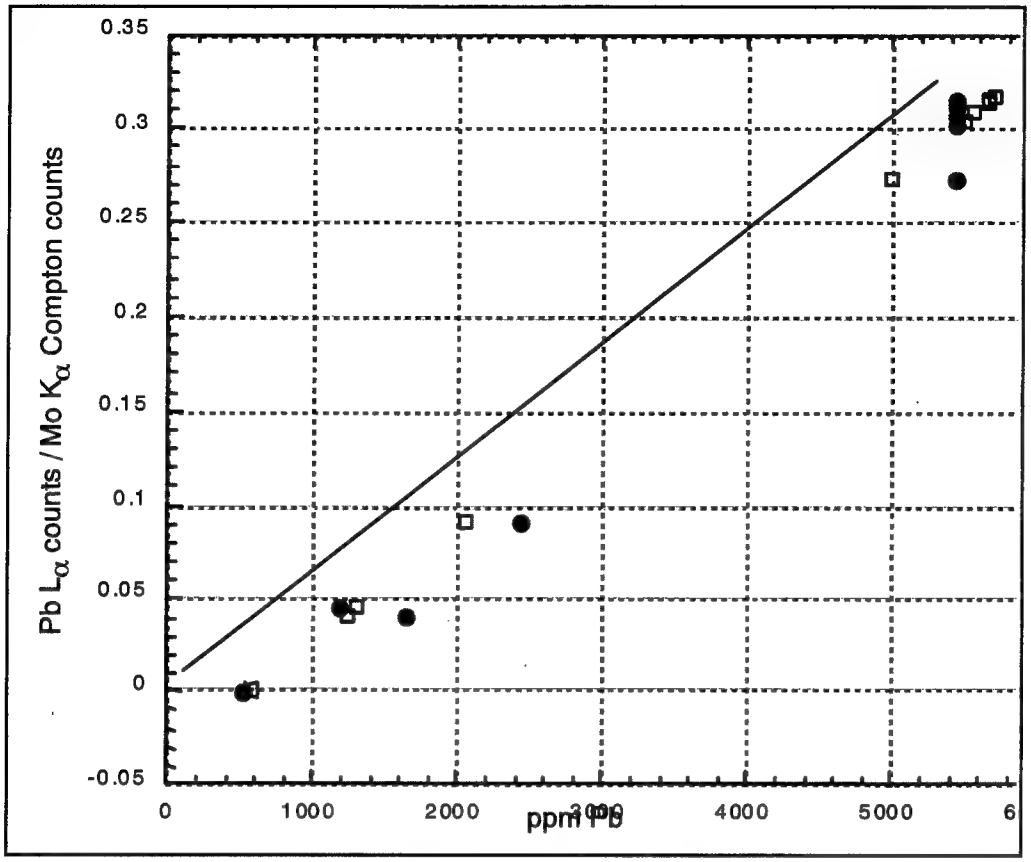

Figure 86. Calibration curve of the SCAPS XRF sensor for lead, the circles are the actual values of the samples used for calibration, the line is the calibration curve, and the squares are the measured values of the calibration samples calculated with the calibration curve

calibration check procedure, the sensor is pushed to the desired depth (referenced to the window depth) and stopped during data collection. For the measurements reported here, data collection times were 100 sec. A Mo x-ray tube was operated at 30kV and 100 microamps. Instrument sensitivities were typically about one count integral under the lead La peak per ppm lead in the soil for 100-sec live time (6 percent dead time). The peaks were integrated over a fixed region about the lead peaks after removal of a linear background. Further details of the field operation of the sensor are reported in detail by Elam (1998). After a spectrum was obtained at a given depth, the penetrometer tip was pushed to the next depth and another 100-sec spectrum is obtained. The typical distance between successive spectra was 5 cm. Figure 87 shows representative spectra of Montana soil, SRM 2710 and Figure 87 shows representative spectra of brass filings taken during initial probe field tests. Figure 88 is representative of spectra obtained from the JAAP at a depth of 1.4 m under typical operating conditions.

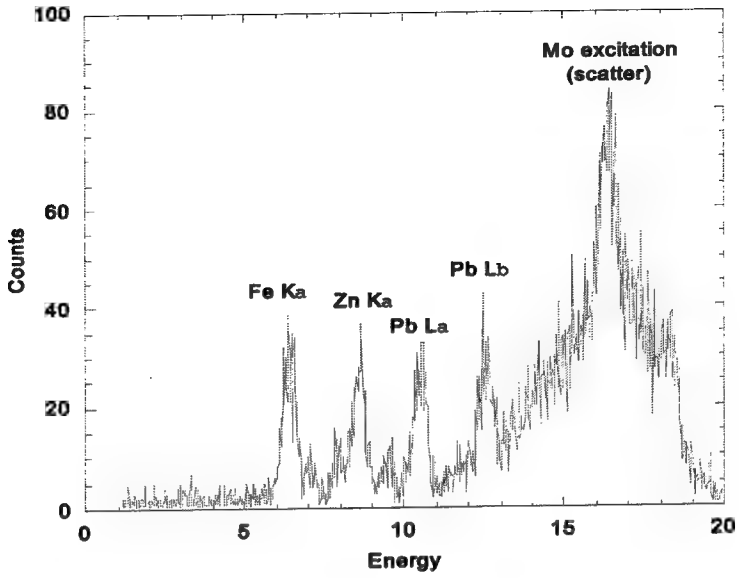

a. Spectrum taken of SRM2710, Montana soil with highly elevated heavy metal contaminants for 100 sec; the sample soil contains about 6,000 ppm each of zinc and lead

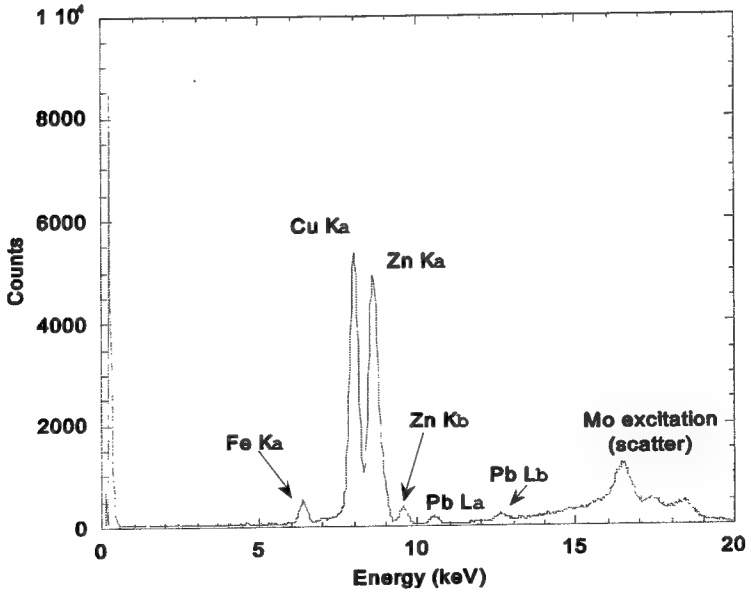

b. Spectrum of brass shavings placed 6 ft bgs during an initial demonstration of the probe at the USAE Waterways Experiment Station. Note the detection of the minority lead in the brass

Figure 87. Representative XRF spectra

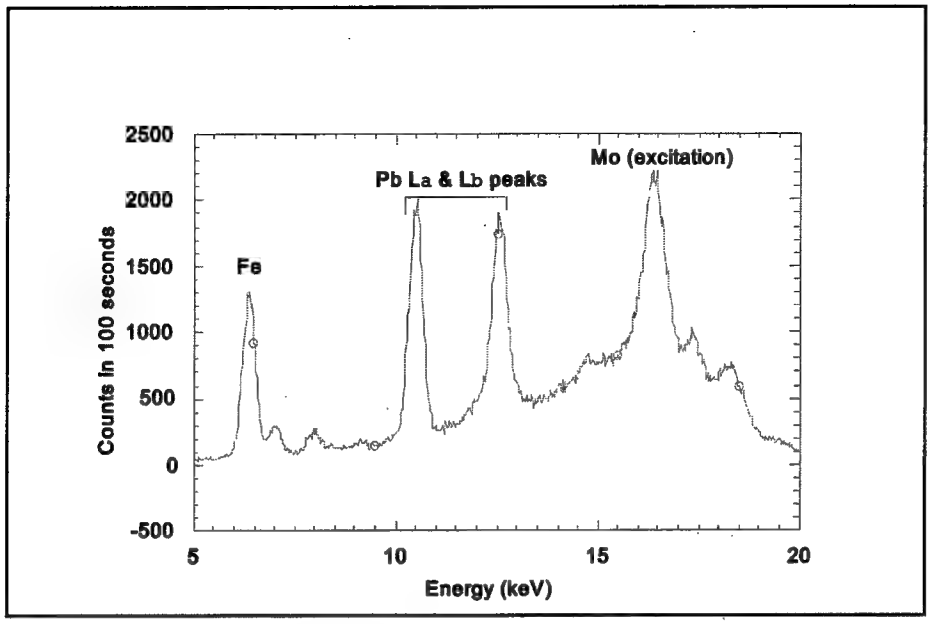

Figure 88. Typical XRF spectrum taken by the SCAPS XRF sensor at a depth of 4.5 ft bgs in hole 6, Lead Azide Area, JAAP; the lead L-alpha and L-beta x-ray emission peaks are clearly visible; these peaks correspond to a lead concentration of about 14,000 ppm

Field Demonstrations: Results/Data

Five field demonstrations were performed in the course of developing the XRF metals sensor probe and establishing operational procedures. Subsurface soil samples for laboratory verification analysis were collected from each sampling location at the site.

J Field, Aberdeen Proving Ground, MD - July 1996
Initial deployment. Faulty x-ray tube electronics - no data acquired.

WES, October 1996
First prototype probe. Electronics and safety lock device successfully demonstrated.

WES, April 1997
Second probe demonstrated. Both probes operable.

JAAP, May 1997
Former lead azide settling pond. This demonstration was conducted at the JAAP. Measurements were made in the lead azide area, which contained a lagoon for wastewater from the manufacture of lead azide primer explosive. The area had since been cleared of building and the lagoon filled. A series of 10 pushes were made in different locations, chosen during the course of the

investigation. The goal was to obtain a range of data with the sensor, and no attempt was made at a complete investigation of the area. The measured concentrations of lead in the soil ranged from below the detection limit to several percent by weight. In some cases, the concentration changes by several orders of magnitude in a distance of 5 cm.

JAAP, October 1997
Lead azide settling pond again– Mock ESTCP ("shakedown") demonstration using three metals probe technologies. All probes operated successfully.

Discussion

Metals analysis via XRF cone penetrometry has proven to be a viable method for obtaining in situ measurements of heavy metal concentrations in underground soil and groundwater. The results agree well with conventional sampling methods and are available in real-time. The SCAPS XRF system uses miniature x-ray tubes that are ruggedized for deployment via direct push techniques, thus negating the need for a radioisotope excitation source. The NRL/WES team currently has two probes operational and has secured two vendors of miniature x-ray tubes. Detection limits are 100 ppm for lead in soil and were obtained by reducing the continuum radiation scattered by the window in the region of the lead peaks. The SERDP-developed XRF technologies were transitioned to ESTCP for demonstration/validation. The ESTCP project includes validation of the sensor performance by the California EPA Certification Program and field demonstrations for regulators and potential commercial partners.

The major technical improvement planned for demonstration under ESTCP is the implementation of continuous data collection while the sensor is being pushed. This has been tested, but software modifications and communication with the SCAPS computer to allow depth readout are needed before transition to ESTCP. No limitations of the sensor performance during push were observed. Detection limits will be improved and performance will be improved at lower energies by optimizing the window design.

Conclusions

Field evaluations of the SCAPS XRF metals probe have demonstrated the capability for rapid detection of subsurface metals higher than element 20 (calcium). The XRF probe can operate both in the vadose and saturated soils, and the response is unaffected by soil moisture or water. Calibration procedures are simple, data are obtained in near real-time, and the need for extensive personnel training is negligible.

Extensive laboratory tests were performed during the development and field use of these probes. Field demonstrations of each of these probes have been performed at a variety of sites to evaluate probe performance and to refine

operational procedures. During FY97, the SERDP funded two very successful field demonstrations conducted at the JAAP.

This highly successful SERDP program has produced two patent applications as well as interest from within DoD, DOE, EPA, and commercial partners. This device is the subject of a book chapter in *Current Protocols and Field Analytical Chemistry* and has prompted changes to the draft EPA method on field-portable x-ray fluorescence measurements.

The SERDP-sponsored XRF technology development work was successfully transitioned to the ESTCP SCAPS metals sensor demonstration/validation program. During 1998, the first ESTCP demonstration was staged at the Lake City Army Ammunition Plant, Independence, MO. The ultimate goal of this program is acceptance by environmental regulators and commercialization of the technology to make it available to a broad array of users.

9 Conclusions

By : Ernesto R. Cespedes, WES

Introduction

The SERDP-funded SCAPS project proved to be a very successful effort to develop, evaluate, and transition innovative site characterization and monitoring technologies. During the course of this project, a number of technologies, such as the Electrochemical probes, the Thermal Desorption Sampler, the LIBS and XRF sensors, and the enhanced LIF and Spectral Gamma systems, were taken from early laboratory proof-of-principle stage to full-scale field use in real-world site characterization operations in minimum time.

The SCAPS project has been showcased by SERDP, ESTCP, and numerous Government agencies as a highly successful environmental technology development project. For the foreseeable future, SCAPS will continue to serve as a prime example of Tri-Service collaboration. As stated by the Peer Review Panel, "the SCAPS program's level of tri-service cooperation is far beyond other environmental programs" (Cespedes and Cargile 1996).

Significant Accomplishments

The SERDP SCAPS project was highly productive in terms of: (a) the number of technologies transitioned to demonstration/validation programs and/or directly to operational field use; (b) the number of patents and patent applications developed during the course of the project; (c) the numerous technical publications including refereed journal articles, conference proceedings, and technical reports; and (d) the number and level of technical presentations and invited talks presented at national and international symposia and conferences.

The following new SCAPS technologies were developed and transitioned as part of the SERDP effort:

a. The Electrochemical Explosives probes were installed in the U.S. Army Engineer District, Tulsa, SCAPS truck and used in actual site characterization efforts at DOE's Pantex, TX, plant. The system underwent further development and was transitioned to the ESTCP program for demonstration/validation.

b. The Electrochemical RCl probe was also used in site characterization efforts onboard Corps District SCAPS and transitioned to ESTCP.

c. The Thermal Desorption VOC sampler was transitioned to the ESTCP program.

d. The RAMAN probes have been used in field evaluations onboard Navy SCAPS trucks.

e. The LIBS Probes (Downhole and Fiber Optic) as well as the XRF probe for metals detection have been transitioned to the ESTCP program.

f. The XeCl LIF (308) probes have been installed in the Navy's operational SCAPS trucks.

g. The Microchip Laser (266-nm) LIF probe has been transitioned to the ESTCP program.

h. Software to provide 3-D visualization of the subsurface stratigraphy and contaminant distribution in the field for a variety of SCAPS probes was developed and transitioned to DoD SCAPS operators.

In addition to the newly developed SCAPS technologies listed above, a number of already existing SCAPS technologies were improved during the course of the SERDP project. These include the fixed wavelength and tunable laser LIF systems, the Multiport Sampler, and the Spectral Gamma Probe. The improved LIF systems have been transitioned to Dem/Val projects, are currently Cal EPA and U.S. EPA certified, and have been installed in DoD, DOE, and commercial SCAPS units conducting operational site characterization operations. The improved Spectral Gamma Probe was transitioned directly to DOE users, and its success led to a DOE-funded effort to develop a combined Spectral Gamma and XRF probe for characterizing mixed waste sites such as DOE's Hanford, WA, facility.

The SCAPS technology development effort produced a number of innovations that resulted in patent applications and patent awards. These are listed in Appendix A. Also listed in Appendix A are the numerous publications produced as part of this effort. In addition to the publications, SCAPS project researchers made numerous technical presentations and demonstrations that resulted in widespread interest in SCAPS related technologies. This interest gave rise to a number of other cone penetrometer-based sensor development efforts such as those funded by the EPA, DOE, and the Advanced Applied Technology Demonstration Facility (AATDF). Finally, during the course of this project, the project's principal investigators participated as invited speakers at

some of the most prestigious national and international technical conferences and symposia. These included those hosted by the Optical Society of America (OSA), the Society of Photo-Optical Instrumentation Engineers (SPIE), the Air and Waste Management Association, the European Symposium on Optics for Environmental and Public Safety, Institute of Electrical and Electronics Engineers (IEEE), the International Geoscience and Remote Sensing Symposium, the American Chemical Society, the American Defense Preparedness Association (ADPA), and the Society of American Military Engineers (SAME). In addition, SCAPS researchers have organized and chaired numerous technical sessions at international conferences and symposia that addressed environmental site characterization and which a forum to publicize and disseminate SCAPS technologies as well as the SERDP Program in general.

Acknowledgments

The SCAPS Peer Review Panel process was instrumental to the success of this effort. The periodic reviews, which included representatives from the user community, ensured that the work was well coordinated, adequate progress was being made, unproductive approaches were redirected or abandoned, and the focus of the project remained on addressing the highest priority user needs. The Panel was very effective in rapidly redirecting work when technical obstacles were encountered or new opportunities arose. Their recommendations were always accepted by the SERDP Scientific Advisory Board and approved by the SERDP Executive Office in a very timely manner.

References

Adams, J. W., Cespedes, E. R., Cooper, S. S., Davis, W. M., Buttner, W. J., and Vickers, W. C. (1995). "Development and testing of cone penetrometer sensor probe for in-situ detection of explosive contaminants." *Field screening methods for hazardous wastes and toxic chemicals, VIP 47 Vol I.* Air and Waste Management Assoc., Pittsburgh, PA, 491-501.

Adams, J. W., Cespedes, E. R., Davis, W. M., Buttner, W. J., and Findlay, M. W. (1997). "Development and testing of cone penetrometer electrochemical sensor probes for chlorinated solvents and explosives." *Field analytical methods for hazardous wastes and toxic chemicals*, VIP 71. Air and Waste Management Assoc., Pittsburgh, PA, 667-670.

Argonne National Laboratory, Environmental Research Div. (1997). "U.S. Army Engineer Waterways Experiment Station spectral gamma probe evaluation report," Internal report, Contract No. W-31-109-Eng-39, Chicago, IL.

Ballard, J. H., and Cullinane, M. J. (1998). "Innovative site characterization and analysis penetrometer system (SCAPS): In-situ sensor and sampling technologies." *Proceedings of the 1998 symposium on the application of geophysics to environmental and engineering problems.* Chicago, IL, 33-42.

Bratton, W. L., Shinn, J. D., and Bratton, J. L. (1993). *Field screening methods for hazardous wastes and toxic chemicals, Vol* 1. Air and Waste Management Association, Pittsburgh, PA, 431-442.

Buttner, W. J., Findlay, M. W., Vickers, W., Davis, W. M., Cespedes, E. R., Cooper, S. S., and Adams, J. W. (1997). "*In-situ* detection of trinitrotoluene and other nitrated explosives in soils," *Analytica Chimica Acta* 17815, 1-9.

Cao, Z., Buttner, W. J., and Stetter, J. R. (1992). "The properties and applications of amperometric gas sensors," *Electroanalysis* 4, 253-266.

Carrabba, M. M., Edmonds, R. B., Rauh, R. D., and Haas, J. W. III. (1991). "Spectroelectrochemical sensing of chlorinated hydrocarbons for field screening and in situ monitoring applications." *Second international symposium on field screening methods for hazardous wastes and toxic chemicals.* Environmental Protection Agency, Las Vegas, NV, 67-73.

Carron, K., Peitersen, L., and Lewis, M. (1992). "Octadecylthiol-modified surface-enhanced Raman spectroscopy substrates: New method for the detection of aromatic compounds," *Environ. Sci. Technol.* 26, 1950-1954.

Cespedes, E. R., Cooper, S. S., Davis, W. M., Buttner, W. J., and Vickers, W. C. (1994). "In situ detection of TNT contamination using electrochemical sensors in cone penetrometer system." *Proceedings of the SPIE conference on optical sensors for environmental and chemical process monitoring.* McLean, VA, 33-42.

Cespedes, E. R., and Cargile, D. M. (1996). "Proceedings of the 2nd annual site characterization and analysis penetrometer system (SCAPS) sensor development workshop, 29-30 August 1995," Miscellaneous Paper SERDP-96-2, U.S. Army Engineer Waterways Experiment Station, Vicksburg, MS.

Cespedes, E. R., Davis, W. M., Ballard J. H., and Buttner, W. J. (1996). "Development and testing of electrochemical sensors for rapid detection of explosive contaminants in soils." *Proceedings of the international geoscience and remote sensing symposium (IGARSS).* Lincoln, NE.

Cespedes, E. R., Miles, B. H., and Lieberman, S. H. (1994). "Development of optical sensors for the site characterization and analysis penetrometer system (SCAPS)." *Proceedings of the international specialty conference on optical sensing for environmental monitoring vol SP89.* Air and Waste Management Association/SPIE, Atlanta, GA, pp 621-632.

Dane, D.H., Oostrom, M., and Missildine, B.C. (1994). *"Determination of capillary pressure-saturation curves involving TCE, water, and air for a sand and a sandy clay loam,"* EPA Project Summary.

Davis, W. M., Cespedes, E. R., Lee, L. T., Powell, J. F., and Goodson, R. A. (1997). "Rapid delineation of subsurface petroleum contamination using the site characterization and analysis penetrometer system," *Environmental Geology* 29, (3-4), 228-237.

Davis, W. M., Wise, M. B., Furey, J. S., and Thompson, C. V. (1997). "Rapid detection of volatile organic compounds in groundwater by in situ purge and direct sampling ion trap mass spectrometry," *Field Anal. Chem. and Tech.* 2, 89-96.

Davis, W. M., Furey, J. S., and Porter, B. (1998). "Field screening of VOCs in ground water using the hydrosparge VOC sensor." *Current Protocols in Field Analytical Chemistry V.* Lopez-Avila, ed., Wiley, New York, 1C.4.1-10.

Doskey, P. V., and Cespedes, E. R. (1998). "Cone penetrometer-deployed chemical sensors." *Encyclopedia of Environmental Analysis and Remediation.* Wiley, New York.

Elam, W. T., Adams, J. W., Hudson, K. R., McDonald, B., and Gilfrich, J. V. (1998). "Subsurface measurement of soil heavy metal concentrations with the SCAPS X-ray fluorescence (XRF) metals sensor." *Field analytical chemistry and technology*. Vol 2, Issue 2.

Elam, W. T. (1998). "Determination of metals in soils by XRF spectrometry via cone penetrometry (SCAPS)." *Current Protocols in Field Analytical Chemistry*. Viorica Lopez-Avila, et al. ed., Wiley, New York, 3B.3.1-3B.3.10.

Elam, W. T., Adams, J. W., Hudson, K. R., Gilfrich, J. V., and McDonald, B. "In-situ environmental XRF," *Advances in X-ray Analysis*. (in preparation).

Elam, W. T., Adams, J. W., Hudson, K. R., McDonald, B., Eng, D., Robitaille, G., and Aggarwal, I. (1997). "Field demonstration of the SCAPS XRF metals sensor." *Field Analytical Methods for Hazardous Wastes and Toxic Chemicals, VIP-71*. Air and Waste Management Assoc., Pittsburgh, PA, 681-689.

Elam, W. T., Whitlock, R. R., and Gilfrich, J. V. (1995). "Use of x-ray fluorescence for in-situ detection of metals." *Proceedings, SPIE. 367*. 59-69.

Elam, W. T., and Gilfrich, J. V. (1995). "Design of an x-ray fluorescence sensor for the cone penetrometer." *Advances in X-ray Analysis* 38, 699-704.

Fleischmann, M., Hendra, P. J., and McQuillan, A. J. (1974). "Raman spectra of pyridine adsorbed at a silver electrode," *Chem.Phys. Lett.* 26, 163-166.

Giauque, R. D., Garret, R. B., and Goda, L. Y. (1979). "Determination of trace elements in light element matrices by x-ray fluorescence spectrometry with incoherent scattered radiation as an internal standard," *Analytical Chemistry* 51, 511-516.

Gilispie, G. D., and St. Germain, R. W. (1995). *Field screening methods for hazardous wastes and toxic chemicals, Vol* 1. Air and Waste Management Associates, Pittsburgh, PA. pp 478-489.

Gillispie, G. D., and St. Germain, R. W. (1995). "Performance characterization of the rapid optical screening tool (ROST)." *Proc. U.S. EPA and A&WMA international symposium on field screening methods for hazardous wastes and toxic chemicals*. Las Vegas, NV, 478-489.

Gillispie, G. D., St. Germain, R. W., and Klingfus, J. L. (1993). "Subsurface optical probes: current status and future prospects." *Field screening methods for hazardous wastes and toxic chemicals*. Las Vegas, NV, 793-805.

Henderson-Kinney, A., and Kenny, J. E. (1995). "Spectroscopy in the field: Emerging techniques for on-site environmental measurements," *Spectroscopy* 10, 32.

Hewitt, A. D. (1994). "Screening for metals by x-ray fluorescence spectrometry/response factor/compton K? Peak normalization analysis," *American Environmental Laboratory*, 24-30.

Hewitt, A. D. (1994). "Comparison of methods for sampling vadose zone soils for determination of trichloroethylene," *Journal of the American Association of Official Analytical Chemist* 77, 458-462.

Jeanmaire, D. L., and van Duyne, R. P. (1977). "Surface Raman spectroelectrochemistry part I. Heterocyclic, aromatic, and aliphatic amines adsorbed at a silver electrode," *J. Electroanal. Chem.* 84, 1-20.

Jenkins, T. F., and Walsh, M. E. (1992). "Development of field screening methods for TNT, 2,4,-DNT, and RDX in soil," *Talanta* 39, 419-428.

Jenkins, T. F., Grant, C. L., Brar, G. S., Thorne, P. G., Schumacher, P. W., and Ranney, T. A. (1997). "Sampling error associated with collection and analysis of soil samples at tnt-contaminated sites," *Field Anal. Chem. and Tech.* 1, 151-163.

Leavell, D. A., Malone, P. G., and Lee, L. T. (1995). "The multiport sampler: an innovative sampling technology." *Proceedings of the Sampling Environmental Media, ASTM STP 1282.* James Howard Morgan, ed., American Society for Testing and Materials, Philadelphia, PA.

Leavell, D. A., and Lee, L. T. (1995). "Design, development, and operation of the multiport sampler," Technical Report GL-95-16, U.S. Army Engineer Waterways Experiment Station, Vicksburg, MS.

Leavell, D. A., Malone, P. G., and Lee, L.T. (1996). "The multiport sampler: An innovative sampling technology," Sampling Environmental Media, ASTM STP 1282, James Howard Morgan, ed., American Society for Testing and Materials, Philadelphia, PA.

Lemire, G. W., Simeonsson, J. B., and Sausa, R. C. (1993). "Monitoring vapor-phase nitro compounds using 226-nm radiation: Fragmentation with subsequent no resonance-enhanced multiphoton ionization detection," *Anal. Chem.* 65, 529-533.

Lieberman, S. H., Theriault, G. A., Cooper, S. S., Malone, P. G., Olsen, R. S., and Lurk, P. W. (1991). " Rapid subsurface *in situ* screening of petroleum hydrocarbon contamination using laser induced fluorescence over optical fibers." *Proceedings of the second international symposium on field screening methods for hazardous wastes and toxic chemicals.* Air and Waste Management Association, Las Vegas, NV, pp 57-63.

Lieberman, S. H. (1993). *Proceedings of the SCAPS Workshop on Sensors for the U. S. Army Environmental Center.* Denver, CO, pp 1-7.

Meidinger, R., St. Germain, R. W., Dohotariu, V., and Gillispie, G. D. (1993). "Fluorescence of aromatic hydrocarbons in aqueous." *Field screening methods for hazardous wastes and toxic chemicals.* 395-403.

McDonald, B., Unsell, C. W., Elam, W. T., Hudson, K. R., and Adams, J. W. "A cone penetrometer x-ray fluorescence tool for the analysis of subsurface heavy metal contamination." *Proceedings 1998 symposium on radiation measurements and applications* (in preparation), Ann Arbor, MI.

Morgan, J. C., Adams, J. W., and Ballard, J. H. (1997). "Field demonstration of the SCAPS cone penetrometer gamma probe for rad-waste detection." *Field analytical methods for hazardous wastes and toxic chemicals,* VIP 71. Air and Waste Management Assoc., Pittsburgh, PA, 600-611.

Morgan, J. C., Adams, J. W., and Ballard, J. H. (1998). "Field use of a cone penetrometer gamma probe for radioactive waste detection," *Field Analytical Chemistry and Technology* 2(2) 111-115.

Morgan, J. C., Fields, M. P., Cargile, D. M., and Adams, J. W. "Results of the use of a cone penetrometer spectral gamma probe for radioactive waste detection at the Savannah River Site," Technical Report EL-98 (in preparation), U.S. Army Engineer Waterways Experiment Stations, Vicksburg, MS.

Mosier-Boss, P.A., Lieberman, S.H., and Newbery, R. (1995). "Fluorescence rejection in Raman spectroscopy by shifted-spectra, edge detection, filtering techniques," *Appl. Spectrosc.* 49, 630-638.

Muilenberg, G. (1997). TSI Incorporated, *http://www.tsi.com/ecs/homepage/ecshome.htm,* (23 January 1997).

Mullen, K., and Carron, K. (1994). "Adsorption of chloinated ethylenes at 1-octanethiol-modified silver surfaces," *Anal. Chem.* 66, 478-483.

Myers, K. F., Brannon, J. M., Karn, R. A., Price, C. B., Eng, D. Y., Strong, A. B., and Cooper, S. S. (1995a). "Laboratory evaluation of a volatile organic compound analysis system for the site characterization and analysis penetrometer system," Technical Report IRRP-95-3, U. S. Army Engineer Waterways Experiment Station, Vicksburg, MS.

_____. (1995b). "Laboratory evaluation of a volatile organic compound analysis system for the site characterization and analysis penetrometer system." *Field screening methods for hazardous wastes and toxic chemicals.* VIP-47 Vol 1. Air and Waste Management Assoc., Pittsburgh, PA, 177-184.

Myers, K.F., Brannon, J.M., Karn, R. A., Price, C. B., Eng, D. Y., and Strong, A. B. (1998). "Thermal desorption VOC sampler: Improvements and field trial performance (Dover AFB)," Technical Report IRRP-98-1, U.S. Army Engineer Waterways Experiment Station, Vicksburg, MS.

Nelson, K. K. (1977). "Matrix corrections for energy dispersive x-ray fluorescence analysis of environmental samples with coherent/incoherent scattered x-rays," *Analytical Chemistry* 49, 641-648.

RCRA Facility Investigation/Remedial Investigation Work Plan for the R-Reactor Seepage Basins/108-4R Overflow Basin Operable Unit (U). (1995). Report No. WRSC-RP-95-537, Westinghouse Savannah River Company, Aiken, SC.

Sausa, R., Pastel, R., Simeonsson, Davis E., Mullane M., Pacquette, H., and Cespedes, E. (1996). "Development studies of LIF sensor for in situ site characterization and analysis of subsurface soil contaminated with trace energetic materials." *Proceedings of the 20th Army Science Conference.* Norfolk, VA.

Shorter, J. H., Wormhoudt, J. W., Adams, E. R., Adams, J. W., Davis, W. M., Buttner, W. J., and Findlay M. W. (1997). "Cone penetrometer detection of energetic marterials in soils." *23rd environmental symposium and exhibition.* American Defense Preparedness Association, New Orleans, LA.

Shriver-Lake, Lisa C., Donner, B., and Ligler, F. (1997). "On-site detection of TNT with a portable fiber optic biosensor," *Environ. Sci. Technol.* 31, 837-841.

Simeonsson, J.B., Lemire, G. W., and Sausa R. C. (1994). "Laser-induced photofragmentation/photoionization spectrometry: A method for detecting ambient oxides of nitrogen," *Anal. Chem.* 66, 2272-2278.

St. Germain, R. W., Gillispie, G. D., and Klingfus, J. L. (1993). "Variable wavelength laser system for field fluorescence." *Field screening methods for hazardous wastes and toxic chemicals.* Las Vegas, NV, 1113-1122.

St. Germain, R. W., and Gillispie, G. D. (1995). "Real-time continuous measurement of subsurface petroleum contamination with the rapid optical screening tool (ROST)." *Proc. U.S. EPA and A&WMA international symposium on field screening methods for hazardous wastes and toxic chemicals.* Las Vegas, NV, 467-477.

Stetter, J. R., Zaromb, S., and Findlay, M. W. (1985). "Monitoring electrochemically active compounds by amperometric gas sensors," *Sensors and Actuators* 6, 269-288.

Stetter, J. R., Zaromb, S., and Findlay, M. W. U.S. Patent #5,055,266. (October 8, 1991), "Methods for detecting toxic gases."

Storey, J. M. E., Shelton, R. D., Barber, T. E., and Wachter, E. A. (1994). "Electrochemical SERS detection of chlorinated hydrocarbons in aqueous solutions," *Appl. Spectrosc.* 48, 1265 -1271.

Strategic Environmental Research and Development Program. (1995). "1995 annual report and five-year (1995-1999) strategic investment plan," Arlington, VA, pp CU-4 - CU-9.

Stromswold, D. C. (1994). "Calibration facilities at Hanford for gamma-ray and fission-neutron well logging," PNL-9958, Pacific Nortwest National Laboratory, Richland, WA.

Stromswold, D. C. (1995). "Calibration facilities for borehole and surface environmental radiation measurements," *Journal of Radioanalytical and Nuclear Chemistry* 194 (2), 393-401.

Swenson, O. F., and Gillispie, G. D. (1996). "REMPI detection of volatile aromatic hydrocarbons in ambient air." *Advanced technologies for environmental monitoring and remediation.* Tuan Vo-Dinh, ed. *Proc. SPIE 2835*, Denver, CO,144-152.

Swenson, O. F., Gillispie, G. D., Cooper, W. F. and Dvorak, M. A. (1997). "Real-time detection of volatile aromatic hydrocarbons in groundwater and soil." *OSA trends in optics and photonics, volume 8, environmental monitoring and instrumentation.* Frank Bucholtz, ed., Optical Society of America, Washington, DC, 14-19.

Swenson, O. F., Gillispie, G. D., and Walls, C. J. (1997). "Detection of organic compounds by ambient pressure MPI." *OSA trends in optics and photonics, volume 8, environmental monitoring and instrumentation.* Frank Bucholtz, ed., Optical Society of America, Washington, DC, 20-24.

ToxFaQs - Trichloroethylene. U.S Department of Health and Human Services, Public Health Service, Agency for Toxic Substances and Disease Registry, http://atsdr1.atsdr.cdc.gov/tfacts19.html (April 1993).

U.S. Environmental Protection Agency. (1994). "Volatile organics by gas chromatography/mass spectrometry (GC/MS): Capillary column technique," SW846 Method 8260A. Washington, DC.

U.S. Environmental Protection Agency. (1995). "Site characterization analysis penetrometer system (SCAPS): Innovative technology evalution report," EPA No. 540/R-95/520, Office of Research and Development, Washington, DC.

Van Benthem, M. H., Mitchell, B. C., Gillispie, G. D., and St. Germain, G. W. (1996). "Chemometric treatment of multimode laser-induced fluorescence (LIF) data of fuel-spiked soils." *Advanced technologies for environmental monitoring and remediation.* Tuan Vo-Dinh, ed. *Proc. SPIE 2835*, Denver, CO, 167-179.

Wise, M. B., Guerin, M. R., Merriweather, R., Thompson, C. V., and Davis, W. M. "Draft EPA Method 8265: Direct sampling ion trap mass spectrometry for the measurement of voaltile organic compounds in water, soil and air," (in preparation), Office of Solid and Hazardous Waste, U.S. Environmental Protection Agency, Washington, DC.

Yinon, J., and Zitrin, S. (1981). *The analysis of explosives.* Pergamon Press, New York.

Appendix A
Publications

Research Area I: Laser-Induced Breakdown Spectroscopy (LIBS)

Patents:

Ballard, J. H., Miles, B. H., and Cress, D. H. U.S. Army Corps of Engineers Case 282, "Laser-induced breakdown spectroscopy for detection of heavy metal soil contaminants."

Ballard, J. H., Miles, B. H., and Cress, D. H. U.S. Army Corps of Engineers Case 400, "Laser-induced Breakdown Spectroscopy For Detection of Heavy Metal Soil Contaminants."

Miles, B. H., Cooper, S. S., Cespedes, E. R., and Theriault, G. A. U.S. Patent 5,757,484 (26 May 1998), "Standoff Laser-induced Breakdown Spectroscopy Penetrometer System."

Miles, B. H., Cortes, J., Ballard, J. H., Everett, J. B., Curtis, J. O., Reed, B. E., and Powell, J. F. U.S. Army Corps of Engineers Case 458, "Apparatus And Method For Real-time Determination of Subsurface Volumetric Moisture Content of Varying Soil Layers In-situ."

Theriault et. al. Navy Case 78165, "Laser Induced Breakdown Spectroscopy Soil Contamination Probe."

Theriault et. al. Navy Case 78881, "A Translation System For Directing an Optical Signal to Predetermined Coordinates."

Papers:

Adams, J. W., Cespedes, E. R., and Miles, B. H. (1997). "Status of emerging technologies for advanced detection devices for characterization and cleanup of contaminated soils and groundwater," HTRW Chemists Workshop, Las Vegas, NV.

Alexander, D. R., and Poulain, D. E. (1997). "Quantitative analysis of the detection limits for heavy metal contaminated soils by laser-induced breakdown spectroscopy," Miscellaneous Paper IRRP-97-2, U.S. Army Engineer Waterways Experiment Station, Vicksburg, MS.

Alexander, D. R., Poulain, D. E., and Cespedes, E. R. (1997). "Detection limits of heavy metals in soils by laser induced breakdown spectroscopy," *Trends in Optics and Photonics (TOPS), Vol* 8, *Environmental Monitoring and Instrumentation*, 8-13.

Alexander, D. R., Poulain, D. E., Khlif, M. S., and Cespedes, E. R. (1996). "Influences on detectability of heavy metals in soils by laser-induced breakdown spectroscopy," IGARSS'96, Lincoln, NE.

Cespedes, E. R., Miles, B. H., and Lieberman, S. H. (1994). "Development of optical sensors for the site characterization and analysis penetrometer system (SCAPS)." *Proceedings of the International symposium on optical sensing for environmental monitoring, Vol SP-89*, pp 621-632.

Cespedes, E. R., Cortes, J., Miles, B. H., and Theriault, G. (1995). "LIBS for in-situ screening of soils contaminated with heavy metals," Optical Society of America annual meeting, Portland, OR.

Cortes, J., Cespedes, E. R., and Miles, B.H. (1996). "Development of laser-induced breakdown spectroscopy for detection of metal contaminants in soils," Technical Report IRRP-96-4, U.S. Army Engineer Waterways Experiment Station, Vicksburg, MS.

Lieberman, S.H., Boss, P. A., Knowles, D. S., and Theriault, G. A. (1995). "Applications of remote spectroscopy for in situ environmental monitoring," IEEE Lasers and Electro-Optics Society 1995 Annual Meeting, San Francisco, CA.

Lieberman, S. H., and Theriault, G.A. (1996). "In situ detection of metals in soils," Optical Society of America Annual Meeting, New York, NY.

Lieberman, S. H., Knowles, D. S., and Theriault, G. A., and Davey, M. (1996). "Remote spectroscopy over optical fibers for in situ measurement of contaminants in soil," Optical Society of America on Laser Application to Chemical and Environmental Analysis, Orlando, FL.

Lieberman, S. H., Theriault, G. A., and Knowles, D. S. (1996). "Fiber-optic chemical sensors: spectroscopic solutions for environmental problems," 1996 XX International Quantum Electronics Conference, Sydney, Australia.

Miles, B. H., Cortes, J., and Cespedes, E. R. (1997). "Laser-induced breakdown spectroscopy (LIBS) detection of heavy metals using a cone penetrometer: System design and field investigation results." *Field analytical methods for hazardous wastes and toxic chemicals.* Air and Waste Management Association, Las Vegas, NV, pp 671-680.

Miziolek, A. W., and Cespedes, E. R. (1997). "Spectroscopic analysis of heavy metal contamination of the environment, Trends in Optics and Photonics (TOPS)," *Environmental Monitoring and Instrumentation* 8, 82-84.

Peach, L. A. (1996). "Laser spectroscopy reveals subsurface contamination," *Laser Focus World.* Pennwell Publishing, Nashua, NH, 23-26, (interview of B.H. Miles regarding DL-LIBS system).

Theriault, G. A., Wingfield, B., and Lieberman, S. H.. (1994). "Fiber-opticbased laser-induced breakdown spectroscopy for remote in-situ measurements of metals in soils." *International symposium on optical sensing for environmental and process monitoring.* McLean, VA.

Theriault G. A., Lieberman, S. H., and Knowles, D. S. (1995). "Laser induced breakdown spectroscopy for rapid delineation of metals in soils." *Proceedings of the U.S. EPA/A&WMA fourth international symposium-field screening methods for hazardous waste and toxic chemicals.* Las Vegas, NV.

Theriault G. A., and Lieberman, S. H. (1994). "A laser-induced breakdown spectroscopy probe for the in situ detection of metal contamination in soils," OSA topical meeting on laser applications to chemical and environmental analysis, Orlando, FL.

Theriault, G. A., and Lieberman, S. H. (1995). "Remote in situ detection of heavy metal contamination in soils using a fiber optic laser-induced breakdown spectroscopy (FO-LIBS) system." *Proceedings SPIE-European symposium on optics for environmental and public safety,* V 2504. Munich FRG.

Theriault, G. A., and Lieberman, S. H. (1996). "Field deployment of a LIBS probe for rapid delineation of metals in soils." *Proceedings SPIE-advanced technologies for environmental monitoring and remediation,* V 2835. Denver, CO.

Theriault, G. A., Bodensteiner, S., and Lieberman, S. H. "A real time fiber-optic libs probe for the *in situ* delineation of metals in soils." *Field analytical chemistry ad technology* (In preparation). Wiley, New York.

Theriault, G. A., Bodensteiner, S., Tripoli, R., and Lieberman, S. H. (1998). "Use of a fiber optic-based, laser-induced breakdown spectroscopy (LIBS) probe for in situ determination of metals in soils," OSA topical meeting on laser applications to chemical and environmental analysis, Orlando, FL.

Research Area II: Laser Induced Fluorescence (LIF)

Patents:

Ballard, J. H., Cooper, S. S., Morgan, J. C., Lawrence, W. R., and Reed, B. E. U.S. Patent 5,548,115 (20 August 1996), "Probe Device for Detecting Contaminants in Subsurface Media."

Cooper, S. S., and Malone, P. G. U.S. Patent 5,128,882 (7 July 1992), "Device for measuring reflectance and fluorescence of in-situ soil."

Papers:

Aggarwal, I. D., Farquharson S., and Koglin, E. (1995). "Capabilities and limitations of a cone-penetrometer-deployed fiber optic laser-induced fluorescence (LIF) petroleum oil and lubricant (POL) sensor." *Optical sensors for environmental and chemical process monitoring.* McGinnis, W. C., Davey, M., Wu, K. D., and Lieberman, S. H. ed., *Proc SPIE Vol 2367*, McLean, VA, 2-16.

Vo-Dinh, T. (1995). "Field results from the SCAPS laser-induced fluorescence (LIF) sensor for in-situ subsurface detection of petroleum hydrocarbons." *Environmental Monitoring and Hazardous Waste Site Remediation.* D. S. Knowles and S. H. Lieberman, ed., *Proc. SPIE Vol 2504*, Bellingham, WA, 297-307.

Symposia presentations:

Andrews, J. M., and Lieberman, S. H. (1995). "Quantitative and qualitative analysis of spectral data obtained from integrated fiber optic fluorometer and cone penetrometer." *Field screening methods for hazardous wastes and toxic chemicals.* 22-24 February, Las Vegas, NV.

Davey, M., Lieberman, S. H., and Wu, K. D. (1995). "In situ determination of petroleum, oil and lubricant products using lser induced fluorescence of polycyclic aromatic hydrocarbons." *Institute of gas technology symposium on gas, oil and environmental biotechnology.* 11-13 December. Colorado Springs, CO. (Abstract only).

Davey, M., Andrews, J. M., and Lieberman, S. H. (1997). "A comparison of alternative excitation wavelengths to induce fluorescence in petroleum, oil and lubricant hydrocarbons." *Symposium proceedings, field analytical methods for hazardous wastes and toxic chemicals.* Las Vegas, NV. (abstract only).

Douglas, G. S., Lieberman, S. H., McGinnis, W. C., and Peven, C. (1995). "The influence of PAH concentration and distribution on real-time in situ measurements of petroleum products in soils using laser induced fluorescence." Presented at *Field Screening Methods for Hazardous Wastes and Toxic Chemicals.* 22-24 February, Las Vegas, NV.

Knowles, D. S., and Lieberman, S. H. (1997). "Techniques for monitoring bioremediation progress using the SCAPS optical cone penetrometer system." *Symposium proceedings, field analytical methods for hazardous wastes and toxic chemicals* (in preparation). Las Vegas, NV.

Lieberman, S. H., McGinnis, W. C., Stang, P. M., and McHugh, D. (1995). "Intercomparison of *in situ* measurements of petroleum hydrocarbons using a cone penetrometer deployed laser-induced fluorescence (LIF) sensor with conventional laboratory-based measurements." *Field screening methods for hazardous wastes and toxic chemicals.* 22-24 February, Las Vegas, NV.

Lieberman, S. H., McGinnis, W. C., Davey, M., Knowles, D. S., and Wu, K. D. (1995). "Field validation of a cone penetrometer deployed laser-induced fluorescence (LIF) sensor for *in situ* measurement of petroleum hydrocarbons in soils." American Defense Preparedness Association. 18-21 April. San Diego, CA. (Abstract only).

Lieberman, S. H., and Knowles, D. S. (1995). "In situ subsurface laser-induced fluorescence measurements for subsurface detection of petroleum hydrocarbons." *European symposium on optics for environmental and public safety.* 19-23 June. Munich, Germany.

Lieberman, S. H. (1995). "Use of laser induced fluorescence (LIF) for real-time field screening of polycyclic aromatic hydrocarbons associated with manufactured gas plants." *International symposium/trade fair on clean-up of manufacuted gas plants.* 19-21 September. Prague, Czech Republic. (Abstract only).

Lieberman, S. H., Boss, P. A., Knowles, D. S., and Theriault, G. A. (1995). "Application of remote spectroscopy for In situ environmental monitoring." *IEEE lasers and electro-optics society 1995 annual meeting.* 30 October - 2 November. San Francisco, CA. (Invited Paper-Abstract only).

Lieberman, S. H., and Hampton, T., Knowles, D., Davey, M., and McGinnis, W. C. (1995). "Comparison of in-situ laser-induced fluorescence (LIF) measurements of petroleum hydrocarbons in soils with conventional laboratory measurements." *10th annual conference on contaminanted soils.* 23-27 October. Amherst, MA. (Abstract only).

Lieberman, S. H., Knowles, D. S., Theriault, G. A., and Davey, M. (1996). "Remote spectroscopy over optical fibers for *in situ* measurement of contaminants in soil." *Optical society of America. Laser application to chemical and environmental analysis.* 18-22 March. Orlando, FL. (Invited Paper-Abstract only).

Lieberman, S. H., and Knowles, D.S. (1996). "Advances in fiber optic based laser-induced fluorescence sensors for *in situ* measurement of petroleum hydrocarbons in soils." *1996 international geoscience and remote sensing symposium.* 27-31 May. Lincoln, NE. (Invited paper-Abstract only).

Lieberman, S. H. (1996). "Laser-induced spectroscopic measurements over optical fibers for in situ environmental analyses." *1996 annual meeting of the division of atomic, molecular and optical physics.* 15-18 May. Ann Arbor, MI. (Invited paper- Abstract only).

McGinnis, W. C., Lieberman, S. H., Davey, M., and Wu, K. D. (1996). "Refinement of in situ laser induced fluorescence measurements using geothechnical data." *Fourth international conference on-site analysis.* 21-24 January. Orlando, FL.

M^{c}Ginnis, W. C., and Lieberman, S. H. (1997). "A case study of field screening for petroleum, oil, and lubricant (POL) contaminants using the SCAPS laser induced fluorescence cone penetrometer system." *Symposium proceedings, field analytical methods for hazardous wastes and toxic chemicals* (in preparation). Las Vegas, NV.

Wingfield, B. H., and Lieberman, S. H. (1996). "In situ subsurface detection of fuel products in soils: Comparison of excitation at 308nm versus 337 nm." *211th American Chemical Society Meeting.* 24-28 March. New Orleans, LA. (Abstract only).

Research Area III: Fiber Optic Raman Sensor (FORS)

Patents:

Boss, P. A., Lieberman, S. H., and Newbery, R. U.S. Patent Application (Navy Case 77310, 1995), "Fiber optic Raman sensor (FORS) using a single excitation fiber and multiple collection fibers."

Boss, P. A., and Boss, R. D. U.S. Patent Application (Navy Case 77803, 1996), "Versatile, thin layer cell for in situ spectroelectrochemistry."

Peer-reviewed publications:

Mosier-Boss, P. A., Lieberman, S. H., and Newbery, R. (1995). "Fluorescence rejection in Raman spectroscopy by shifted-spectra, edge detection, and FFT filtering techniques," *Appl. Spectrosc.* 49, 630 -638.

Mosier-Boss, P. A., Newbery, R., Szpak, S., Lieberman, S. H., and Rovang, J. W. (1996). "Versatile, low volume, thin layer cell for *In Situ* spectroelectrochemistry," *Anal. Chem.* 68, 3277-3282.

Conference/Symposium Proceedings:

Mosier-Boss, P. A., Lieberman, S. H., and Newbery, R. (1995). "Use of edge detection and FFT filtering techniques to reject fluorescence in Raman spectra." *Proceedings of the fourth international symposium on field screening methods for hazardous wastes and toxic chemicals,* Environmental Protection Agency, Las Vegas, NV, 1155-1162.

Mosier-Boss, P. A., Newbery, R., and Lieberman, S. H. (1997). "Development of a cone penetrometer deployed solvent sensor using a SERS fiber optic Raman probe." *Proceedings of the international symposium on field screening methods for hazardous wastes and toxic chemicals.* Environmental Protection Agency, Las Vegas, NV, 588 -599.

Mosier-Boss, P. A., and Lieberman, S. H. (1998). "Detection of subsurface solvent contamination using a cone penetrometer deployed SERS fiber optic probe." *Proceedings of the second biennial international conference on chemical measurement and monitoring of the environment.* Ottawa, Canada, 65-70.

Presentations:

Lieberman, S. H., Norita, C. A., and Mosier-Boss, P. A. (1997). "Cone penetrometer deployed *In Situ* video imaging system for characterizing sub-surface soil properties and contaminants." *First international conference and industrial exhibition 'Field Screening Europe,'* Karlsruhe, Germany, September.

Mosier-Boss, P. A., and Lieberman, S. H. (1997). "Remote Raman spectroscopy of subsurface environments: technical challenges and solutions," *24th Conference of the Federation of Analytical Chemistry and Spectroscopy Societies.* Providence, RI.

Published Text Books or Book Chapters:

Mosier-Boss, P. A., and Lieberman, S. H. (1998). "Determination of VOCs using a cone penetrometer-deployed solvent sensor with a SERS fiber-optic probe." Current Protocols in Field Analytical Chemistry. Viorica Lopez-Avila et al., ed., Wiley, New York, 1.F1.1-1.F.1.23.

Research Area IV: Electrochemical Sensors

Patent:

Stetter, J. R., Zaromb, S., and Findlay, M. W. U.S. Patent 5,055,266 (8 October 1991), "Method for detecting toxic gases."

Peer-reviewed publications:

Buttner, W. J., Findlay, M., Vickers, M. W., Davis, W. M., Cespedes, E. R., Cooper, S. S., and Adams, J. W. (1997). "*In-situ* detection of trinitrotoluene and other nitrated explosives in soils," *Analytica Chimica Acta*, 17815, 1-9.

Technical Reports:

Cespedes, E. R., Davis, W. M., Adams, J. W., and Hall, G. J. (1998). "Results of the site characterization and analysis penetrometer system (SCAPS) explosives sensor field testing - Landfill No. 3 (ADS 1200), Pantex, TX."

Mortensen, D. J., and Buttner, W. J. (1996). *Operating manual for the TRI RCL/SCAPS probe,* Contract DACA39-95-K-0016, (in preparation) Transducer Research, Inc., Aurora, IL.

Powell, J. F., Davis, W. M., Eng, D. Y., Adams, J. W., and Murray, M. C. (1998). "Results of the site characterization and analysis penetrometer system (SCAPS) explosives sensor field testing - Area 17 and 63, Longhorn Army Ammunition Plant, TX."

Conference/Symposium Proceedings:

Adams, J. W., Cespedes, E. R., Cooper, S. S., Davis, W. M., Buttner, W. J., and Vickers, W. C. (1995). "Development and testing of cone penetrometer sensor probe for in-situ detection of explosive contaminants," *Field Screening Methods for Hazardous Wastes and Toxic Chemicals, VIP* 47 *Vol* I. Air and Waste Management Assoc., Pittsburgh, PA, 491-501.

Adams, J. W., Cespedes, E. R., Davis, W. M., Buttner, W. J., and Findlay, M. W. (1997). "Development and testing of cone penetrometer electrochemical sensor probes for chlorinated solvents and explosives," *Field Analytical Methods for Hazardous Wastes and Toxic Chemicals, VIP* 71, Air and Waste Management Assoc., Pittsburgh, PA, 667-670.

Cespedes, E. R., Cooper, S. S., Davis, W. M., Buttner, W. J., and Vickers, W. C. (1995). "In situ detection of TNT contamination using electrochemical sensors in cone penetrometer system," *Optical sensors for environmental and chemical process monitoring, Proc. SPIE* 2367, I.D. Aggarwal, S. Farquharson, E. Koglin, ed., Bellingham, WA, 33-42.

Shorter, J. H., Wormhoudt, J. W., Cespedes, E. R., Adams, J. W., Davis, W. M., Buttner, W. J., and Findlay, M. W. (1997). "Cone penetrometer detection of energetic materials in soils." *Proceedings 23rd environmental symposium and exhibition, American Defense Preparedness Assoc.* New Orleans, 481-486.

Published Technical Abstracts:

Findlay, M. W., Vickers, W., Buttner, W. J., Cespedes, E. R., Davis, W. M., and Cooper, S. S. (1995). "Measurement of TNT and other explosive contamination in soils using electrochemical sensors." *Proceedings of the environmental sensors symposium, electrochemical society, Vol* 95-2, 1555.

Presentations:

Adams, J. W., Cespedes, E. R., and Miles, B. H. (1997). "Status of emerging technologies for advanced detection devices for characterization and cleanup of contaminated soils and groundwater." HTRW Chemists Workshop, Las Vegas NV, March.

Cespedes, E. R., Davis, W. M., Ballard, J. H., and Buttner, W. J. (1996). "Development and testing of electrochemical sensors for rapid detection of explosive contaminants in soils." *IGARSS '96: 1996 international geoscience and remote sensing symposium: Remote sensing for a sustainable future.* Institute of Electrical and Electronics Engineers, Piscataway, NJ.

Research Area V: Spectral Gamma Sensor

Patents:

Ballard, J. H., and Morgan, J. C. U.S. Patent 5,744,730 (28 April 1998), "Subsurface in-situ radon gas detection/penetrometer system."

Reed, B. E., Eng, D. Y., Register, B. A., Ballard, J. H., and Morgan, J. C. U.S. Patent 5,635,710 (3 June 1997), "Subsurface penetrometer radiation sensor probe and system."

U.S. Pat. Application 09/018,881 (Case No. COE461 (status pending)), "A system for detection of radioactive elements and metal contaminants in subsurface soil."

Peer-reviewed publications:

Morgan, J. C., Adams, J. W., and Ballard, J. H., (1998). "Field use of a cone penetrometer gamma probe for radioactive waste detection," *Field Analytical Chemistry and Technology* 425, 129-135.

Technical Reports:

Morgan, J. C., Fields, M. P., Cargile, D. M., and Adams, J. W. "Results of the use of a cone penetrometer spectral gamma probe for radioactive waste detection at the Savannah River Site," Technical Report (in preparation), U.S. Army Engineer Waterways Experiment Station, Vicksburg, MS, April.

Conference/Symposium Proceedings:

Morgan, J. C., Adams, J. W., and Ballard, J. H. (1997). "Field demonstration of the SCAPS cone penetrometer gamma probe for rad-waste detection." *Field analytical methods for hazardous wastes and toxic chemicals, VIP* 71. Air and Waste Management Assoc., Pittsburgh, PA, 600-611.

Presentations:

Adams, J. W., Cespedes, E. R., and Miles, B. H. (1997). "Status of emerging technologies for advanced detection devices for characterization and cleanup of contaminated soils and groundwater," *7th combined innovative tech transfer and chemistry workshop, Annual corps chemists meeting.* Las Vegas, NV.

Adams, J. W. (1997). "DOE rad characterization," U.S. Army Engineer Waterways Experiment Station Environmental Laboratory GPRA Review, USAEWES, Vicksburg, MS.

Research Area VI: SCAPS Samplers

Patent:

Peters, J. F., Leavell, D. A., Lee, L. T., Cooper, S S., Malone, P. G., and Peterson, R. W. U.S. Patent 5,358,057 (25 October 1994), "A modular device for collecting multiple fluid samples from soil using a cone penetrometer."

X-Ray Fluorescence (XRF) Sensor

Patent (applied for):

Case COE-461 (June, 1997), "A system for detection of radioactive elements and metal contaminants in subsurface soil."

Papers:

Adams, J. W., and Eng, D. Y. (1995). "Use of ceramics in emerging environmental characterization techniques," *Bull. Am. Cer. Soc.* (3)75, SXIII-69-96.

Adams, J. W., Cespedes, E. R., and Miles, B.H. (1997). "Status of emerging technologies for advanced detection devices for characterization and cleanup of contaminated soils and groundwater." HTRW Chemists Workshop. Las Vegas, NV.

Elam, W. T., Adams, J. W., Hudson, K. R., McDonald, B., and Gilfrich, J. V. (1998). "Subsurface measurement of soil heavy metal concentrations with the SCAPS x-ray fluorescence (XRF) metals sensor," *Field Analytical Chemistry and Technology* 2(2), 97-102.

Elam, W. T. (1998). "Determination of metals in soils by XRF spectrometry via cone penetrometry (SCAPS)." *Current protocols in field analytical chemistry*. Viorica Lopez-Avila et al., ed., Wiley, New York, 3B.3.1-3B.3.10.

Elam, W. T., Adams, J. W., Hudson, K. R., Gilfrich, J. V. and McDonald, B. "In-situ environmental XRF." *Advances in x-ray analysis* (in preparation).

Elam, W. T., Adams, J. W., Hudson, K. R., Eng, D., Robitaille, G., and Aggarwal, I. (1997). "Field demonstration of the SCAPS XRF metals sensor." *Field analytical methods for hazardous wastes and toxic chemicals, VIP* 71. Air and Waste Management Assoc., Pittsburgh, PA, 681-689.

Elam, W. T., Adams, J. W., Hudson, K. R., McDonald, B. and Gilfrich, J.V. (1998). "Use of the SCAPS XRF metals sensor to detect subsurface lead contamination." *Proceedings EnviroAnalysis '98, Ottawa, Canada.*

McDonald, B., Unsell, C. W., Elam, W. T., Hudson, K. R., and Adams, J. W. (1998). "Cone penetrometer x-ray fluorescence tool for the analysis of subsurface heavy metal contamination." *Proceedings, 1998 symposium on radiation measurements and applications.* Ann Arbor, MI.

"X-ray metals sensor for the cone penetrometer." Navy Case No. 77,638. (in preparation).

REPORT DOCUMENTATION PAGE

Form Approved
OMB No. 0704-0188

1. AGENCY USE ONLY *(Leave blank)*	2. REPORT DATE	3. REPORT TYPE AND DATES COVERED
	September 1999	Final report

4. TITLE AND SUBTITLE
Tri-Service Site Characterization and Analysis Penetrometer System (SCAPS) Accelerated Sensor Development Project - Final Report

5. FUNDING NUMBERS

6. AUTHOR(S)
Ernesto R. Cespedes, Stephen H. Lieberman, Bruce J. Nielsen, George E. Robitaille

7. PERFORMING ORGANIZATION NAME(S) AND ADDRESS(ES)
U.S. Army Engineer Research and Development Center, Waterways Experiment Station, 3909 Halls Ferry Road, Vicksburg, MS 39180-6199; Space and Naval Warfare Systems Command, 53605 Hull Street, San Diego, CA 92152-5410; U.S. Air Force Research Laboratory, 139 Barnes Drive, Tyndall Air Force Baes, Florida 32403-5323; U.S. Army Environmental Center, Aberdeen Proving Ground, Maryland 31010-5401

8. PERFORMING ORGANIZATION REPORT NUMBER
Technical Report SERDP-99-3

9. SPONSORING/MONITORING AGENCY NAME(S) AND ADDRESS(ES)
SERDP Program Office
901 North Stuart Street, Suite 203
Arlington, VA 22203

10. SPONSORING/MONITORING AGENCY REPORT NUMBER

11. SUPPLEMENTARY NOTES
Available from National Technical Information Service, 5285 Port Royal Road, Springfield, VA 22161.

12a. DISTRIBUTION/AVAILABILITY STATEMENT
Approved for public release; distribution is unlimited.

12b. DISTRIBUTION CODE

13. ABSTRACT *(Maximum 200 words)*

In 1994, the Strategic Environmental Research and Development Program (SERDP) funded a Tri-Service effort to accelerate the development and fielding of environmental sensing technologies to extend the capabilities of the Site Characterization and Analysis Penetrometer System (SCAPS). This effort, which was completed in 1998, produced a wide range of SCAPS sensors, samplers, and supporting technologies that allow SCAPS to detect, delineate, and map subsurface contaminants including petroleum, oils, and lubricants (POL), toxic metals, explosives and energetics, volatile organic compounds (VOC), and radioactive wastes. This report describes the various SCAPS sensors developed as part of the SERDP-funded effort including laser induced fluorescense, Raman spectroscopy, laser induced breakdown spectroscopy, X-ray fluorescence, electrochemical sensor, biosensor, and spectral gamma probes. In addition, the development and testing of cone-penetrometer based samplers, including thermal desorption and multiport samplers, are detailed. Results of laboratory evaluation and field validation studies are presented, and technology transfer accomplishments are described. Included in this report is a bibliography of technical papers, reports, presentations, and patents produced during the course of this project.

14. SUBJECT TERMS

Cone penetrometer	Spectroscopy
Environmental sensors	Site characterization
In situ sensors	Site screening

15. NUMBER OF PAGES
184

16. PRICE CODE

17. SECURITY CLASSIFICATION OF REPORT	18. SECURITY CLASSIFICATION OF THIS PAGE	19. SECURITY CLASSIFICATION OF ABSTRACT	20. LIMITATION OF ABSTRACT
UNCLASSIFIED	UNCLASSIFIED		